4-30-2020

Understanding the Toxicity of Single Hydrocarbons, Oil, and Dispersed Oil: A Species Sensitivity Assessment for Five Atlantic Coral Species

Nicholas R. Turner
Nova Southeastern University

Dissertation of
Nicholas R. Turner

Submitted in Partial Fulfillment of the Requirements for the Degree of

Doctorate of Philosophy
Ph.D. Oceanography/Marine Biology

Nova Southeastern University
Halmos College of Natural Sciences and Oceanography

April 2020

Approved:
Dissertation Committee

Major Professor: D. Abigail Renegar, Ph.D.

Committee Member: Jose Lopez, Ph.D.

Committee Member: Thomas Parkerton, Ph.D.

Committee Member: Bernhard Riegl, Ph.D.

HALMOS COLLEGE OF NATURAL SCIENCES AND OCEANOGRAPHY

UNDERSTANDING THE TOXICITY OF SINGLE HYDROCARBONS, OIL, AND DISPERSED OIL: A SPECIES SENSITIVITY ASSESSMENT FOR FIVE ATLANTIC CORAL SPECIES

By

Nicholas R Turner

Submitted to the Faculty of
Halmos College of Natural Sciences and Oceanography
in partial fulfillment of the requirements for
the degree of Doctorate of Philosophy

Nova Southeastern University

June 2nd, 2020

`

ABTRACT

Coral reefs are keystone coastal ecosystems that are at risk of exposure to petroleum hydrocarbons from a range of sources, including oil spill incidents and chronic runoff, and are usually one of the highest valued natural resources for protection in Net Environmental Benefit Analysis (NEBA)/Spill Impact Mitigation Assessment (SIMA) of response methods and environmental damage. Previous research evaluating hydrocarbon impacts to corals has resulted in no clear characterization of sensitivity, as work has generally focused on higher-level effects, compounded by significant variability in experimental methodology. This represents an important knowledge gap in oil spill preparedness and response as it relates to the potential impact of oil spills to the coral animal and its symbiotic zooxanthellae. This research was designed to address this gap, using a standardized toxicity testing protocol to evaluate effects of the petroleum/dispersant system the Atlantic shallow-water coral species *Acropora cervicornis, Porites astreoides, Siderastera siderea, Stephanocoenia intersepta,* and *Solenastrea bournoni.* The central objective of the Coral-Tox project was to provide lethal and sub-lethal endpoints of hydrocarbon exposure for five key Atlantic coral species in order to support effective decision-making and response should a spill occur near coral reefs.

The relative sensitivity of these scleractinian coral species to hydrocarbon exposure was assessed with 48-h assays using 1-methylnaphthalene, phenanthrene, and toluene, as well as non-dispersed and chemically dispersed MC252 crude oil. Effects were evaluated based on physical coral condition, mortality, photosynthetic efficiency, growth rate, and gene expression. While the threatened species *A. cervicornis* is the most sensitive of those tested, the acute endpoints for the single-compound tests, and the oil and chemically dispersed oil exposures indicated that corals are comparatively more resilient to narcotic chemical exposure than other coastal marine species, possibly due to the lipid-rich nature of coral tissue and their ability to secrete mucus. Typically, mortality is used to compare the effects of contaminants, but sublethal impacts are necessary for assessing impacts of petroleum spills in the environment, particularly when evaluating the relative effects of a spill to different ecosystem components included in a NEBA/SIMA. Gene expression results were used to evaluate effects of the contaminants at levels below the onset of observable physiological changes or lethality. Identifying impact pathways of hydrocarbon exposure to corals from the genomic to organismal levels provides a framework for the prediction of oil impacts on the coral animal, significantly improving model inputs to predict the effects of spill responses in coastal tropical environments.

KEY WORDS: 1-methylnaphthalene, phenanthrene, toluene, toxicity, MC252, oil, dispersant, Corexit

TABLE OF CONTENTS

LIST OF TABLES

CHAPTER 1

CHAPTER 2

CHAPTER 3

CHAPTER 4

LIST OF FIGURES

CHAPTER 1

CHAPTER 2

CHAPTER 4

CHAPTER 5

CHAPTER 1- UNCERTAINTY IN OIL TOXICITY TO CORAL

1.1 INTRODUCTION

Coral reefs are commonly regarded as one of the most diverse and complex marine communities, providing intrinsic beauty, economic and tourism value, incubators for fisheries, and erosion protection to the planet's tropical shorelines. Coral reefs exist in oligotrophic seas worldwide, including South Florida, the Gulf of Mexico, and the Caribbean Sea, providing an essential aspect of the ecology of subtropical oceans. Additionally, coral reefs are vital to the geochemical mass balance of the oceans in regard to fluxes of magnesium, calcium, strontium, and carbonate (Knap et al. 1983). The coral animal is fundamental to the reef, providing shelter from predators and substrate for colonization of algae and invertebrates, and acting as a direct source of nutrients (Loya and Rinkevich 1980, Shigenaka 2001, Haapkylae et al. 2007).

Coral reefs are one of the world's most threatened ecological resources due to a variety of environmental stressors, including those related to urban development of the coastal environments they inhabit. The adjacent increase in human population density has elevated the possibility of anthropogenic impacts on these ecosystems, and the more persistent, and often more frequent occurrence leaves little time for recovery (Haapkylae et al. 2007). Human dominance of coastal areas has led to increased sediment, nutrients, and other pollutant inputs into the sea that have been measurable for the last 30+ years (Knap et al. 1983, Shigenaka 2001).

Shallow-water coral reef ecosystems have an elevated risk of exposure to petroleum hydrocarbons due to their proximity to coastlines and shipping channels. Coral reefs of the US and elsewhere are ecosystems that have been, and could be again impacted by future spills and mitigation measures, especially with respect to increased oil exploration activities near Cuba and increased port expansion activities. Thus, detailed knowledge about the potential adverse effects of oil on coral reefs are needed to provide data for improving impact assessment tools for response planning and decision-making if real-world exposures occur.

1.1.1 Statement of the problem

Previous research on hydrocarbon toxicity to corals and coral reefs has been previously reviewed (Turner and Renegar 2017). Publications which considered the effects of hydrocarbons on 34 species of coral from 23 genera, both from Hexacorallia and Octocorallia, encompassing shallow, intermediate and deep-water species were summarized. However, where toxicity data for scleractinian corals exist, methodological inconsistencies frequently make a comparison of

results difficult. A significant issue in most of these studies was the lack of quantitative characterizations of exposure media; of the 46 laboratory exposures reviewed, only 9 reported measured treatment concentrations. The use of nominal concentrations can result in over- or underestimation toxicity due to variable solubility and volatility of constituent hydrocarbons. Additionally, substantial inconsistencies in the evaluation of coral health/mortality during exposure, variability in assay condition, toxicant utilized, and dosing regimen were also common (Singer et al. 2000, Aurand and Coelho 2005).

Differences in toxicant preparation methods prior to exposure can also lead to profound effects on the distribution of constituent hydrocarbons in the test media, and results of bioassays completed with one oil, may not be extrapolated to those completed with another. The extensive variation in methodology has led to a spectrum of observations, which range from no effect to complete mortality. Further, past studies have generally focused on community-level effects, therefore relatively little is known about effects on the individual, cellular, and sub-cellular levels. Impacts of environmental and chemical stressors on corals, in particular, are poorly understood at the cellular and subcellular levels (Venn et al. 2009), and focused studies at the molecular level will provide much-needed information into the cause of the observed physiological responses.

From the perspective of Oil Spill Preparedness and Response (OSPR), coral reefs, with a particular focus on the impacts on the coral animal itself, represent one of the highest valued natural resources for protection in Net Environmental Benefit Analysis (NEBA) of response methods and environmental damage (Shigenaka 2001). Overall, a significant data gap exists in oil spill preparedness and response as it relates to the potential impact of oil spills on coral reefs, thus, targeted hydrocarbon toxicity studies are vital to accurate assessment of coral resilience following hydrocarbon exposure. To fill this data gap, a standardized toxicity testing protocol for adult scleractinian corals that is tailored to the unique nature of corals and considers coral response using multiple high-resolution metrics has been developed. (Renegar et al. 2015, Turner 2016).

1.1.2 Statement of the significance of the work

The sum of experimental results, when integrated into response support tools, will provide input to managers for the visualization, prediction, and understanding of oil impacts on the coral animal and related habitats at variable severity levels. This will allow determination of thresholds

of acceptable/ unacceptable impact, and prediction of impact severity and choice of treatment based on expected impact, not just in terms of mortality. Different scenarios of coral impact can also be evaluated for various levels of acute, chronic exposures that can be used for making policy decisions.

This applied science approach to a practical issue allows improvement in decision-frameworks for reaction and mitigation and provides much-needed information to be used in Net Environmental Benefit Analysis (NEBA) or Spill Impact Mitigation Assessment (SIMA) of predicted impacts and response methods in coral reef environments following an oil spill. This research is designed with this end in mind, and builds upon an existing collaboration between academia, government, industry, and responders, with the goal of bridging the gap between science and decision-making by providing data that fill existing knowledge deficiencies and supports predictive modeling tools.

1.2 BACKGROUND AND APPROACH

This research, primarily intended to fill critical information gaps for oil spill response decision-makers, was developed with input from research partners in government and the response community in order to design study outputs that would integrate with existing toxicity models and existing and emerging oil spill fate models that predict oil exposures in the field over time and space to better inform response decision-makers on the potential impact of transported spilled oil or dispersed oil on coral reefs. It was envisioned that if toxicity endpoint data were available, then it would be possible to predict the effects of transported concentrations of dispersed and degraded oil plumes on exposed coral communities. Chemical dispersants remove or prevent surface oil by reducing oil droplet size, thus enhancing dissolution and increasing hydrocarbon concentrations in the water column (National Academies of Sciences and Medicine 2019). Understanding the effects of these increased water column concentrations on coral requires knowledge of the fate and effects for the individual compounds in the aqueous phase. Theoretically, if critical toxicity endpoints were identified for every petroleum compound, it would be possible to evaluate potential effects associated with different response options in the proximate presence of corals and coral reefs following fate modelling.

The first phase of the proposed research included a suite of experiments that investigated single hydrocarbon toxicity to five ecologically relevant Atlantic shallow-water corals (*Acropora cervicornis, Solenastrea bournoni, Stephanocoenia intersepta, Siderastrea siderea,* and *Porites*

astreoides). The initial focus was to obtain effect concentrations for three individual hydrocarbons (1-methylnaphthalene (1MN), phenanthrene (PHE), and toluene (TOL) with each of the five coral species. The effects of single hydrocarbon exposures were investigated using a variety of endpoints (visible condition, physiological, and transcriptomic) to evaluate the observed response and potential linkages at different levels of biological organization including molecular, sub-cellular and whole organism. Each 48-hour bioassay was conducted in the continuous-flow exposure system designed by Renegar et al. (2017b), which utilized a passive dosing method (Butler et al. 2013) to determine the effect and mortality endpoints for each species.

The second phase of this research was to input effect concentrations for corals into the Target Lipid Model (TLM), which can be used to predict the toxicity of dissolved hydrocarbons and related mixtures (Di Toro et al. 2000, McGrath et al. 2005, McGrath et al. 2018). PETROTOX (Redman et al. 2012a) and an oil solubility model (Redman 2015)were used to estimate the dissolved oil exposures and predicted impacts of a well characterized crude oil, which was then verified using bioassays with this physically and chemically-dispersed crude oil and two coral species. Aqueous hydrocarbon concentrations were quantified and characterized to assess the accuracy of predicted aqueous concentrations predicted by the solubility model.

The final phase of this research was a quantitative risk assessment examining the impacts of a potential spill in close proximity to Port Everglades, Florida. The port is scheduled to be dredged in the near future in order to increase the size and capacity of ships entering the channel. Tankers regularly transport diesel, jet fuel, and gasoline to Port Everglades, and the port expansion will facilitate the travel of larger, more completely full ships into close proximity with the Southeast Florida Coral Reef Tract. Using data generated in this research, a risk assessment was performed on a hypothetical cargo spill, to identify the impacts that may result.

1.2.1 Modeling effects of hydrocarbons

Crude oil and its derivatives (e.g. petroleum products such as diesels and heavy fuel oils) are complex mixtures containing thousands of compounds, with significant variability in composition between different oils depending on the source and manufacturing conditions (NRC 2003, National Academies of Sciences and Medicine 2019). Differences in solubility, persistence, bio- and photo-transformation, and oxidation of constituent compounds in oils results in different toxic impacts between oils or between the same oil in different environments (NRC 2005, Redman and Parkerton 2015). Predicting toxicity is further confounded by the

effects of different methods of preparation of aquatic exposure media on the dissolution, relative concentration, and bioavailability of constituent hydrocarbons in the exposure media (Bejarano et al. 2014).

Single hydrocarbon testing provides an alternative to the use of oil water accommodated fraction (WAF) as exposure media in toxicity studies. The effects of single compound tests are input into the TLM to establish a critical target lipid body burden (CTLBB), which is the hypothetical hydrocarbon lipid concentration at the site of toxic action for the specific organism. The site of action for most narcotic chemicals is presumed to be lipid in nature and related to cellular membranes. The TLM relies on the fact that most hydrocarbons found in crude oil exhibit acute toxicity via narcosis, and differences in chemical toxicity can be attributed to differences in partitioning of the chemical into the target lipid (Di Toro et al. 2000, Kipka and Di Toro 2009). Polycyclic aromatic hydrocarbons (PAHs) exhibit acute narcotic effects with toxicity correlated to hydrophobicity, which results in increased partitioning across permeable membranes into target lipids, thus resulting in increased toxicity.

The TLM-derived CTLBB can be used to compare species sensitivity, but more importantly, provides the information to predict the toxicity of other narcotic chemicals. The organism CTLBB and individual chemical logKow are used in the TLM to predict the effect concentration for each specific hydrocarbon. The TLM framework can also be combined with the additive toxic unit (TU) model to predict the concentrations and toxicities of all dissolved oil constituents found in more complex mixtures (Landrum et al. 2012, Redman et al. 2012a). The TU-TLM paradigm provides the means to describe and predict the toxicity of dissolved hydrocarbon mixtures, like oil, based on laboratory determined endpoints from single compound testing (McGrath et al. 2005, NRC 2005, McGrath and Di Toro 2009, Redman et al. 2012a).

The TLM estimates the CTLBB (µmol chemical/ g lipid) using the specific endpoint [i.e., the concentration lethal to 50% of the population: LC50 (mmol/L)] and the target lipid-water partition coefficient (K_{LW}), which is defined as the ratio of chemical concentration in the lipid (C_L) to the aqueous concentration (C_W).

1) $$CTLBB = LC_{50} * K_{LW}$$

2) $$K_{LW} = \frac{C_L}{C_W}$$

Experimental determination of the LC50 for a specific narcotic chemical allows calculation of an organism's CTLBB using the TLM.

3) $$\log LC_{50} = \log CTLBB - \log K_{LW}$$

The TLM uses K_{LW}, which is calculated using the linear free energy relationship between K_{LW} and the octanol-water partition coefficient (K_{OW}), as octanol has been determined a good surrogate for organism lipid tissues.

4) $$\log K_{LW} = -0.936 * \log K_{OW}$$

The TLM assumes that the target lipid has the same chemical partitioning property in all organisms, therefore the universal narcosis slope (-0.936) is representative of this ubiquitous mode of action (McGrath and Di Toro 2009). Combining Equations 3 and 4 results in the TLM.

5) $$\log LC_{50} = \log CTLBB - 0.936 * \log K_{OW}$$

McGrath and Di Toro (2009) refined the TLM to include chemical class correction factors for hydrocarbons with different affinities for the target lipid site, which in turn express increased toxicity. A re-evaluation of the TLM (McGrath et al. 2018) now includes an acute database of 79 species and updated narcosis slope and chemical class correction factors (slope=-0.940; Δc: MAHs= -0.025, PAHs= -0.364).

6) $$\log LC_{50} = \log CTLBB - 0.940 * \log K_{OW} + \Delta c$$

The species-specific CTLBB must be determined in a controlled laboratory experiment by measuring the LC50 for a single hydrocarbon with known K_{OW}. The CTLBB is expressed in µmol chemical/g octanol, but because of the relationship between K_{OW} and K_{LW}, the units are assumed to be µmol chemical/g lipid (McGrath et al. 2004). If TLM assumptions are true, and partitioning into organismal lipid is the same for all species, the CTLBB can be used to estimate the acute LC50 for other hydrocarbons with the same toxic modes of action using their respective K_{OW}.

The additive TU approach to evaluating mixture toxicity is a means of normalizing the toxicity of different chemicals in a mixture (Di Toro and McGrath 2000). The TU is the ratio of the aqueous concentration (Cw) to the effect concentration (LC50).

7) $$TU = \frac{C_W}{LC_{50}}$$

Hydrocarbons are known to have an additive effect (Capuzzo 1987, Di Toro and McGrath 2000, Barata et al. 2005, Redman et al. 2012a, Butler et al. 2013), and combining the toxic effect of all constituents' results in a convenient metric for predicting mixture toxicity.

8) $$TU_{mixture} = \sum_i TU_i$$

The TLM and the additive TU model are used to predict the toxicity of chemical mixtures with known concentrations. In an ideal world, the concentration of every chemical in the mixture would be known, but that is not feasible. A speciated oil solubility model uses physical properties of the chemical mixture (i.e., solubility, Kow, and Henry's Constant) and the exposure scenario (i.e., water volume, headspace) to predict dissolved concentrations of a subset of speciated hydrocarbons in the test oil (Redman and Parkerton 2015). Although the differences between the predicted and measured dissolved concentrations for this subset of hydrocarbon compounds are used to identify the presence of droplet oil in a test system, the model can also assign TU for each of the constituents in the aqueous phase. The estimated individual component concentrations (speciated solubility model) and the estimated endpoint concentrations (TLM) are used to calculate a TU for each component found in the oil. TUs are summed across all constituents and used as the basis for crude oil toxicity prediction in this study, i.e. the predicted oil loading causing a 50% response (LL50), corresponding to ∑TU=1. If the combined TU for a chemical mixture is greater than 1, the mixture is toxic at that concentration (Di Toro and McGrath 2000, McGrath and Di Toro 2009).

Contrary to the speciated solubility model, PETROTOX is model developed to produce toxicity estimates based on the whole dissolved oil, not just a speciated subset that have been measured (Redman et al. 2012a). Toxic units derived from PETROTOX will always be higher than the solubility model because they capture every compound expected to be present. The overall composition of the parent oil is input into PETROTOX to assign TUs to representative hydrocarbon blocks, before using the total TUs to determine a loading that will cause a 50% response. The predicted oil loading is assumed to be protective of 50% of the population exposed, and represents the oil loading that results in a WAF that causes 50% effects.

1.2.2 Passive dosing

Determining effect concentrations of individual hydrocarbons for TLM calibration must be completed using a constant concentration throughout the exposure to provide reliable data to

generate dose-response curves (McGrath and Di Toro 2009, Butler et al. 2013, Redman and Parkerton 2015). Most petroleum PAHs are sparingly soluble, and obtaining constant exposure concentrations can be challenging due to loss mechanisms (sorption, volatilization, and degradation) (Smith et al. 2010, Butler et al. 2013). The passive dosing technique was developed to combat the issue of degradation whereby the chemical is partitioned from a solvent solution into a biocompatible polymer, such as polydimethylsiloxane (PDMS), and placed in seawater to allow equilibration. The excessive amount of hydrocarbon loaded into the PDMS O-rings has been proven to produce a constant aqueous concentration for the exposure duration despite potential losses that occur in the test system (Smith et al. 2010, Butler et al. 2013, Renegar et al. 2017b).

1.2.3 Gene expression

There is an increasing number of genomic and proteomic tools that focus endpoints at earlier stages of the stress response by examining gene alterations following exposures to stressors. The earliest of these stages is the transcriptome, resulting from the transcription of DNA to mRNA. Alterations in mRNA expression of the transcriptome are the most sensitive biomarkers for physiological responses to environmental stress (Woo et al. 2014). Levels of mRNA provide a snapshot of transcriptional activity, and the changes in transcript levels often indicate a change in the level of a gene product following translation (Nikinmaa and Rytkönen 2011). Impacts can be diagnosed and quantified by comparing target gene basal expression with levels that are altered in response to environmental contaminants or experimental conditions.

Gene expression analysis is one of the most efficient ways to determine the molecular mechanisms of acclimatization, adaptation, and response to natural and anthropogenic stressors (Morgan et al. 2001, Moll et al. 2014). Sequencing the transcriptome is a viable and cost-efficient alternative to whole genome sequencing for methods focusing on the protein-coding regions of DNA. Typical RNASeq methods sequence the whole transcriptome and have become increasingly utilized as cost per sequenced base has been reduced over the last decade according to the National Human Genome Research Institute (Wetterstrand 2018). Although sequencing costs have diminished in recent years, sample preparation and data processing are still major cost factors in high-throughput screenings (Metzker 2009). QuantSeq (Lexogen) is a new robust and simple method for mRNA sequencing that increases the precision of gene expression measurements by only generating a single read at the 3’ end of each transcript. This makes it

ideal for multiplexing, which ultimately reduces the cost for accurately determining gene expression.

Studies of gene expression show physiological effects of contaminants prior to the onset of observational changes. These early indicators of stress were investigated to identify possible dose-response relationships, and how changes in genomic response may be linked to in-vivo effects. The gene expression results aid in defining the effects of low-level exposures indicative of real-world scenarios and provide data necessary for modeling impacts of petroleum mixtures. This approach will also likely identify and further characterize specific genes related to hydrocarbon toxicity stress. Past research has identified genes of a "chemical defensome" in marine invertebrates, which includes an integrated network of genes and pathways that allow an organism to defend against toxic chemicals (Goldstone et al. 2006). Additionally, the mixed-function oxidase system, which is the main pathway induced during exposure to xenobiotics, has been identified in numerous cnidarian species (Ramos and Garcia 2007, Downs et al. 2012, Shinzato et al. 2012). This pathway includes cytochrome p450 monooxygenase and numerous other conjugating and antioxidant enzymes (i.e., glutathione-s-transferase and multi-xenobiotic resistance protein) which have been previously correlated with increases in aromatic hydrocarbons in tissues.

1.3 GOALS AND HYPOTHESES

The overarching goal of this research was to build a foundation for effective decision-making should a spill potentially impact coral reefs. To reflect the complexity of the coral animal, evaluating the effects of any contaminant requires several levels of analysis. Lethality provided information necessary to model effects in terms of survival, but sublethal indicators provide more useful information to make decisions during a spill response. The steps followed for completing this process are outlined in Figure 1.1.

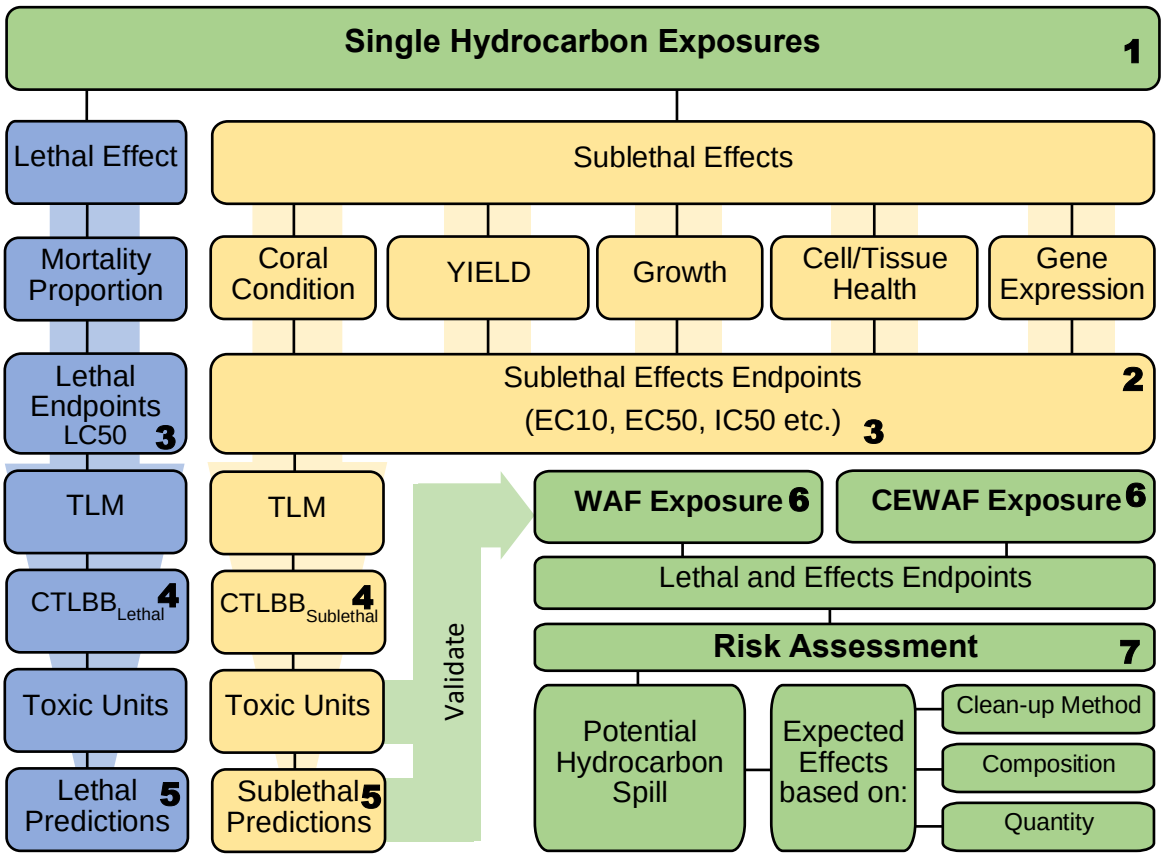

Figure 1.1 Flow chart outlining the steps and completed goals of the research. Bold numbers correspond to the goals listed in the text. This process was completed for all coral species, with the exception of only two species in the WAF and CEWAF exposures

This research included a variety of toxicity assays that were designed to achieve the planned goals and provide useful information to spill responders. Each single hydrocarbon exposure completed with each species generated data required to assess the overall effects of the toxicants (HO1- HO6). As an example, observational changes to the coral were assessed to determine the effect on visual condition to evaluate hypothesis 1. All hypotheses and associated assessment metrics can be found in Table 1.1.

Table 1.1 Hypotheses tested during exposures to all coral species used in this study

Hypothesis	Assessment Metric
H_O 1: Exposure to 1-methylnaphthalene, phenanthrene, or toluene will not affect the visual condition of each coral species.	Coral Condition
H_O 2: Exposure to 1-methylnaphthalene, phenanthrene, or toluene will not affect the survival of each coral species.	Mortality
H_O 3: Exposure to 1-methylnaphthalene, phenanthrene, or toluene will not affect the photosynthetic efficiency of each coral species.	Photosynthetic Yield
H_O 4: Exposure to 1-methylnaphthalene, phenanthrene, or toluene will not affect the growth of each coral species.	Calcification
H_O 5: Exposure to 1-methylnaphthalene, phenanthrene, or toluene will not affect the tissue and cellular characteristics of each coral species.	Histological Analysis
H_O 6: Exposure to 1-methylnaphthalene, phenanthrene, or toluene will not affect gene expression of each coral species.	Transcriptome Sequencing
H_O 7: Exposure to oil WAF or CEWAF will not affect the visual condition of each coral species.	Coral Condition
H_O 8: Exposure to oil WAF or CEWAF will not affect the survival of each coral species.	Mortality
H_O 9: Exposure to oil WAF or CEWAF will not affect the photosynthetic efficiency of each coral species.	Photosynthetic Yield
H_O 10: Exposure to oil WAF or CEWAF will not affect the growth of each coral species.	Calcification
H_O 11: Exposure to oil WAF or CEWAF will not affect the tissue and cellular characteristics of each coral species.	Histological Analysis
H_O 12: Exposure to oil WAF or CEWAF will not affect gene expression of each coral species.	Transcriptome Sequencing
H_O 13: WAF and CEWAF will cause the same effects on the coral species.	All

Testing hypotheses H_O1- H_O6 completed goal 1 of this project and resulted in data necessary to model the effects endpoints in terms of all assessment metrics (goals 2 and 3). Linking H_O1- H_O5 with H_O6 was completed following annotation of the expressed gene sequences. Differentially expressed genes were annotated, and KEGG database searches provided functional information to compare the observed change in expression with observed physiologic changes. The following is a list of goals that correspond to the bold numbers in Fig. 1.1.

1. Completed single hydrocarbon exposures for each coral species (1-methylnaphthalene, phenanthrene, and toluene)
    a. Refined dosing protocol and assessment metrics
    b. Generated lethal and sublethal data
2. Modeled effects using all assessment metrics.

3. Determined effect concentrations for lethality, median effect, and other hazard concentrations.
4. Used the TLM to calculate the CTLBB for lethality and sub lethal effects for each coral species
5. Used solubility model to assess the toxicity of exposures using WAF and CEWAF and toxic units
6. Verified the predicted lethality and effects with controlled laboratory exposures
    a. Determined lethal and sublethal effects endpoints for WAF and CEWAF to facilitate assessment of dispersed oil toxicity
7. Used the information gained to complete a risk assessment examining the impacts of a hypothetical hydrocarbon spill and response options near Florida reefs.

Creating models from the observed effects of the single hydrocarbon assays ultimately resulted in the information necessary to generate CTLBBs for each coral species (goal 4) and promote the assessment of crude oil toxicity using the solubility model and TUs (goal 5). To satisfy goal 6, two coral species were exposed to WAF and CEWAF to test hypotheses H_O7-H_O12 (Table 1). Analyzing the same effects as the single hydrocarbon tests verified the accuracy of modeled toxicity predictions from TU assessment. In addition to verifying TU predictions of toxicity, the WAF and CEWAF exposures facilitated a comparison of physically dispersed, and chemically dispersed oil toxicity (H_O13). The risk assessment was completed based on potential future hydrocarbon spills that may impact the Florida Reef Tract (goal 7). Completion of these goals resulted in an assessment of the effects of a possible hydrocarbon spill on coral species in the western Atlantic. The goal of this work is to have this information included in contingency plans, and aid in effective decision making should an oil spill impact these areas.

CHAPTER 2- SINGLE COMPOUND TOXICITY AND THE TARGET LIPID MODEL

2.1 INTRODUCTION

In order to determine the toxicity of crude oil and fill the gap in the understanding of the effects of an oil spill on coral, the toxicity of multiple single compounds was first investigated. The complexity and varying concentrations of constituents in crude oil results in differences in toxicity between oils, or between the same oil in different environments (NRC 2005, Butler et al. 2013, Redman and Parkerton 2015). Measuring the toxicity of all oils, in all environmental conditions is unfeasible, and predicting toxicity is confounded by the effects of different methods of exposure media preparation, relative concentrations, and bioavailability of constituent hydrocarbons in the exposure media (Bejarano et al. 2014, Redman and Parkerton 2015). Alternatively, toxicity of crude oils can be assessed by determining the toxicity of single compounds, and using the effects concentrations as inputs to commonly used toxicological models like the Target Lipid Model (TLM). The TLM is used to estimate a critical target lipid body burden (CTLBB) based on laboratory determined effects endpoints (McGrath et al. 2005, NRC 2005, Redman et al. 2012a, Butler et al. 2013, McGrath et al. 2018). The TLM framework can also be combined with the additive toxic unit (TU) model to predict the concentrations and toxicities of dissolved oil constituents found in more complex mixtures (Landrum et al. 2012, Redman et al. 2012a). In this way, TU can be used to predict toxicities of different oils given their measured or estimated dissolved oil exposures.

The initial phase of this work was to develop inputs to the TLM by assessing the toxicity of several individual hydrocarbons in controlled laboratory exposures. This suite of experiments investigated single hydrocarbon toxicity to five ecologically relevant Atlantic shallow-water corals (*Acropora cervicornis, Porites astreoides, Siderastrea siderea, Stephanocoenia intersepta,* and *Solenastrea bournoni*). The acute toxicity of three individual hydrocarbons (1-methylnaphthalene (1MN), phenanthrene (PHE), and toluene (TOL) was assessed with each of the five coral species, with the exception of no PHE exposure to *S. bournoni*. Current oil spill models predict effects with pseudo components that represent each of the dominating hydrocarbon classes in the aqueous phase of most water-soluble fractions of crude oil; monoaromatic hydrocarbons (MAHs), two-ring polyaromatic hydrocarbons (PAHs), and three-ring PAHs (French-McCay 2002, 2004). According to the pseudo components used by current oil toxicity models (SIMAP/OILMAP), one-, two-, and three-ring aromatic hydrocarbons are regarded as key contributors to the toxicity of surface oil

spills to aquatic life, although this model also predicts the fate and effects of 8 other pseudo components (French-McCay 2004).

The effects of TOL, 1MN, and PHE exposures were investigated using multiple 48-hour bioassays conducted in the continuous-flow exposure system designed by Renegar et al. (2017b), which utilized a passive dosing methodology to determine the effect and mortality endpoints for each species. The second phase of this chapter was to input the endpoints determined for each coral into the TLM, in order to estimate the target lipid concentration that caused the observed responses. This protocol has been previously applied to one species of shallow-water coral and significant lethal and sublethal impacts of a single hydrocarbon have been demonstrated (Renegar et al. 2017b). Further experimentation utilizing this testing protocol with additional coral species contributed to a more complete picture of hydrocarbon toxicity to scleractinian corals.

2.2 METHODS

2.2.1 Organism collection

The coral species utilized in this research, *Acropora cervicornis, Porites astreoides, Siderastrea siderea, Stephanocoenia intersepta,* and *Solenastrea bournoni,* are common in shallow depths and were chosen because of their widespread distribution and suitability to fragmentation and experimentation. Branch tips of *A* cervicornis were snipped from colonies at the Nova Southeastern University's Offshore Coral Nursery, while the remaining coral species were hand-collected by divers from a nearshore reef in Broward County, FL within close proximity to the nursery. Colonies were returned to the laboratory and fragmented (2-3 cm branch tips for *A. cervicornis,* and 4 cm^2 fragments for all others) for use in the exposure system. Branching species were attached with a minimal amount of cyanoacrylate gel glue (The Original Super Glue Corporation) to individually numbered aragonite bases (2 cm diameter, 0.25 cm thickness), and all corals were acclimated to laboratory conditions in a 1100-L indoor recirculating seawater system for 2-4 wk prior to the exposures, as well as during the post-exposure period. The laboratory holding system was maintained at 35 PSU (using artificial seawater prepared with reverse osmosis water and TropicMarin sea salt) and 26ºC, with water motion supplied by dedicated powerheads and a wave maker. Artificial light was provided by LEDs (Radian XR30W G4 Pro) that were programmed to mimic sunrise and sunset (photoperiod 12:12) with a spectrum suited for coral growth. Ultraviolet radiation was removed from the LED spectrum to avoid phototransformation of test substances during the exposure period.

2.2.2 Experimental design

Experiments were conducted using a continuous flow recirculating passive dosing system which employs polydimethylsiloxane (PDMS) O-rings as a partition-controlled chemical reservoir system with 24 independent dosing chamber/vessel replicates (Figure 2.1) Each experiment included a 2 wk pre-exposure period to establish baseline coral health, a 48 h constant exposure, and a 4 wk post-exposure period to assess recovery potential. Six treatments were used, including a seawater control and 5 concentrations of TOL, 1MN, or PHE, with 4 replicate dosing systems per treatment. No O-ring or methanol (MeOH) controls were used as these treatments were previously demonstrated to have no significant effect (Renegar et al. 2017b). The seawater control was utilized to provide baseline performance in the absence of toxicant to ensure test conditions and organism health were maintained over 48 h.

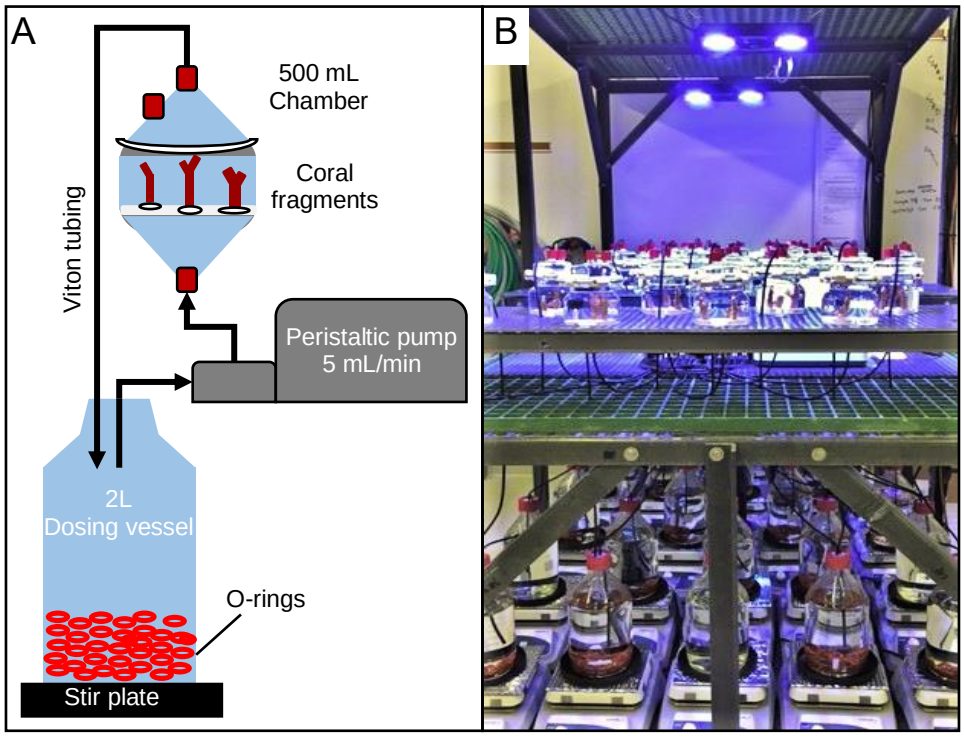

Figure 2.1 A) Schematic and B) Actual recirculating-flow exposure system. Exposure chambers were connected to a multi-channel peristaltic pump by Viton tubing (black arrows) with a flow rate of 5 mL/min. Each chamber was supplied by a separate 2-L dosing vessel containing variably loaded O-rings

Before the start of the exposure period, PDMS O-rings (O-Rings West, Part number: SF70 212 and 002, mean O-ring mass 1.06g) were cleaned by rinsing in ethyl acetate (Fisher Scientific) (24 h), methanol (Fisher Scientific) (3x in 24 h), and deionized water (3x in 24 h), then dried at 110°C for 1 h. Cleaned PDMS O-rings were loaded with each hydrocarbon in methanol. Stock solutions of TOL (Sigma Aldrich), 1MN (Acros Organics, 97%), or PHE (Sigma Aldrich) were prepared by dissolving known amounts of hydrocarbon in methanol using the equation:

$$C_{MeOH} = \left[K_{MeOH-PDMS} + \left[\frac{V_{PDMS,A}}{V_{MeOH}}\right]\right] * \left[K_{PDMS-Water} + \left[\frac{V_{Water}}{V_{PDMS,D}}\right]\right] * C_{Target}$$

where C_{MeOH} is the concentration of hydrocarbon added to methanol (mg/L); C_{target} is the target concentration in seawater (mg/L); V_{MeOH} is the volume of the methanol dosing solution (mL); $V_{PDMS,A}$ is the volume of PDMS O-ring acceptor in the methanol stock solution (mL); $V_{PDMS,D}$ is the volume of PDMS O-ring donor in the aqueous test media (mL); V_{water} is the volume of seawater in the recirculating flow-through system (mL); $K_{MeOH\text{-}PDMS}$ is the hydrocarbon's partition coefficient between methanol and PDMS; and $K_{PDMS\text{-}Water}$ is the hydrocarbon's partition coefficient between PDMS and water (Butler 2013). The partition coefficients, number of O-rings, volumes, and calculated depletion of hydrocarbon in MeOH loading solutions and PDMS reservoirs for each exposure are summarized in Table S2.1 with an example loading calculation and examples of depletion calculations available in Equation S2.1. The number of O-rings and volume of loading solutions were adjusted to limit depletion for each of the hydrocarbons in each phase.

Calculated amounts of hydrocarbon for each treatment level (Table S2.2) were added to 500- or 1000-mL volumetric flasks of MeOH and mixed on a magnetic stir plate at room temperature (24 °C) for 1-2 h until dissolved. PDMS O-rings were added to vessels containing MeOH stock solutions and placed on an orbital shaker for 72 h to allow partitioning of hydrocarbon into the PDMS O-rings (Butler et al. 2013, Turner 2016). In order to produce variable treatment concentrations across replicates, loaded O-rings were transferred to randomly assigned dosing systems filled with seawater from the laboratory holding system after being filtered to 1 µm (Polymicro) and UV sterilized. The dosing system, when full, contained less than 10% headspace to limit volatile loss of contaminant from the dissolved phase. Dosing vessels were stirred vigorously throughout the 20-h equilibration period to ensure targeted concentrations were

reached. Following the equilibration period, randomly assigned corals were added to each chamber (N=3), and the test initiated. Corals were not fed, and lighting was provided as described above. Along with monitoring the coral fragments, equipment was monitored for continuous operation throughout the duration of exposure.

Following the 48-h exposures, one coral from each chamber was immediately preserved for gene expression analysis (Chapter 4), while the remaining coral fragments were transferred back to the acclimation system and immediately analyzed for photosynthetic efficiency and growth. After these measurements, one coral from each chamber was fixed for histological analysis of cellular and tissue changes, which is assessed elsewhere and not within this dissertation. In order to assess the potential for recovery after hydrocarbon exposure, remaining corals were held over a 4-wk post-exposure recovery period during which the coral fragments were maintained under the same conditions as described for pre-exposure. Recovery was assessed by monitoring the condition of each coral using the same health endpoints evaluated following 48 h test substance exposure. At the end of the recovery period, all remaining corals were fixed for histological analysis.

2.2.3 Hydrocarbon Chemistry

Chemical analysis was performed to verify the stability of the concentration throughout the exposure. Samples were collected at the beginning (0 h, immediately prior to addition of coral fragments), and end (48 h) of the exposure for 1-methylnaphthalene and phenanthrene, and also at 24 h exposure to toluene. Water samples for 1MN and PHE were collected from the effluent line of each chamber in 20 mL volatile organic analyte vials (Thermo Scientific) with Teflon-lined caps and preserved at 4°C until quantification. Water samples for toluene analysis were collected in 40 ml certified volatile organic analyte vials (Thermo Scientific) with no headspace, and acidified with 70µL of 6M hydrochloric acid (HCl) before analysis by AEL Laboratory using EPA Method 8260 for VOCs by GC/MS (Shimadzu QP2010SE with EST Purge & Trap).

Sample analysis of 1-methylnaphthalene and phenanthrene was completed by Florida International University using fluorometry (Horiba Aqualog Spectrofluorometer). Briefly, certified standards of 1-methylnaphthalene or phenanthrene were obtained from Ark Pharm (Libertyville, IL, USA). Stock solutions were prepared with dichloromethane analytical grade quality (Burdick and Jackson, Fisher Scientific, Fairlawn, NJ, USA) and stored at -20 °C. Working solutions were further diluted in ultrapure water (18.2 MΩ cm-1) obtained by a

Nanopure Infinity Ultrapure Water system or HPLC grade water from Fisher Scientific. Samples were preserved at 4°C and allowed to reach room temperature before analysis. A calibration curve was produced in artificial saltwater (35 PSU). A six-point calibration curve based on the fluorescence intensity value was established to create a linear regression plot. The criterion for acceptance is that the calibration relationship must have an r2>0.990. As a quality control procedure, blanks were run to determine that no emission was observed at the wavelengths (excitation and emission) used for 1-methylnaphthalene or phenanthrene. Also, a calibration standard at 0.5 ppm was analyzed at the end of each analytical batch to assess deviations from the initial calibration; calibration verifications were all within the method criteria outlined by the analyzing laboratory.

2.2.4 Assessment Endpoints

Metrics used to evaluate the effects of each compound were chosen based on previous work. The following metrics will aid in understanding the full effect of the chemical on each of the coral species.

Coral condition and mortality

Coral condition was visually assessed using a semi-quantitative four-level scoring system, with zero being within normal limits, and three being severely affected. This scoring system was adapted from a histologically verified stress index developed for real-time coral health assessment, and has been previously used for evaluation of hydrocarbon effects on another coral species (Renegar et al. 2015, Renegar et al. 2017b). Changes in coloration, polyp extension/retraction, tissue swelling, tissue attenuation, and mucus production were considered with a precision level of 0.5 (Table S2.3). The individual scores for each criterion were summed and divided by the total maximum score possible to obtain a single percent effect at each time point, for each coral fragment. The maximum score for an individual coral is 12, which is the sum of 5 categories scored from 0-3. This is because tissue swelling and tissue attenuation are scored as one category, whereas the total of the two categories can never exceed a maximum of 3. A coral that scores greater than 1.5 for tissue swelling cannot score greater than 1.5 for tissue attenuation, as the two criteria are opposite responses to stress (attenuation of 3 results in swelling of 0, as there is no tissue left to swell). The maximum score possible using this system is 12, and percent effect was determined using this maximum score. Coral condition was assessed weekly during the pre-exposure and post-exposure periods. During the exposure, coral

condition was assessed hourly for the first 8 h after exposure initiation, and every 12 h thereafter for the remainder of the 48-h exposure. At each time point measured, the percent effect of each replicate fragment was averaged to determine a single percent effect for each chamber.

Percent mortality was also visually assessed, consistent with established methods of tissue mortality determination in corals (Lirman et al. 2013). Coral mortality was identified by severe tissue attenuation to the point of skeletal element exposure, or through sloughing of tissue after large amounts of swelling and mucus release. Initially, mortality was recorded at 24 and 48 h, but without the ability to open the chambers, could not be confirmed until the end of the exposure (48 h). Partial coral fragment mortality also occurred in some species and was visually assigned a percent mortality score at 10% intervals. The percent mortality scores for the three replicate fragments were averaged to provide a chamber percent mortality, whereas the number of dead fragments (not always a whole number) was normalized to the number of total fragments in each chamber. The relationship between coral mortality and measured treatment concentration formed the basis for LC50 determination.

Photosynthetic efficiency

A pulse-amplitude-modulation (PAM) fluorometer (Diving-PAM, Walz, Germany) was utilized as an indicator of the physiological status of the autotrophic endosymbiotic zooxanthellae prior to the exposure, immediately after the exposure period, and for the remainder of the post-exposure period. PAM fluorometry measures the light-adapted effective quantum yield [$(F_m–F_o)/F_m$ or $\Delta F/F_m$] of the autotrophic endosymbiotic zooxanthellae by applying a saturation pulse of light and determining yield from the ratio of initial fluorescence (F_o) to maximum fluorescence (F_m). The measuring parameters on the Diving-PAM (gain, measuring light and saturation pulse intensity, and saturation width) were adjusted to best suit each coral species (Table S2.4). Light programs were paused at an intensity and spectrum equivalent to 30 minutes post-sunrise for the duration of each set of measurements to ensure differences in photosynthetic efficiency are not due to changes in light over the 2-3 h measurement period. Measurements were taken from every 90 deg around the circumference of the branch tip for branching species, and one in each quadrant for massive corals (n=4 for all corals), to represent the whole coral fragment. Using measurements taken twice during pre-exposure holding, immediately before and after each exposure, and after one week and one-month recovery, the

change in yield was determined for four time periods: baseline, 48 h exposure, 7 days post-exposure recovery, and 28 days post-exposure recovery.

Growth

Calcification of the coral fragments was evaluated using buoyant wet weight (Davies 1989). Buoyant weight determination is a non-destructive method of measuring growth rates for corals over short time intervals, which removes variability between fragments resulting from tissue thickness and provides weights explicitly related to the mass of the skeleton. Measurements were made one week-, and immediately prior to the exposure to determine a baseline growth rate. Immediately following the exposure, after one week of recovery, and at the end of four weeks of recovery, measurements were also made. Growth rates are expressed as mg gained or lost per day between these measurements, and the change in growth rates (mg/d) was determined for each of the time periods to provide the basis for determining the growth rate inhibition following exposure to each compound.

2.2.5 Statistical analysis

Data were tested for normality (Shapiro-Wilk) and homoscedasticity (Levene's), transformed to satisfy parametric assumptions, or nonparametric methods were used. Parametric (ANOVA) or nonparametric (Kruskal-Wallis) analysis of variance were used to determine the effects of the treatment groups on each measured parameter at each time point. Tukey's Unequal N HSD (parametric) or Conover's pairwise test for multiple comparisons (nonparametric) were used for post-hoc analysis when treatment effects were identified. All statistical tests were performed using R statistical software (V3.6.1) with significance determined using an alpha of 0.05. To determine the presence of treatment effects on each parameter, a mean hydrocarbon concentration for each treatment was determined using the geometric means of the four replicate chamber concentrations. These treatment levels are from here on referred to as the TOL dose, 1MN dose, and PHE dose.

Effect concentrations were determined with the *drc* package in R, and were based on subacute (coral condition, photosynthetic efficiency, growth rate, and gene expression) and acute (mortality) effects at the end of the exposure period (Ritz et al. 2015). The *drm* (dose response model) used to determine single compound effects in each test utilized the measured hydrocarbon concentrations and percent effect in each chamber to determine the endpoints for each coral species and test substance. Effects associated with each chamber replicate were individually modeled to

ensure variability of each response was captured. The log-logistic 4-parameter *drm* was used to determine the 50% effect concentrations (EC50), with maximum effect level fixed at 100%, as the scores were a proportion of the total effect possible. In order to estimate inhibition, the relative change in quantum yield or growth rate from before and after each exposure was calculated. If the *drm* for that relationship was significant, it was used to estimate the 50% inhibition concentrations (IC50) using the log-logistic 4-parameter model, but maximum effects were not fixed. The log-logistic 2-parameter *drm* was used to determine the 50% lethal concentrations (LC50), which uses a binomial logistic distribution to assess proportions. These models use self-starting functions that initially estimate the model parameters using the maximum likelihood principle. Estimates of all effect concentrations were made with the effect dose (ED) function, which utilizes the delta method to estimate 95% confidence intervals. Effect concentrations (EC50 and LC50) were input into the TLM equation to calculate CTLBBs (McGrath et al. 2018).

2.2.6 Water Quality

Samples for basic water quality were collected at the start and end of the exposure. Nutrients [ammonia (NH_3), nitrite (NO_2), nitrate (NO_3), phosphate (PO_4)] were measured with a HACH DR850 colorimeter; pH, dissolved oxygen (DO) and temperature were measured with a YSI 556 Multiprobe System; and alkalinity was determined by potentiometric titration with a Mettler-Toledo DL22 autotitrator.

2.3 RESULTS

The results of all exposures are summarized and available in the GRIIDC data repository under the CTOX project. The dataset identifiers for each exposure are listed at the end of this chapter in section 2.6- Single Compound Data Availability. These files contain all coral condition scores for all time points measured, as well as the individual growth and yield measurements and mortality. The water quality measurements for each exposure are also found in the repository files, and are summarized below.

2.3.1 Water Quality

Water quality measurements were made on each individual chamber of all exposures completed. In the 14 experiments described here, there were no significant differences in temperature between any of the doses at any time ($p>0.05$). Significant differences in nutrient concentrations (PO_4, NH_3, NO_2, and NO_3) were not generally present, except in few cases where

high levels of exposure resulted in necrosis. These differences are highlighted below, with implications for their significant contribution to the observed toxicity included in the discussion.

Exposure to TOL produced significantly elevated nutrient levels in four of the five completed tests, driven primarily by increases in NO2 concentration. The top four doses to *A. cervicornis* and *P. astreoides,* and the top three doses to *S. intersepta*, resulted in significantly increased NO_2 concentrations compared to controls. Toluene also resulted in increases in NH_3 in the *A. cervicornis* 72.7 mg/L and *P. astreoides* 114.2 mg/L doses. The *P. astreoides* exposure resulted in increased PO_4 levels in the two highest doses of TOL, while exposure to *S. siderea* resulted in significantly increased levels of PO_4, NO_3, and NO_2 in the highest dose tested compared to controls. Following exposure to 1MN, significantly elevated levels of NH_3 and PO_4 were only observed in the highest dose of the *A. cervicornis* exposure, while NO_2 was significantly elevated in the top four doses. In addition, NO_3 was significantly higher in the top two doses of the *A. cervicornis* exposure, and the highest dose in the *S. siderea* exposure. There were no significant differences in any nutrient concentration following exposure to PHE.

Dissolved oxygen showed significant reductions compared to controls and/or low doses following exposure to all three compounds tested. Significant reductions in DO were observed after TOL exposure in the top four *A. cervicornis, S. siderea,* and *S. bournoni* doses, top two *S. intersepta* doses, and all *P. astreoides* doses compared to controls. The three highest doses of 1MN to *A. cervicornis, P. astreoides,* and *S. intersepta,* four highest doses of 1MN to *S. siderea,* and all 1MN doses to *S. bournoni*, had significant reductions in DO compared to controls ($p<0.05$). Phenanthrene exposure resulted in less of a reduction in DO, with significant declines in the highest dose of *P. astreoides* and the three highest doses of *S. intersepta*.

Significant decreases ($p<0.05$) in pH were also observed following 1MN and PHE. Compared to controls, significantly reduced pH was observed following 1MN exposure in the two highest *A. cervicornis* and the three highest *P. astreoides* doses. The three highest, and 804 µg/L *S. intersepta* doses, as well as the high *S. bournoni* dose also had significantly lower pH following 1MN exposure. Reductions in pH were also observed following exposure to PHE, whereas all doses to *A. cervicornis* except the controls, and the highest *S. intersepta* dose had significantly lower pH compared to controls. Exposure to TOL produced a slightly different pattern of pH reduction compared to 1MN and PHE. Following TOL exposure, pH was significantly reduced in *A. cervicornis* doses of 55.9 mg/L, 72.2 mg/L, and 97.1 mg/L compared

to controls, but not in the highest treatment tested (155.0 mg/L). Additionally, mid-level TOL doses in the *P. astreoides* (81 mg/L) and *S. siderea* (66.3 mg/L) exposures showed reduced pH, as well as the top three and four doses of *S. intersepta and S. bournoni,* respectively.

Alkalinity was generally found to be significantly higher ($p<0.05$) in the high doses of all three compounds tested compared to controls. Following TOL exposure, alkalinity was significantly higher in the top four doses of *A. cervicornis, P. astreoides,* and *S. siderea*, and the highest treatments of *S. intersepta* and *S. bournoni.* Alkalinity was also significantly elevated in the highest dose of 1MN to *A. cervicornis,* and the top two and three highest doses to *P. astreoides,* and *S. siderea,* respectively. Exposure to PHE resulted in less significant differences, with only the highest dose of both *P. astreoides* and *S. siderea* having significantly elevated alkalinity compared to controls.

2.3.1 Toluene

Chemistry

The measured concentration of TOL in each chamber at T0 and T48 for all tests is provided in Appendix 1 (Tables S2.5- S2.9). In each exposure, the concentration of TOL was stable over time, with average chamber coefficients of variation (CVs) of 14.2% (*A. cervicornis)*, 11.7% (*P. astreoides)*, 10.3% (*S. siderea)*, 6.7% (*S. intersepta)*, and 8.4% (*S. bournoni)*. The average TOL concentrations in the replicate chambers of each treatment group were averaged to determine a mean TOL dose that was used to identify treatment effects. The mean TOL doses for all treatments are listed in Table 2.1, and exhibited CVs of 6.3% (*A. cervicornis)*, 11.7 % (*P. astreoides)*, 4.5% (*S. siderea)*, 3.4% (*S. intersepta)*, 4.3% (*S. bournoni)*, indicating consistency in aqueous concentrations between treatment replicates for all species tested. Figure 2.2 shows the consistency in the mean aqueous concentrations for each TOL dose over time for all species tested (Panels A-E). Toluene is a mono-aromatic, volatile compound, and passive dosing resulted in stable concentrations over time, with TOL concentrations increasing slightly in most treatments between 0–48 h of exposure.

Table 2.1 Mean measured concentration of TOL in each dose for all species tested

		Mean TOL Concentration[a]				
Species	Control	25 mg/L	75 mg/L	100 mg/L	145 mg/L	225 mg/L
Acropora cervicornis	<MDL[b]	19.2 (±2.2)	55.9 (±1.7)	72.7 (±3.0)	97.1 (±2.2)	155.0 (±16.2)
Porites astreoides	<MDL	16.9 (±1.5)	69.0 (±3.6)	80.9 (±1.0)	114.2 (±3.8)	175.8 (±3.6)
Siderastrea siderea	<MDL	19.2 (±1.5)	66.3 (±2.8)	88.7 (±3.6)	124.5 (±2.1)	184.0 (±8.1)
Stephanocoenia intersepta	<MDL	25.9 (±0.5)	79.4 (±4.0)	97.2 (±1.9)	136.0 (±6.3)	NA
Solenastrea bournoni	<MDL	23.7 (±0.5)	67.5 (±2.0)	78.1 (±8.3)	124.7 (±3.7)	196.4 (±5.4)

[a] mg/L (± standard error)
[b]minimum detection limit

Coral condition

Coral condition was scored throughout all TOL exposures using criteria previously outlined. The effect of TOL dose on the overall coral condition of all species resulted in consistent and statistically significant effects from one hour, through the completion of the 48-h exposure (Figure 2.3). The individual scores for each coral or chamber are available in the GRIIDC data repository.

Acropora cervicornis. Figure 2.3.A shows the mean coral condition scores for all doses of TOL to *A. cervicornis.* The coral condition scores of the 19.2 mg/L lowest dose were significantly higher than controls from 4–48 h of exposure. All other higher doses scored significantly higher than controls after just 1 h of exposure.

Porites astreoides. The effects of TOL on the coral condition of *P. astreoides* are found in Figure 2.3.B. The lowest dose, 16.9 mg/L, scored similar to controls until 12 h exposure, when it scored significantly higher for the first time. All other doses scored significantly higher than controls after 1 h exposure, through 48 h.

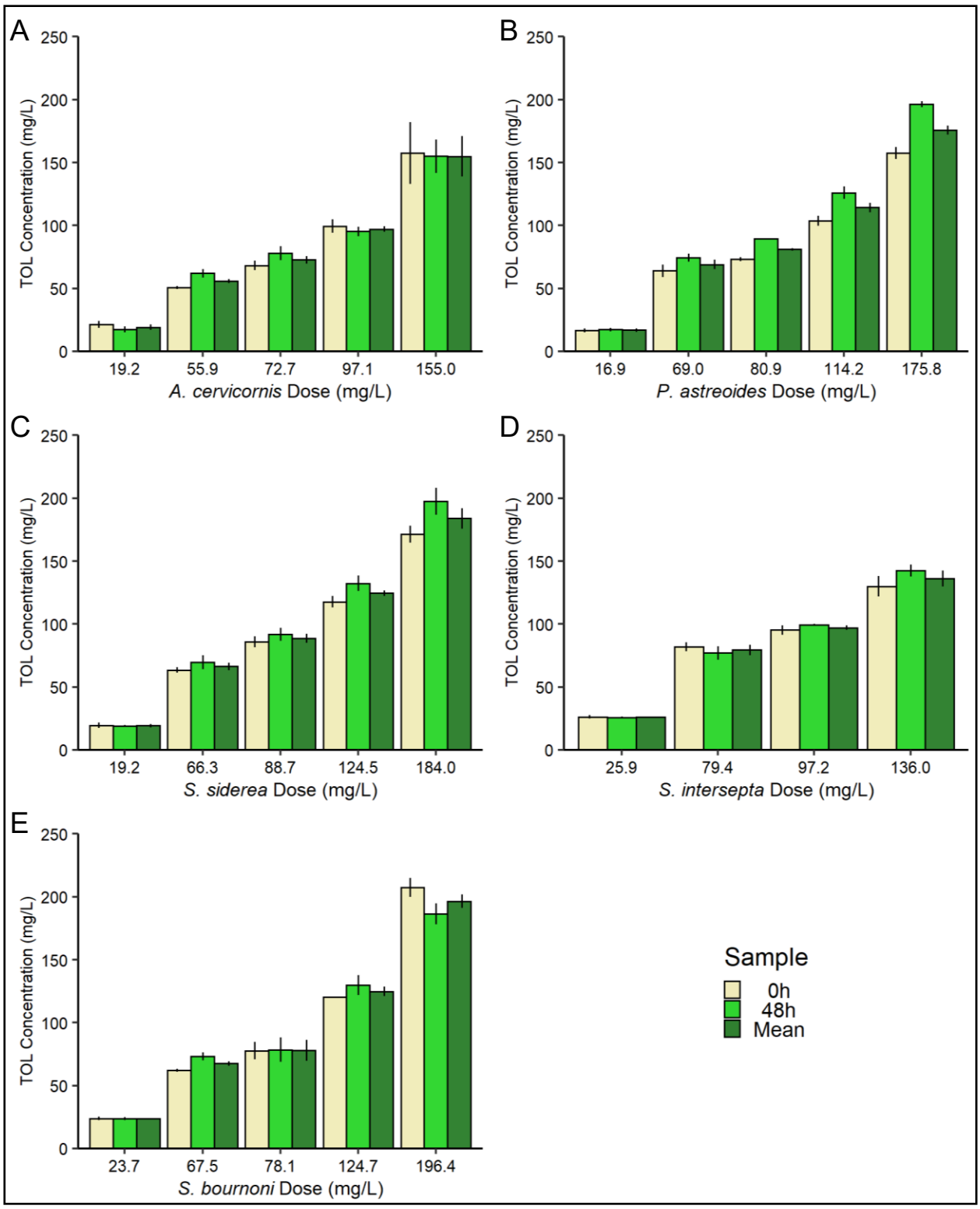

Figure 2.2 Mean measured concentration of TOL in each dose for all species tested. Error bars = standard error, n=4

Siderastrea siderea. The coral condition (Figure 2.3.C) showed a similar pattern as previous corals described, with significantly effects at all time points, mainly due to differences in the top four doses. The lowest TOL dose was significantly different from control corals from 4 h to 8 h exposure, and again at 48 h. All other doses scored significantly higher than controls at all time points through 48 h.

Stephanocoenia intersepta. The coral condition scores for the lowest dose of TOL to *S. intersepta* (Figure 2.3.D) became significantly different from controls from 6 h to 8 h exposure, then again at 48 h. Coral condition scores of all other doses remained significantly elevated compared to controls throughout the 48 h exposure.

Solenastrea bournoni. The coral condition scores of *S. bournoni* following TOL exposure are shown in Figure 2.3.E. The lowest dose, 23.7 mg/L, scored significantly higher than controls at 2 and 3 h of exposure, but scored similar for all other time points. From 5 h through 48 h of exposure, the 67.5 mg/L, and higher doses, scored significantly higher than controls.

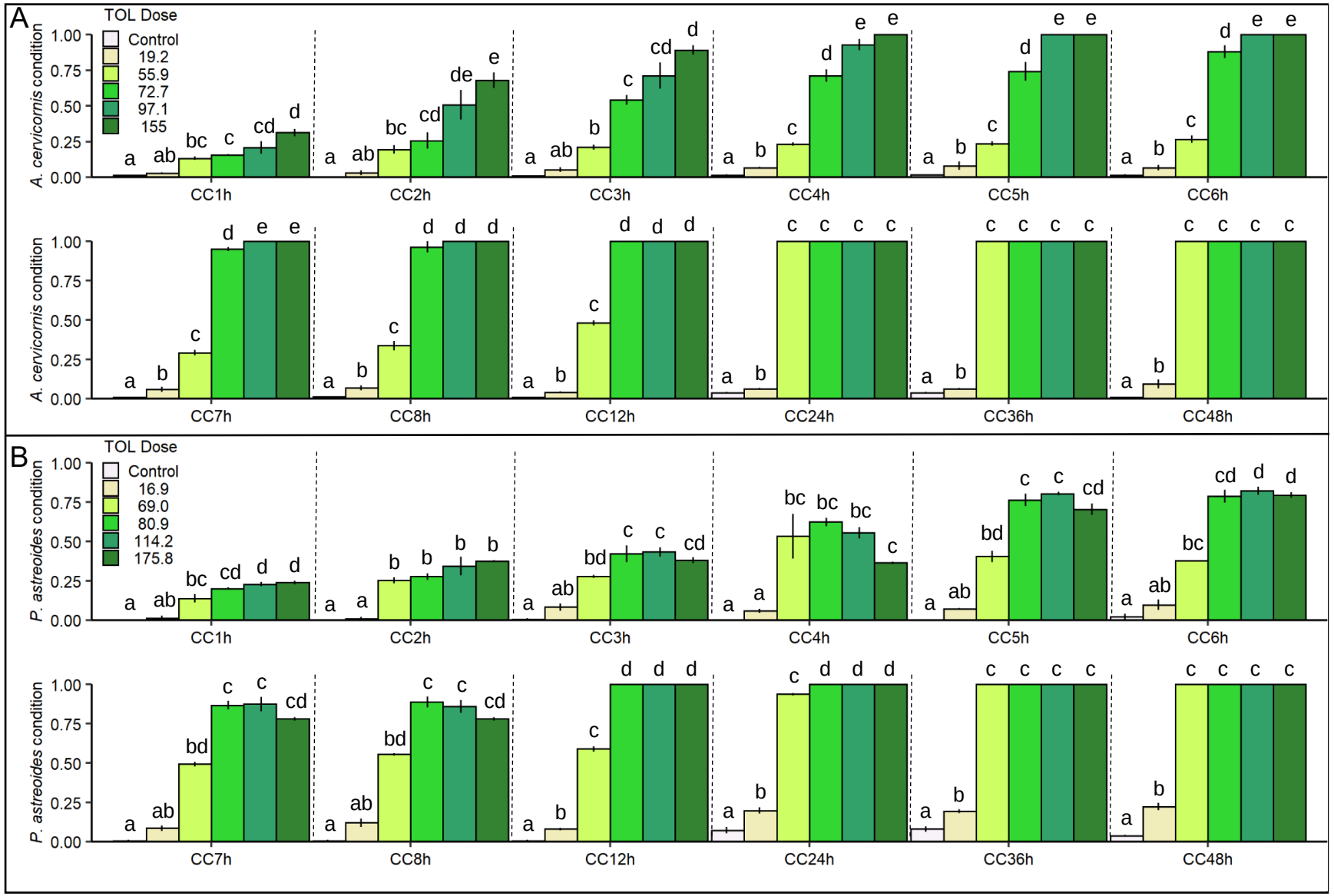

Figure 2.3 Coral condition scores for A) *A. cervicornis*, B) *P. astreoides*, C) *S. siderea*, D) *S. intersepta*, and E) *S. bournoni* following exposure to TOL. Letters above bars represent statistically similar groups, error bars= standard error

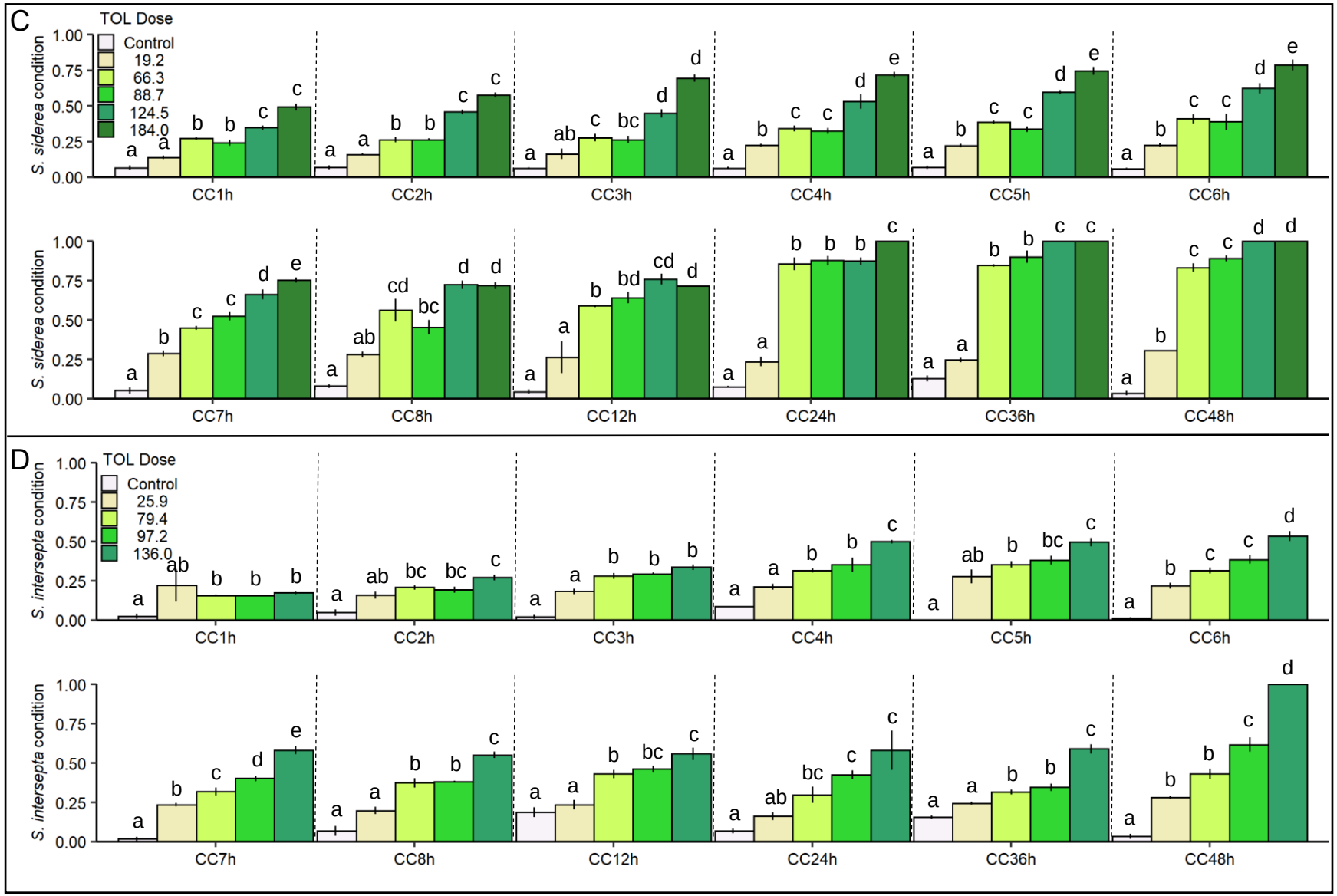

Figure 2.3 (cont'd). Coral condition scores for A) *A. cervicornis*, B) *P. astreoides*, C) *S. siderea*, D) *S. intersepta*, and E) *S. bournoni* following exposure to TOL. Letters above bars represent statistically similar groups, error bars= standard error

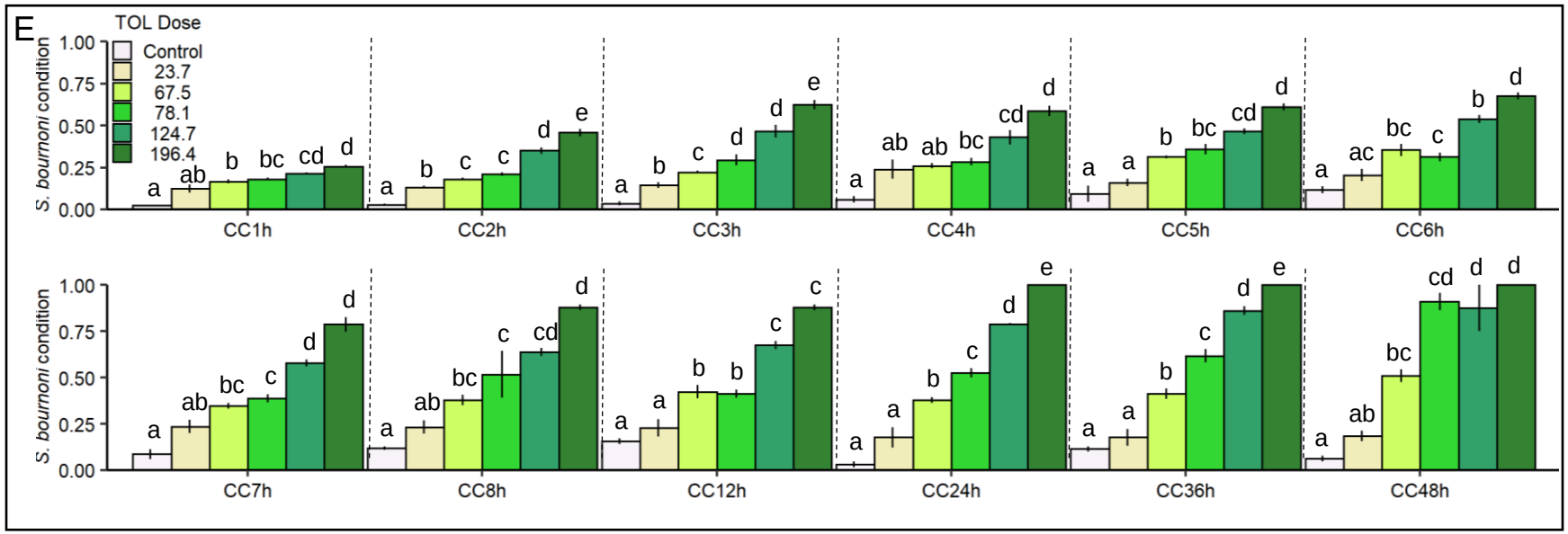

Figure 2.3 (cont'd). Coral condition scores for A) *A. cervicornis*, B) *P. astreoides*, C) *S. siderea*, D) *S. intersepta*, and E) *S. bournoni* following exposure to TOL. Letters above bars represent statistically similar groups, error bars= standard error

Photosynthetic efficiency

Photosynthetic efficiency was determined for each coral by measuring the effective quantum yield (Fm-Fo/Fm) for each coral. The mean quantum yield was determined for each TOL dose, at designated intervals as shown in Figure 2.4 and was compared between surviving doses at each time interval, for each of the species tested. There were no significant differences in quantum yield across any dose of the *A. cervicornis* exposure for all time periods (Figure 2.4.A). Figure 2.4.B shows the quantum yield for *P. astreoides* for all time points, with a significant decline evident in the 69.0 mg/L dose following the exposure. This was based off a single fragment that was considered 100% dead shortly after obtaining this poor-quality reading (low Fo) immediately after the exposure. By 7 days of post-exposure recovery, there were no longer significant differences between TOL doses, as the yield of the 16.9 mg/L corals remained similar to controls and no other treatments were alive. Significant declines in quantum yield from TOL exposure were also observable for *S. siderea, S. intersepta*, and *S. bournoni* (Figure 2.4. C, D, and E, respectively). The *S. siderea* 66.3 mg/L dose had a significantly reduced yield compared to controls, while the yields of the surviving higher doses were unreadable due to low initial fluorescence signals, presumably due to bleaching. Toluene exposure to *S. intersepta* significantly reduced quantum yield in the 79.4 mg/L and 97.2 mg/L doses compared to controls. The 67.5 and 78.1 mg/L TOL doses of the *S. bournoni* exposure also produced significantly lower quantum yields compared to controls. Following 7 d of post-exposure recovery, no significant differences in quantum yield between TOL doses were observable for any species tested, which was maintained through 28 d of recovery.

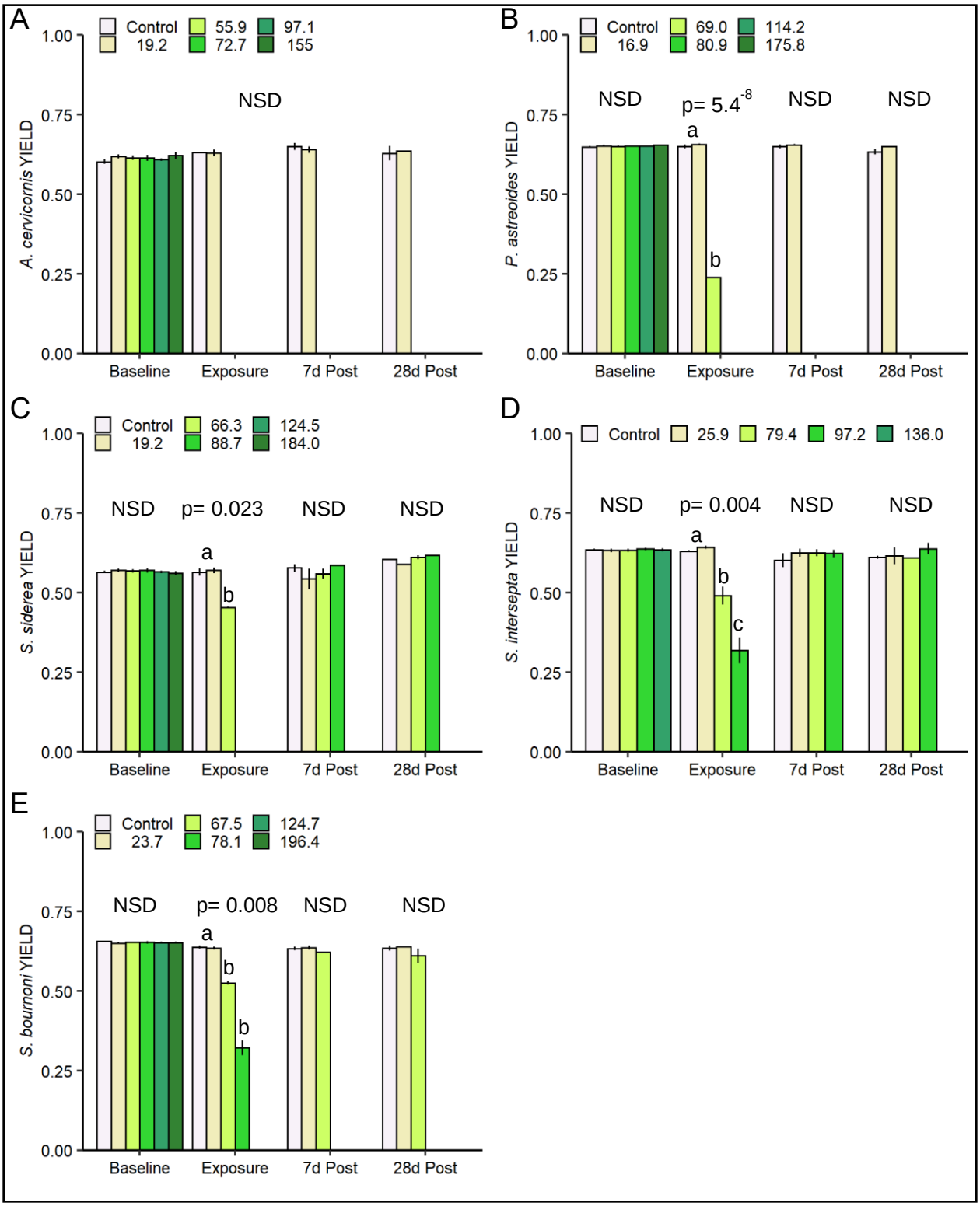

Figure 2.4 Mean Quantum Yield for A) *A. cervicornis*, B) *P. astreoides*, C) *S. siderea*, D) *S. intersepta*, and E) *S. bournoni* for the indicated time periods. Letters above bars represent statistically similar groups, error bars= standard error, NSD= no significant differences (p>0.05)

Growth

Mean growth rates, expressed as mass gain per day for the number of days in the observation period (mg/day), for each TOL dose during each exposure period are shown in Figure 2.5 Exposure of TOL to *A. cervicornis* (Fig. 2.5.A), *P. astreoides* (Fig. 2.5.B), *S. siderea* (Fig. 2.5.C), and *S. bournoni* (Fig. 2.5.E) resulted in no significant differences in growth rate across all doses and time periods. However, the growth rate of the 97.2 mg/L dose of the *S. intersepta* exposure was significantly reduced compared to the 25.9 mg/L dose following exposure, but was not significantly different than controls (Fig. 2.5.D).

Mortality

Each coral fragment was visually assessed for the presence of lesions, and a percent mortality was assigned. The mean mortality percentages for each dose of all TOL exposures are shown in Figure 2.6 and Table S.2.10. There was high mortality across many of the TOL doses at 48 h, and overall, TOL produced statistically significant levels of mortality in all exposures. Four of the six TOL doses in both *A. cervicornis* and *P. astreoides* exposures resulted in 100% mortality after 48 h, with the high doses confirmed dead after 24 h. Exposure to *S. siderea* resulted in total mortality in the two highest doses, while TOL doses of 66.3 mg/L and 88.7 mg/L resulted in 41.7% and 85% mortality, respectively. The *S. bournoni* exposure resulted in 100% mortality in the two highest doses, and 99% in the 78.1 mg/L TOL dose. There was 6.3% mortality in the 67.5 mg/L dose, slightly less than *S. siderea* at a similar level. There was 100% survival in the controls and the lowest doses of TOL for each of these coral species. The *S. intersepta* exposure had comparatively more survival, with TOL doses as high as 97.2 mg/L resulting in 100% survival and only the highest TOL dose (136.0 mg/L) resulted in 100% mortality.

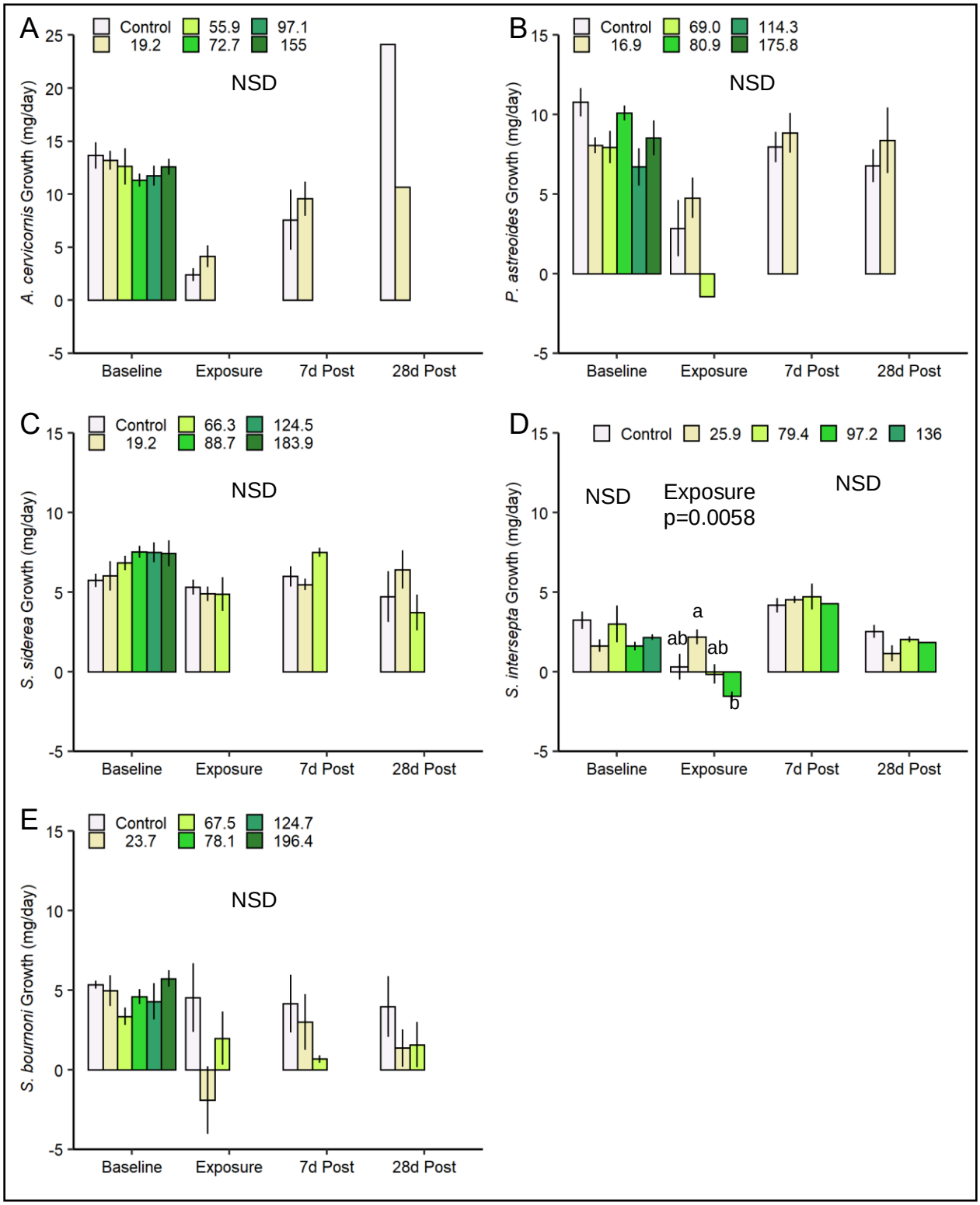

Figure 2.5 Mean growth rate for A) *A. cervicornis*, B) *P. astreoides*, C) *S. siderea*, D) *S. intersepta*, and E) *S. bournoni* for the indicated time periods. Letters above bars represent statistically similar groups, error bars= standard error, NSD= no significant differences (p>0.05)

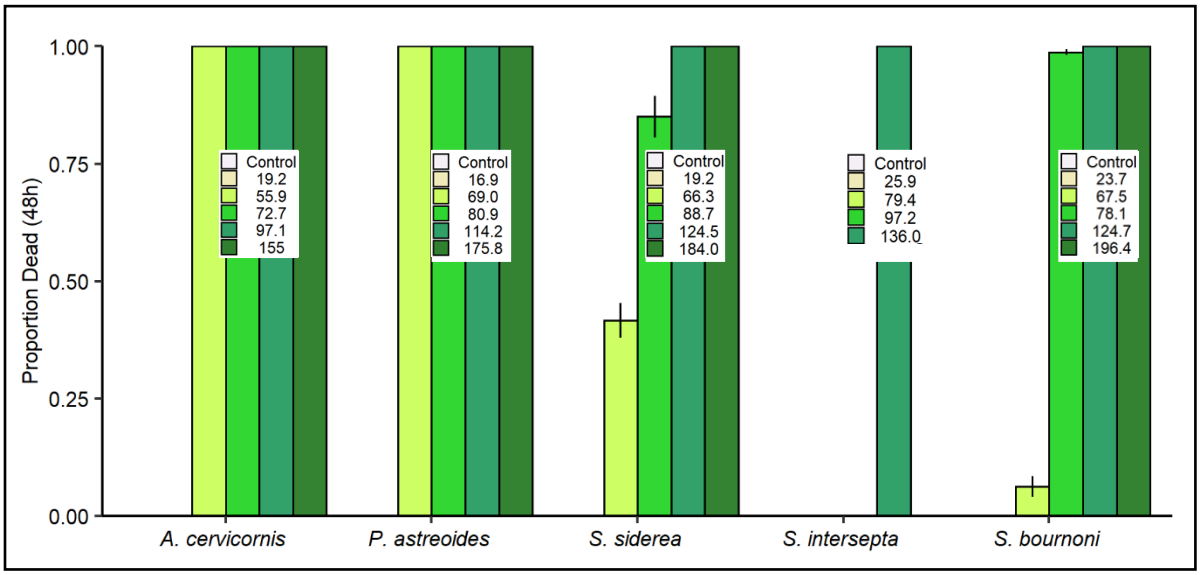

Figure 2.6 Proportion of coral dead after 48 h exposure to TOL for all coral species tested. Individual legends include the TOL dose group (mg/L) for each coral exposure.

2.3.2 1-Methylnaphthalene

Chemistry

Overall, measured concentrations were lower than the target, but maintained similar levels amongst each dose, and across tests completed. The exception to this is the *P. astreoides* exposure, which was due to incorrectly loading the o-rings with double the amount of 1MN (Table S2.2).The individual chamber concentrations at T0 and T48 h are available in the SI (Tables S.2.11-15), and reveal a constant aqueous 1MN concentration throughout time in each chamber, resulting in an average CV of 7.4% (*A. cervicornis)*, 1.9% (*P. astreoides)*, 5.4% (*S. siderea)*, 5.1% (*S. intersepta)*, and 3.4% (*S. bournoni)* for each test. The average 1MN dose measured in each treatment for all species (Table 2.2) was used to calculate a CV of 1.7% (*A. cervicornis)*, 0.9% (*P. astreoides)*, 1.0% (*S. siderea)*, 0.8% (*S. intersepta)*, 0.7% (*S. bournoni).* This indicates high consistency in average aqueous concentrations amongst treatment replicates in all 1MN exposures (Figure 2.7).

Table 2.2 Mean 1MN concentration in each exposure treatment for all corals tested in this study

	1MN concentration[a]					
Species	Control	1000 µg/L	2000 µg/L	4000 µg/L	8000 µg/L	16000 µg/L
Acropora cervicornis	<MDL[b]	745 (±14)	1501 (±14)	2775 (±67)	5370 (±108)	9434 (±124)
Porites astreoides	<MDL	1522 (±20)	2868 (±26)	5236 (±8)	8293 (±113)	12530 (±108)
Siderastrea siderea	<MDL	828 (±7)	1614 (±18)	3030 (±22)	5876 (±97)	10332 (±68)
Stephanocoenia intersepta	<MDL	805 (±7)	1616 (±17)	2955 (±16)	5610 (±55)	9019 (±51)
Solenastrea bournoni	<MDL	788 (±4)	1719 (±15)	3081 (±14)	5712 (±69)	10293 (±59)

[a] µg/L (± standard error)
[b]minimum detection limit

Coral condition

The effects of 1MN on each coral species were scored as before and are summarized in Figure 2.8, and show consistent and significant effects of 1MN dose on all corals tested. The individual scores for each coral or chamber are available in the GRIIDC data repository.

Acropora cervicornis. After 1 h exposure, the coral condition of *A. cervicornis* (Figure 2.8.A) doses at and above 2775 ug/L 1MN were significantly higher than controls and remained so for the duration of the exposure. The 1501 µg/L dose exhibited significantly elevated scores compared to controls from 2–4 h, 6–7 h, and 24–36 h of exposure, but not at 48 h. The coral condition of the 745 µg/L dose remained statistically similar to controls throughout the 48-h exposure.

Porites astreoides. The effects of 1MN on *P. astreoides* are summarized in Figure 2.8.B, and show significant impacts to coral condition. After 1 h, 1MN doses 5236 µg/L and above, scored significantly higher than controls for the remainder of the exposure. The 2868 µg/L dose also scored significantly higher than controls after 1 h, but at 24, 36, and 48 h, elevated effects in the controls eliminated this significance. The coral condition of the 1522 µg/L dose did not score significantly different than controls at any time point.

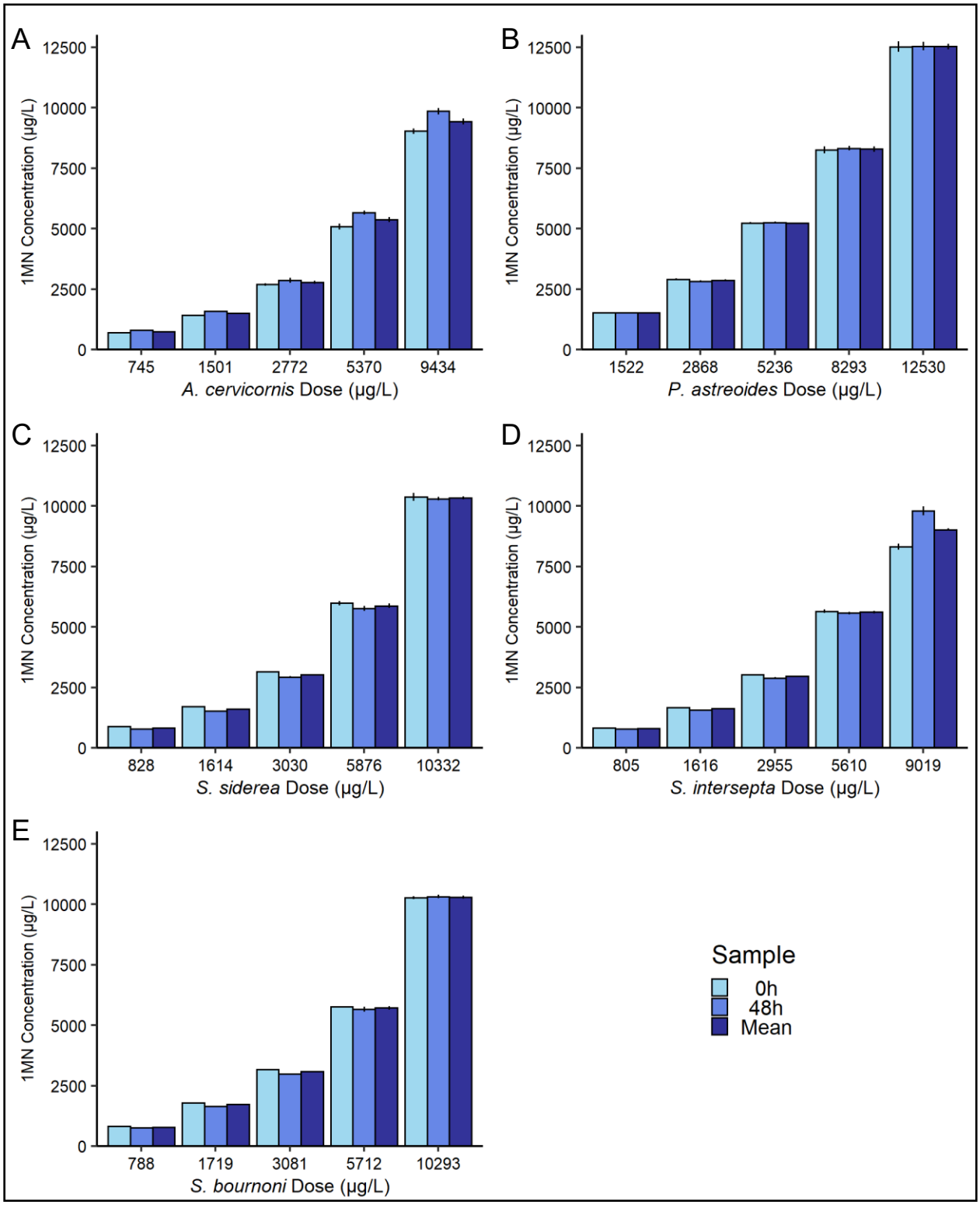

Figure 2.7 Measured concentration of 1MN in treatment group over time for all species tested. Error bars = standard error

Siderastrea siderea. The effects of 1MN on *S. siderea* coral condition are shown in Figure 2.8.C, and indicate significant differences in the highest dose (10332 µg/L) from 1–48 h exposure. Doses 3030 µg/L and 5876 µg/L scored significantly higher than controls from 2–3 h, and 1–3 h of exposure, respectively. Both doses also scored significantly higher than controls from 5–48 h of exposure to 1MN. The pattern observed for the 1614 µg/L dose was similar, with significantly elevated scores compared to controls from 2–3 h exposure, and again from 6–48 h. The coral condition of the lowest dose (828 µg/L) only scored higher than controls at 48 h of exposure.

Stephanocoenia intersepta. Significant impacts on coral condition of *S. intersepta* (Figure 2.8.D) were observed from 1–4 h exposure, and again from 24–48 h. The initial differences in coral condition from 1–4 h were from significantly elevated scores in the three highest 1MN doses, 2955 µg/L, 5610 µg/L, and 9019 µg/L. At 24 h and 36 h exposure, only the 9019 µg/L dose scored significantly higher than controls. After 48 h exposure to 1MN, the coral condition of all doses above 1616 µg/L scored significantly higher than controls

Solenastrea bournoni. The coral condition of *S. bournoni* (Figure 2.8.E) shows significant effects following exposure to 1MN after 1 h. The top three doses of 1MN all scored significantly higher than controls for the entire exposure. The 1719 µg/L dose initially scored higher than controls at 1 h, and again from 4–48 h of exposure to 1MN. The lowest dose (788 µg/L) scored significantly higher than controls for the first time at 36 h and 48 h.

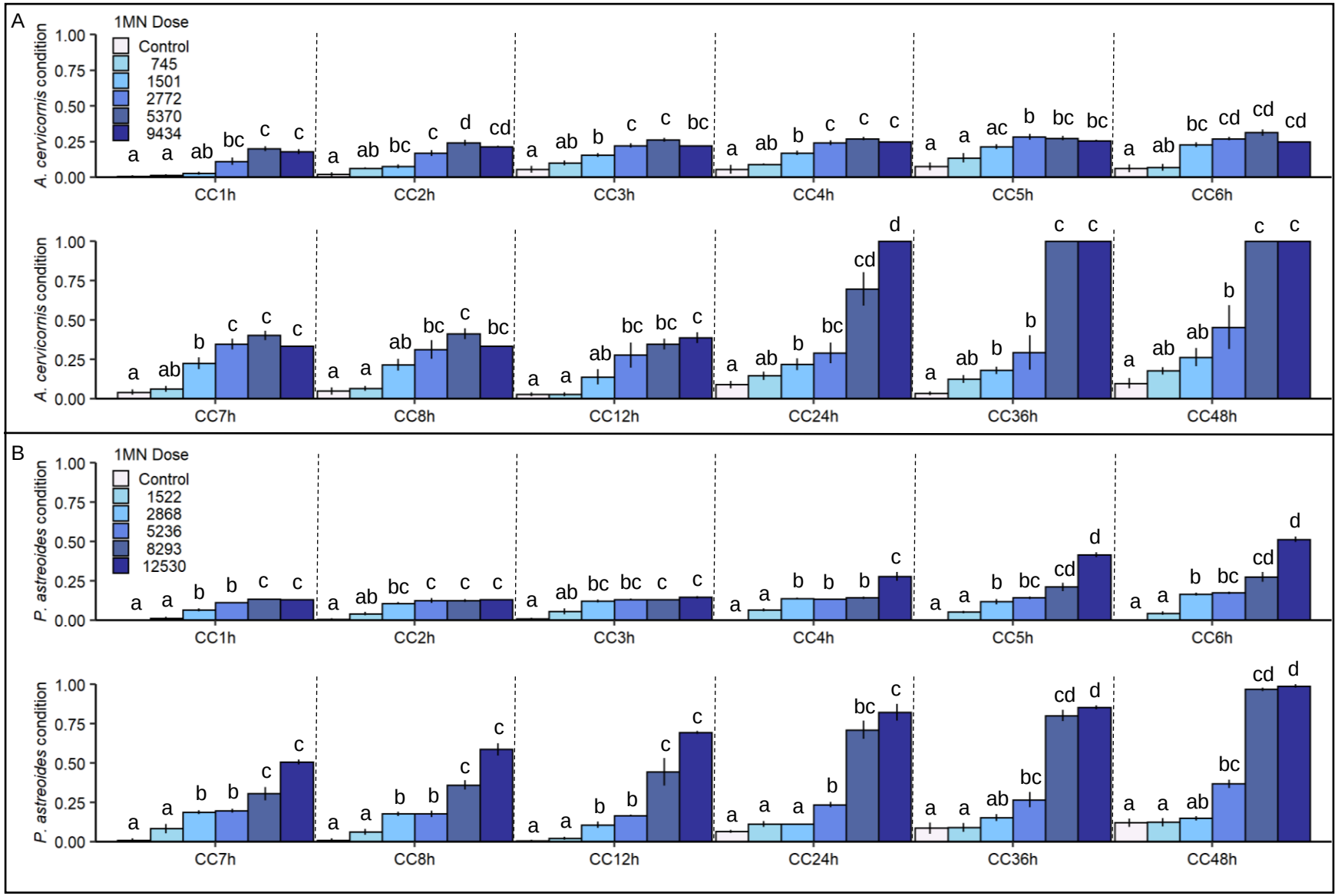

Figure 2.8 Coral condition scores for A) *A. cervicornis*, B) *P. astreoides*, C) *S. siderea*, D) *S. intersepta*, and D) *S. bournoni* following exposure to 1MN. Letters above bars represent statistically similar groups, error bars= standard error

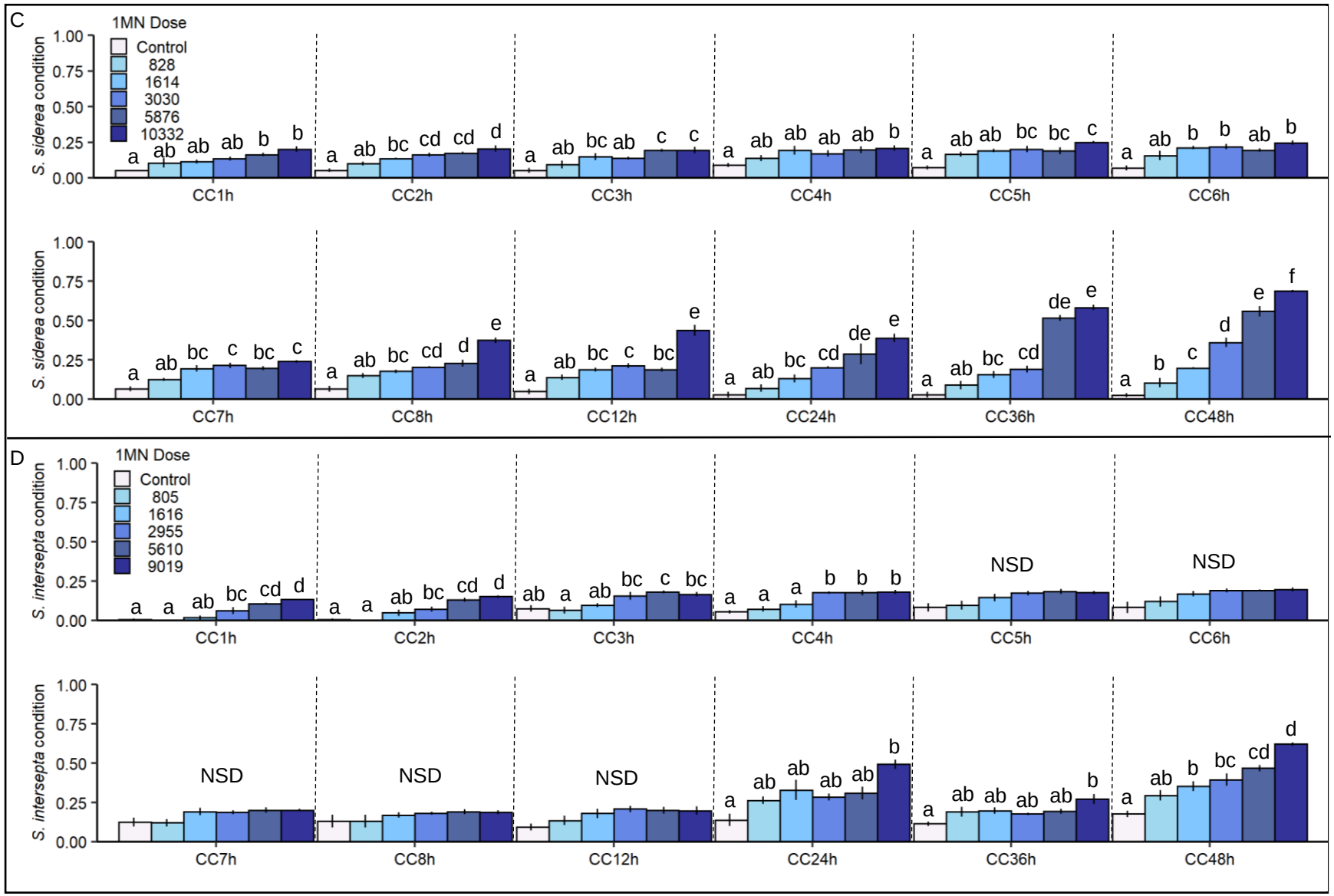

Figure 2.8 (cont'd). Coral condition scores for A) *A. cervicornis*, B) *P. astreoides*, C) *S. siderea*, D) *S. intersepta*, and D) *S. bournoni* following exposure to 1MN. Letters above bars represent statistically similar groups, error bars= standard error

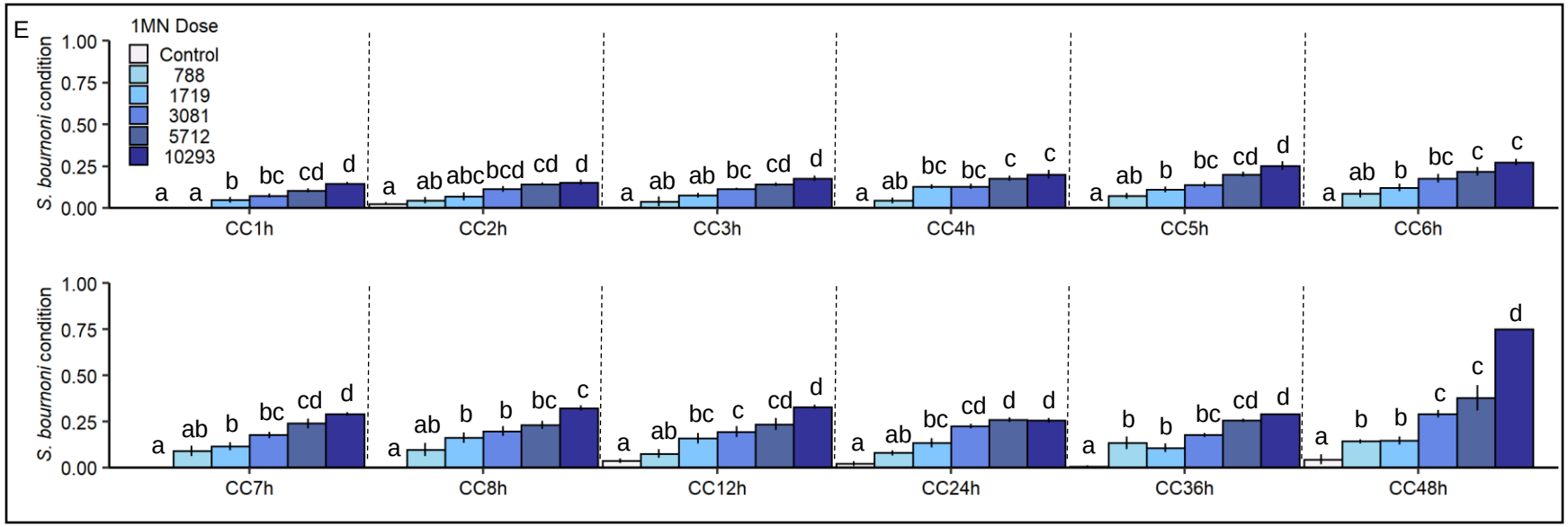

Figure 2.8 (cont'd). Coral condition scores for A) *A. cervicornis*, B) *P. astreoides*, C) *S. siderea*, D) *S. intersepta*, and D) *S. bournoni* following exposure to 1MN. Letters above bars represent statistically similar groups, error bars= standard error

Photosynthetic efficiency

The effects of 1MN on the photosynthetic efficiency of all corals tested are shown in Figure 2.9. Mean effective quantum yield was measured at four time periods, and significant differences were observed between surviving doses immediately following all five tests with 1MN. Quantum yield of the highest surviving dose of *A. cervicornis* (2775 µg/L 1MN) was significantly lower than controls and the other surviving doses (Fig 2.9.A). The 5236 µg/L and higher doses of the *P. astreoides* exposure (Fig. 2.9.B), and the doses 3030 µg/L and higher to *S. siderea* (Fig. 2.9.C) resulted in yields significantly lower than controls. The highest *S. intersepta* dose measured the only significantly lower quantum yield compared to controls (Fig. 2.9.D). Additionally, the 5610 µg/L dose had significantly lower yield compared to the 1616 µg/L and 2955 µg/L 1MN doses, but not controls. Exposure to 1MN also significantly reduced yield in the two highest *S. bournoni* doses compared to controls (Fig. 2.9.E). There were no significant differences in effective quantum yield between doses of any species after 7 or 28 d post-exposure recovery in clean seawater.

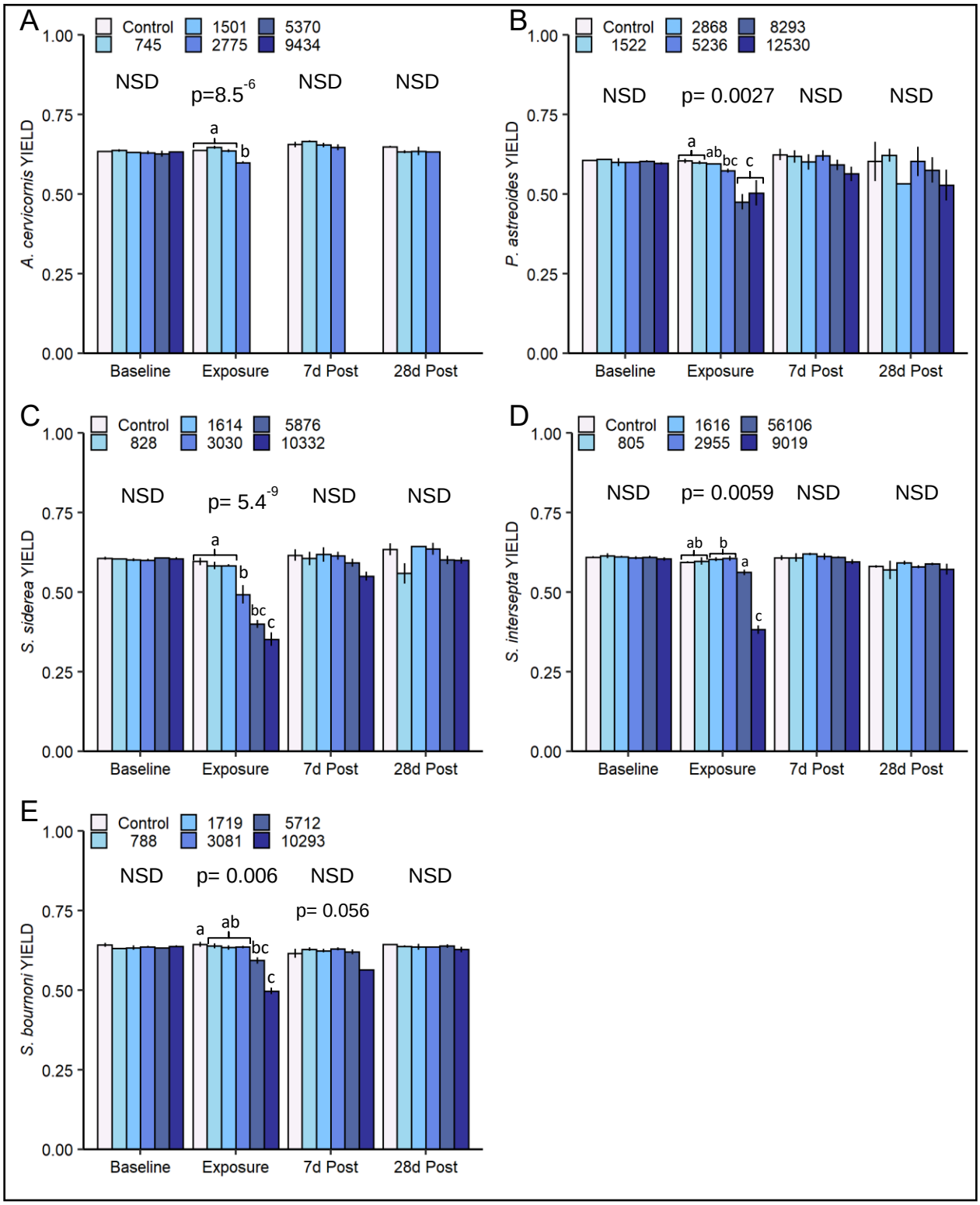

Figure 2.9 Mean Quantum Yield for A) *A. cervicornis*, B) *P. astreoides*, C) *S. siderea*, D) *S. intersepta*, and D) *S. bournoni* for the indicated time periods. Letters above bars represent statistically similar groups, error bars= standard error

Growth

The mean growth rate of each species during each exposure period are shown in Figure 2.10. Although some doses appear to have reduced growth rate, there were no significant differences during any period of the 1MN exposures to *A. cervicornis* (Fig. 2.10.A), *S. intersepta* (Fig. 2.10.D), and *S. bournoni* (Fig. 2.10.E). Following exposure to 1MN, there were significant differences in the growth rate of *P. astreoides* doses (Fig. 2.10.B). Although there were observable declines in the growth rate of the higher doses, and increases in growth rate of the 2868 µg/L dose, post-hoc analysis failed to reveal significant differences from the control corals. However, the growth rate of the 8293 µg/L dose was reduced enough to be significantly less that the increased growth rate of the 2868 µg/L dose, but not controls. The reduced growth rates observed in the higher doses following exposure remained for 7 d post-exposure recovery, but were not significant. Exposure to 1MN also produced significant differences in growth rate of *S. siderea* doses (Fig. 2.10.C). Following exposure, the same pattern observed in the *P. astreoides* exposure occurred, whereas the growth rates of the high doses were reduced, the low-mid doses were increased, but neither were significantly different from controls. However, growth rates of the 10332 µg/L dose were significantly less than the 828 µg/L dose. Following 7 d post exposure recovery, there were significant differences in growth rate of *S. siderea* treatments (p=0.0003), specifically, the three highest doses were growing significantly less than the control and 1614 µg/L doses. After 28 d post exposure recovery, there were no significant differences in the growth rate of any species tested.

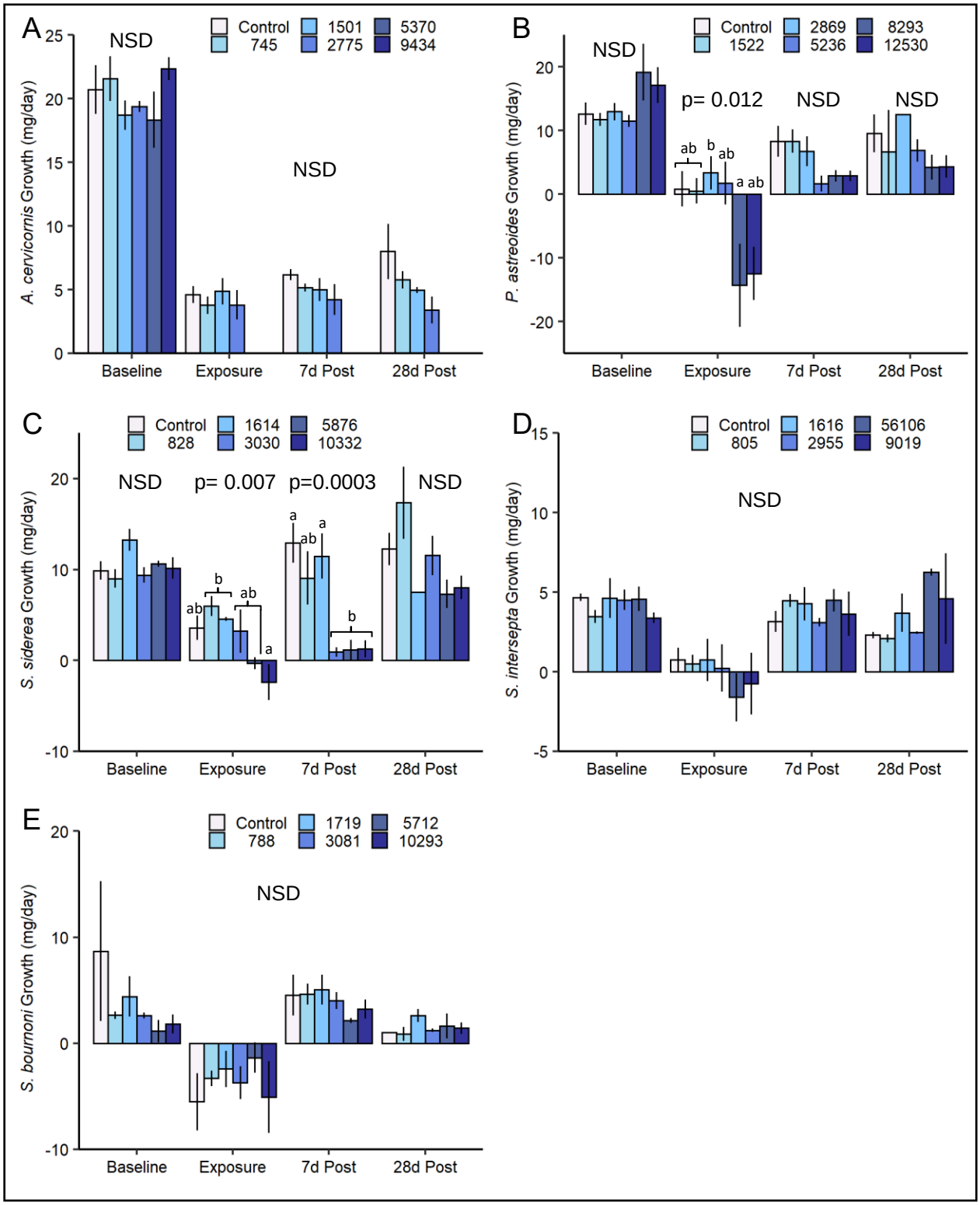

Figure 2.10 Mean growth rate for A) *A. cervicornis*, B) *P. astreoides*, C) *S. siderea*, D) *S. intersepta*, and D) *S. bournoni* for the indicated time periods. Letters above bars represent statistically similar groups, error bars= standard error

Mortality

Following each exposure to 1MN, mortality was visually assessed in each chamber and a mean level of mortality was determined for each dose (Figure 2.11, Table S2.10). There was less mortality compared to the TOL exposure, with some species exhibiting high survival, even at higher doses of 1MN. Although less than TOL, there were significant differences in mortality between doses of 1MN to all coral species. The *A. cervicornis* exposure produced the highest mortality of all 1MN exposures, with the two highest doses 100% dead at 48 h. The mid-range doses, 1501 µg/L and 2775 µg/L, resulted in low mortality, and controls and 745 µg/L had 100% survival. Exposure of *P. astreoides* to 1MN resulted in 50.4 % mortality in the highest dose, while the 8293 µg/L dose resulted in 25.8% mortality after 48 h. The two lower doses of 1MN, 1521 µg/L and 2868 µg/L, resulted in 8.3% and no mortality, respectively. Following the 48-h exposure, there was low mortality in one fragment of the controls, resulting in a mean dose mortality level of 0.42% for controls. The *S. siderea, S. intersepta,* and *S. bournoni* exposures resulted in similar patterns of mortality, where the controls and three lowest doses of 1MN exhibited no mortality after 48 h. Mortality in the two highest doses of these exposures was variable, but the maximum observed mortality for each test was 5% for *S. siderea,* 18.3% for *S. intersepta,* and 6.3% for *S. bournoni*.

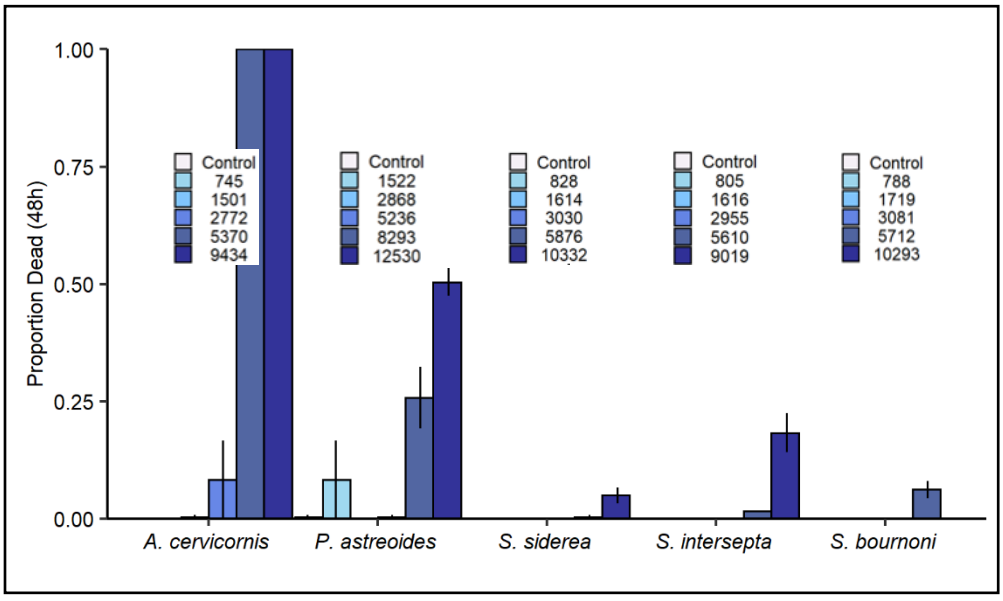

Figure 2.11 Proportion of coral dead after 48 h exposure to 1MN for all coral species tested. Individual legends include the 1MN dose group (µg/L) for each coral exposure

2.3.3 Phenanthrene

Chemistry

All PHE exposures were similarly loaded (Table S2.2), and as such, the level of PHE in each dose was similar between tests. Measured concentrations fell short of target levels, but this was anticipated as the doses were designed to approach solubility in seawater (690 µg/L) (Shaw 1989). Although the concentrations of each dose do not vary geometrically as intended, the mean level of each treatment was significantly different than the levels of all other treatments. Additionally, passive dosing succeeded at maintaining stable concentrations throughout the 48-h exposure (Tables S2.16-19), indicated by an average CV of 8.4% (*A. cervicornis)*, 3.6% (*P. astreoides)*, 3.5% (*S. siderea)*, and 4.9% (*S. intersepta*), for each test. The average PHE dose measure in each treatment (Table 2.3) was used to calculate a CV of 2.9% (*A. cervicornis)*, 2.9% (*P. astreoides)*, 2.8% (*S. siderea)*, and 1.9% (*S. intersepta)*. The low CVs amongst treatment replicates indicated consistent aqueous concentrations were achieved in all exposures (Figure 2.12).

Table 2.3 Mean measured concentration for the target PHE doses of all exposures

Species	Mean PHE Concentration[a]					
	Control	125 µg/L	250 µg/L	500 µg/L	1000 µg/L	2000 µg/L
Acropora cervicornis	<MDL[b]	92 (±2)	202 (±6)	369 (±11)	454 (±16)	656 (±20)
Porites astreoides	<MDL	77 (±3)	181 (±4)	390 (±6)	501 (±16)	654 (±23)
Siderastrea siderea	<MDL	110 (±1)	196 (±4)	373 (±8)	456 (±4)	518 (±41)
Stephanocoenia intersepta	<MDL	68 (±2)	167 (±1)	345 (±4)	440 (±12)	544 (±13)

[a] µg/L (± standard error)
[b]minimum detection limit

Coral condition

The changes to coral condition of all four species exposed to PHE are summarized in Figure 2.13, and show significant effects of dose in all exposures. Exposure to PHE resulted in significantly elevated coral condition scores compared to controls, but in most tests, the coral condition of the highest doses of PHE did not reach a 50% response.

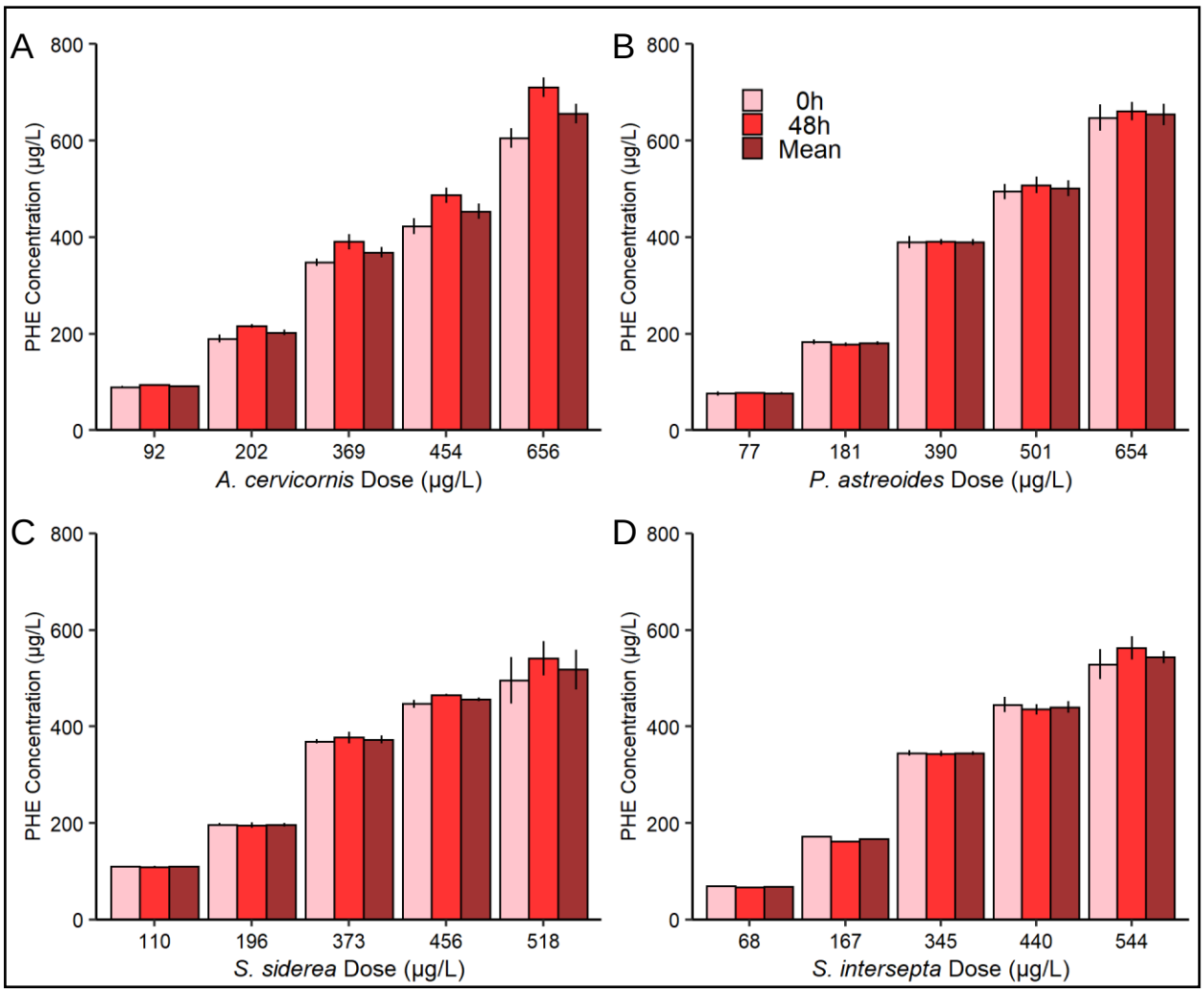

Figure 2.12 Measured concentration of PHE in each dose at 0 h and 48 h of all exposures

Acropora cervicornis. Coral condition for all time points of the *A. cervicornis* exposure to PHE are shown in Figure 2.13.A. There were significant effects of PHE dose on the coral condition for all time points measured. Following 1 h of exposure, doses at 202 µg/L and higher, scored significantly higher than controls and the 92 µg/L dose. The coral condition of the 92 µg/L dose increased at 4 h, to no longer significantly less than the four highest doses, but remained statistically similar to controls.

Porites astreoides. The coral condition scores for all *P. astreoides* doses are summarized in Figure 2.13.B, and shows significant effects at all time points measured. The top three doses of PHE (390 µg/L, 501 µg/L, and 654 µg/L) scored significantly higher than controls at 1 h, and remained elevated through 48 h. The coral condition score of the 181 µg/L PHE dose was similar to controls for all time points except 7 h and 12 h.

Siderastrea siderea. Figure 2.13.C summarizes the coral condition scores for all doses of PHE to *S. siderea*. Although significant effects were present from 1 h through 48 h, scores of most doses were not immediately elevated compared to controls. Compared to controls, the 518 µg/L dose scored significantly higher at 1 h, followed by the 456 µg/L dose scoring significantly higher at 2 h. The mid-range PHE doses, 196 µg/L and 373 µg/L, scored higher after 4 h and 3 h respectively, but fluctuated with regard to significant differences from controls through 24 h. At 24 h, all doses at and above 196 µg/L, scored significantly higher than controls. The coral condition of the 110 µg/L dose was not significantly different than controls at any time point during exposure to PHE.µ

Stephanocoenia intersepta. Coral condition scores for the *S. intersepta* doses exposed to PHE are summarized in Figure 2.13.D. There were significant effects of PHE dose on the coral condition scores with the four highest doses significantly elevated compared to controls from 1–24 h of exposure. At 24 h, the coral condition scores of the three highest doses (345, 440, and 544 µg/L) were significantly higher than controls. After 36 h, all doses 68 µg/L and above, except the 167 µg/L dose, scored significantly higher than controls. The coral condition of all doses at and above 167 µg/L scored significantly higher than controls at 48 h.

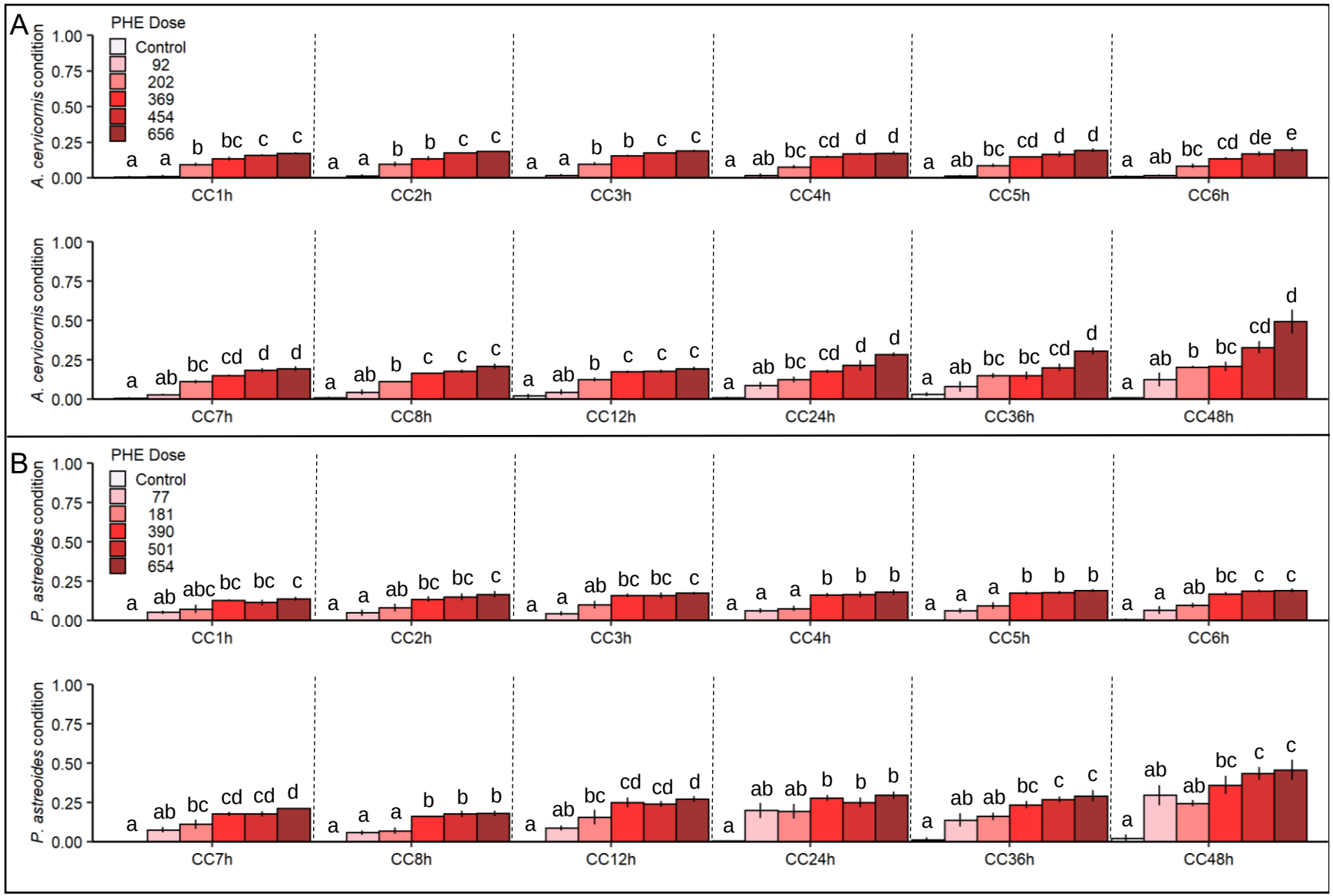

Figure 2.13 Coral condition scores for A) *A. cervicornis*, B) *P. astreoides*, C) *S. siderea*, and D) *S. intersepta* following exposure to PHE. Letters above bars represent statistically similar groups, error bars= standard error

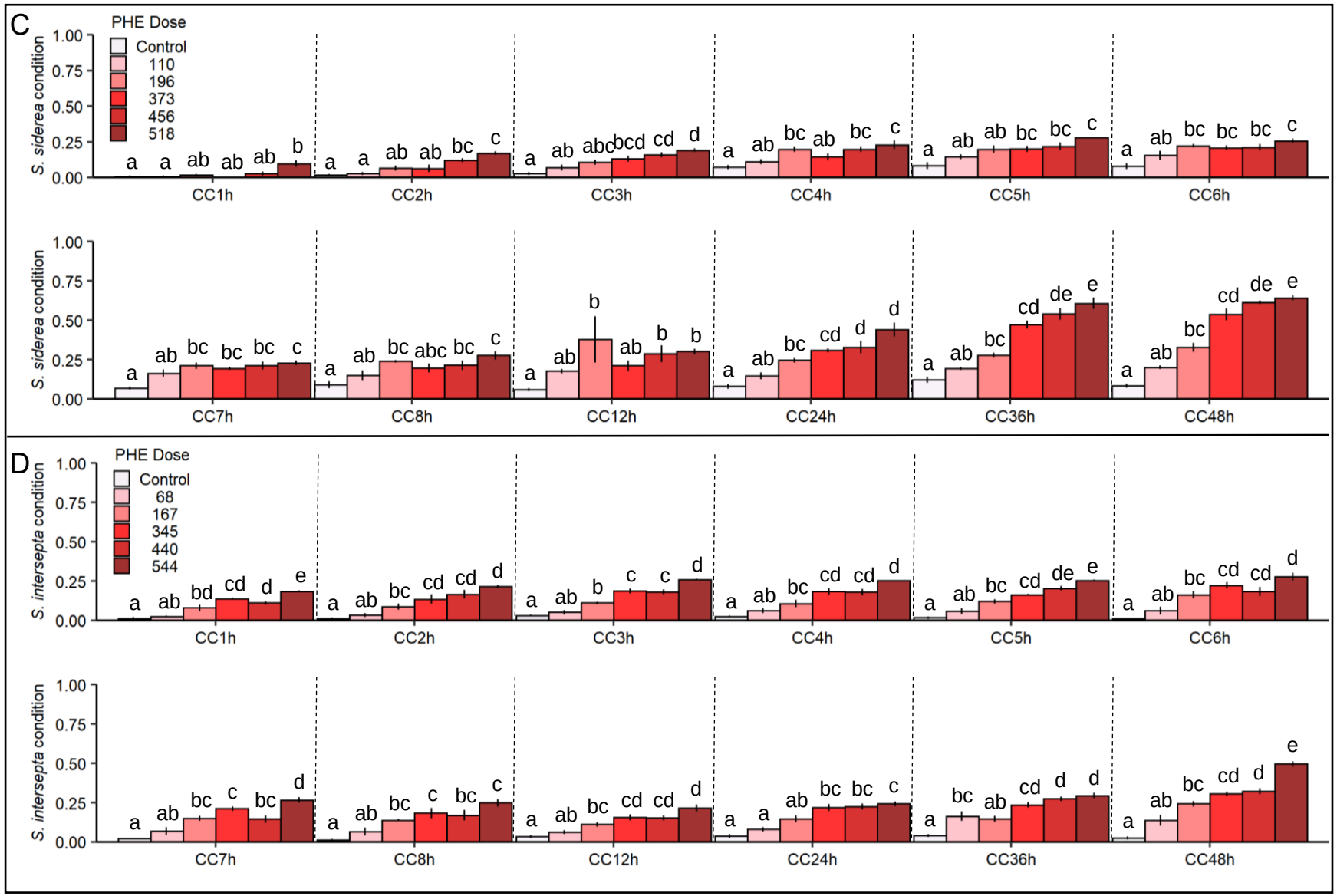

Figure 2.13 (cont'd). Coral condition scores for A) *A. cervicornis*, B) *P. astreoides*, C) *S. siderea*, and D) *S. intersepta* following exposure to PHE. Letters above bars represent statistically similar groups, error bars= standard error

Photosynthetic efficiency

The mean effective quantum yield was measured for all time periods of the PHE exposures, and changes to the yield of each PHE dose of all species assessed are summarized in Figure 2.14. No significant differences were present at any time point of the *A. cervicornis* exposure (Fig. 2.14.A). Following exposure, there were significant effects of PHE dose on the yield of *P. astreoides* (Fig. 2.14.B), but no significant differences were identified with post-hoc analysis. The yields of *S. siderea* doses were also significantly impacted by PHE dose (Fig. 2.14.C), specifically, yields of the 373.2 µg/L, 456 µg/L, and the 517.9 µg/L doses were all significantly less than the control, 109.8 ugL and 196.4 µg/L doses. There were no significant effects of PHE dose on the yield of *S. intersepta* (Fig. 2.14.D). In addition, after 7 d post, and again at 28 d post exposure recovery following exposure to PHE, no significant differences in mean quantum yield were observed for any species examined.

Growth

The mean growth rates of each dose following exposure to PHE are summarized in Figure 2.15. Overall, there were some declines in growth rates of higher doses, but none were significant. There was no significant effect of PHE dose on the growth rate of any coral tested.

Mortality

Mortality was assessed in each chamber and a mean dose level was determined for each coral exposure to PHE (Table S2.10). Comparatively, exposure to PHE resulted in the lowest mortality of all three hydrocarbons examined. There was no, or very low (<5%) mortality in three of the four coral species tested with PHE. The only exposure to result in a significant level of mortality at 48 h was the *A. cervicornis* exposure, with the highest mortality (33.8%) observed in the top dose of PHE. Additionally, the 453.8 µg/L dose also resulted in 8.3% mortality after 48 h exposure to PHE.

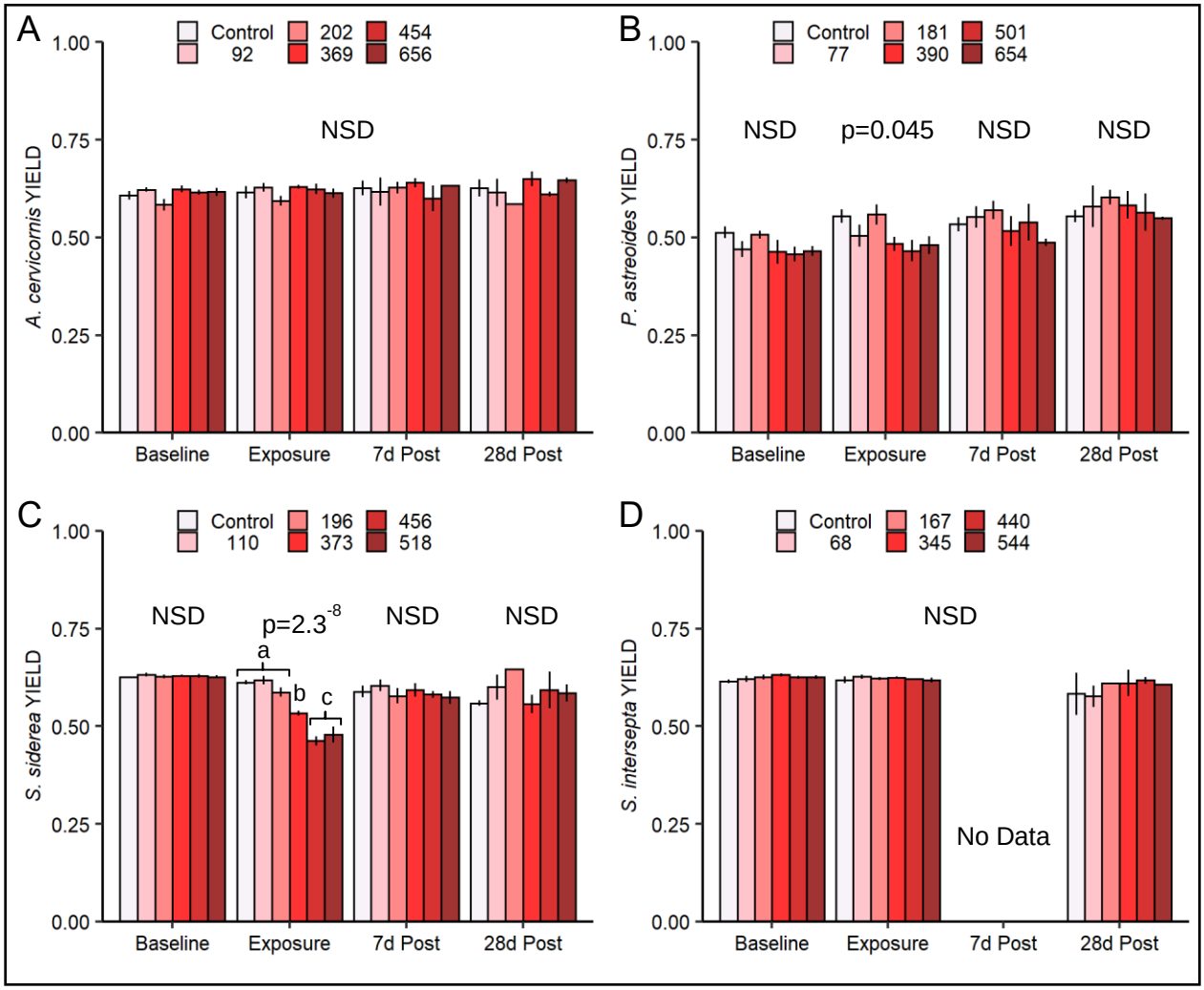

Figure 2.14 Mean Quantum Yield for A) *A. cervicornis*, B) *P. astreoides*, C) *S. siderea*, and D) *S. intersepta* for the indicated time periods. Letters above bars represent statistically similar groups, error bars= standard error

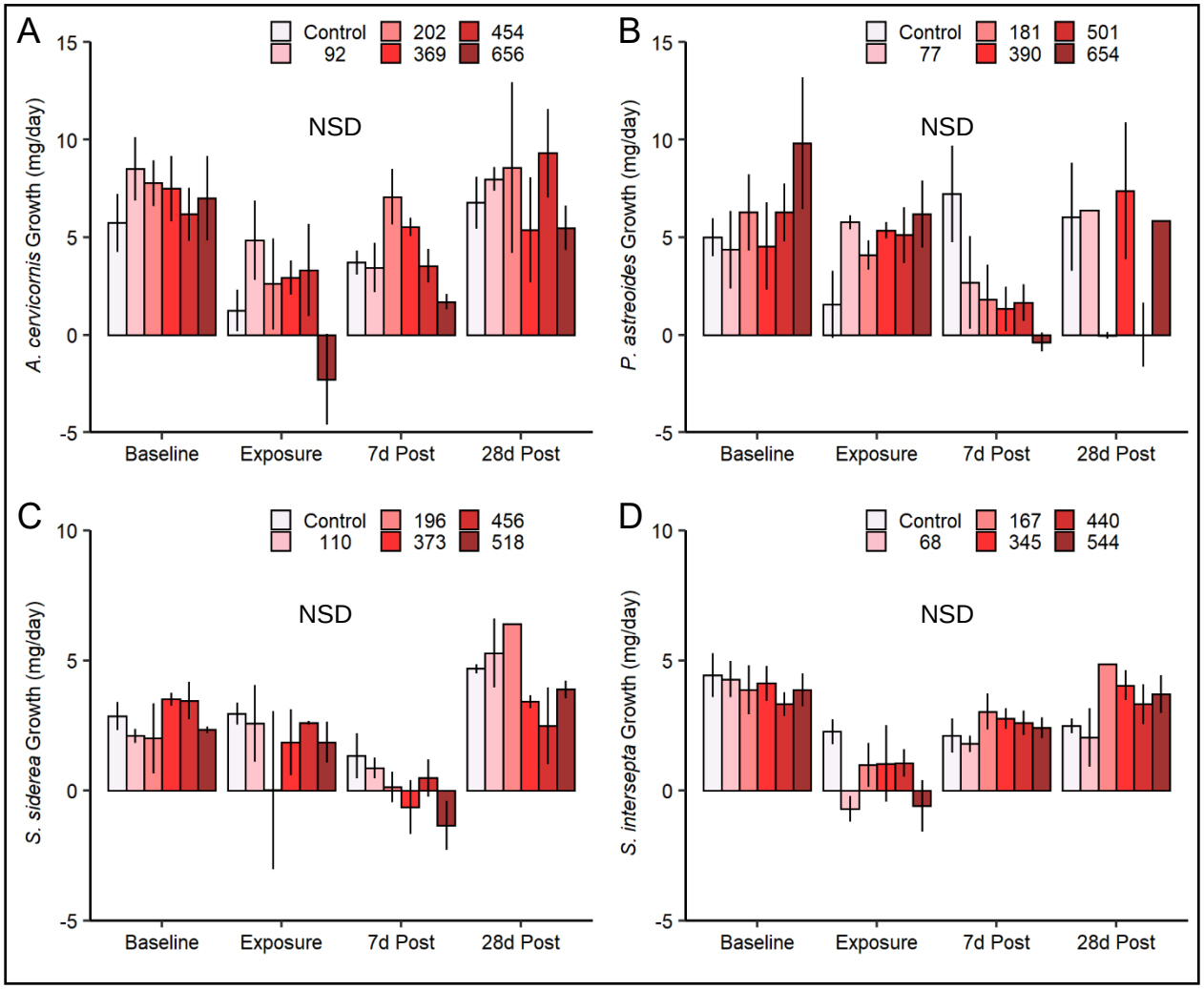

Figure 2.15 Mean growth rate for A) *A. cervicornis*, B) *P. astreoides*, C) *S. siderea*, and D) *S. intersepta* for the indicated time periods. Letters above bars represent statistically similar groups, error bars= standard error

2.3.4 Effect Concentrations and Species Sensitivity

The responses of each coral species were used as inputs to the *drm* models to estimate effect concentrations for the previously described parameters that were significantly impacted by exposure to the specific hydrocarbons. The significant TOL, 1MN, and PHE dose effects on the coral condition of each species were used to estimate the EC10 and EC50 for each coral/hydrocarbon exposure, in order to calculate observable effect concentrations. Additionally, hydrocarbon dose effects to photosynthetic efficiency and growth that were previously determined significant, were used to calculate inhibition concentrations (IC50). The LC50 for each coral was determined from the mortality levels previously described, as a measure of the

acute toxic endpoint for each hydrocarbon. Table 2.4 summarizes these subacute and acute effect concentrations for each coral with all compounds tested.

The subacute effects to coral condition for each *A. cervicornis* exposure are shown in Figure 2.17.A. There was a significant positive relationship between the concentration of each compound and the increasing effect observed ($p<0.001$), producing estimates of EC50 that are the lowest for all corals examined here, 31.2 mg/L TOL, 3126 µg/L 1MN, and 752 µg/L PHE. Exposure to 1MN also caused significant effects to quantum yield (Fig. 2.17.B), which were used to calculate an $IC50_{YIELD}$ of 1539 µg/L. Acute effects of all compounds on *A. cervcornis* (Fig. 2.17.C) were used to determine LC50s of 35.9 mg/L TOL, 3421 µg/L 1MN, and 719 µg/L PHE.

Table 2.4 Subacute and acute effect concentrations calculated from each coral exposure

Species	Chemical	EC10	EC50	$IC50_{YIELD}$	LC50
A. cervicornis	Toluene (mg/L)	23.2 (21.2-25.3)	31.2 (28.7-33.6)	NA	35.9 (CNC)
P. astreoides		16.0 (12.6-19.4)	27.9 (24.2-31.6)	NA	35.4 (CNC)
S. siderea		10.9 (8.4-13.4)	30.6 (26.8-34.4)	35.3 (7-64)	68.3 (57.9-78.8)
S. intersepta		65.3 (47.7-82.8)	92.5 (83.8-101.2)	92.1 (35-149)	109.5 (CNC)
S. bournoni		20.0 (4.6-35.3)	50.6 (33.8-67.4)	70.5 (66-74)	69.7 (62.8-76.6)
A. cervicornis	1-methylnaphthalene (µg/L)	1945 (1013-2872)	3126 (2573-3678)	1540 (1509-1570)	3421 (2667-4174)
P. astreoides		4593 (4342-4844)	5819 (5594-6045)	5993 (3685-8300)	14427 (6190- >>)
S. siderea		857 (596-1119)	5189 (4583-5794)	3431 (2630-4233)	> solubility
S. intersepta		673 (42-1304)	9294 (6370-12217)	12288 (CNC)	11787 (4956-18618)
S. bournoni		2355 (1048-3663)	7127 (5945-8310)	7433 (2400-12465)	> solubility
A. cervicornis	Phenanthrene (µg/L)	216 (0-443)	[a]752 (535-969)	NA	[a]719 (558-881)
P. astreoides		19 (0-169)	> solubility	181 (153-210)	> solubility
S. siderea		84 (54-114)	373 (330-417)	302 (200-402)	> solubility
S. intersepta		67 (8-126)	[a]829 (564-1093)	NA	> solubility

[a] > highest concentration and estimate extrapolated
CNC= could not calculate

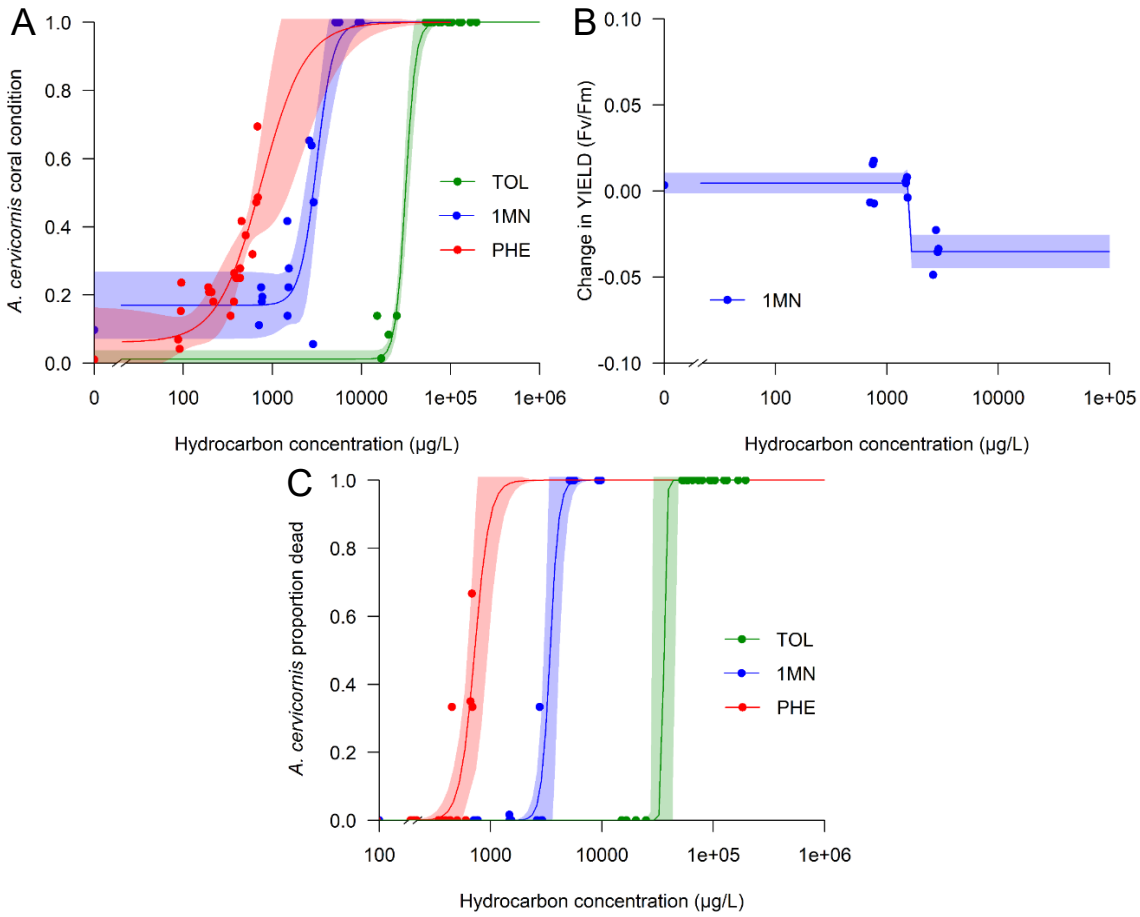

Figure 2.16 Dose response curves for the significant effects on A) subacute coral condition, B) photosynthetic efficiency, and C) acute lethality of *A. cervicornis* following exposure to TOL, 1MN, and PHE.

The subacute impacts to *P. astreoides* used to determine the EC50 for each compound are shown in Figure 2.18.A. Impacts to *P. astreoides* were comparatively less severe than exposures of *A. cervicornis*, but still produced significantly elevated effects used to determine EC50s of 27.9 mg/L TOL and 5819 µg/L 1MN. The *drc* model for PHE appears to predict an EC50 around 1300 µg/L, but a non-significant model fit (p=0.12), coupled with an estimate that is greater than solubility in seawater, suggests this value is unreliable and the maximum effect of PHE on *P. astreoides* was not high enough to calculate an EC50. Significant impacts to both quantum yield (Fig. 2.18. B) and growth (Fig. 2.18.C) of *P. astreoides* were used to estimate inhibition concentrations for each parameter. Thus, an $IC50_{YIELD}$ of 5993 µg/L was estimated following exposure to 1MN, and 181 µg/L was calculated following PHE exposure. Additionally, the *drm*

for the change in growth rate following exposure to 1MN was highly significant ($p= 2.2^{-16}$), prompting calculation of an $IC50_{GROWTH}$ of 8052 µg/L (95% CI= 7961–8144 µg/L). Mortality following each *P. astreoides* exposure (Fig. 2.18.D) was used to estimate LC50s of 35.4 mg/L TOL, and 14427 µg/L 1MN.

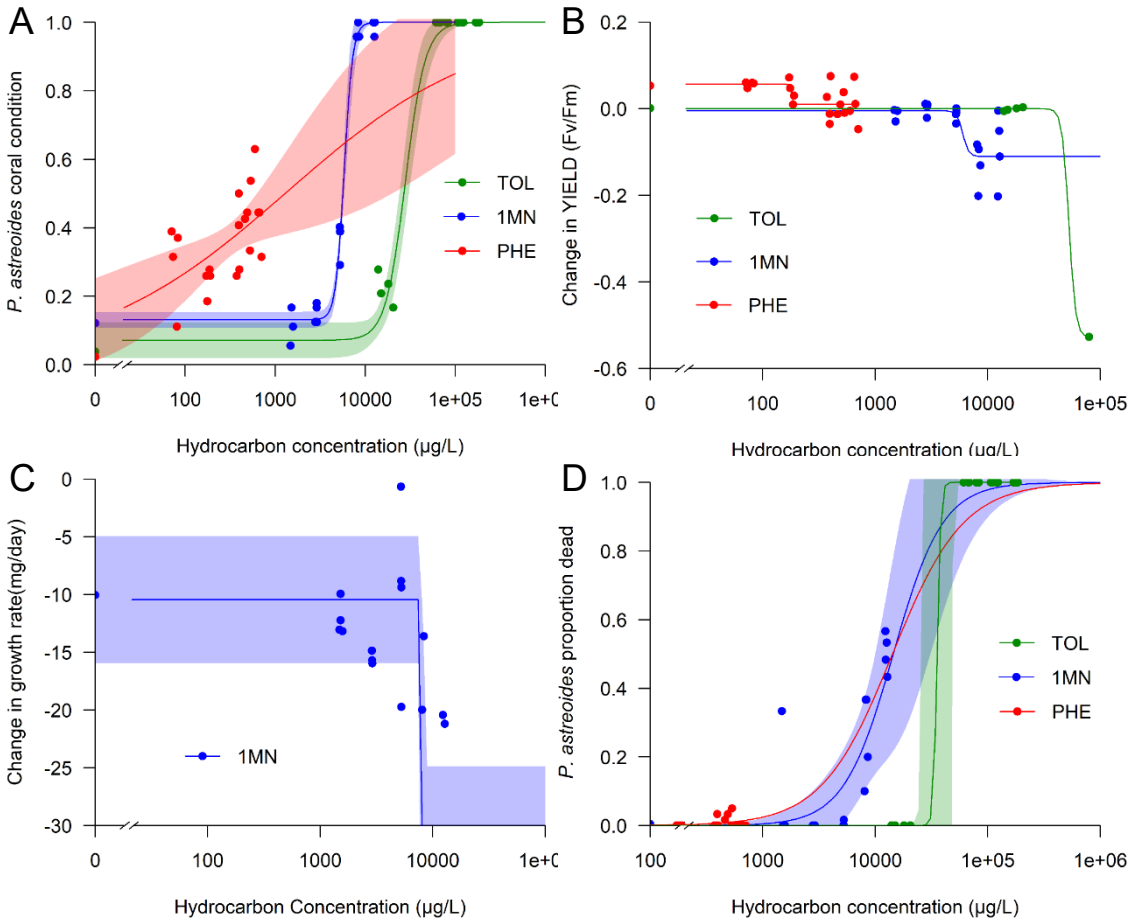

Figure 2. 17 Dose response curves for the significant effects on A) subacute coral condition, B) photosynthetic efficiency, C) growth, and D) acute lethality of P. astreoides following exposure to TOL, 1MN, and PHE.

The EC50 for each compound was determined from the impacts to *S. siderea*, which are summarized in Figure 2.19.A. The effects on coral condition increased with increasing hydrocarbon concentration in a significantly positive relationship for all three compounds tested, producing EC50s of 30.6 mg/L TOL, 5189 µg/L 1MN, and 373 µg/L PHE. Quantum yield (Fig. 2.19.B) and growth (Fig. 2.19.C) of *S. siderea* were both significantly impacted and therefore, changes to both were used to measure inhibition concentrations for each parameter. The

calculated $IC50_{YIELD}$ for TOL and 1MN was 35.3 mg/L TOL and 3431 µg/L 1MN, respectively, while the PHE $IC50_{YIELD}$ was 301 µg/L. The *drm* model for the effects of 1MN on growth was not significant (p=0.15), but was still used to estimate an $IC50_{GROWTH}$ of 3388 µg/L (95% CI= 0–8149 µg/L). Mortality of *S. siderea* following exposure to all three compounds is in Figure 2.19.D, but only TOL produced enough mortality for a significant model fit, which resulted in an LC50 of 68.3 mg/L TOL.

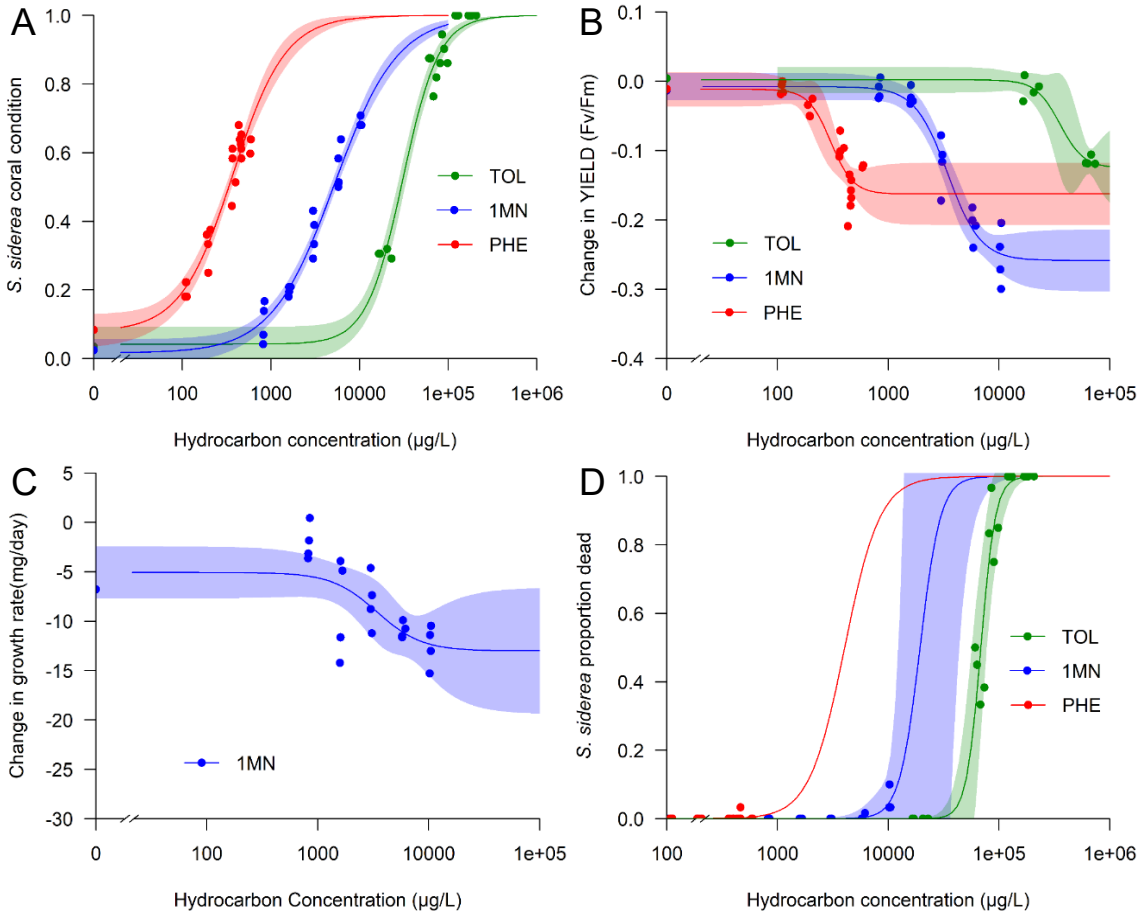

Figure 2.18 Dose response curves for the significant effects on A) subacute coral condition, B) photosynthetic efficiency, C) growth, and D) acute lethality of *S. siderea* following exposure to TOL, 1MN, and PHE.

The subacute effects on the coral condition of *S. intersepta* following exposure to all three compounds are shown in Figure 2.20.A. Although effects generally occurred at a higher concentration when compared to the previously described species, there was still a significant positive relationship between concentration and effect observed (p<0.01). These effects were

used to estimate EC50s of 92.5 mg/L TOL, 9293 µg/L 1MN, and 828 µg/L PHE, with the latter two at, or slightly above, the maximum concentrations obtained at these loadings. Consistent with previous species, significant declines in quantum yield were present following exposures to TOL and 1MN (Fig. 2.20.B), leading to estimates of 92.1 mg/L TOL and 12288 µg/L 1MN for $IC50_{YIELD}$. Significant mortality levels for TOL and 1MN were used to estimate LC50s of 109.5 mg/L TOL and 11787 µg/L 1MN respectively (Fig. 2.20.C).

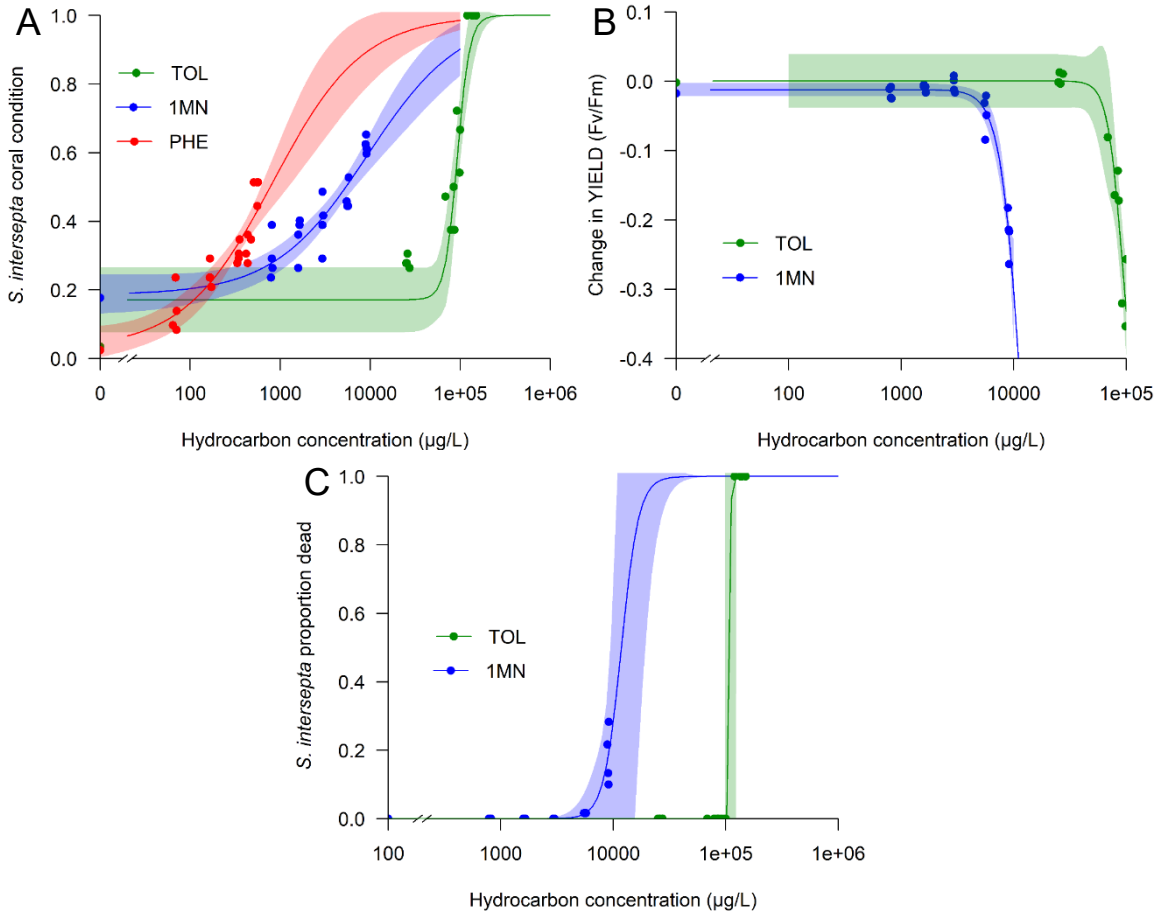

Figure 2. 19 Dose response curves for the significant effects on A) subacute coral condition, B) photosynthetic efficiency, and C) acute lethality of *S. intersepta* following exposure to TOL, 1MN, and PHE.

The effects of TOL and 1MN on *S. bournoni* are summarized in Figure 2.21, and were used to estimate effect endpoints following both exposures. Subacute effects to coral condition (Fig. 2.21.A) were used to estimate EC50s of 50.6 mg/L TOL and 7127 µg/L 1MN. The significant declines in quantum yield (Fig. 2.21.B) were both used to estimate IC50s of 70.5

mg/L TOL and 7433 µg/L 1MN following both exposures. Exposure to 1MN did not result in sufficient levels of mortality in *S. bournoni*, so the only reliable estimate of LC50 is 69.7 mg/L TOL (Fig. 2.21.C).

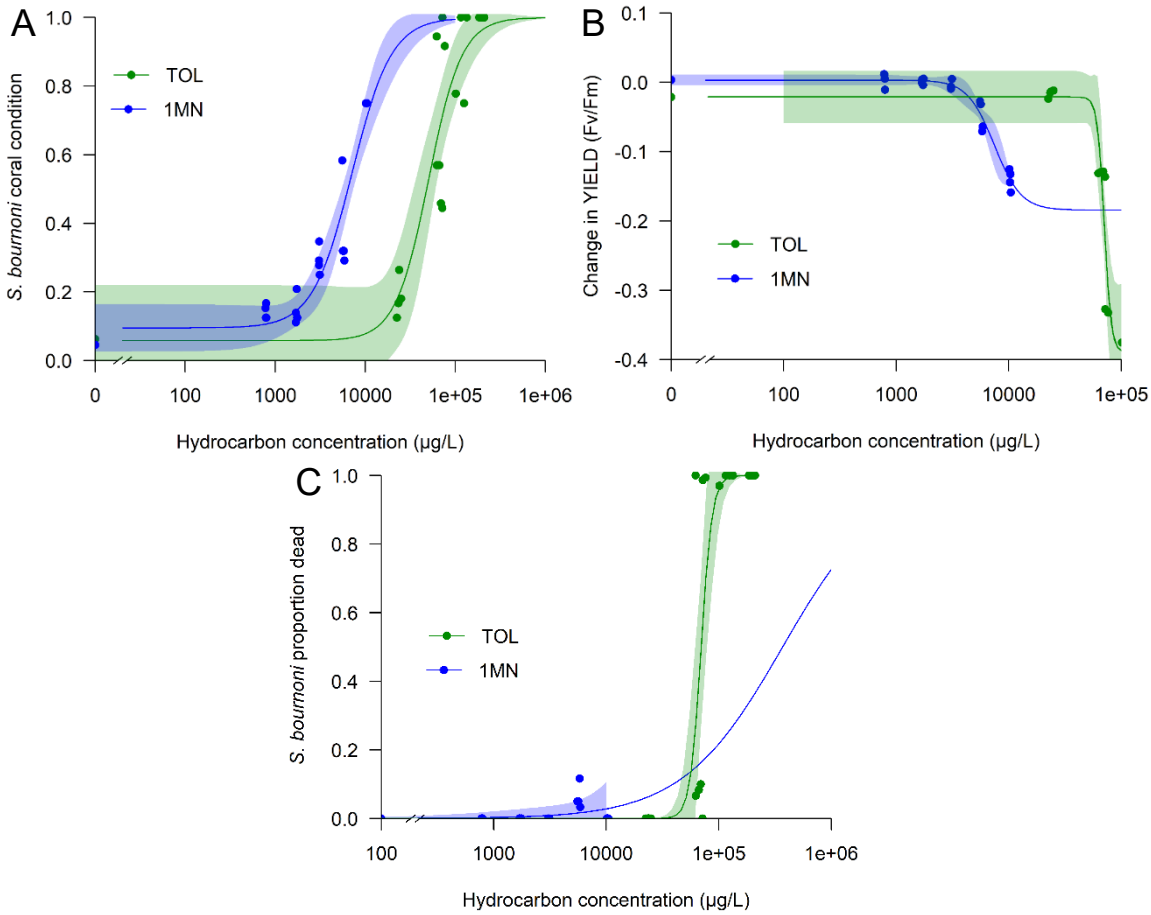

Figure 2.20 Dose response curves for the significant effects on A) subacute coral condition, B) photosynthetic efficiency, and C) acute lethality of *S. bournoni* following exposure to TOL and 1MN.

2.3.5 Target Lipid Model

The endpoints determined for each coral are useful for species sensitivity comparisons when data for that specific hydrocarbon exists. In order to broaden the comparison of species sensitivity, the TLM was used to estimate subacute and acute target lipid body burdens from the specific sublethal or lethal endpoints determined. Similarity in the sublethal endpoints (i.e. condition, photosynthetic efficiency, growth) investigated for each coral suggest an average of EC50 and IC50 values was the most appropriate input to the TLM. EC50 and LC50s were fit to the TLM to calculate corresponding critical target lipid body burdens for sub-lethal

($CTLBB_{Sublethal}$) and lethal ($CTLBB_{Lethal}$) effects (Table 2.5). Further, E/LC50 values estimated above the solubility limit of any chemical were excluded from calculation of body burdens given their unreliability.

The $CTLBB_{Sublethal}$ for each coral was derived by regressing the Log EC50 (adjusted with Δc) with the Log Kow of each compound, and using the TLMs universal narcosis slope (-0.940) to produce a line with a y-intercept equal to the $CTLBB_{Sublethal}$ for that species (Figure 2.22.A—E). The uncertainty in the y-intercept resulted in the error associated with the body burden estimate, and was derived by reducing the residuals of the endpoints and the TLM.

Table 2.5 The TLM applied to the subacute and acute endpoints determined for each coral to estimate CTLBBs for effect and lethality

Species	CTLBB Sublethal				CTLBB Lethal			
	Log (mM)	SE	µmol/g	SE	Log (mM)	SE	µmol/g	SE
Acropora cervicornis	2.231	0.005	170.0	1.3	2.257	0.002	180.9	0.6
Porites astreoides	2.307	0.050	202.9	15.4	2.556	0.136	359.9	76.5
Siderastrea siderea	2.315	0.021	206.6	6.7	2.473	-	297.4	-
Stephanocoenia intersepta	2.560	0.027	362.8	14.8	2.758	0.006	572.2	5.4
Solenastrea bournoni	2.481	0.019	302.4	8.7	2.482	-	303.5	-

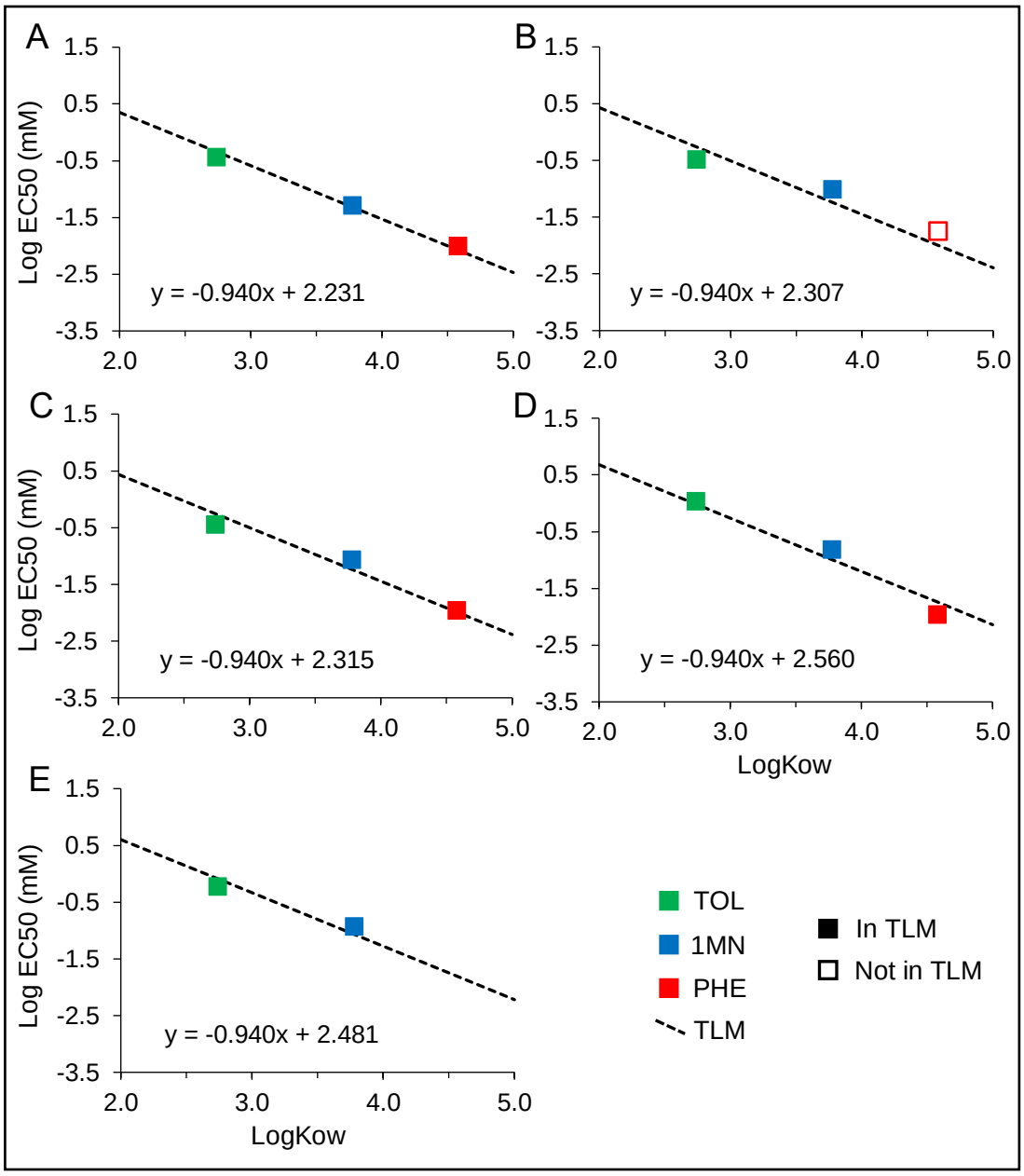

Figure 2. 21 The Target Lipid Model fit to the EC50 values measured for each single compound exposure

Similarly, measured lethal effects endpoints were used to estimate a $CTLBB_{Lethal}$ for each species using the same method but substituting log LC50 (Fig 2.23.A—E). The TLM was used to produce a line with a y-intercept equal to the $CTLBB_{Lethal}$ for that species. Many of the estimated lethal endpoints were well above solubility of the chemical in seawater due to the low mortality in many of the exposures, and were not used in these regressions.

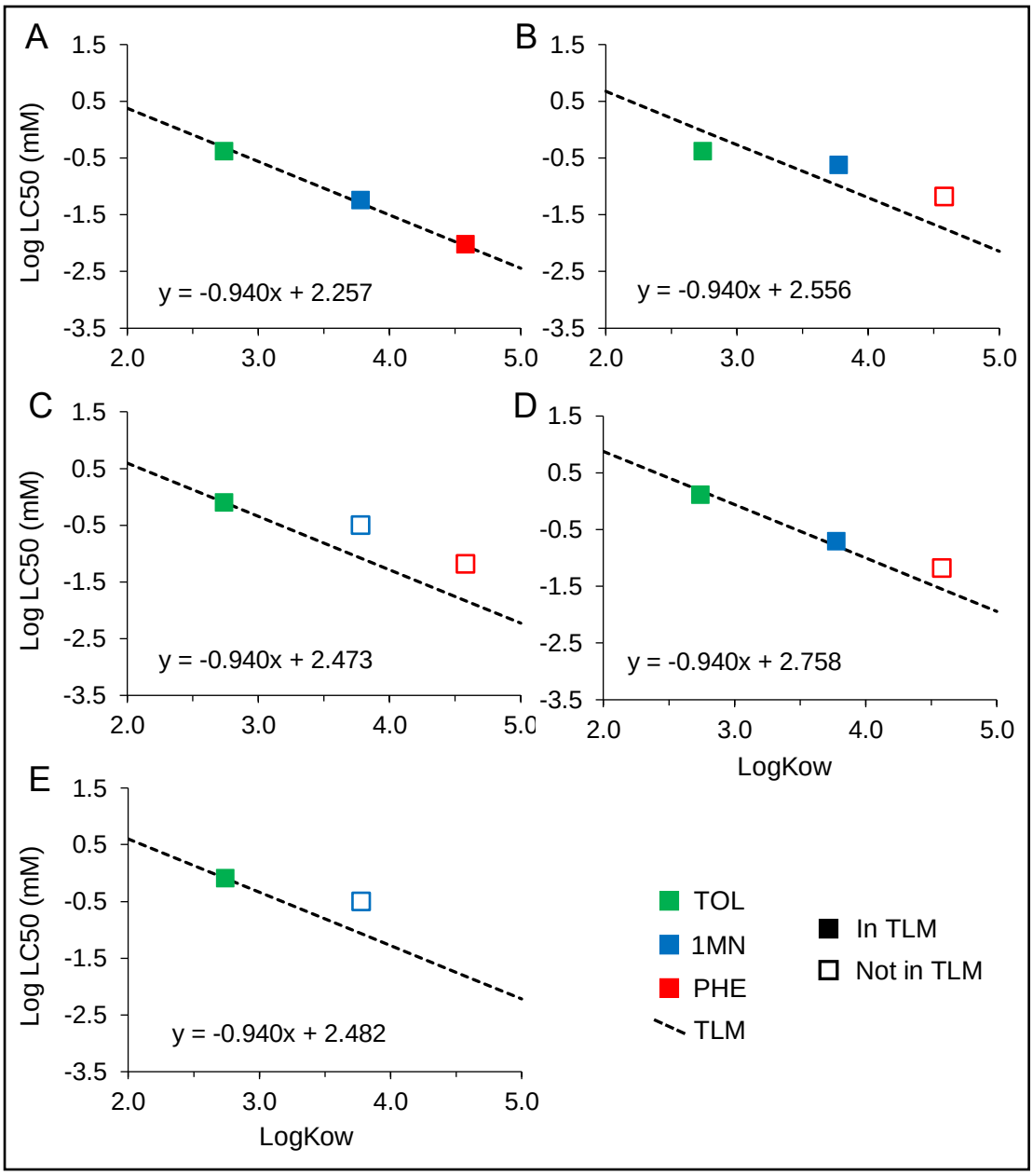

Figure 2.22 The Target Lipid Model fit to the LC50 values measured for each single compound exposure

The calculated body burdens for each coral species were compared with other species for which this information was available, and are shown in Figure 2.24. Both $CTLBB_{Sublethal}$ (Fig. 2.24 blue diamonds) and $CTLBB_{Lethal}$ (Fig. 2.24 red diamonds) calculated here have been included in the comparison with CTLBBs of the 79 species previously measured (McGrath et al. 2018). The most sensitive coral tested here, as indicated by the lowest of all calculated CTLBBs is from *A. cervicornis* (sublethal) and ranks higher than a majority of species (74%) previously

assessed. Due to uncertainty in the CTLBB estimates of all species, the actual percentile for the coral species tested here may be slightly higher or lower. However, even if the error of CTLBBs is considered, all corals ranked more resilient than 60% of the other species. Additionally, the highest values recorded in this comparison are from corals tested here, making these species some of the most resilient organisms for which this data is available.

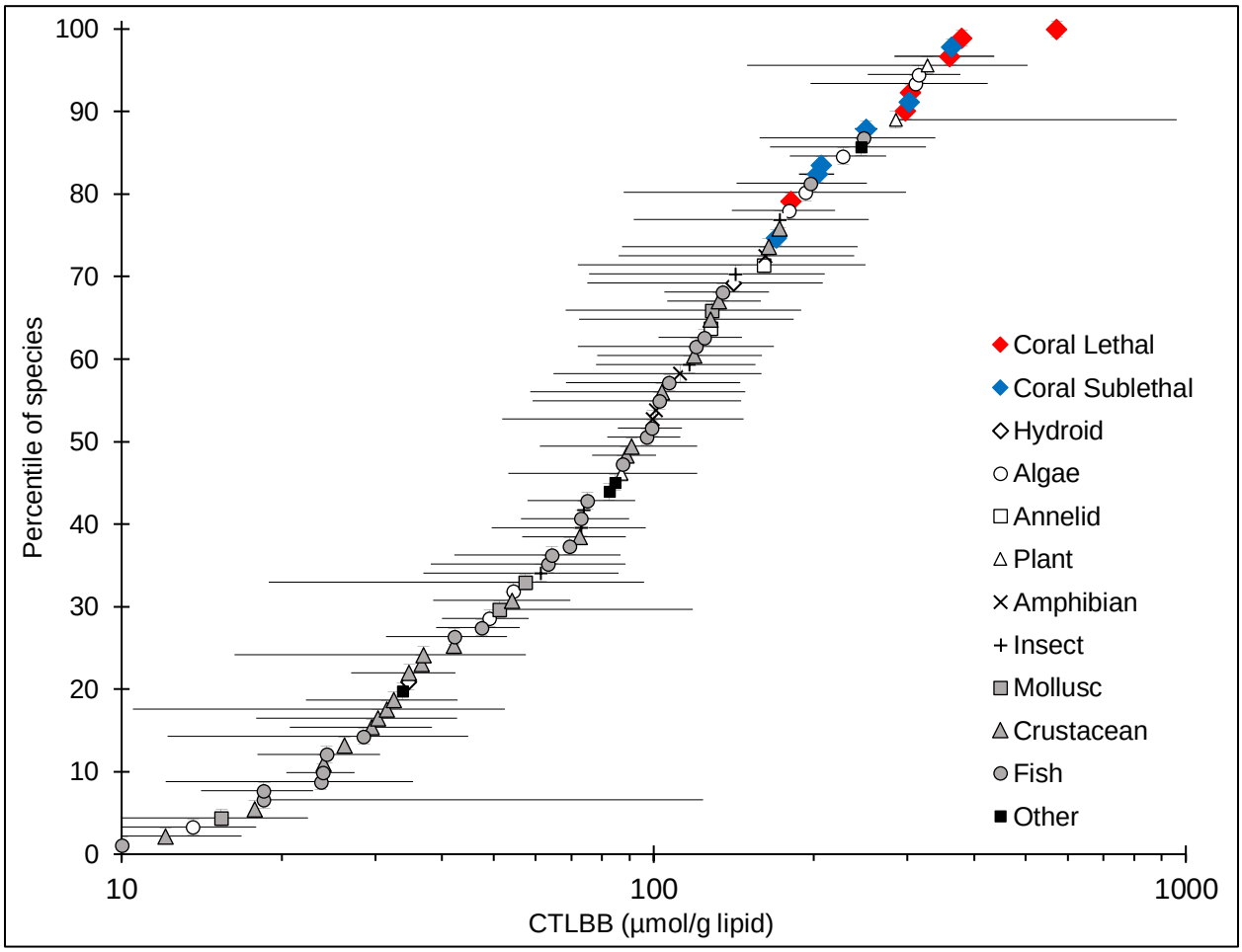

Figure 2.23 Comparison of CTLBBs with those listed in the acute database of McGrath et al. (2018). Filled diamonds represent $CTLBB_{Sublethal}$ (blue) and $CTLBB_{Lethal}$ (red) for the coral species tested here.

2.4 DISCUSSION

Corals exhibit a range of responses to single PAH exposures, with a degree of variability between hydrocarbons tested, and species. Throughout the exposures, control corals maintained normal polyp extension and mucus production, with no tissue swelling or attenuation.

Occasionally, control corals would receive low scores for polyp extension, presumably due to physical disturbance of the test system, but otherwise, effects on controls across all exposures were minimal. Corals exposed to low hydrocarbon concentrations (or high concentrations over short time scales) exhibited polyp retraction compared to controls and elevated mucus production. Tissue swelling of the coenenchyme was also frequently observed in response to hydrocarbon exposure, although polyp swelling and distension was also evident in some species; frequently accompanied by delayed response to stimulus (Renegar et al. 2017b). At higher concentrations, responses included tightly retracted polyps, followed by lightening of coloration and bleaching. Highly stressed corals had severe polyp retraction, with degradation of the coenenchyme, exposure of skeletal elements and tissue loss or mortality.

The TOL exposure produced severe effects, with higher doses of all tests resulting in immediate disruption of normal coral behavior, eventually leading to complete mortality. Lower doses showed effects, but were delayed in comparison to high levels. Overall, the order of effects observed within each species was similar between TOL doses, but the speed of onset of each subacute effect was dependent upon the dose. High doses exhibited rapid and severe effects, including tight polyp retraction, large amounts of mucus secreted, and in most cases extreme tissue swelling. Later in the exposure, these severe effects resulted in tissue attenuation and eventual maximum scores and death. Mid-range doses exhibited many of these same responses, except they were delayed, usually becoming severely impacted after 12—24 h exposure, leading to maximum effects and mortality by 48 h in some species. Low doses of TOL exhibited polyp retraction and some tissue swelling, but remained alive with little to no tissue attenuation.

The coral condition of all species was also significantly affected by exposure to 1MN, with some effects immediate. Although not as severe as TOL, exposure to 1MN produced immediate effects in high doses that lead to mortality in much the same pattern. At high doses, polyps were tightly retracted, with tissue swelling of the coenenchyme evident. Tissue swelling subsided and was replaced by tissue recession and attenuation, exposing skeletal septa on the ridges of corallites. At moderate doses, 1MN resulted in tissue swelling, with eventual polyp retraction and slight tissue attenuation. Low doses showed some effects to polyp retraction, but typically remained similar to, or slightly different than controls.

The effects of PHE on the coral condition of the four species examined were less severe than TOL and 1MN, with some tests failing to result in adequate effects required to facilitate the

calculation of endpoints. Effects of the high concentrations were less severe, with most of the scores attributed to polyp retraction and some tissue attenuation. Corals in the moderate and low exposure doses exhibited some polyp retraction, but typically did not show signs of tissue attenuation. Toxicity of PHE appeared to be constrained by solubility, or the 48-h exposure time limit. The toxicity of these compounds is time dependent, and the higher LogKow compounds require more time to partition into membranes and cause effects (French-McCay 2002, McGrath et al. 2018).

The effects of all three compounds on the quantum yield and growth of all species tested were initially present but were absent by 7 d post exposure. In higher doses, surviving corals exhibited significant declines in quantum yield immediately following most exposures, but had recovered to pre-exposure levels and not significant from controls by 7 d post exposure. Effects on growth rates were even more limited, with higher doses of three exposures causing significant declines immediately following the tests. By 7 d post exposure, only the growth of *S. siderea* exposed to high doses of 1MN remained significantly decreased, but increased to within control levels by 28 d post exposure.

Nutrient concentrations followed a pattern of significance that mirrored the severity of effects caused the contaminant in each exposure. In exposures that resulted in the highest effects and mortality, concentrations of NH3, NO2, NO3, and PO4 were elevated in doses with the greatest impacts. Exposure to TOL produced the most significant nutrient concentrations, followed by 1MN, which had elevated nutrient levels in the high dose of the *A. cervicornis* exposure. There were no significant nutrient differences following exposure to PHE, the test with the least effect overall. Dissolved oxygen levels were depressed in many of the hydrocarbon doses that had increased effects, most prominently following TOL exposure. The elevated nutrients and decreased DO in doses with the highest effects were likely due to necrosis and decomposition, but could also be due to elevated respiration in the stressed physiology of the exposed corals. Additional pH and DO measurements were taken at the onset of mortality or significant mucus release (24 h) in corals exposed to the higher concentrations of compounds, and showed levels similar to the start of the exposure. Necrosis of tissue would increase nutrient levels due to decomposition, which in turn depresses O2 and pH, and the significant differences were likely in response to mortality and tissue degradation/mucous release, and are believed to have accumulated in response to damage caused by the contaminant. Therefore, the observed

decreases in pH and DO at 48h were concluded to be the result of coral tissue necrosis or decomposition of excess mucus at the highest concentrations tested.

Alkalinity, a measure of the available ions in seawater for calcification, was significantly higher in hydrocarbon doses that had the greatest overall effects. Although only few exposures resulted in statistically significant differences in growth after exposure, this may be due to decreased calcification in high doses of hydrocarbon. The pH was also significantly altered, whereas the TOL and 1MN exposures produced significantly depleted pH in most exposures. In exposures with greater overall effects measured, such as those in the TOL exposures, the mid-range doses produced lower pH than the high doses. This is likely due to immediate effects and lethality preventing the time required for stress in the coral to elevate CO2.

The coral responses to all three hydrocarbons were used to estimate acute and subacute endpoints for effect and lethality, and these values (EC50 and LC50) were fit to the TLM to calculate corresponding critical target lipid body burdens for effect and lethality. The relationship between calculated EC50s and chemical log K_{ow} shows the subacute effect concentration determined as function of the partitioning behavior of the compound. Because log Kow is a proxy for lipid-water partitioning, the $CTLBB_{Sublethal}$ calculated from this relationship is therefore an estimate of the organismal target lipid hydrocarbon concentration that caused the 50% subacute effect. The $CTLBB_{Sublethal}$ and $CTLBB_{Lethal}$ calculated for *A. cervicornis*, *P. astreoides*, *S. siderea*, *S. intersepta*, and *S. bournoni* were compared to calculated values for other species for which this data is available. The $CTLBB_{Lethal}$ for the corals (red diamonds), except for *A. cervicornis*, indicates that these scleractinian coral species are more resilient to narcotic chemical exposure, compared to a majority of other species for which similar data is available.

For single hydrocarbons such as TOL, 1MN, and PHE the mode of action underlying baseline toxicity is narcosis, or the non-specific partitioning of chemicals into biological membranes and membrane-protein interfaces; the function of the lipid membranes is altered due to an increase in fluidity of the membranes, which accompanies solubilization of the narcotic chemical (van Wezel and Opperhuizen 1995). The acute and subacute endpoints determined indicate that corals are comparatively more resilient to narcotic chemical exposure than other coastal marine species. For brief periods on the order of days, corals are capable of secreting significant quantities of lipid-rich mucus through pores in mucocyte membranes either onto the

coral surface, or into the gastrovascular cavity. Corals are therefore covered in a layer of lipid-rich mucus that, in addition to its protective role, may efficiently and actively depurate lipophilic chemicals. This would only temporarily prevent chemical concentration in structural lipids from reaching a damaging concentration, as extended periods of exposure would eventually exhaust mucus production capabilities and result in sublethal effects or mortality.

The lipid content of the organism has been observed to have a significant positive linear relationship to the acute toxicity endpoint (Geyer et al. 1993, Geyer et al. 1994). This is particularly relevant to coral tissue, which has a relatively high total lipid content (≈8-34%), consisting of structural and storage components that can vary based on multiple environmental factors (Imbs 2013, Towle et al. 2015). Cnidarians have a large and diverse group of total lipids that are composed of non-polar storage lipids (wax esters and triglycerides), polar structural lipids (phospholipids), and additional symbiont (zooxanthellae) lipids. For scleractinian corals, the significant lipid storage reserves (22-32% of total) are accompanied by a large amount of structural lipid (10-18% of total) (Imbs 2013) which may serve in a protective role during exposure to non-polar chemicals, and may in part explain the relative resilience of corals compared to other species. Balance between storage and structural lipids is important for species specific thermal resistance in corals, and loss of symbiotic zooxanthellae (bleaching) resulting from ocean warming can significantly reduce total coral lipid content (Yamashiro et al. 2005, Imbs and Yakovleva 2012). Zooxanthellae densities are known to reduce in relation to other environmental factors (ocean warming, acidification, land-based sources of pollution), which would reduce overall storage lipid ratios and cause a significant decline in coral storage lipids following increased utilization of energy reserves. Additionally, short-term exposure to elevated temperatures has also been shown to decline polar structural lipids of the coral animal (Imbs and Yakovleva 2012). Changes in the environment that lead to reductions in structural lipids could potentially lead to disruptions in normal processes at lower levels of contaminant.

The corals used in these experimental exposures are sourced from the offshore waters of Broward County, Florida, and are thus exposed to chronic levels of land-based sources of pollution, including hydrocarbons from shipping and boating activities. The tested corals therefore have the potential to be reasonable surrogates of coral species expected to be exposed in the field. However, additional research is needed to understand the effects of compounding environmental factors (temperature, ultraviolet light, and pressure) and stress, and further

elucidate oil impacts and impact thresholds of petroleum hydrocarbons on scleractinian corals and related habitats.

2.5 CONCLUSION

The objective of this research was to form a more complete understanding of petroleum hydrocarbon toxicity to shallow-water scleractinian corals, by application of a standard test protocol to determine scientifically defensible toxicity benchmarks for multiple Atlantic shallow-water coral species. The tested species were found to have a variable range of species-specific physical responses to petroleum hydrocarbon exposures, with greater impacts observed in branching corals compared to massive corals. The acute and sub-acute endpoints, and associated CTLBBs, implicates the tested coral species (except for Acropora cervicornis) as generally more resilient to narcotic chemical exposure compared to other taxa for which similar data is available.

2.6 SINGLE COMPOUND DATA AVAILABILITY

The results of all exposures are summarized and available in the GRIIDC data repository (https://data.gulfresearchinitiative.org/) under the CoralTox project. All coral condition scores for all time points measured, as well as the individual growth and yield measurements, mortality, and water quality are included within. Table 2.6 contains the Unique Dataset Identifier and the DOI for all single compound exposures.

Table 2. 6 GRIIDC Dataset information for all single compound exposures

Dataset Name	UDI	DOI
Toxicity of 1-methylnaphthalene to *Acropora cervicornis*	R6.x825.000:0001	10.7266/N7NP22ZB
Toxicity of 1-methylnaphthalene to *Siderastrea siderea*	R6.x825.000:0002	10.7266/n7-d2ww-0y33
Toxicity of 1-methylnaphthalene to *Porites astreoides*	R6.x825.000:0003	10.7266/N7DF6PSG
Toxicity of 1-methylnaphthalene to *Stephanocoenia intersepta*	R6.x825.000:0004	10.7266/n7-6ynk-8q14
Toxicity of 1-methylnaphthalene to *Solenastrea bournoni*	R6.x825.000:0005	10.7266/n7-4bhj-qj29
Toxicity of phenanthrene to *Acropora cervicornis*	R6.x825.000:0006	10.7266/n7-r2gb-px96
Toxicity of phenanthrene to *Siderastrea siderea*	R6.x825.000:0007	10.7266/n7-2h81-ay91
Toxicity of phenanthrene to *Porites astreoides*	R6.x825.000:0008	10.7266/n7-4f3v-1394
Toxicity of phenanthrene to *Stephanocoenia intersepta*	R6.x825.000:0009	10.7266/n7-d030-p651
Toxicity of toluene to *Acropora cervicornis*	R6.x825.000:0011	10.7266/n7-ejhs-rs70
Toxicity of toluene to *Porites astreoides*	R6.x825.000:0012	10.7266/n7-gk76-6d98
Toxicity of toluene to *Siderastrea siderea*	R6.x825.000:0013	10.7266/n7-r6jc-bz50
Toxicity of toluene to *Stephanocoenia intersepta*	R6.x825.000:0014	10.7266/n7-g2v6-0s84
Toxicity of toluene to *Solenastrea bournoni*	R6.x825.000:0015	10.7266/n7-3ms6-e633

CHAPTER 3- OIL AND DISPERSED OIL TOXICITY

3.1 INTRODUCTION

The complexity and variable concentration of constituents in crude oil results in differences in toxicity between oils, or between the same oil in different environments, which complicates comparability between tests (NRC 2005, Redman and Parkerton 2015, National Academies of Sciences and Medicine 2019). Measuring the toxicity of all oils, in all environmental conditions is unfeasible, and predicting toxicity is confounded by the effects of different methods of exposure media preparation, relative concentrations, and bioavailability of constituent hydrocarbons in the exposure media (Bejarano et al. 2014, Redman and Parkerton 2015). Alternatively, the toxicity of crude oils can be assessed by determining the toxicity endpoints for single compounds, and employing the Target Lipid Model (TLM) and an oil solubility model to assign toxic units to evaluate the toxicity of dissolved hydrocarbon mixtures (McGrath et al. 2005, McGrath and Di Toro 2009, Redman et al. 2012b, National Academies of Sciences and Medicine 2019).

The initial phase of this work developed inputs to the TLM by assessing the toxicity of several individual hydrocarbons to multiple species of coral in controlled laboratory exposures. Given the log Kow and measured toxicity of each single compound, the CTLBB was derived. Body burdens were calculated from sublethal (EC50) and lethal endpoints (LC50), providing both $CTLBB_{Sublethal}$ and $CTLBB_{Lethal}$. The previously calculated body burdens for the corals in this study indicated relatively high resilience compared to other species, and the central objective of this work was to confirm this resiliency using crude oil and dispersed oil exposures, and to compare effects of each using the toxic unit approach.

The calculated $CTLBB_{Sublethal}$ and $CTLBB_{Lethal}$ for each species were used as inputs to an oil solubility model (Redman 2015) in order to predict subacute and acute toxic endpoints, in addition to determining an LL50 for each coral using PETROTOX (Redman et al. 2012a). The oil solubility model predicts the aqueous concentration of a subset of speciated hydrocarbons (Table S3.1) in the water-soluble fraction (WSF) of whole oil using the parent oil composition and exposure assay conditions. The predicted aqueous phase concentrations are divided by the estimated endpoint (subacute or acute) predicted from the TLM in order to calculate a toxic unit (TU) for each component found in the oil. If the $CTLBB_{Sublethal}$ was used in the model, the estimated TUs referred to the sublethal effect, while the use of $CTLBB_{Lethal}$ resulted in lethal TU

estimates. Regardless of the type, TUs from the subset of hydrocarbons were summed across all constituents and used as the basis for crude oil effects and lethality predictions. This approach produced estimates of oil loadings that would result in significant effects for both species using the TLM and derived TU, which were validated following exposure to MC252 crude oil.

In addition to assessing the relative accuracy of the TU predictions with measured impacts, the TU approach was employed to evaluate the comparative toxicity of crude oil water accommodated fraction (WAF) and chemically-enhanced water accommodated fraction (CEWAF) for two Atlantic coral species. Estimating TU for each compound in the mixture provided a means to evaluate the toxic contribution of different hydrocarbon classes based on the dissolved constituents, as is the recommended method for comparisons of physically and chemically dispersed oil according to the National Academies of Sciences and Medicine (2019).

3.2 METHODS

Experiments with WAF and CEWAF were conducted in the same exposure system, using the same assessment metrics as described for the single hydrocarbon exposures. Five treatments and a seawater control were tested in each of exposures, with three coral fragments in each of the four replicates of the treatment. All exposures were conducted with 24 independent dosing chamber/vessel replicates, which were connected and monitored as previously described in Chapter 2.

3.2.1 Organism collection

The coral species utilized in the WAF and CEWAF exposures were *Acropora cervicornis* and *Porites astreoides,* due to their previously determined relative sensitivity and ease of collection. Fragments of *A. cervicornis* were again collected from the Nova Southeastern University's Offshore Coral Nursery, while *P. astreoides* were collected from a nearshore reef in Broward County, FL within close proximity to the nursery. Colonies were returned to the laboratory and fragmented (2-3 cm branch tips for *A. cervicornis,* and 4 cm^2 fragments for *P. astreoides*) for use in the exposure system. Branching species were attached with a minimal amount of cyanoacrylate gel glue to small numbered aragonite bases, and all corals were acclimated to laboratory conditions in a 1100 L indoor recirculating seawater system for 2-4 wk prior to the exposures, as well as during the post-exposure period. The laboratory holding system was maintained at 35 PSU (using artificial seawater prepared with reverse osmosis water and TropicMarin sea salt) and 26ºC, with water motion supplied by dedicated powerheads and a

wave maker. Artificial light was provided by LEDs (Radion XR30W G4 Pro) that were programmed to mimic sunrise and sunset (photoperiod 12:12) with a spectrum suited for coral growth. Ultraviolet radiation was removed from the LED spectrum to avoid phototransformation of toxicant during the exposure.

3.2.2 Experimental design

Each experiment included a 2 wk pre-exposure period to establish baseline coral health, a 48-h constant exposure, and a 4 wk post-exposure period to assess recovery potential. Five treatments and a seawater control were tested in each of exposures, with three coral fragments in each of four replicates. Corals were not fed, and lighting was provided as described for single compound testing. Along with monitoring the coral fragments, solutions and equipment were monitored for continuous operation within designated limits throughout the duration of exposure.

Exposure to WAF and CEWAF were conducted in the continuous flow toxicity system previously discussed, but recirculation and contaminant delivery were adjusted to reflect the complexity of each dosing media. Collaborative work with Texas A&M GERG lab has aided in the development of a passive-dosing protocol for toxicity tests with crude oil (Redman et al. 2017, Bera et al. 2018), where instead of using silicon O-rings as a partition-controlled chemical reservoir system, the WAF exposures employed oil-loaded silicon tubing. The technique involved injecting oil into silicon tubing, which has been shown to produce a very similar WAF compared to previous physical mixing protocols, without the complicating factor of oil droplets in the exposure media (Bera et al. 2018). Individual exposure chambers were connected to the 2-L dosing vessels by Viton tubing via a Cole-Parmer multihead peristaltic pump, with a flow rate of 5 mL/min. All chambers and vessels were sealed by caps with Teflon-lined septa, and connectors were used to attach Viton tubing. Dosing systems were filled with seawater from the laboratory holding system after being filtered to 1 µm (Polymicro) and UV sterilized, resulting in less than 10% headspace to limit volatile loss of contaminant from the dissolved phase. For each treatment replicate, a predetermined amount of oil was injected into the medical grade silicone tubing (A-M Systems Inc., WA, dimensions of 0.058 X 0.077 X 0.0095-inch) using a gas tight Hamilton syringe, and both ends of the tubing were knotted tightly. The loaded silicone tubing was loosely coiled, submerged, and suspended in each 2 L dosing vessel. The peristaltic pumps were started, and the systems were given 20 h for equilibration; dosing vessels were vigorously stirred throughout the equilibration and exposure periods to ensure partitioning of hydrocarbons

into the aqueous phase. Following the equilibration period, randomly assigned corals were added to each chamber (N=3), and the test initiated.

Recirculating the media in CEWAF exposures was not an option due to the nature of dispersed oil, therefore the exposure system was altered for compatibility with a flow-through dispersed oil exposure. As it cannot be passively dosed, preparation of CEWAF followed standard CROSERF protocol (Aurand and Coelho 2005), with predetermined amounts of oil injected into the mixing vessel, followed by a 1:20 (dispersant:oil) volume of Corexit 9500A before being sealed. Each exposure replicate was independently loaded with oil and dispersant, mixed for 18 h and settled for 4 h prior to dosing the chambers. Due to the volume of media required to supply each chamber over 48 h, dosing vessels were replaced with fresh oil/dispersant mixtures at 24 h that were also independently loaded, mixed, and settled as described previously. Once chambers were full, the randomly assigned corals were added to each chamber (N=3), and the test initiated.

Following the 48-h exposures, one coral from each chamber was immediately preserved for gene expression analysis (Chapter 4), while the remaining coral fragments were transferred back to the acclimation system and immediately analyzed for photosynthetic efficiency and growth. After these measurements, one coral from each chamber was fixed for histological analysis of cellular and tissue changes after 48 h of hydrocarbon exposure. In order to assess the potential for recovery after hydrocarbon exposure, remaining corals were given a 4-wk post-exposure recovery period during which the coral fragments were maintained under the same conditions as described for pre-exposure. Recovery was assessed by monitoring the condition of each coral using the same health metrics as the exposure. At the end of the recovery period, all remaining corals were fixed for histological analysis.

3.2.3 Analytical confirmation of test exposures

Water samples from WAF and CEWAF experiments were collected for analysis of estimated oil equivalents (EOE), volatile organic compounds (VOCs), and total and speciated petroleum aromatic hydrocarbons (TPAH). While EOE was monitored at 0 h and 48 h to verify the stability of aqueous concentrations, VOCs and PAHs were only measured at 48 h. Because passive dosing systems were used for WAF experiments, concentrations of petroleum hydrocarbons from oil were expected to be constant during the period of the experiments.

Measurement of EOE followed the methods described in detail by (Wade et al. 2011, Bera et al. 2018). In summary, maximum intensity at optimal wavelengths (Ex=260, Em=372.05 nm) for crude oil (MC252) were determined and six-point calibration curve was generated using a range of oil concentrations (0.1 mg/L – 10mg/L). Different amounts (0.1 mg/L – 10mg/L) of crude oil were dissolved in dichloromethane to make the calibration standards. The water samples were extracted with dichloromethane and their fluorescence emissions were measured at the predetermined optimal wavelengths. EOE measures aromatic hydrocarbons that contain unsaturated bonds in their structure, which are calibrated against the calibration curve made with known MC252 oil loadings to determine overall aqueous hydrocarbon concentrations.

Water samples for VOCs were collected in 40 ml certified volatile organic analyte vials (Thermo Scientific) with no headspace, and acidified with 70µL of 6M hydrochloric acid (HCl). Samples were analyzed by EPA Method 8260 at AEL Laboratories (Miramar, FL) for VOC measurements in GCMS (Shimadzu QP2010SE with EST Purge & Trap).

For TPAH measurements, the methods of (Wade et al. 2017, Bera et al. 2018) were followed. Water samples (300-500 mL) were collected at 48 h and 100-300 mL dichloromethane was added to each sample for preservation. Samples were spiked with aromatic and aliphatic surrogates (d8-naphthalene, d10-acenaphthene, d10-phenanthrene, d12-chrysene, and d12-perylene for PAHs and d26-nC_{12}, d42-nC_{20}, d50-nC_{24}, and d62-nC_{30} for aliphatic) before extraction with DCM (total 200 mL) in a separatory funnel. The extracts were boiled down (in 55°C water bath) to final volume of 1 mL and GC internal standards were added. The details of temperature program, column used, and quantification method are described in (Bera et al. 2018), and the individual aromatic hydrocarbons determined using this method with associated quantitation limits are listed in Table S3.2. A total of 46 speciated hydrocarbons were determined, which represents a broader target list than the 18 PAHs that are included in the National Status and Trends (NS&T) target list.

3.2.4 Assessment metrics

Metrics used to evaluate the effects of WAF and CEWAF were identical to those used in the single compound testing. As before, metrics were chosen to aid in understanding the full effect of the contaminant on each of the coral species. Coral condition was assessed weekly during the pre-exposure and post-exposure periods, and hourly for the first 8 h after exposure initiation, and every 12 h thereafter for the remainder of the 48-h exposure. Changes in

coloration, polyp extension/retraction, tissue swelling, tissue attenuation, and mucus production were evaluated using the aforementioned coral condition scoring rubric, and were used to determine the sublethal effects endpoints. Mortality was also initially assessed at each time point, but the inability to open the chambers prevented determination of mortality until the end of the exposure (48 h). In some cases, it was possible to identify coral death at 24-36 h, but only mortality at 48 h was discussed here. The relationship between coral mortality and hydrocarbon concentration formed the basis for calculation of the lethal effect endpoints.

Measurements of photosynthetic efficiency were made with a pulse-amplitude-modulation (PAM) fluorometer (Diving-PAM, Walz, Germany). Effective quantum yield was utilized used as an indicator of the physiological status of the autotrophic endosymbiotic zooxanthellae prior to the exposure, immediately after the exposure period, and for the remainder of the post-exposure period. PAM fluorometry measures the light-adapted effective quantum yield [$(F_m–F_o)/F_m$ or $\Delta F/F_m$] of the autotrophic endosymbiotic zooxanthellae by applying a saturation pulse of light and determining yield from the ratio of initial fluorescence (F_o) to maximum fluorescence (F_m). The data collection strategy and measuring parameters were consistent with those used in the single hydrocarbon tests. Using measurements taken twice during pre-exposure holding, immediately before and after each exposure, and after one week and one-month recovery, the change in yield was determined for the time periods: baseline, exposure, 7 days post-exposure recovery, and 28 days post-exposure recovery.

Calcification of the coral fragments was also evaluated using buoyant wet weight determination. Measurements were made one week-, and immediately prior to the exposure to determine a baseline growth rate. Immediately following the exposure, after one week of recovery, and at the end of four weeks of recovery, measurements were also made to determine growth rates (mg gained or lost per day) between these measurements. As before, the change in these rates (mg/d) was determined between each of the time periods to provide the basis for determining the reduction in growth rate following exposure to the contaminant.

3.2.5 Statistical analysis

Data were tested for normality (Shapiro-Wilk) and homoscedasticity (Levenes), transformed to satisfy parametric assumptions, or nonparametric methods were used. Parametric (ANOVA) or nonparametric (Kruskal-Wallis) analysis of variance were used to determine the effects of the treatment groups on each measured parameter at each time point. Tukey’s Unequal

N HSD (parametric) or Conover's pairwise test for multiple comparisons (nonparametric) were used for post-hoc analysis when treatment effects were identified. All statistical tests were performed using R statistical software (V3.6.1) with significance determined using an alpha of 0.05. The geometric mean EOE concentration was determined from the individual chamber replicates of each treatment group, and used to determine the presence of treatment effects on each parameter.

Endpoint concentrations were determined with the *drc* package in R, and were based on subacute (coral condition, photosynthetic efficiency, and growth rate) and acute (mortality) effects at the end of the exposure period (Ritz et al. 2015). The *drm* (dose response model) was used to determine effects of WAF and CEWAF in each test, and because the chambers were variably loaded and independently dosed, the effects associated with each replicate were individually modeled to ensure variability of each response was captured. The dependent variable used in each model was either the sublethal or lethal effects, while the independent variable was adjusted to accurately reflect treatment-dependent exposures (i.e. nominal oil loading, EOE, and TPAH). The log-logistic 4-parameter *drm* was used to determine the 50% effect concentration (EC50) using coral condition scores and mean EOE, while log-logistic 2-parameter *drm* was used to determine the 50% lethal concentration (LC50) from mortality and EOE data. The oil and dispersed oil loadings were used to predict the 50% effect loading (EL50), and the 50% lethal loading (LL50) endpoints, while endpoints were also calculated for each coral species based on aqueous TPAH measurements ($EC50_{PAH}$ and $LC50_{PAH}$).

3.2.6 Water Quality

Water samples for basic water quality were collected at the start and end of the exposure. Nutrients [ammonia (NH_3), nitrite (NO_2), nitrate (NO_3), phosphate (PO_4)] were measured with a HACH DR850 colorimeter; pH, dissolved oxygen (DO) and temperature were measured with a YSI 556 Multiprobe System; and alkalinity was determined by potentiometric titration with a Mettler-Toledo DL22 autotitrator.

3.3 RESULTS

3.3.1 Hydrocarbon Characterization

WAF

In both exposures to crude oil, WAF was generated by passive dosing with whole oil loaded into silicone tubing. The average amount of oil loaded in each treatment, and the resulting mean aqueous EOE and TPAH concentrations are listed in Table 3.1; individual chamber measurements are available in Table S3.3 and S3.4. Both exposures produced aqueous concentrations at or near solubility in the highest loadings used, with some differences in lower loadings due to an elevated dissolved phase measured in the *A. cervicornis* exposure. Figure 3.1.A shows a maximum aqueous concentration of 528 µg/L produced in either exposure, suggesting solubility had been reached.

Table 3.1 Summarized hydrocarbon concentrations for oil WAF exposures to *A. cervicornis* and *P. astreoides*

Species	MC252 Loading[a]	EOE Concentration[b]			TPAH Concentration[b]	
		Mean	se	% change	Mean	sd
A. cervicornis	0	<MDL	NA	NA	<MDL	NA
	12.2	308	18	55.2	23	1
	49.4	304	39	-23.2	74	6
	247.1	392	10	9.5	191	10
	747.9	512	19	-3.6	246	11
	1216.1	527	11	-9.0	274	14
P. astreoides	0	<MDL	NA	NA	<MDL	NA
	12.2	46	10	-0.6	22	2
	49.1	95	8	-9.1	77	16
	243.5	428	17	-7.7	145	27
	760.9	501	32	-7.9	216	7
	1221.7	528	31	-2.2	244	1

[a] mg/L; [b] µg/L

In the *A. cervicornis* exposure, an increase in oil loading from 747.9 mg/L to 1216.1 mg/L only increased the mean EOE concentration in the WAF from 512 µg/L to 527 µg/L. Figure 3.1B and C show the 0 and 48 h, as well as the mean aqueous concentration for each treatment of the *A. cervicornis* and *P. astreoides* WAF exposures, respectively. The two lowest treatments of the *A. cervicornis* exposure resulted in elevated and highly fluctuating dissolved concentrations (+55% and – 23% over time), suggesting a leak in the silicon tubing, or some loss

to the atmosphere. All other treatments had little to no droplets, with consistent dissolved EOE concentrations over time, with an average coefficient of variation (CV) of 18% (*A. cervicornis*) and 10.6% (*P. astreoides*) across all chambers. The variation between replicates of each treatment was also low in both exposures, resulting in a mean CV of 5.4% (*A. cervicornis*) and 9.4% (*P. astreoides*).

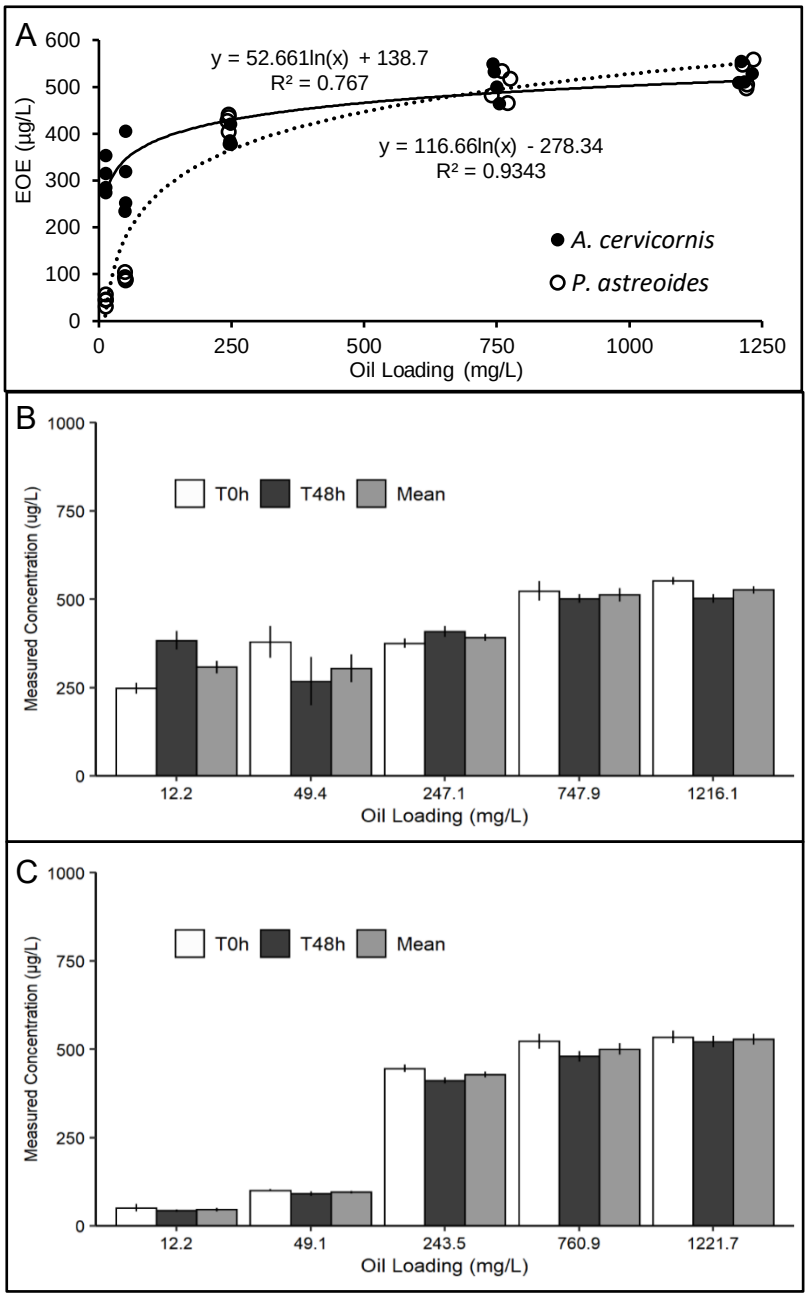

Figure 3. 1 Achieved hydrocarbon concentration in WAFs produced from passive dosing of oil. A) Mean aqueous concentration produced from each loading in the *A. cervicornis* (filled circles and solid line) and *P. astreoides* exposures (open circles and dashed line), and the 0h, 48h, and mean concentration for B) *A. cervicornis* and C) *P. astreoides* treatments.

The WAF produced from each loading of both coral exposures was also analyzed for a target list of aromatic hydrocarbons and the individual measurements are available in Table S3.5 and S3.6. The mean measured PAHs from naphthalene through C4-chrysene for all loadings of both coral exposures are shown Figure 3.2. Overall, the concentrations of the individual PAHs and their alkylated derivatives increased with increased oil loading, with even the lowest loadings producing measurable levels of PAHs. Across all loadings, 1-methylnapthalene and naphthalene were the dominant PAHs measured (100-150 µg/L), with fluorene, phenanthrene, and their alkylated derivatives measuring comparatively lower (< 5 µg/L), but still considerably above background levels. The pattern of dissolved PAHs in these exposures reflected the concentration of the individual PAHs in the parent oil, with high levels of alkylated PAHs.

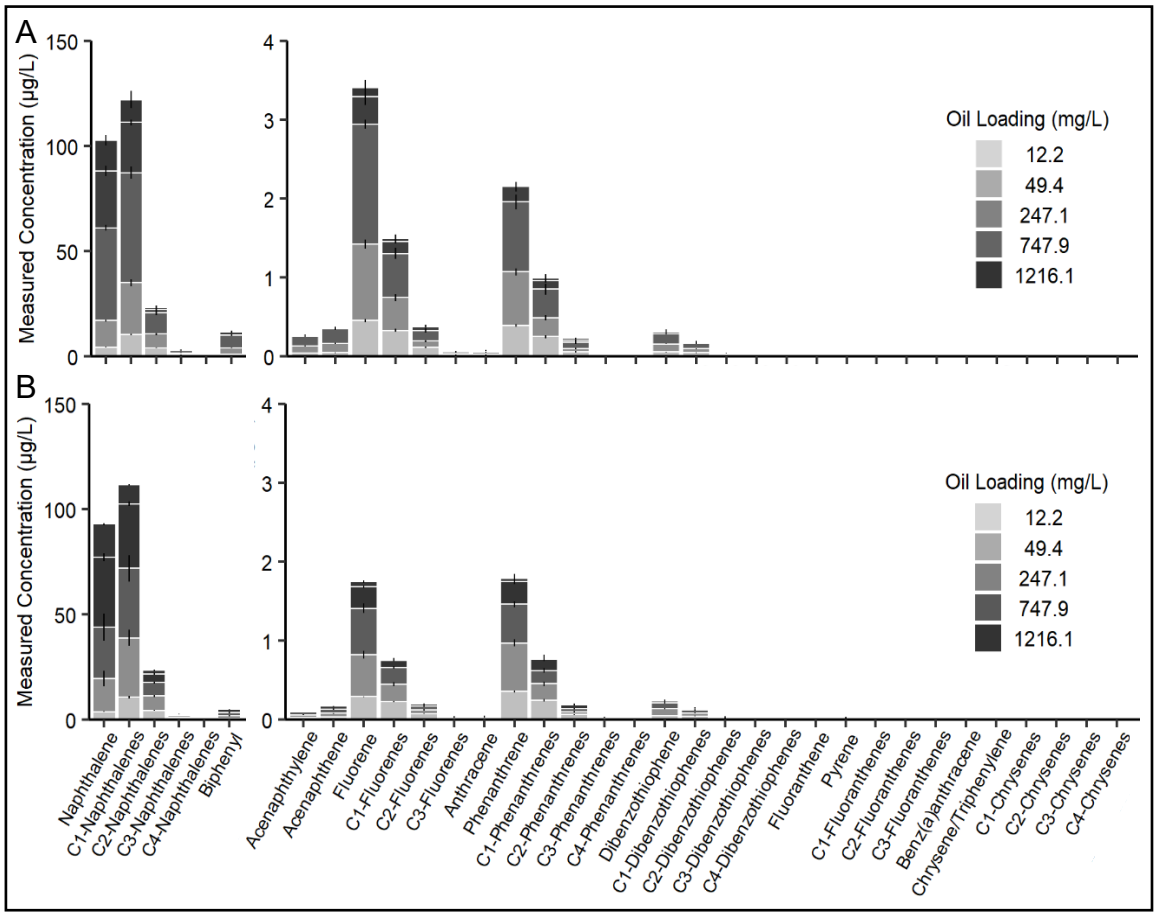

Figure 3.2 Measured PAHs for WAF exposures to A) *A. cervicornis* and B) *P. astreoides*. Note the change in the y-axis between biphenyl and acenaphthylene. Error bars=sd

CEWAF

Oil and dispersant were added to seawater to produce the individual CEWAFs for each treatment replicate of both exposures. Table 3.2 shows the mean oil loading, EOE and TPAH concentration for each treatment of both exposures (individual chamber values are in Table S3.7 and S3.8). As expected, increases in oil and dispersant loading resulted in an overall increase in the dissolved concentrations due to droplet dissolution. Compared to similar oil loadings from WAF exposures, addition of dispersant resulted in 10–100 times higher average EOE concentrations. Figure 3.3.A shows the achieved mean EOE from each oil and dispersant loading for both exposures. Dispersant addition resulted in CEWAF hydrocarbon levels above the solubility observed in the WAF exposures, presumable due to the increase in droplet concentrations. There was also more variation in aqueous concentrations of treatment replicates (CV = 13 % *A. cervicornis* and 21 % *P. astreoides*). Additionally, the variation in aqueous concentrations within each chamber over time was higher in CEWAF exposures (CV = 35% *A. cervicornis* and 27 % *P. astreoides*) compared to WAF (Figure 3.3.B and C).

Table 3.2 Hydrocarbon characterization for all *A. cervicornis* and *P. astreoides* treatments exposed to CEWAF

Species	MC252 Loading[a]	EOE Concentration[b]			TPAH Concentration[b]	
		Mean	se	% change	Mean	sd
A. cervicornis	0	<MDL	NA	NA	<MDL	NA
	10.1	319	56	78	45	2
	25.3	769	108	105	88	6
	50.8	1786	191	29	136	12
	250.6	26704	5392	0.7	504	152
	734.8	91261	3016	-7	1064	100
P. astreoides	0	<MDL	NA	NA	<MDL	NA
	10.6	214	13	-21	39	2
	51.3	2654	596	-33	132	8
	125.5	18063	10214	-49	313	160
	226.0	34790	4340	3	523	133
	751.1	172454	12819	62	2201	93

[a] mg/L; [b] µg/L

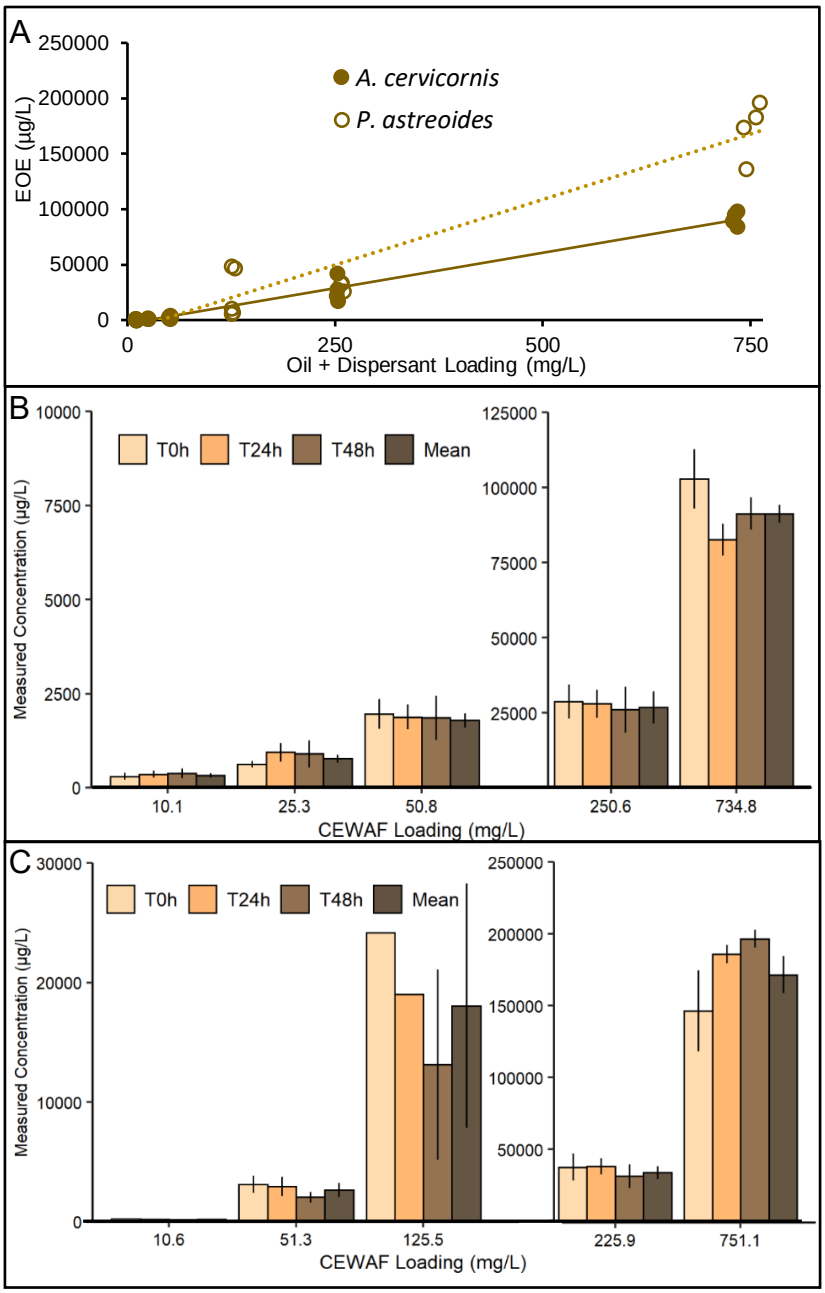

Figure 3.3 Achieved hydrocarbon concentration in CEWAFs produced from variably loading oil and dispersant (20:1). A) Mean aqueous concentration produced from each loading in the *A. cervicornis* (filled circles and solid line) and *P. astreoides* exposures (open circles and dashed line) and the 0h, 24, and 48 h, and mean concentration for B) *A. cervicornis* and C) *P. astreoides* treatments.

The same target list of PAHs measured following WAF exposure were also measured in each of the chambers following exposure to CEWAF (Table S3.9 and S3.10). Figure 3.4 shows the mean concentration of each PAH for all loadings of both CEWAF exposures. The composition dissolved PAH profiles of CEWAF exposures revealed compositional differences

that changed as loadings increased. At lower loadings of both CEWAF exposures (≤ 50mg/L), a PAH profile similar to WAF loadings of the same level was observed. Aqueous concentrations of naphthalene and 1-methylnaphthlene were between 10-20% higher in CEWAF exposures, while increases of 5-10x the concentration of fluoranthene, phenanthrene, and methylated derivatives were observed at this level. At loadings near 250 mg/L, naphthalene and 1-methlynaphthalene in CEWAF exposures were 42-57% higher than WAF exposures, with increases of 10-20x observed for fluoranthene, and phenanthrene (and methylated derivatives). The highest common loading of WAF and CEWAF exposures, roughly 750 mg/L, produced aqueous PAH profiles with the most drastic differences. Naphthalene in CEWAF increased by 47% and 166%, while 1-methylnaphthalene was 140% and 400% higher than WAF exposures for *A. cervicornis* and *P. astreoides*, respectively. The concentrations of fluoranthene and methylated derivatives did not increase as drastically, only being 2-10x the WAF levels, while phenanthrene was much more enhanced in CEWAF compared to WAF, with levels 20-50x higher. Overall, all PAHs were enhanced in CEWAF exposures compared to WAF, but more drastic increases in the ≥ 3-ring PAHs were observed, particularly at loadings at and above 125.5 mg/L.

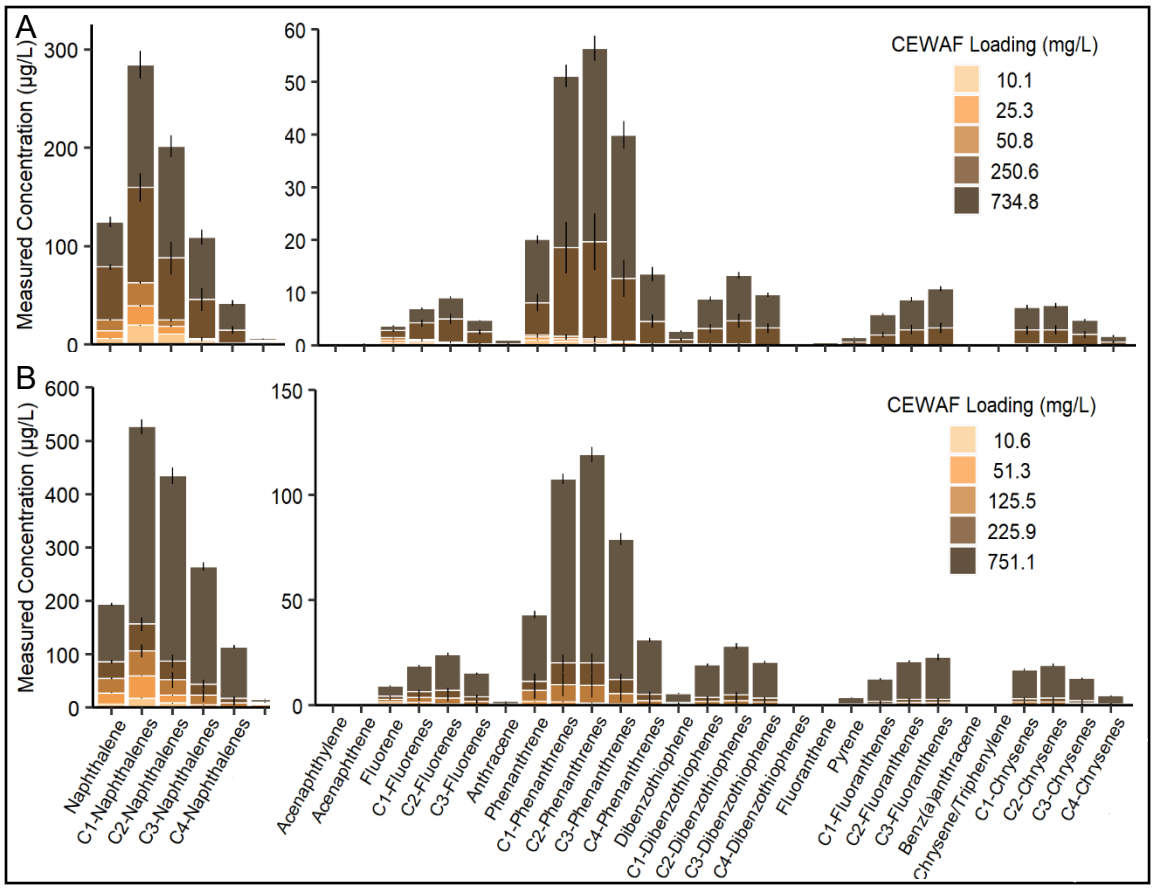

Figure 3.4 Measured PAHs for CEWAF exposures to A) *A. cervicornis* and B) *P. astreoides.* Note the change in the y-axis between biphenyl and acenaphthylene. Error bars=sd

3.3.2 Impacts of exposure to WAF and CEWAF

WAF

Impacts to the coral condition scores of *A. cervicornis* and *P. astreoides* from exposures to crude oil WAF were significant at all tested time points (Figure 3.5). Overall, maximum coral condition scores were less than 50% in both exposures, with *A. cervicornis* experiencing a slightly higher maximum effect (43.4%) compared to *P. astreoides* (38.2%). From 1–48 h, the coral condition of *A.* cervicornis showed significantly elevated scores in the top doses of WAF compared to controls. The 392 µg/L WAF dose resulted in significantly elevated scores compared to controls from 1–12 h, and again at 36 h, but not at 48 h. The 308 and 304 µg/L WAF doses resulted in limited impacts to coral condition, with no significant differences compared to controls, except at 7 h when the 304 µg/L dose was significantly higher. By 48 h, only WAF doses at and above 512 µg/L EOE scored significantly higher than controls.

The coral condition of *P. astreoides* was similarly impacted, but to a comparatively lesser extent than *A. cervicornis.* The top two doses of WAF (501 µg/L and 528 µg/L) scored significantly higher than controls for the entire 48 h exposure. The mid-level dose, 428 µg/L WAF, was significantly higher than controls from 3-24 h, and again at 48 h. The coral condition of the 95 µg/L WAF doses scored similar to controls until 48 h, when it scored significantly higher for the first time. The lowest dose, 46 µg/L WAF, did not score significantly higher than controls at any time point.

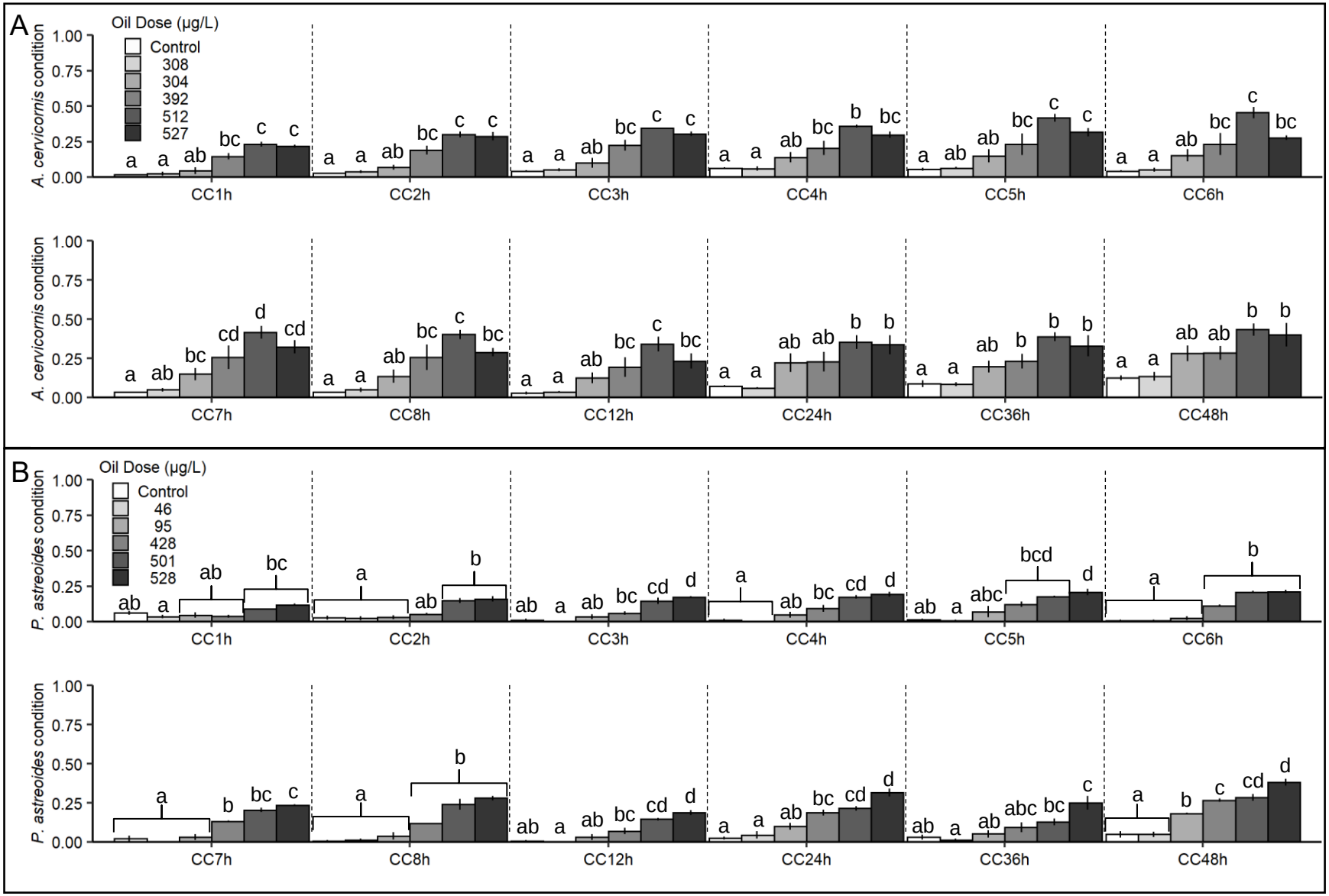

Figure 3.5 Sublethal effects determined with coral condition scores of A) *A. cervicornis* and B) *P. astreoides* during exposure to WAF. Bars with the same letter on each time point were not significantly different, error bars= standard error, n=4.

There were no significant differences in growth rates for either coral, for any of the time periods assessed (Figure S3.1). Declines in growth rate did occur, but high variability within treatment groups and control effects eclipsed a clear trend. The mean quantum yield for each treatment group is shown in Figure 3.6, and shows few impacts following exposure to WAF. There were significant effects of exposure on the yield of *A. cervicornis*, but none of the treatments were statistically different than controls. The yield of the 512 µg/L WAF dose was significantly lower than the 304 µg/L and 392 µg/L WAF doses, but remained similar to controls. A declined growth rate in the 512 µg/L dose was also observed during the baseline assessment period, although not significant.

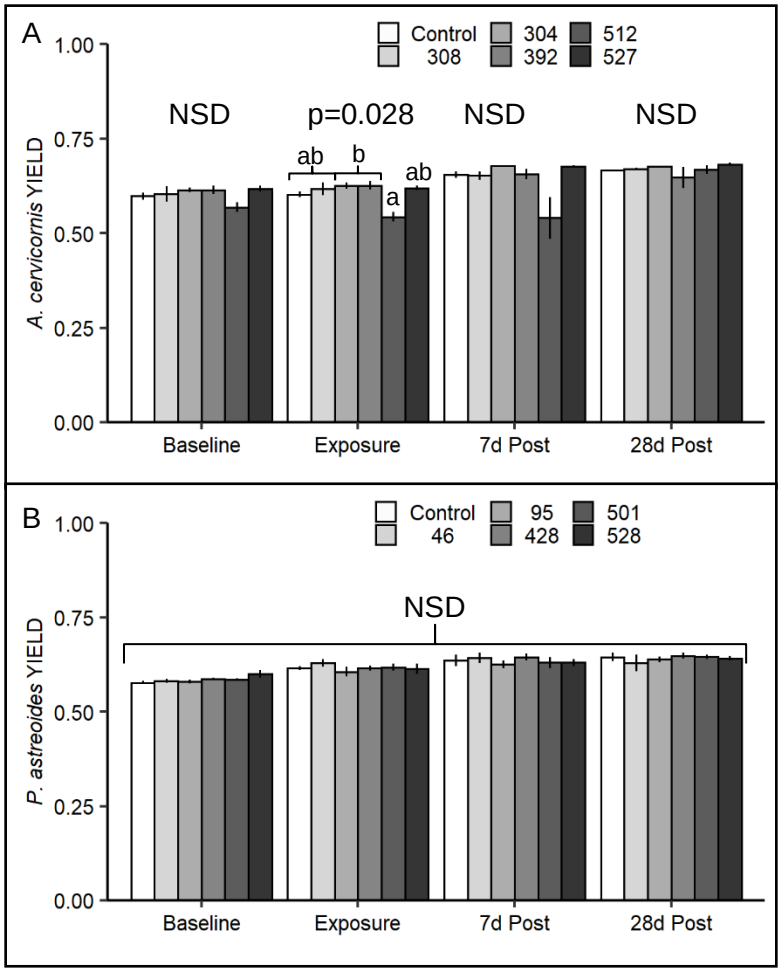

Figure 3.6 Effects of WAF treatments (µg/L) on A) *A. cervicornis* and B) *P. astreoides* quantum yield for the indicated time periods

Mortality was visually assessed at the end of the exposure for both species. There was only one dead fragment of *A. cervicornis* from the highest WAF dose, resulting in a maximum treatment mortality of 8.3%. All other treatments of both tests resulted in no mortality following exposure to crude oil WAF.

CEWAF

Consistent with results of the WAF testing, mean coral condition scores were significantly impacted at all time points of both coral exposures to CEWAF (Figure 3.7). Overall, effects to the coral condition after 48 h were minimal in low to moderate levels of CEWAF (10–36 % effect), and severe in the highest treatments (100%). Important to note, the highest treatment of each exposure, 91261 µg/L *A. cervicornis* and 172454 µg/L *P. astreoides*, were not hourly scored due to the inability to see through suspended oil, but eventual total mortality allowed a 100% effect to be assigned these levels. From 1–48 h exposure, *A. cervicornis* condition scores were significantly elevated in the 1786 µg/L 26704 µg/L CEWAF doses compared to controls. The 770 µg/L CEWAF dose first scored significantly higher than controls at 2 h, and remained higher through 48 h. The lowest CEWAF dose, 319 µg/L, scored significantly higher than controls from 6–7 h, and 12 h exposure, with scores again elevated at 48 h. Exposure to CEWAF resulted in significantly elevated coral condition scores of *P. astreoides* after 1 h. Compared to controls, scores of the 18063 µg/L and 34790 µg/L CEWAF doses remained significantly higher through 48 h, with maximum effects of 36.5 and 50 %, respectively. The 2654 µg/L CEWAF dose resulted in elevated condition scores at 3 h, 6–8 h, and from 24–48 h, while the lowest dose, 214 µg/L, only scored significantly higher than controls at 24 and 48 h.

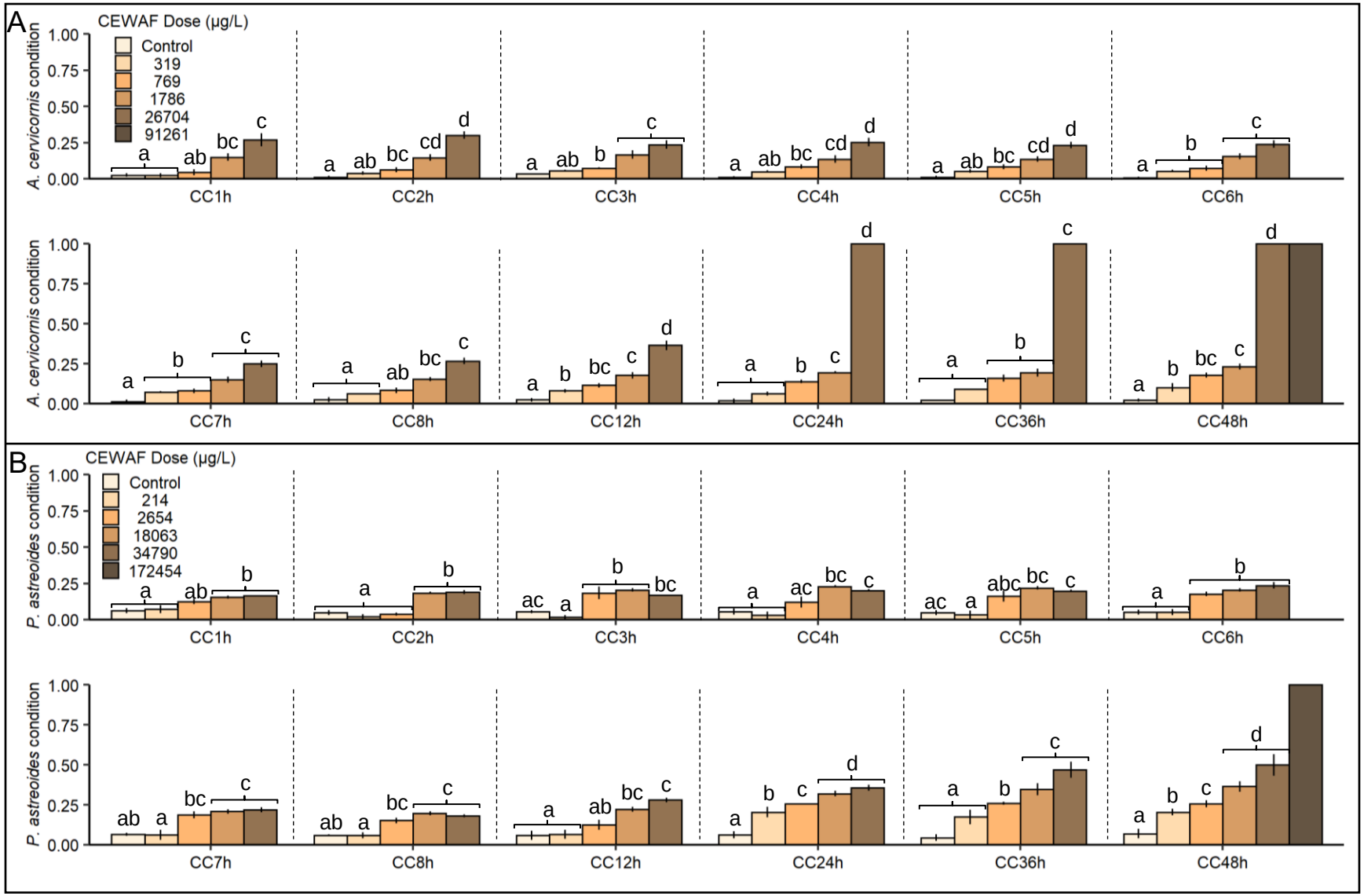

Figure 3.7 Sublethal effects determined with coral condition scores of A) *A. cervicornis* and B) *P. astreoides* during exposure to WAF. Bars with the same letter on each time point were not significantly different, error bars= standard error, n=4.

The growth rate of *A. cervicornis* was not significantly impacted by CEWAF exposure at any measured time period (Figure 3.8.A). Reductions in growth rate were observed in all treatments including controls, but none were significantly different. The growth rates of *P. astreoides* were significantly impacted during the CEWAF exposure (Fig. 3.8.B). Although reductions in growth rates are observed across all treatments, post-hoc analysis failed to resolve differences between treatment groups. The mean quantum yield for either coral species was not significantly impacted by exposure to CEWAF at any of the measured time periods (Figure S3.2).

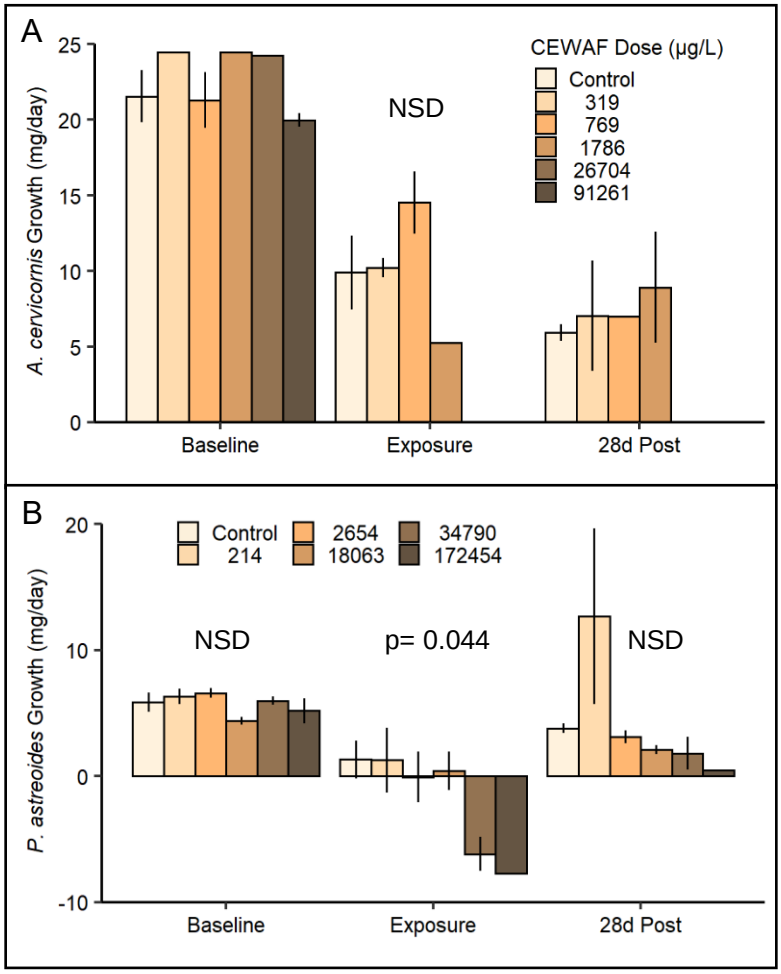

Figure 3.8 Growth rate (mg/day) at each time point of the A) *A. cervicornis* and B) *P. astreoides* CEWAF exposures

Exposure to CEWAF resulted in no mortality in low-moderate treatments, with 100% mortality in the highest treatments of both coral exposures. The 26704 µg/L and 91261 µg/L CEWAF doses to *A. cervicornis,* and the 172454 µg/L CEWAF dose to *P.* astreoides caused

100% mortality after 48 h exposure. One fragment of *P. astreoides* in the highest CEWAF dose initially appeared to survive the exposure, but died with 24 h recovery and was therefore assumed dead at 48 h.

3.3.3 Endpoints and Species Sensitivity

The significant sublethal and lethal effects incurred from exposure to WAF and CEWAF were used to calculate sublethal and lethal endpoint concentrations for both coral species using the *drc* package in R. Figure 3.9 shows the models produced using the coral condition of each species and measured EOE, oil loading, or measured TPAH concentrations from WAF and CEWAF exposures. Sublethal endpoints were determined for multiple methods of hydrocarbon characterization to increase the comparability between exposures in this study (Table 3.3). In general, the low-level effects in the highest WAF treatments (38.2–43.4%) resulted in model predictions of EC50 and $EC50_{PAH}$ for both species slightly above the highest concentrations measured. In contrast, high effects in CEWAF exposures produced confident estimates of EC50 that were 6X higher for *A. cervicornis* and 28x higher for *P. astreoides* exposed to WAF (Fig. 3.9.A, D). The $EC50_{PAH}$ values were also confidently estimated following CEWAF exposure (Fig. 3.9.C, F), which showed a reduction in the *A. cervicornis* estimate, and a slight increase in the *P. astreoides* TPAH endpoint compared to their respective WAF exposures. Oil loading levels were also used to calculate EL50 values for all exposures and resulted in a similar trend for both species (Fig. 3.9.B, E). Exposure to WAF produced estimates of EL50 above the highest loading used, while CEWAF exposures resulted in higher effects at lower loadings, and EL50 values of 82.3 mg/L for *A. cervicornis* and 239.1 mg/L for *P. astreoides*.

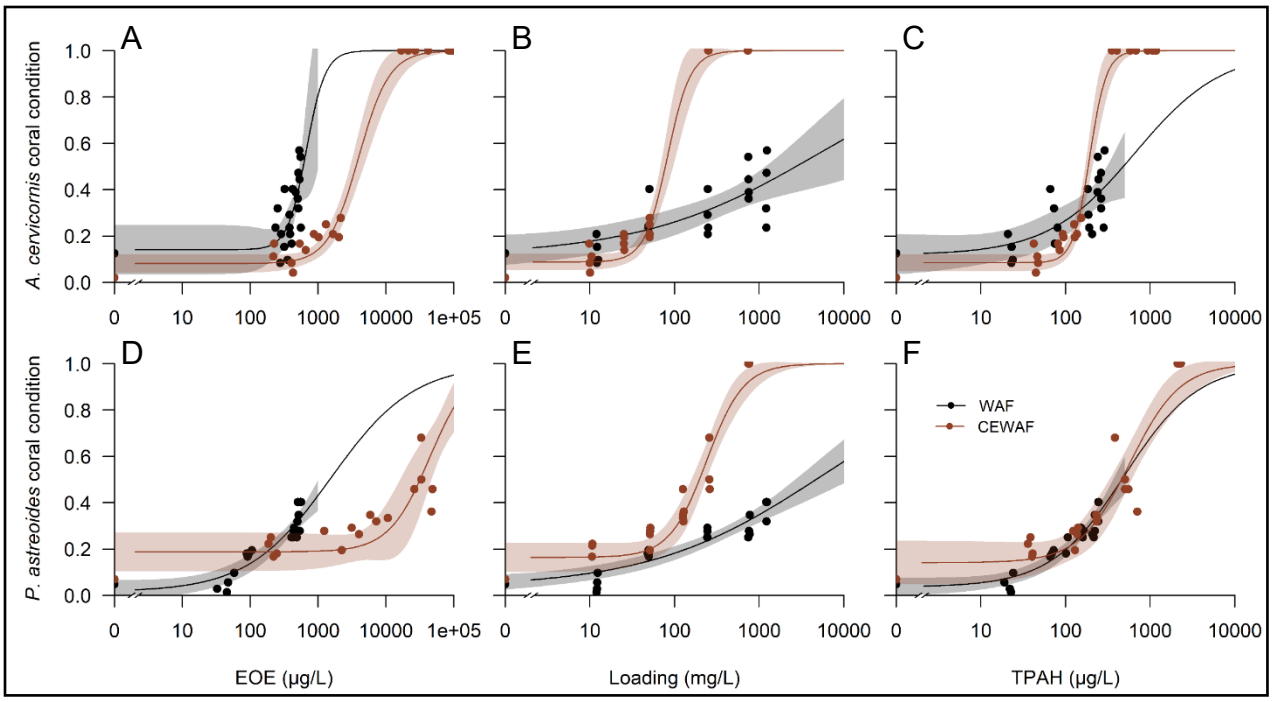

Figure 3.9 Dose response curves for the coral condition of *A. cervicornis* and *P. astreoides* after 48 h exposure to WAF and CEWAF. A&D) EOE concentration in each chamber used for EC50, B&E) Oil loading of each chamber used for EL50, and C&F) TPAH concentration in each chamber used for $EC50_{PAH}$. Points indicate the mean score and concentration of each chamber. Lines and shading represent the *drc* model and 95% confidence interval for each relationship.

Changes to the growth rates and quantum yields of both species were also evaluated for the WAF or CEWAF exposures to determine the level that produced a 50% inhibition in the growth rate ($IC50_{GROWTH}$) or yield ($IC50_{YIELD}$). The only significant effects of WAF exposure were on the change in quantum yield of *A. cervicornis*, which produced a highly significant $IC50_{YIELD}$ of 386 µg/L (95% CI= 378–393 µg/L, $p= 2.2^{-16}$) following the 48 h exposure (Figure S3.3). Exposure to CEWAF resulted in significant treatment effects on growth of *P. astreoides*, but model estimates of $IC50_{GROWTH}$ (17862 µg/L) were not-significant (p=0.596). No significant differences in *A. cervicornis* growth or quantum yield occurred following exposure to CEWAF.

Table 3.3 Calculated effect and lethal endpoints for WAF and CEWAF exposures to *A. cervicornis* and *P. astreoides*

Endpoint	Units	*Acropora cervicornis*		*Porites astreoides*	
		WAF	CEWAF	WAF	CEWAF
EC10	µg/l	332 (157-508)	1264 (790-1738)	70 (3-137)	9679 (0-23812)
EC50	µg/l	670[a]	3951 (2993-4910)	1547[a]	43879 (22971-64787)
$EC50_{PAH}$	µg/l	658.9[a]	192.5 (172-213)	496.3[a]	572.6 (370-775)
EL50	mg/L	> 1216.1	82.3 (68-97)	> 1221.7	239.1 (188-291)
LC50	µg/l	> solubility	6045	> solubility	82179
$LC50_{PAH}$	µg/l	> solubility	231.1	> solubility	1202.2
LL50	mg/L	> 1216.1	112.5	> 1221.7	435.6

[a] > highest concentration and estimate extrapolated

The proportion of coral fragments dead in each chamber at 48 h was used to calculate lethal endpoint for exposures that resulted in enough mortality. Figure 3.10 shows the *drc* models produced from mortality data following exposures to WAF and CEWAF. Although some mortality was present in the highest dose (8.3%), estimates of lethal endpoints from WAF exposure to *A. cervicornis* were above the highest concentration measured or amount of oil loaded, and were not significant. No mortality in the *P. astreoides* WAF exposure also prevented determination of lethal endpoints. Both exposures to CEWAF resulted in 100% mortality in high doses, resulting in estimates of lethal endpoints for both species (Table 3.3), but an absence of partial mortality prevented determination of confidence intervals for all measured parameters. The CEWAF LC50 determined from aqueous hydrocarbon concentrations was 10X lower for *A. cervicornis* (6045µg/L) compared to *P. astreoides* (82179 µg/L).

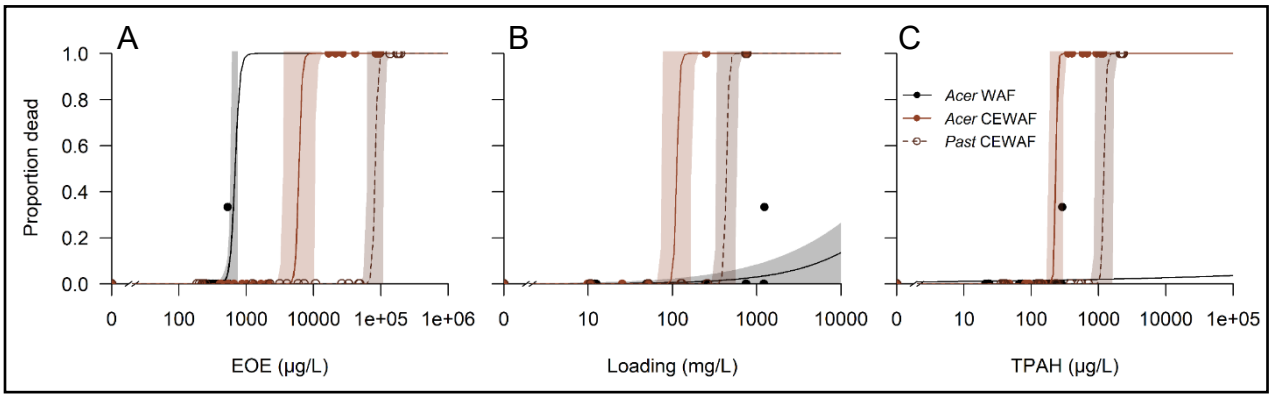

Figure 3.10 Dose response curves for lethality of *A. cervicornis* and *P. astreoides* after 48 h exposure to WAF and CEWAF. A) EOE concentration in each chamber used for LC50, B) Oil loading of each chamber used for LL50, and C) TPAH concentration in each chamber used for $LC50_{PAH}$. Points indicate the mean score and concentration of each chamber. Lines and shading represent the *drc* model and 95% confidence interval for each relationship.

3.3.4 PETROTOX, the Solubility Model, and Toxic Units

PETROTOX

The whole oil composition, test system parameters, and organism CTLBB were input to PETROTOX to generate and estimated LL50 for both coral species. Using the 1500+ compounds in the PETROTOX database, TU were assigned used to assess the toxic contribution of hydrocarbon classes. The TU contributions of each hydrocarbon class are a function of test oil composition, and are therefore the same for *A. cervicornis* and *P. astreoides.* The lightweight aromatic composition of this oil was estimated to result in a WAF dominated by MAHs (45%) and 2-ring PAHs (34%), with 5% contribution from ≥3-ring PAHs, together combining for 84% of the TU estimated here. The TUs generated by PETROTOX were used to estimate effects of increasing oil loadings as a means of generating an LL50s for both coral species. PETROTOX estimated maximum TU of 0.85 (*A. cervicornis*) and 0.73 (*P. astreoides*), resulting in estimates of LL50 >1000 mg/L loading for both species, presumably due to solubility constraints.

Speciated Solubility Model: WAF

The MC252 oil composition and average loading for each treatment were input into the speciated solubility model previously described, to simulate the dissolved concentrations for select hydrocarbons of both WAF exposures (Figure 3.11). Overall, predicted and measured dissolved hydrocarbon concentrations correlated well within each treatment for both exposures (Spearman R= 0.963-0.976 for all treatments). As the distance of each point to the 1:1 line indicates, the model generally overestimated the aqueous concentration of most monoaromatics, while underestimating the aqueous concentration of many ≥3-ring PAHs compared to the measured values.

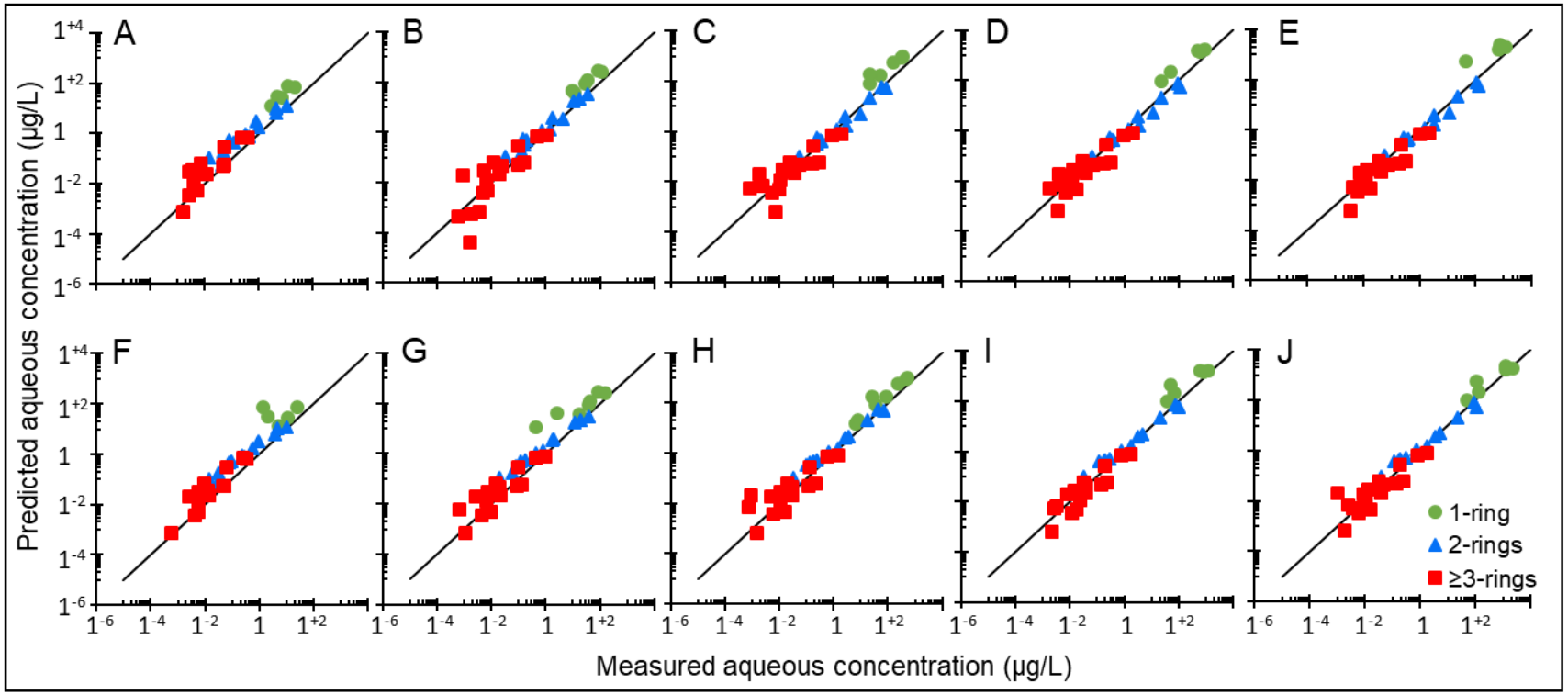

Figure 3.11 Predicted vs measured concentrations of 1-, 2-, and ≥3-ring aromatic hydrocarbons in the *Acropora* cervicornis A) 12.2 mg/L, B) 49.4 mg/L, C) 247.1 mg/L, D) 747.9 mg/L, E) 1216.1 mg/L oil loadings, and *Porites astreoides* F) 12.2 mg/L, G) 49.1 mg/L, H) 243.5 mg/L, I) 760.9 mg/L, and J) 1221.7 mg/L oil loadings

Deviation of measured concentrations from predicted values depended on the hydrocarbon class, but also on the oil loading (Figure 3.12). Monoaromatic hydrocarbons and VOCs were difficult to measure, and were on average 63.0% (*A. cervicornis*) and 50% (*P. astreoides*) less than predicted values for compounds above minimum detection, regardless of the oil loading. The predicted concentration of di-aromatic PAHs was more accurate than MAHs, with aqueous concentrations on average of 6.7% and 36% less than estimated levels for *A. cervicornis* and *P. astreoides*, respectively. Oil loading had a positive effect on this relationship in the *A. cervicornis* WAF exposure, with low loadings producing aqueous concentrations 32-56% lower than predicted, while high loadings resulted in measured concentrations 20-25% higher than predicted levels. This pattern was also observed in the *P. astreoides* exposure, although measured concentrations were less than predictions across all oil loadings (64.6-14.1%). Aromatics with ≥3 rings were on average 64.6% and 30% above estimated levels for *A. cervicornis* and *P. astreoides* exposures, respectively, and exhibited a similar pattern across oil loadings as observed for di-aromatics. For both species tested, low oil loadings produced a WAF with aqueous concentrations less than predicted, while mid-range and high oil loadings produced higher than predicted levels of ≥3-ring PAHs.

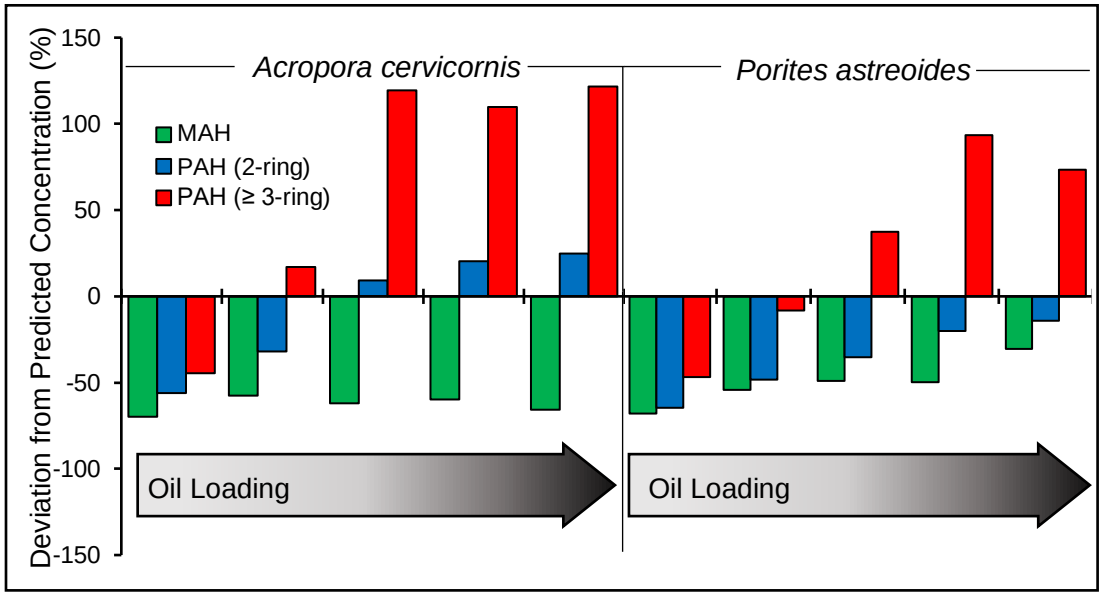

Figure 3.12 The difference between measured and predicted concentration of aromatic hydrocarbons for WAF exposures to *A. cervicornis* and *P. astreoides.*

Speciated Solubility Model: CEWAF

The oil loadings used in the dispersed oil tests were also input into the oil solubility calculator in order to simulate the resulting WAF if no dispersant were applied. Although the solubility calculator is not meant to predict the composition of dissolved compounds in CEWAF, it does provide an estimated baseline concentration for each hydrocarbon for comparison with measured values following dispersant application. Figure 3.13 shows the comparison of predicted and measured concentration for all detected aromatic hydrocarbons of 1-, 2-, or ≥3-rings in the CEWAF exposures. Consistent with WAF exposures, the measured concentrations of MAHs were less than predicted values by 17.2-72.1 % for both species across all dispersed oil loadings, except the highest *P. astreoides* loading, which resulted in MAH concentrations 117% higher than predicted. The lowest loadings of both species also produced lower than expected levels of 2-ring PAHs, measuring 10.1 and 27.3% less than predictions. The two highest dispersed oil loadings for both species produced variable levels of 2-ring aromatics up to 4588% predicted concentrations. This increase in measured concentrations extended into the ≥3-ring PAHs, with nearly all dispersed oil loadings producing over 100% higher levels than predicted for oil with no dispersant applied.

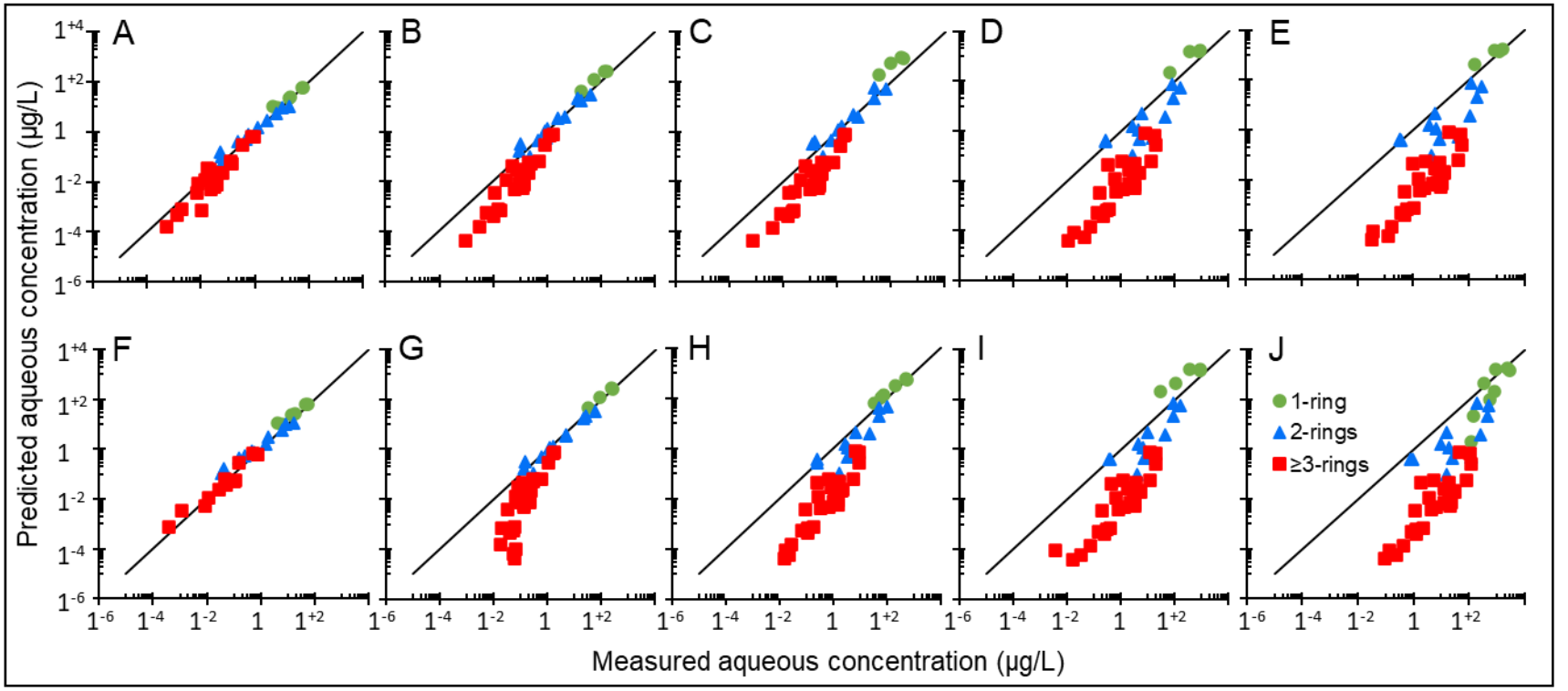

Figure 3.13 Predicted vs measured concentrations of aromatic hydrocarbons in the *Acropora cervicornis* A) 10.1 mg/L, B) 25.3 mg/L, C) 50.8 mg/L, D) 250.6 mg/L, E) 734.8 mg/L dispersed oil loadings, and *Porites astreoides* F) 10.1 mg/L, G) 51.3 mg/L, H) 125.5 mg/L, I) 226.0 mg/L, and J) 751.1 mg/L dispersed oil loadings.

Speciated Solubility Model: Toxic Units

The TLM derived species specific CTLBBs were used in the oil solubility calculator to estimate toxic units (TU) for the simulated WAF produced from all oil loadings of both coral exposures (Table 3.4). Measured aqueous concentrations were not used to predict TU, because only a small fraction of the compounds were measurable above detection limits. Measured concentrations of nearly all MAHs and PAHs were similar to, or slightly less than predicted levels, which provided cause to assess WAF TU using the predicted concentrations of all compounds included in the solubility model. Sublethal (from the ETLBB) and lethal (from the CTLBB) TU were assessed for each of the loadings used, but only the more sensitive sublethal TU are outlined in detail. The total lethal TU estimated for *A. cervicornis* and *P. astreoides* resulted in an overestimation of toxicity, as there was a lack of mortality in both WAF exposures.

Table 3.4 The toxic units and predicted effects for *A. cervicornis* and *P. astreoides* following WAF exposure

	MC252 Loading[a]	EOE[b]	TPAH[c]	Sublethal Effect			Lethal Effect		
				TU[d] sum	Predicted %	Measured %	TU sum	Predicted %	Measured %
A. cervicornis	12.2	308	22.6	0.143	7.2	13.5	0.150	7.5	0.0
	49.4	304	73.5	0.297	14.8	28.1	0.296	14.8	0.0
	247.1	392	191.3	0.536	26.8	28.5	0.520	26.0	0.0
	747.9	512	246.4	0.674	33.7	43.4	0.649	32.5	0.0
	1216.1	527	273.5	0.722	36.1	39.9	0.694	34.7	8.3
P. astreoides	12.2	46	21.9	0.120	6.0	4.9	0.076	3.8	0.0
	49.1	95	77.0	0.248	12.4	18.1	0.148	7.4	0.0
	243.5	428	145.1	0.447	22.3	26.7	0.260	13.0	0.0
	760.9	501	216.2	0.566	28.3	28.5	0.327	16.4	0.0
	1221.7	528	243.6	0.602	30.1	38.2	0.347	17.3	0.0

[a] mg/L; [b] estimated oil equivalents (µg/L); [c] Total polyaromatic hydrocarbon (µg/L); [d] Total toxic units

The $CTLBB_{Sublethal}$ was used to estimate sublethal effect TU to predict the impacts of WAF exposure on both species. Figure 3.14 shows the total effect TU, and TU of each hydrocarbon class predicted for both *A. cervicornis* and *P. astreoides* exposures to WAF (Table S3.11). The toxicity of a mixture is assumed to be represented by the total TU in the dissolved phase, which was predicted to reach a maximum level dependent upon the level of hydrocarbon dissolved in each WAF.

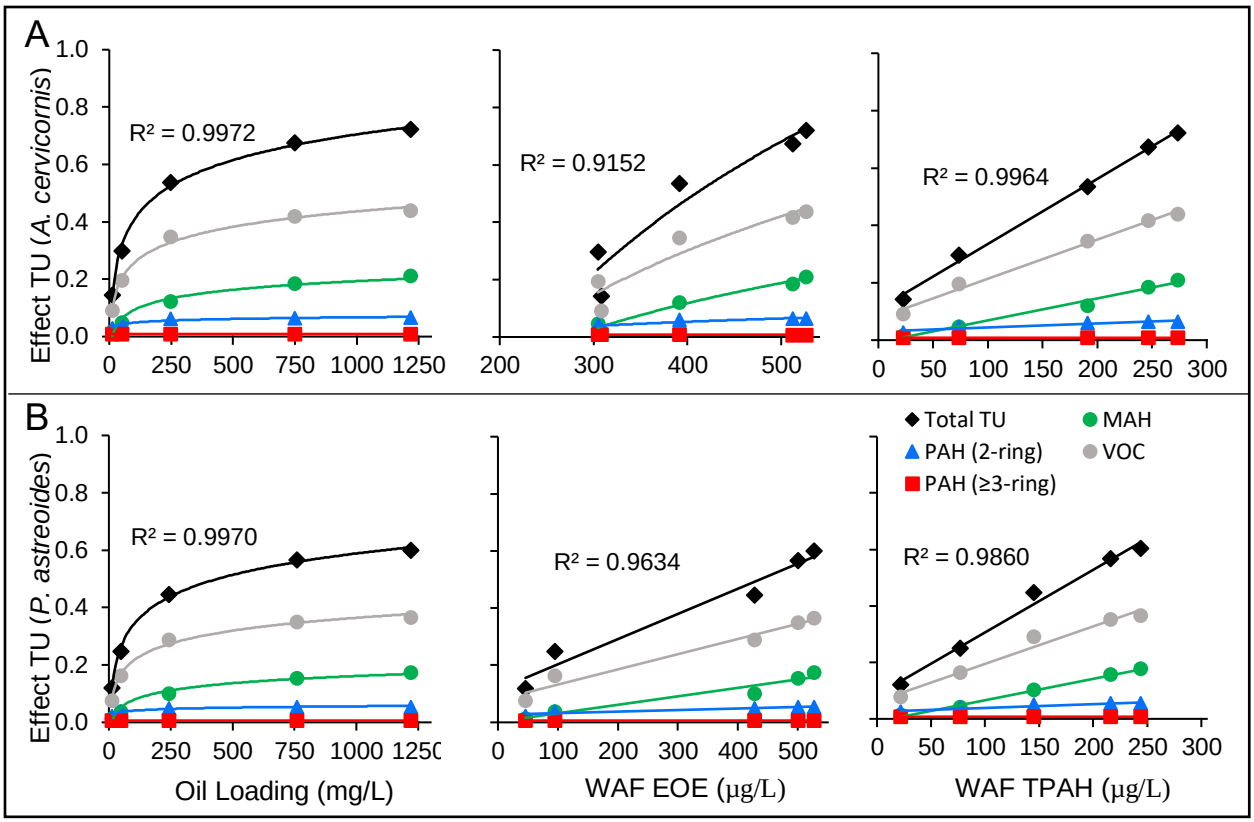

Figure 3.14 A) *A. cervicornis* and B) *P. astreoides* sublethal toxic units determined by oil loading, EOE, and TPAH for multiple hydrocarbon classes of WAF exposures

For both exposures, average WAF TU contributions were dominated by VOCs (63.3%) and MAHs (21.2%), followed by 2-ring PAHs (13.0%), and ≥3-ring PAHs (2.5%) (Figure 3.15). The effect TUs for each treatment group were summed and used to predict the sublethal percent effect for both species at all oil loading levels (Table 3.4). Maximum TU of 0.722 in *A. cervicornis* and 0.602 in *P. astreoides* suggested maximum sublethal effects of WAF exposure were 36.1% and 30.1%, respectively. The relationships between total sublethal effect TUs and either loading, EOE, or TPAH concentrations, can be used to calculate effect endpoints for each parameter, but total effect TU were less than 1 (<50% effect), so EL50, EC50, and $EC50_{PAH}$ were estimated above the highest value measured.

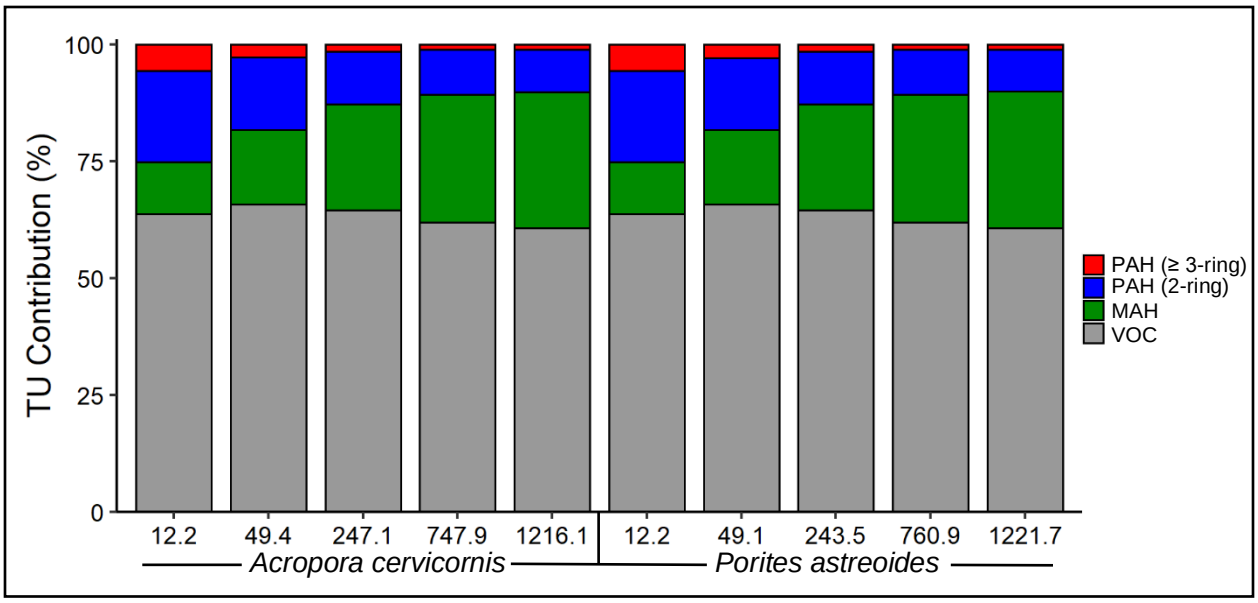

Figure 3.15 The contribution of hydrocarbon classes to the total predicted TU from multiple oil loadings (mg/L) during WAF exposures to *A. cervicornis* and *P. astreoides*

The $CTLBB_{Sublethal}$ and $CTLBB_{Lethal}$ were also used to estimate effect and lethal TU for dispersed oil exposures to both species, but characterizing the TU for CEWAF required a combination of measured and predicted aqueous concentrations because the model was not designed to predict dispersant effects on hydrocarbon dissolution. Although dispersant was used, measurements of detected MAHs in the CEWAF were generally less than or agreed well with the values predicted for undispersed oil, except in the highest dispersed oil loadings. Measurements of MAHs and VOCs for each compound were used if detected, or predicted levels were used to ensure the minimum levels of these hydrocarbon classes were represented in TU analysis of each CEWAF. The total TUs for each dispersed oil loading for both corals indicated maximum sublethal and lethal effects (100%) would occur following exposure to CEWAF (Table 3.5).

The total sublethal effect TU, as well as the contribution of each of hydrocarbon class, for the dispersed oil loadings, EOE, and TPAH are shown in Figure 3.16. The actual effect TU contribution of each hydrocarbon class to the total TU of each dispersed oil loading is available in Table S3.12. The dissolved phase measured in CEWAF exposures did not reach a maximum concentration as observed in the WAF exposure, which resulted in a near linear increase in TU with dispersed oil loading as a function of the presence of droplets.

Table 3.5 The toxic units and predicted effects for *A. cervicornis* and *P. astreoides* following CEWAF exposure

	MC252 Loading[a]	EOE[b]	TPAH[c]	Sublethal Effect			Lethal Effect		
				TU[d] sum	Predicted %	Measured %	TU sum	Predicted %	Measured %
A. cervicornis	10.1	319	45.1	0.132	6.6	10.1	0.126	6.3	0.0
	25.3	769	88.3	0.318	15.9	17.7	0.299	14.9	0.0
	50.8	1786	135.9	0.542	27.1	23.3	0.495	24.7	0.0
	250.6	26704	503.7	1.525	76.3	100.0	1.434	71.7	100.0
	734.8	91261	1063.7	3.248	162.4	100.0	3.053	152.6	100.0
P. astreoides	10.6	214	38.8	0.103	5.2	20.5	0.058	2.9	0.0
	51.3	2654	132.4	0.299	14.9	25.7	0.168	8.4	0.0
	125.5	18063	312.6	0.741	37.0	36.5	0.418	20.9	0.0
	226.0	34790	523.3	1.327	66.3	50.0	0.748	37.4	0.0
	751.1	172454	2200.7	5.686	284.3	100.0	3.206	160.3	100.0

[a] mg/L; [b] estimated oil equivalents (µg/L); [c] Total polyaromatic hydrocarbon (µg/L); [d] Total toxic units

The TU contributions of each hydrocarbon class to the total TU for the CEWAF exposures are shown in Figure 3.17. For the *A.* cervicornis exposure, lower loadings of dispersed oil (10.1 mg/L, 25.3 mg/L, and 50.8 mg/L) resulted in CEWAF with effect TU dominated by VOCs (62-64%) and 2-ring PAHs (14-21%), while TU of higher loadings were dominated by 2- and 3-ring PAHs (24-26% and 42-56%, respectively). The *P. astreoides* exposure resulted in a similar pattern, with VOCs accounting for 56-68% of the effect TU from low dispersed oil loadings (10.6 mg/L and 51.3 mg/L), but declined to only 6% of the TU in the 751.1 mg/L loading. As dispersed oil loading increased, the TU contribution of the 2-ring PAHs increased from 17-30%, while the contribution from ≥3-ring PAHs increased from 5-58% of the total TU. For each species, the total sublethal effect TU for each loading were used to estimate sublethal effects (Table 3.5). For both species, effects of dispersed oil loadings less than 125.5 mg/L were expected to be low, while the two highest loadings of both CEWAF exposures were expected to result in high sublethal effects, *A.cervicornis* with 76 and 100%, and *P. astreoides* 66 and 100%.

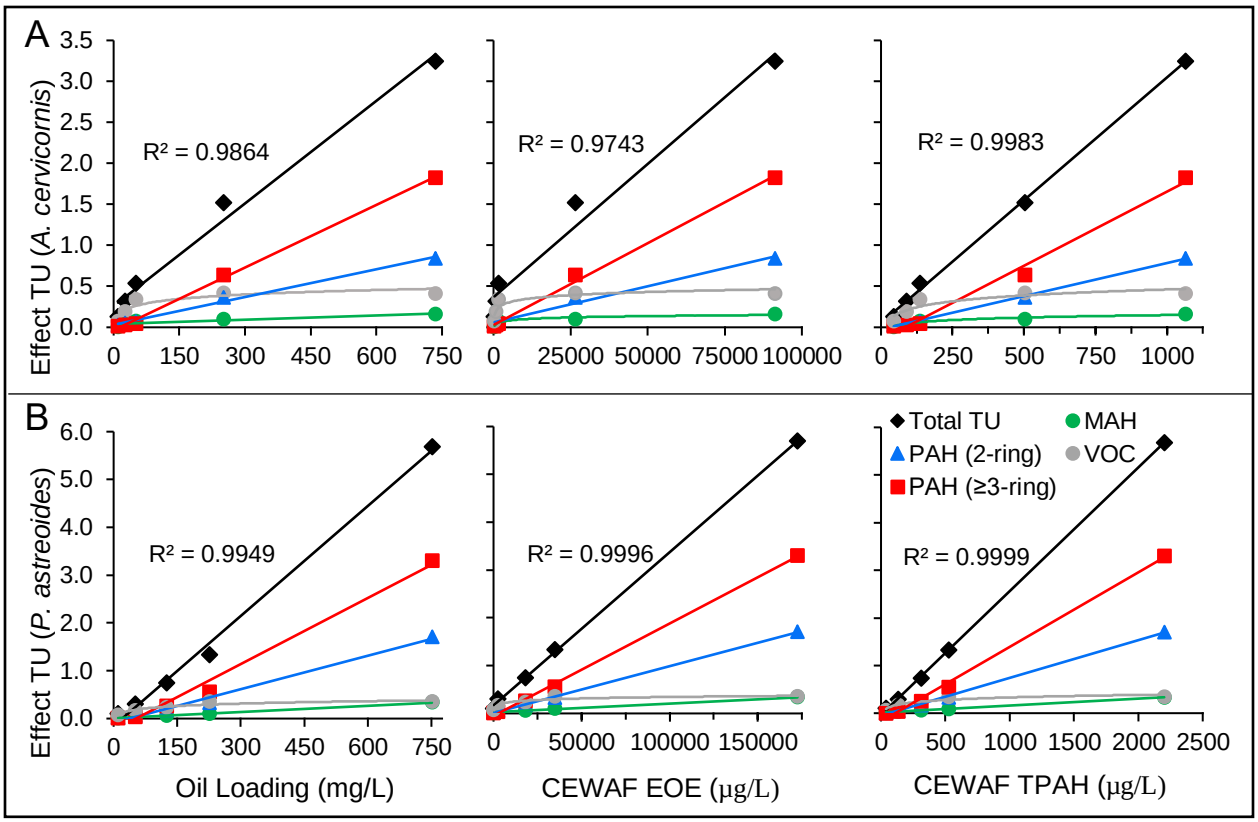

Figure 3.16 A) *A. cervicornis* and B) *P. astreoides* toxic units determined by oil loading, EOE, and TPAH for multiple hydrocarbon classes of the CEWAF exposures

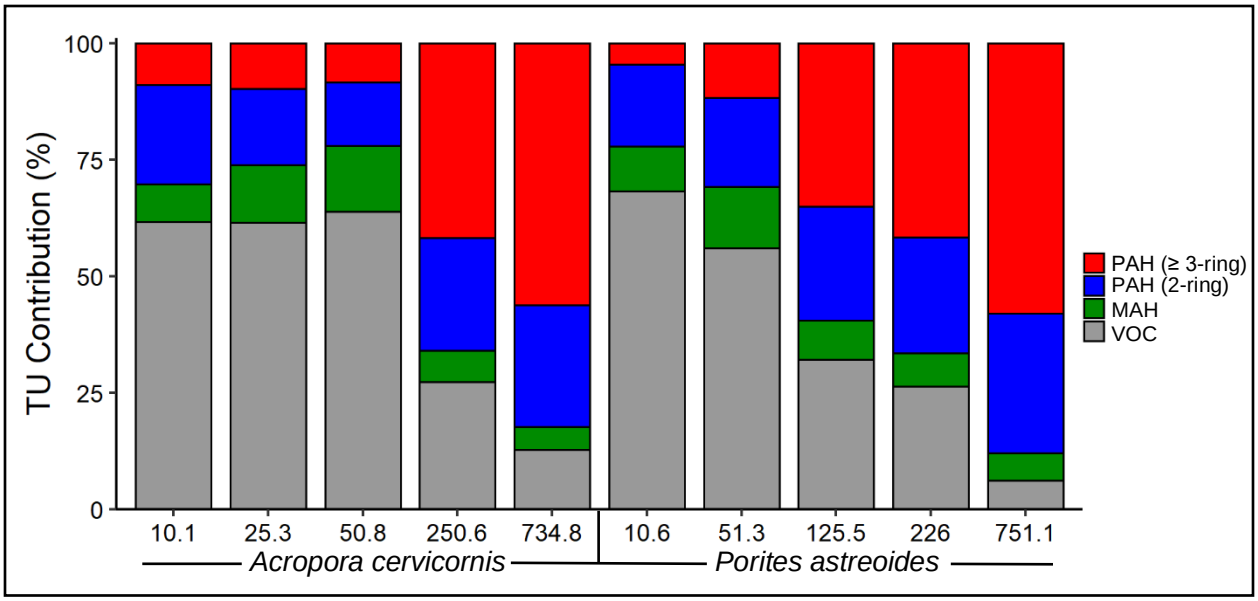

Figure 3.17 The contribution of hydrocarbon classes to the total predicted TU from multiple dispersed oil loadings (mg/L) during CEWAF exposures to *A. cervicornis* and *P. astreoides*.

The relationships between effects estimated from TU and either loading, EOE, or TPAH concentrations, were used to estimate effect endpoints for each species following CEWAF exposure (Table 3.6). The calculated loading, EOE, or TPAH that resulted in a sublethal TU of 1, was used as the estimated EL50, EC50, and $EC50_{PAH}$ values for both corals following exposure to the CEWAF. Similarly, the LL50, LC50, and $LC50_{PAH}$ were estimated from the loading, EOE, or TPAH that resulted in a lethal TU of 1.

Table 3.6 Sublethal and lethal effects endpoints determined for *A. cervicornis* and *P. astreoides* following exposure to WAF and CEWAF

Exposure	Endpoint	*Acropora cervicornis*		*Porites astreoides*	
		TU Predicted	Measured	TU Predicted	Measured
WAF	EL50 (mg/L)	>1216.1	>1216.1	> 1221.7	> 1221.7
	EC50 (µg/L)	> 527	> 527	> 528	> 528
	$EC50_{PAH}$ (µg/L)	> 273.5	> 273.5	> 243.6	> 243.6
	LL50 (mg/L)	>1216.1	>1216.1	> 1221.7	> 1221.7
	LC50 (µg/L)	> 527	> 527	> 528	> 528
	$LC50_{PAH}$ (µg/L)	> 273.5	> 273.5	> 243.6	> 243.6
CEWAF	EL50 (mg/L)	176.5	82.3	150.1	239.1
	EC50(µg/L)	439	3951.4	445	43878.7
	$EC50_{PAH}$ (µg/L)	204	192.5	174	572.6
	LL50 (mg/L)	195.0	112.5	253.0	435.6
	LC50(µg/L)	451	6044.5	760	82179
	$LC50_{PAH}$ (µg/L)	215	231.1	260	1202.2

3.3.5 Water Quality

Water quality measurements were made on each individual chamber of all exposures completed, and measurements can be found in the GRIIDC data repository. For the four experiments described here, there were no significant differences in temperature between any of the doses at any time ($p>0.05$). Consistent with observations made during single compound testing (Chapter 2), the pH and DO of higher treatments (391 µg/L and above, both exposures) decreased slightly (≈0.2 pH and ≤1 mg/L O_2) but significantly following both WAF exposures. CEWAF also produced similar significant declines in pH and DO in the higher treatments, but these declines were minimal. Significant differences in nutrient concentrations (PO_4, NH_3, NO_2, and NO_3) were not present following WAF exposures or CEWAF exposure to *A. cervicornis*.

However, there was significant elevation of NO_2 and NO_3 following *P. astreoides* exposure to CEWAF, whereas all treatments at and above 2654 µg/L were higher than controls.

3.4 DISCUSSION

The work described here includes multiple experiments assessing the toxicity of the WAF and CEWAF of crude oil on two coral species. Specific focus was given to the comparisons of WAF and CEWAF toxicity among each species, although species sensitivity differences were also examined. Additionally, an oil solubility model was used to calculate toxic units as a means of increasing comparability between the tests completed, and to assess the accuracy of predicted effects and lethality for each exposure completed.

3.4.1 Concentration and Composition of WAF and CEWAF

Assessing the toxicity of WAF and CEWAF required analytical confirmation of the exposure media, both in terms of overall achieved aqueous concentrations, as well as the composition of each mixture. The aqueous hydrocarbon concentrations following both WAF exposures were limited by the partitioning behavior of the compounds from the silicon tubing to a level higher than solubility. The maximum concentrations achieved in this exposure were near solubility of the oil in seawater, as the highest loadings in both tests resulted in very similar values (Fig. 3.1). There was less than ±10% fluctuation in the dissolved hydrocarbon concentrations (EOE) of each exposure treatment, except the two low treatments of *A. cervicornis* fluctuated more than anticipated. Otherwise, passive dosing produced stable aqueous concentrations across a variety of oil loadings, and resulted in varying treatments of WAF exposure to both coral species without the formation of droplet oil. Exposure WAFs were assessed for PAH content, and revealed a composition dominated by PAHs with lower numbers of aromatic rings (≤ 3) (Fig. 3.2). Additionally, the distribution of PAHs in each WAF were in a similar ratio as observed in the parent oil.

The addition of Corexit 9500A dispersant created a CEWAF with higher dissolved concentrations compared to similar loadings of undispersed oil. Total hydrocarbon estimates breached the highest concentrations measured in WAF exposures, with the increase more drastic at higher loadings. This increase in concentration did not plateau, and maintained a linear relationship (Fig. 3.3), with high treatments of both exposures creating CEWAF with visible oil droplets even after settling the exposure media, which adhered to walls of the exposure chambers. Compared to WAF tests, the CEWAF exposures had more variability regarding total

dissolved hydrocarbon levels within each treatment, especially the *P. astreoides* 125.5 mg/L dispersed oil loading. The replacement of CEWAF supply at 24 h, or the variability in dispersant effectiveness due to small differences in media preparation energy for each chamber may have led to small differences in the level of dispersed hydrocarbon over time. Nonetheless, treatments of CEWAF maintained relatively consistent hydrocarbon levels over time, possibly due to a buffering capacity of the droplets in the highest concentrations.

The PAH concentrations measured in CEWAF exposures were consistently higher than those measured in WAF exposures, although the increases were not as drastic as observed in EOE measurements. Low CEWAF treatments resulted in 2–3X the TPAH concentration compared to WAF treatments of similar oil loading. Additionally, the high CEWAF treatments produced 4-8X the TPAH levels of high WAF treatments. Naphthalenes, specifically 1-methylnaphthalene and other alkylated derivatives, were 2-3X the level measured during WAF exposures of similar oil loading. Aromatic hydrocarbons with three or more rings were enriched in the CEWAF exposures compared to WAF, with some compounds 10X higher in the CEWAF treatments (Fig. 3.4). Additionally, higher loadings produced CEWAF with measurable levels of PAHs up to and including chrysenes, which were not found in the highest WAF loadings tested.

3.4.2 Impacts and species sensitivity

Exposures of both organisms to WAF caused significantly elevated condition scores at all time points, but these effects were limited in extent. The maximum sublethal effects resulting from coral condition changes observed in *A. cervicornis* were slightly higher than *P. astreoides*, but failed to breach 50% in either test, even at the highest loadings. Growth rate and quantum yield changes were also minimal, with no clear trend observable for either species. These sublethal effects were designed to obtain endpoint concentrations (EC50, $EC50_{PAH}$, and EL50), but limited responses to WAF exposure produced extrapolated estimates of each endpoint that are all above the highest value measured for each parameter (Table 3.3). The highest oil loadings produced WAF with hydrocarbon concentrations near solubility, which were below the level to cause adequate partitioning of hydrocarbon into each coral species, therefore limiting the sublethal effects of each WAF. Additionally, only one fragment of *A. cervicornis* died, preventing calculation of any lethal endpoint for either coral species following exposure to WAF.

The effects imposed by both CEWAF exposures were comparatively more severe than WAF exposures, with two treatments of *A. cervicornis*, and one treatment of *P. astreoides*

resulting in 100% mortality. However, impacts were relatively similar at low doses of WAF and CEWAF (~10-50 mg/L loadings), as illustrated by the low ends of the *drc* models for all measured parameters (Fig. 3.9). As loadings increased above 125.5 mg/L, the sublethal effects of CEWAF exposures occurred more quickly, and to a higher overall extent when compared with sublethal effects resulting from similar non-dispersed oil loadings. At loadings around 250 mg/L, *A. cervicornis* were 28.5% impacted by WAF and 100% impacted by CEWAF, while sublethal impacts to *P. astreoides* were 26.7% in WAF and 50% in CEWAF (Tables 3.4 and 3.5). The increased effects resulting from CEWAF exposures were used to generate reliable estimates of all sublethal and lethal endpoint concentrations within the range of measured values for each parameter (Table 3.3).

Sublethal endpoints calculated from effects were used to compare the toxicity of WAF and CEWAF, but also the sensitivity of each coral species. Although endpoints calculated from WAF exposures were above the highest values tested, some effects were estimated to occur just outside of the range of concentrations used and were still used to compare with endpoints from CEWAF exposures. According to aqueous concentrations (EOE), calculated EC50 values were 6X (*A. cervicornis)* and 28X (*P. astreoides*) higher in CEWAF exposures when compared to the estimated WAF values, indicating the effects were occurring due to a higher amount of dissolved and particulate hydrocarbon in the exposure media (Figure 3.9). Contrary to EC50 values, EL50 estimates from CEWAF exposures were considerably lower than the estimated values from WAF testing, which indicated less oil was required to elicit a 50% sublethal effect in both coral species if it is dispersed. Compared to WAF exposures, higher sublethal impacts were measured in similar loadings of CEWAF because of the elevated dissolved phase/ droplet concentrations resulting from dispersant addition, which led to the increase in EC50, and a decrease in EL50 for *A. cervicornis* and *P. astreoides*. The sublethal effects of WAF and CEWAF on both coral species were also defined by the TPAH concentrations in the dissolved phase of both tests. The $EC50_{PAH}$ calculated from the CEWAF exposure to *A. cervicornis* was less than the WAF estimated value, while the *P. astreoides* $EC50_{PAH}$ was slightly higher, although estimates from both WAF tests were above the highest PAH concentrations measured. Figure 3.9.F illustrates the similarity in effect between WAF and CEWAF exposures to both species as defined by the aqueous TPAH concentrations.

The dissolved hydrocarbon concentrations were also used to assess impacts to growth and photosynthetic efficiency of both coral species following WAF and CEWAF exposures. There were very limited significant treatment effects in any test, but those that were present were used to calculate IC50 values. Exposure to WAF only significantly impacted the quantum yield of *A. cervicornis*, producing an $IC50_{YIELD}$ of 386 µg/L. Although within the range of concentrations measured, the $IC50_{YIELD}$ refers to a concentration that represented only a 5% decline in the photosynthetic efficiency. This also occurred for *P. astreoides* following CEWAF exposure, where the $IC50_{YIELD}$ was estimated at 9124 µg/L (non-significant), but only represented an 8% decline in photosynthetic efficiency. It appears that exposure to hydrocarbons may impact the photosynthetic efficiency of the corals, but over this time scale the effects were limited, and only representative of a 2-8% decline. Although an $IC50_{YIELD}$ less than the EC50 indicates a higher sensitivity measurement, it was only indicative of small changes to the photosynthetic efficiency, which were only significant in *A. cervicornis.* Exposure to CEWAF also produced significant treatment effects on growth of *P. astreoides*, but there was high variability in this trend, resulting in a non-significant $IC50_{GROWTH}$.

3.4.3 Toxic units and predicted effects

As a means of predicting the effects of the whole oil, PETROTOX was used to identify the LL50 expected from exposure to MC252 oil WAF. Due to solubility limits and no droplets, maximum concentrations in the dissolved phase were not predicted to reach a level to induce major effects to either coral species. This resulted in estimates of LL50 above 1000 mg/L loading for both coral species, which were both confirmed following WAF exposures; limited aqueous concentrations resulted in limited effects that were below 50% at the highest loadings (>1200 mg/L loading).

This next step in the prediction of mixture toxicity involved estimating the aqueous concentrations for a subset of hydrocarbons using the oil solubility calculator. According to the compounds measured, WAF exposures resulted in concentrations less than predicted, although this relationship was loading and hydrocarbon class dependent (Figure 3.12). Although some deviation from predicted values occurred, the agreement was within an order of magnitude for most compounds and the predicted concentrations were used for all compounds in the model to assign TU for the sublethal effects on each coral. The solubility calculator was also used to infer the concentrations of compounds below detection limits for the CEWAF exposures. Although

the model was not designed to predict the dissolved fraction of dispersed oil fractions, it did provide minimum exposure levels to estimate TU for compounds expected to be present but not measured. For some of the compounds, predicted values were still higher than measured concentrations, particularly in the low dispersed oil loadings, but most compounds measured much higher than predicted.

In order to avoid missing toxic contributions from compounds below detection, WAF exposures used predicted concentrations for TU, while CEWAF exposures used the combination of predicted and measured values previously described. The TU predicted for WAF were dominated by VOCs and MAHs, which are both volatile and likely experienced loss over both 48-h exposures. According to TU, PAHs were the least contributors to toxicity across all WAF loadings (Fig. 3.15), presumably due to their low aqueous solubility compared to MAHs and VOCs. The calculated TUs for each WAF treatment were used to predict the sublethal effects expected to occur in each exposure, which agreed well with measured effects at all loadings (Table 3.4). Sublethal effects of *A. cervicornis* treatments were slightly underpredicted by a maximum of 9.7%, with the highest effects measuring 3.8% higher than the effects predicted. Sublethal effects were also underestimated for a majority of the *P. astreoides* WAF treatments, but were all within 10.2% of the effects measured.

Alternative to WAF, addition of dispersant produced a CEWAF with TU dominated by different hydrocarbon classes at different loadings (Fig. 3.17). The more soluble VOCs and MAHs dominated low dispersed oil loadings, while loadings above 125.5 mg/L were dominated by ≥3-ring PAHs, some of which were not measured in WAF exposures at these loadings (ex: chrysenes). It appears that the solubility of PAHs was increased by dispersant addition at higher loadings, resulting in the observed increase in TU that obscured the contribution of other hydrocarbon classes. The sublethal effects predicted for low loadings of both coral species (10.1-125.5 mg/L) were similar to measured effects, or slightly underpredicted. The effects measured in low treatments of *A. cervicornis* were within 5% of measured effects, but effects were underpredicted by 23.7% in the 250.6 mg/L loading. Sublethal effects estimated for *P. astreoides* were underpredicted by as much as 15.3% in the lowest loading, but were more accurate as concentrations increased, eventually resulting in overpredictions of effect in the higher loadings.

The effects predicted from TU were relatively accurate for both WAF and CEWAF, although the model over predicted the dissolved concentration of some hydrocarbon classes (ex:

MAH). Compared to the model, measured hydrocarbon levels were depleted in the more volatile components, which were consistently found to be the highest contributors to the TU of each coral species in all exposures to WAF, and the lowest doses of CEWAF. It is possible that the model was predicting exposure concentrations accurately in each WAF, but loss of the most volatile components occurred during sampling, as samples were collected at 48 h from the effluent line of the chambers and thus, could not be collected faster than a flow rate of 5 ml/min. If this suspected loss had not occurred, the predicted concentrations may have been representative of the actual exposure concentrations, resulting in TU that accurately represented the effects. It is also possible that the enrichment of ≥3-ring PAHs compared to predicted levels in most treatments negated the loss of toxic contributions from depleted, more soluble components, producing estimates that were close to observed effects.

The total TU relationships in Figures 3.15 and 3.16 were used to estimate the effect endpoints in Table 3.6. Predictions of effect were representative of measured effect in both species, and all estimated and measured endpoints from the TU of WAF exposures were above the highest value tested for each coral. The TU estimated for CEWAF exposures produced values of each endpoint that were lower than WAF, due to the increase in TU contributions of compounds dissolved in the high CEWAF treatments. The greater toxicity of high CEWAF treatments is represented by an increase in the total TU compared to similar WAF loadings. For both species, EL50 estimates from TU were within roughly 100 mg/L loading. The estimated EL50 from TU of *A. cervicornis* was higher than measured, which suggested the presence of TU contributions absent from the model, resulting in an underprediction of toxicity. However, TU predicted a CEWAF EL50 for *P. astreoides* that was lower than measured, which implied some TU contribution in the model that was higher than represented by the measured components. The EC50 estimated from TU of both exposures to CEWAF was much lower than measured, possibly due to the high levels of droplet oil in high treatments complicating the measurement of dissolved phase. The solubility model relates toxicity to the dissolved hydrocarbon fraction, and TU for the dissolved PAHs produced an effect endpoint for *A. cervicornis* most similar to the measured value. The EC50PAH estimated from TU of *P. astreoides* was less than measured, which implied a higher amount of PAH than measured.

The lethal endpoints were also used to determine TU that represented the lethal effect of each WAF and CEWAF exposure. For both coral species, maximum lethal effects of WAF were

predicted higher than measured, as no mortality occurred. The lethal effects estimated for CEWAF exposures, resulted in estimates of percent mortality that were relatively similar to measured levels (Table 3.5). The partial mortality estimated for lower treatment levels by total TU less than 1 was overestimated, as no mortality at these levels occurred. If the total TU passed 1 for either species, the measured toxicity was typically 100%, but estimated slightly lower. The endpoints estimated from the lethal TU of each species were compared with endpoints calculated with measured mortality, which showed a similar pattern as observed for sublethal effects.

3.4.4 Toxicity of WAF and CEWAF

Comparisons of toxicity typically involve the use of some effect concentration measured for both compounds, or chemical mixtures. If comparisons of the WAF and CEWAF toxicity examined here were made with only one of the measured parameters, results may be misinterpreted. The EC50 for both coral species reflected higher values for CEWAF, which by way of EC50 comparisons, implied WAF was more toxic, as less was required to cause a 50% effect. Alternatively, CEWAF EL50 values were much less, as WAF estimates were all above the concentration achieved by the highest loading. This implied less oil was required to cause the effect if it is chemically dispersed, suggesting CEWAF was more toxic, or there was some difference in composition that altered the toxicity. Further analysis of the mixture composition revealed varying levels of PAHs that are known to exert different toxic contributions to hydrocarbon mixtures. Simple comparison of EC50 or EL50 would fail to identify the shift in compounds responsible for the altered toxicity.

Chemical dispersion preferentially increased the concentration of PAHs at high loading levels, much more than any loading of WAF. Comparisons of toxicity were made with $EC50_{PAH}$ of WAF and CEWAF, which were shown to account for most of the elevated TU contributions in CEWAF, and resulted in some similarity in estimated toxicity for both mixtures. The CEWAF $EC50_{PAH}$ for *A. cervicornis* was about 50% lower than the value calculated for WAF. Based on the PAH composition, less CEWAF was required to cause a 50% effect in *A. cervicornis*, presumably because the ratio of ≥3-ring PAHs was increased well beyond the solubility in WAF. Increased TU contribution of these compounds compared to the MAH and VOC dominated WAF loadings, reflected the increase in toxicity observed at the highest concentrations of CEWAF. Alternatively, CEWAF exposure to *P. astreoides* produced an EC50PAH very similar to the (not-significant) WAF estimate, which was estimated outside the measured level of TPAH,

and could have been higher. However, the similarity in estimated for EC50PAH of *P. astreoides* does imply that the toxicity of both mixtures was highly related to the dissolved PAH composition, which is altered in the presence of chemical dispersants.

The toxicity of WAF and CEWAF to both corals is complex and determining if dispersed oil was more toxic required analysis of the dissolved components in each mixture. It appears that dispersed oil was more toxic to both corals because it required less oil to cause a similar effect. However, measurement of CEWAF aqueous concentrations showed much higher hydrocarbon levels that were responsible for the increased effect at certain loadings. Lower loadings of dispersed oil did not enhance the contribution of TU from larger ringed structures as observed in loadings of 125.5 mg/L and above. It appears that levels of dispersed oil above 100 mg/L are more toxic than non-dispersed oil, as the concentration and thus toxic contribution, of the more insoluble components reaches a supply great enough to breach solubility compared to other hydrocarbon classes. This is consistent with similar findings by the National Academies of Sciences and Medicine (2019), which identified increased toxicity for dispersed oil compared to oil, when loaded at 100 mg/L or more. The increased toxicity is presumably linked to either an increase in droplet/ dissolved concentrations, or some inherent toxicity contributed by the concentration of dispersant required to effectively disperse 100 mg/L of oil. In this research, it was apparent by PAH analysis that the concentration of components not normally soluble in WAF were enhanced by chemical dispersion at these higher loadings, which increased the TU contribution, thus increasing the toxicity of CEWAF for these coral species.

3.5 CONCLUSION

In this chapter, PETROTOX and a speciated oil solubility model estimates of LL50 using TU were validated, and used to compare effects of WAF and CEWAF for two coral species. Compared to other organisms, and consistent with species sensitivity comparisons with CTLBB, both coral species were minimally impacted by exposure to oil WAF. Overall, impacts to both corals were higher in CEWAF exposures compared to WAF, which was due to elevated aqueous hydrocarbon concentrations in the higher treatments. Toxicity at low doses appears comparable, as TU were comparable for WAF and CEWAF, but doses above 125.5 mg/L were more toxic if dispersants were applied. These findings are consistent with other research that has identified an increase in toxicity for dispersants when applied at these loadings.

3.6 WAF AND CEWAF DATA AVAILABILITY

The results of the WAF and CEWAF exposures are summarized and available in the GRIIDC data repository (https://data.gulfresearchinitiative.org/) under the CTOX project. All coral condition scores for all time points measured, as well as the individual growth and yield measurements, mortality, and water quality are included within. Table 3.7 contains the Unique Dataset Identifier and the DOI for all WAF and CEWAF exposures.

Table 3. 7 GRIIDC Dataset information for WAF and CEWAF exposures to *A. cervicornis* and *P. astreoides*

Dataset Name	UDI	DOI
Toxicity of oil WAF to *Acropora cervicornis*	R6.x825.000:0016	10.7266/JP55N1SR
Toxicity of oil WAF to *Porites astreoides*	R6.x825.000:0017	10.7266/J5XEDFDJ
Toxicity of oil CEWAF to *Acropora cervicornis*	R6.x825.000:0018	10.7266/3KGEEMKX
Toxicity of oil CEWAF to *Porites astreoides*	R6.x825.000:0019	10.7266/04Q6DDFB

CHAPTER 4- TRANSCRIPTOME SEQUENCING AND GENE EXPRESSION

4.1 INTRODUCTION

The Coral-Tox project was designed to fill the knowledge gap in hydrocarbon toxicity to corals by determining the relative sensitivity of the Atlantic scleractinian corals *Acropora cervicornis, Porites astreoides,, Siderastrea siderea, Stephanocoenia intersepta,* and *Solenastrea bournoni* to single hydrocarbons, oil, and chemically dispersed oil. The present study utilized the test protocol described in Chapters 2 and 3 to evaluate the observed response and potential linkages at different levels of biological organization including molecular, sub-cellular and whole organism. Effects summarized elsewhere considered coral response using multiple high-resolution metrics, and have indicated relatively high resiliency for these corals compared to other species with regards mortality.

Mortality is commonly used to compare the relative effects of contaminants on different organisms, but corals (and most multicellular organisms) exhibit multiple levels of response to various levels of natural and anthropogenic stressors (Morgan et al. 2001). Scleractinian corals are colonial, and the impacts assessed at the community level include changes to percent coral cover, bleaching, and reduced biodiversity (Edge et al. 2013). Corals also respond to stressors at the population level through the loss of individual colonies and changes in reproductive viability (Morgan et al. 2001, Downs et al. 2012). Alteration of physiological processes is the principal component of these changes, resulting from changes to growth, respiration, and calcification rates, and reproduction (Morgan et al. 2017). Although measuring physiological decline gives a clear picture of how the coral is responding, it does not identify specific stressors or determine underlying biological mechanisms causing the response (Morgan et al. 2001, Edge et al. 2013). Additionally, these responses generally occur after declining health is evident, and perhaps beyond recovery. Because researchers typically utilize physiological indicators, impacts of environmental and chemical stressors on corals are poorly understood at the cellular and subcellular levels (Venn et al. 2009). Focused studies at the molecular level of stress responses in corals provide much needed information into the cause of the observed physiological disturbance.

For some species, low-level exposures that cause sublethal effects may be more important for assessing impacts of petroleum spills in the environment. This is especially true when evaluating the relative effects of an oil spill to different ecosystem components included in

Net Environmental Benefit Analysis (NEBA) or Spill Impact Mitigation Assessment (SIMA). In order to prevent impacts to keystone species that may already be affected by anthropogenic disturbance, these analyses should emphasize early sublethal indicators of stress. The earliest and most sensitive biomarkers for physiological responses to stress are likely in the transcriptome (RNA messages); studies of which show physiological effects of contaminants prior to the onset of observational changes.

The transcription of DNA to mRNA results in the transcriptome. Changes in gene transcription represent the initial step in stress response, and levels of mRNA provide a snapshot of transcriptional activity indicative of the current physiological status of the organism. Changes in transcript levels often indicate a change in the level of a gene product following translation (Nikinmaa and Rytkönen 2011), and impacts of stressors can be diagnosed and quantified by comparing target gene basal expression with levels that are altered in response to environmental contaminants or experimental conditions. Altered expression of mRNA following disturbance can be detected within minutes of onset, and will disappear rapidly after removal of the stressor. During this time, abundance of the mRNAs provides evidence that very specific gene expression has changed, the patterns of which can be used to infer which class of stressor is causing the observed response. Because of this, mRNA biomarkers may be especially useful in diagnosing causative agents of stress, and if the specific gene in question is evolutionarily conserved, it can be used for many species.

Transcriptome sequencing uses standard RNASeq (Ruiz-Jones and Palumbi 2015), which employs methods similar to whole genome sequencing; RNA is reverse transcribed into cDNA, amplified, purified, and sequenced. Sequencing the transcriptome expands the number of identifiable genes compared to microarrays (Karako-Lampert et al. 2014) by sequencing all of the mRNA present in the sample following extraction and isolation. Once assembled, the sequences in the transcriptome are analyzed for homology to other known sequences using BLAST alignments, and function is assigned via the KEGG pathway database or other similar functional annotation platform (Shinzato et al. 2014) (Yum et al. 2017). Gene expression analysis is one of the most efficient ways to determine the molecular mechanisms of acclimatization, adaptation, and response to natural and anthropogenic stressors (Morgan et al. 2001, Barshis et al. 2013, Moll et al. 2014). Impacts can be diagnosed and quantified by

analyzing target genes with expression levels that are altered in response to environmental contaminants.

Recent advances in RNA sequencing have produced a rapid and cost effective method for gene discovery via transcriptome sequencing (Kitchen et al. 2015). RNAseq has become the quantitative method of choice to profile transcription levels, as the technique provides an unbiased approach to discovering functional processes through identification and quantification of differentially expressed genes between experimental treatments. There have been multiple coral genomes produced over the past decade (Genbank -*A. digitifera* GCA_000222465.2, *A. millepora* GCA_004143615.1, *Montipora capitata* GCA_006542545.1, *Orbicella faveolata* GCA_002042975.1, *Pocillopora damicornis* GCA_003704095.1, *Porites rus* GCA_900290455.1, and *Stylophora pistillata* GCA_002571385.1) that aid in annotation of coral transcriptomes. Additionally, transcriptome sequences are useful in identifying coding regions of the genome, specifically where intronic and intergenic sequences are embedded.

Primarily, toxicologists focus on the mechanisms of action and exposures that produce acute and chronic pathologies. Ecotoxicogenomics has emerged in order to determine the mechanism of toxic action at the gene level (Nikinmaa and Rytkönen 2011, 2012). Organisms use a variety of molecular mechanisms to survive environmental fluctuations, as well as contaminant exposures (Edge et al. 2013). These responses are complex and involve many genes, typically resulting in changes to baseline gene expression, which in turn alter the physiology and behavior of the organism. Following an exposure, gene expression profiling exhibits altered transcript levels related to protecting cellular structures, repairing damage, and maintaining normal cellular functions. Quantifying gene expression reveals the mechanisms behind a biological response, and can also be used to identify stress response in individuals and populations prior to the onset of functional alterations. One of the major limitations with ecotoxicogenomic studies is the lack of combined functional and genomic information, as gene expression is controlled at several steps, including transcription, RNA processing and transport, mRNA stability, translation, and protein stability, which can all be regulated by environmental conditions and contaminants (Nikinmaa and Rytkönen 2011, 2012).

This chapter describes the RNA sequencing portion of the Coral-Tox project, where the transcriptomes of four corals (*Acropora cervicornis, Porites astreoides, Porites divaricata,* and *Siderastrea* siderea), and the gene expression of most previously completed exposures (Chapters

2 and 3), were sequenced and characterized. Full, reference transcriptomes were generated and annotated for select coral species to aid in the identification of the short sequences produced from gene expression profiling using Quantseq (Lexogen) Kits. Samples from each species were preserved for analysis of gene expression following each 48-hour exposure. Laboratory exposures in this program were designed with the goal of determining sublethal and lethal endpoints for these species, and integrating differential gene expression into this analysis further characterized the low-level, sublethal exposures that are indicative of real-world scenarios. Outputs generated from this work will improve coral species sensitivity inputs for modeling of spill response options during NEBA and SIMA activities. Additionally, this work provides needed data to substantially improve oil-spill response decisions on the predicted effects of oil spills and clean-up methods on corals.

4.2 METHODS

4.2.1 Experimental organisms and exposures

The coral species utilized in this research, *Acropora cervicornis, Porites astreoides, Siderastrea siderea, Stephanocoenia intersepta,* and *Solenastrea bournoni,* are common in shallow depths and were chosen because of their widespread distribution and suitability to fragmentation and experimentation. Branch tips of *A* cervicornis were collected from the Nova Southeastern University Offshore Coral Nursery, with the remaining coral species collected from the nearshore reef in Broward County, FL. Colonies were returned to the laboratory and fragmented for use in the exposure system. Branching species were attached with a minimal amount of cyanoacrylate gel glue to small numbered aragonite bases, and all corals were acclimated to laboratory conditions in a 1100 L indoor laboratory culture system. Artificial seawater (prepared with reverse osmosis water and TropicMarin sea salt) was used; the system was maintained at 35 PSU and 26°C, with artificial light provided by LED lights (Radion XR30W G4 Pro). Corals were maintained in this system during the pre-exposure and post-exposure recovery periods.

Coral exposures to TOL, 1MN, PHE, WAF, and CEWAF are described in detail in Chapters 2 and 3. Briefly, experiments were conducted using a continuous flow recirculating passive dosing system with multiple treatment levels over 48 h. Assessment metrics, results, and implications for findings are previously discussed. However, one fragment from each exposure

chamber was immediately preserved following the exposure, and the remaining methodology and results will focus on these fragments.

4.2.2 Reference transcriptomes

Sample preparation, RNA extraction, and sequencing

Samples for full transcriptome sequencing were taken from coral colonies under the care of the Marine Toxicology Laboratory of Nova Southeastern University (Florida, USA) that were originally collected from nearshore reefs in Broward County for use in the previously described exposures. Two fragments (1-2 cm branch tip or 2 cm^2 tissue) of each species were preserved in RNALater Stabilizing Solution (Thermo Fisher Scientific) and frozen at -80C until thawed for extraction. Tissue (approximately 200 mg) was scraped from a majority of the skeleton into 2 mL bead-beating centrifuge tubes containing 0.7 mm garnet beads (Qiagen; Part #13123) and 1 mL of TRIzol (Ambion Life Technologies, CA). The depth of tissue sampled was dependent upon the level of live tissue skeletal perforation for each species, and skeleton up to and including the depth of the deepest gastrodermal tissue was included in the sample. Samples were lightly homogenized with a PowerLyzer 24 (MoBio Laboratories) at 1000 RPM, for 2 cycles of 20 seconds, with a one-minute delay between cycles to prevent high temperatures. The low RPM was used to denude the skeleton and prevent complete skeletal homogenization, which complicated this process in early attempts. The lightly homogenized samples were incubated for 5 min, then centrifuged to remove skeletal debris. Total RNA was extracted from the supernatant using a modified protocol (SI Protocol 4.1) consisting of TRIzol RNA isolation through phase separation with chloroform (Sigma-Aldrich Part #25668, Molecular-grade) followed by RNA precipitation with isopropanol (Sigma-Aldrich Part #59304, Molecular-grade), before being washed in ethanol (Thermo Fisher Scientific, Part #BP2818, Molecular-grade) twice and resuspended in DEPC treated water (Thermo Fisher Scientific, Part #J70783, Molecular-grade).

The total RNA concentration was determined using a Qubit Digital Flourometer 2.0 (Life Technologies), the integrity (RIN) checked using automated gel electrophoresis on an Agilent 2200 Tapestation, and the purity was determined with a NanoDrop Spectophotometer 2.0. Contaminating phenol and salts were present in a majority of the samples, and removed with an additional ammonium acetate precipitation (SI Protocol 4.2) and subsequent ethanol washes (x2). Quality and quantity were re-evaluated (Table S4.1) before samples were sent to Genewiz for library preparation and sequencing on an Illumina HISeq.

Sequence annotation and functional analysis

Transcriptomes were assembled *de novo* following adapter and quality trimming (Trimmomatic v0.36). The sequences from two samples of each species (Table S4.2) were combined and assembled (Trinity v2.5) into one transcriptome with a minimum contig length of 200bp. Statistics were generated for each assembled reference transcriptome and EMBOSS tools getorf were used to determine open reading frames that were annotated by Diamond BLASTx alignments to the *nr* database. All species in this study contain endosymbiotic dinoflagellates, and therefore, extracted RNA is expected to contain coral host and algal symbiont. The BLASTx annotation was used to group the sequenced transcripts into Cnidarian, Zooxanthellae, other organism, and unidentified.

Sequences identified as Cnidarian were input Functional Analysis module with Blast2Go annotation (OmicsBox 2019) to facilitate functional characterization. This program streamlined the functional annotation of genes in a list of sequences, starting with a BLASTx alingnment to the *nr* database with an expected E-value cutoff of 10^{-6}. Each transcript was assigned a gene name and functional category based on its best match to sequences in online databases (Gene Ontolgy (GO) and Kyoto Encyclopedia of Genes and Genomes (KEGG)). Each Cnidarian transcriptome was simultaneously analyzed with InterPro, UniProt, Ensembl, and others, and mapping results were merged to GO results to form one merged annotation for each species. The merged annotations for each species were used to determine the number of genes present in functional categories (biological processes, molecular functions, and cellular components) within functional analysis pipeline.

4.2.3 Gene expression

Sample preparation, RNA extraction, and sequencing

Following each laboratory exposure, one fragment from each chamber was collected and assessed for gene expression; high concentrations were often removed as only surviving corals were used. Samples were immediately preserved in RNALater Stabilizing Solution, stored for 24 h at 4°C, and frozen at -80C until thawed for extraction. Total RNA from each sample was individually extracted by cutting roughly 100 mg of tissue and skeleton into 2 mL centrifuge tubes containing 0.7 mm garnet beads and 1 mL of TRIzol. Samples were lightly homogenized with a PowerLyzer at 1000 RPM for 2 cycles of 20 seconds, with a one-minute delay between

cycles, then centrifuged at 12,000 G for 10 min to remove skeletal debris. RNA from *A. cervicornis*, *S. sidera*, *S. intersepta*, and *S. bournoni* was extracted from each supernatant using the same modified protocol (SI Protocol 4.1) consisting of TRIzol RNA through phase separation with chloroform, followed by RNA precipitation with isopropanol before being washed in ethanol twice and resuspended in DEPC treated water. Due to continuous contamination and low RNA yield using the previous method, total RNA from *P. astreoides* samples was extracted from using the TRIzol manufacturer's protocol through phase separation with chloroform, then equal volume 100% ethanol was added and the RNEasy (Qiagen RNEasy Mini Kit, Part #74104) protocol was utilized to bind, wash, and elute the RNA (SI Protocol 4.3). The total RNA concentration of each sample was determined using a Qubit Digital Flourometer, and purity was determined on the NanoDrop Spectrophotometer.

In order to determine a treatment-based pattern of gene expression, prior to cDNA library preparation, total RNA from each treatment replicate was equally pooled, producing one sample per treatment for all exposures completed. This produced a total of 73 samples, split across the 13 single compound, WAF, and CEWAF exposures (Table 4.1). Some exposures were not sampled due to no exposure or due to mortality at the end of the exposure, but others were not included downstream due to lack of quantity and quality of extracted RNA (e.g., *P. astreoides*-CEWAF, *S. siderea*-TOL). Contaminating DNA was removed from all pooled samples with TURBO DNA-free kit (Invitrogen, Thermo Fisher Scientific) treatment. RNA in these pooled samples was quantified on a Qubit Digital Flourometer, and the integrity (RIN) checked using automated gel electrophoresis on the Agilent Tapestation (Table S4.3).

Table 4.1 Number of samples for sequencing from each exposure after pooling treatment replicates

Exposure	*A. cervicornis*	*P. astreoides*	*S. siderea*	*S. intersepta*	*S. bournoni*
TOL	2	2	*	4	3
1MN	4	4	4	6	5
PHE	5	6	6	6	-
WAF	6	6	-	-	-
CEWAF	4	*	-	-	-

Library preparation of each pooled sample followed standard QuantSeq methods (Lexogen- 3' mRNA-Seq FWD Library Prep Kit for Illumina), which required a low initial input volume without the need for polyadenylated RNA enrichment or ribosomal RNA removal. Input volumes of RNA were normalized within each treatment, so that samples being analyzed contained similar RNA inputs to allow comparison of gene counts following sequencing. Following library preparation and amplification, libraries were sequenced by Lexogen to generate one short (50-100 base pairs) fragment per transcript, in each sample.

Sequence annotation and differential gene expression

The raw sequences for each of the sequenced libraries were analyzed using a modified transcript-level-analysis workflow (OmicsBox 2019) beginning with fastqc assessment (Andrews 2010)and sequence trimming (Trimmomatic V0.38) (Bolger et al. 2014). All sequences were trimmed for Illumina adapters, length (6 bp removed from 5' end and a minimum 20 bp total length), and quality (Q≥25). The quality of the trimmed sequences was assessed again using fastqc before gene count tables for each sample/library were generated. The modified workflow used Bowtie2 (Langmead and Salzberg 2012) to align the trimmed sequences in each library (fastq) to the reference transcriptome (fasta) previously generated for each coral. Count tables were then generated from transcript-level quantification using RSEM (Li and Dewey 2011) and the generated alignment files (BAM) for each coral species, and were filtered for low counts according to standard practices (minimum of 5 counts in ≥25% of samples).

Gene expression of each sample was assessed using differential gene expression analysis in Omicsbox (Tarazona et al. 2011). Individual pairwise comparisons were made between the control and all treatments within each exposure, using the generated count tables and the Pairwise Differential Expression Analysis (without replicates) method suitable for samples with no replicates. This software is based on the NOISeq R package (Bioconductor (Tarazona et al. 2015)), which compared samples of two experimental conditions by simulating replicates. In this study, 4 replicates were simulated, with 25% contribution from each, as this is the true number of fragments with standardized input in the pooled library that was sequenced. For each treatment level, the intensity of differential expression from the control was indicated by a $\log_2$ fold change for each gene identified. The list of differentially expressed genes for each sample was filtered to include only those that were expressed and identified in all samples of that specific exposure, and had $\log_2$ fold changes of ≤ -2 or ≥ 2. After filtering, the average $\log_2$ fold change for up-regulated

genes was multiplied by the number of up-regulated genes, and the average $\log_2$ fold change for down regulated genes was multiplied by the number of down-regulated genes, and the absolute value of each was summed. The result was an estimate of the overall change in gene expression compared to controls for each treatment, of each exposure. This was based on genes that were present in all samples of each exposure, and was termed the differential gene expression intensity (DGEI).

A dose-response analysis was used to determine the concentration of each contaminant that caused a significant change in the gene expression of *A. cervicornis*. The concentration of each contaminant that caused a 50% change in the DGEI (DEC50) was determined with the *drc* package in R (Ritz et al. 2015). Each dose-response model utilized the measured hydrocarbon concentrations (1MN and PHE) or the estimated oil equivalents (EOE) concentration (WAF), and the DEGI calculated for each exposure treatment to determine the endpoints for each coral species and test substance. The 2-parameter asymptotic regression (AR.2) was fit to the data, with minimum effects fixed at 0, because the DEGI for each treatment is the difference from the respective control treatment. Similar to previous effects endpoints determined (Chapters 2 and 3), the ED function was used to determine the DEC50 from each model fit.

4.3 RESULTS

4.3.1 Exposures

The effects of each exposure are summarized in Chapters 2 and 3. Coral response was used to estimate acute and subacute endpoints for sublethal effects and mortality; these values (EC50 and LC50) were input into the TLM to calculate corresponding CTLBBs for effect and lethality. The subacute and acute endpoints used to derive CTLBBs for *A. cervicornis*, *P. astreoides*, *S. siderea*, and *S. intersepta* were compared to calculated values for other species for which this data is available and indicated that these scleractinian coral species are comparatively more resilient to narcotic chemical exposure than a majority of the other species, regardless of whether comparisons are made with the effect or lethality endpoints.

4.3.2 Reference transcriptomes

The four transcriptomes described here yielded an average of 100.19 million reads per library (range 87.91-119.78 million reads) with >93% of all reads having a mean Q score of > 35.8 (Table S4.2). Following quality and adaptor filtering, assembly of the remaining reads

produced between 553 thousand and 1.9 million contigs for each coral holobiont (Table 4.2). Assembled transcriptomes varied in size, with the shortest length and lowest number of contigs in the *A. cervicornis* transcriptome, while the largest transcriptome sequenced here had four times the contigs sequenced, and double the length (*S. siderea*). Both species in the genus *Porites* produced transcriptomes with similar contig numbers and total length, and identical GC content.

Table 4.2 Statistics for the four assembled reference transcriptomes.

	A. cervicornis	*P. divaricata*	*P. astreoides*	*S. siderea*
# Contigs	553,673	916,155	997,495	1,983,922
# Contigs >1000	168,268	220,068	188,214	283,937
# Contigs >10000	1,324	1,186	812	237
Largest Contig	29,963	28,793	45,131	41,466
Total Length	602,437,966	800,190,465	752,536,063	1,209,831,816
Mean Length	1088.08	873.42	754.43	609.82
N50	2101	1575	1227	840
GC%	42.81	42.46	42.46	41.51
#Ns	0	0	0	0

The assembled transcriptomes for each species were filtered by taxonomic origin using a Diamond BLASTx alignment to the *nr* database. There were a variable number of transcripts for each species that aligned with sequences of any origin, and the majority of contigs in each transcriptome did not match any known sequences (Table 4.3). The number of transcripts identified as Cnidarian and Zooxanthellae were remarkably similar between *A. cervicornis*, *P. divaricata*, and *P. astreoides*, with *S. siderea* having a larger number of both. Additionally, the transcriptome of *S. siderea* contained the largest number of unidentified sequences that did not align to any known sequence in the *nr* database. Figure 4.1 shows the contribution of each category to the whole sequenced transcriptome of each coral species. All transcriptomes appear to contain similar levels, with *A. cervicornis* having the highest ratio of transcripts identified as Cnidarian (37%) and zooxanthellae (12%). Although the transcriptome of *S. siderea* was substantially larger, the ratio of each category was highly similar to both *Porites* spp., with all three transcriptomes consisting of 17-25% Cnidarian, 5-6% zooxanthellae, and 63-65% unidentified

Table 4.3 Number of sequences identified from Diamond BLASTx alignment.

	A. cervicornis	*P. divaricata*	*P. astreoides*	*S. siderea*
Total Assembly	553,673	916,155	997,495	1,983,922
Cnidarian	204,597	231,744	225,893	345,267
Zooxanthellae	64,881	50,818	61,639	102,882
Other Organism	30,720	39,718	83,063	238,958
Unidentified	253,475	593,875	626,900	1,296,815

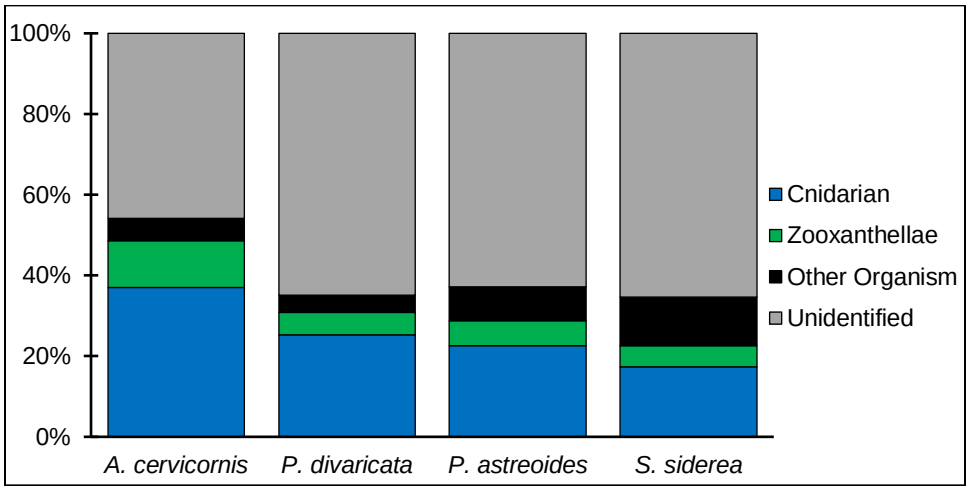

Figure 4.1 Percent contribution of sequence identities to the total transcriptome sequenced for each coral.

The sequenced transcripts identified as Cnidarian were annotated using Blast2Go homology searches, with +99% of sequences matching previously identified genes. This additional alignment was included because the previous alignments used a database that lacked genomes that have been sequenced in recent years. The references transcriptomes for *A. cervicornis, P. astreoides,* and *S. siderea* are each summarized in Figures 4.2, 4.3, and 4.4, respectively. As expected, transcripts from *A. cervicornis* predominantly aligned to sequences identified as *Acropora* in origin, but genes identified from distantly related Indo-Pacific corals were also present (Fig. 4.2.A).

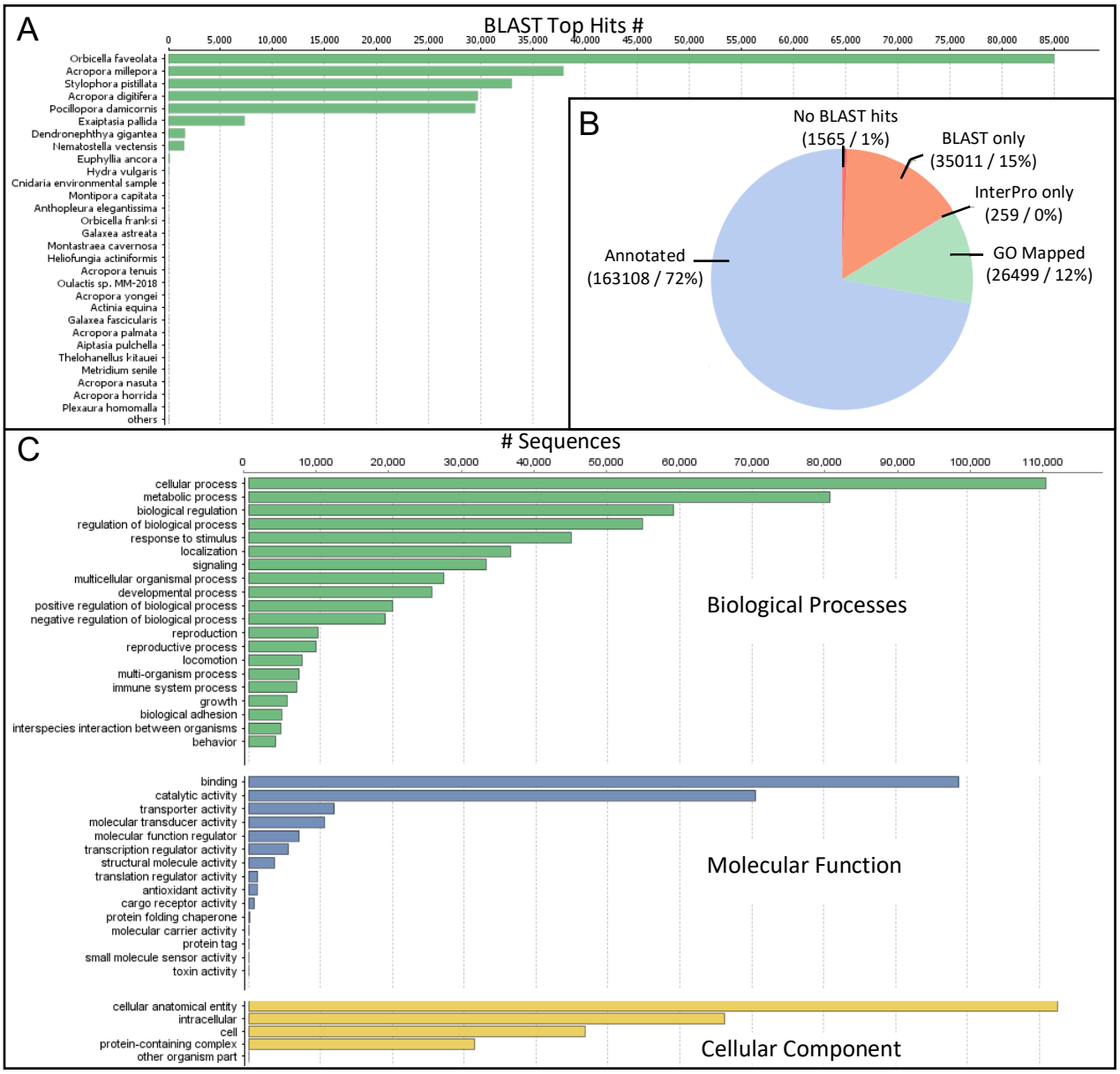

Figure 4.2 A) BLAST alignment and B) annotation statistics for the *Acropora cervicornis* transcriptome with C) level 2 GO functional classification

Transcriptomes from *P. astreoides* and *S. siderea* were dominated by genes previously identified from *Orbicella faveolata*, a similar morphological coral from the Atlantic (Figs. 4.3.A and 4.4.A). Because the transcripts were previously filtered for coral origin, the BLAST alignments were highly successful for all species (Figures 4.2.B, 4.3.B, and 4.4.B), and were used to produce GO mapping terms for each transcriptome, resulting in functional annotation for 66-72% of the Cnidarian genes with BLAST matches. The GO terms were broadly distributed across the three domains (biological processes, molecular functions, and cellular components)

and the percentages of sequences mapped to a given sub-ontology were highly similar for all three species here (Figures 4.2.C, 4.3.C, and 4.4.C).

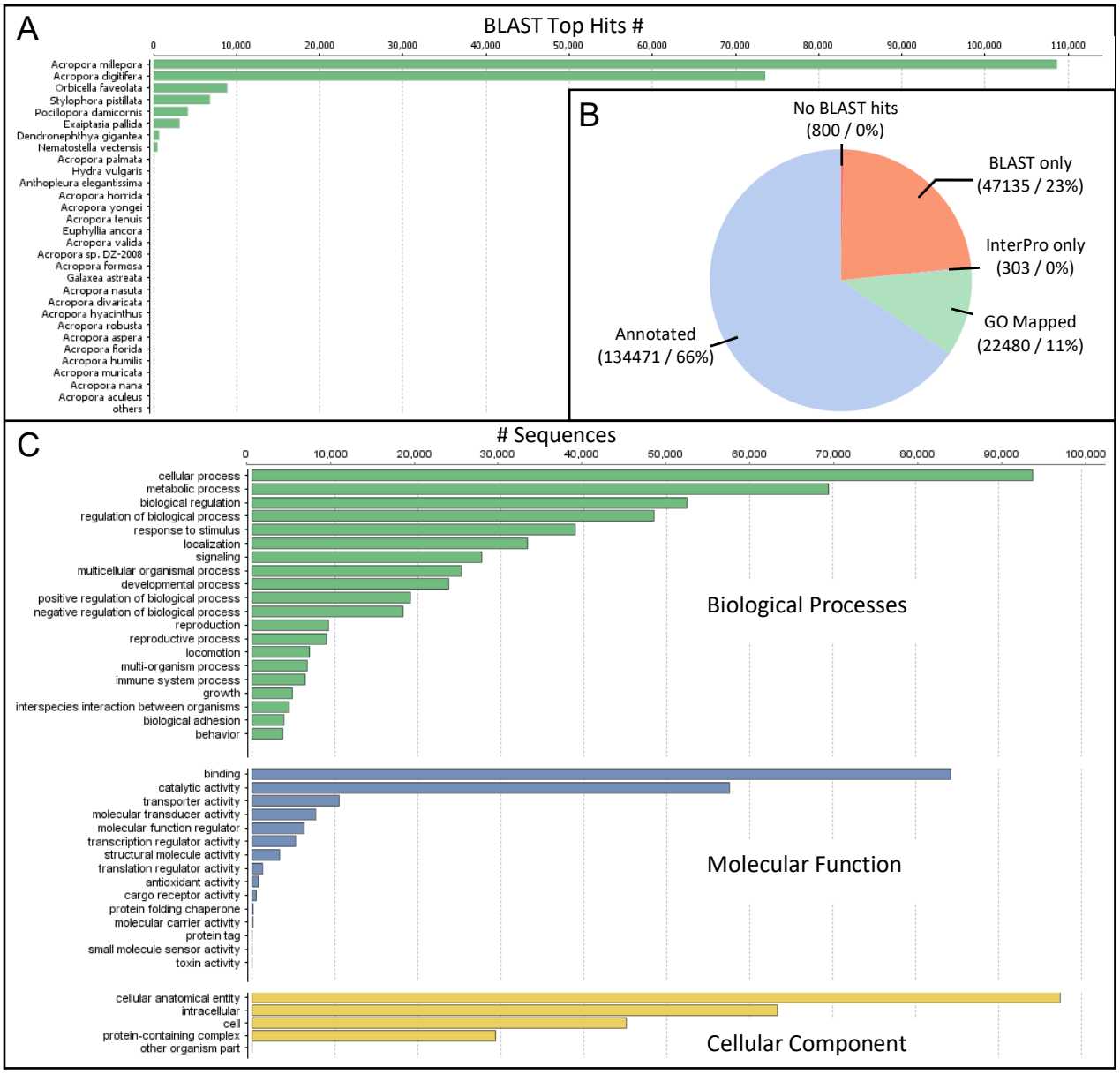

Figure 4.3 A) BLAST alignment and B) annotation statistics for the *Porites astreoides* transcriptome with C) level 2 GO functional classification

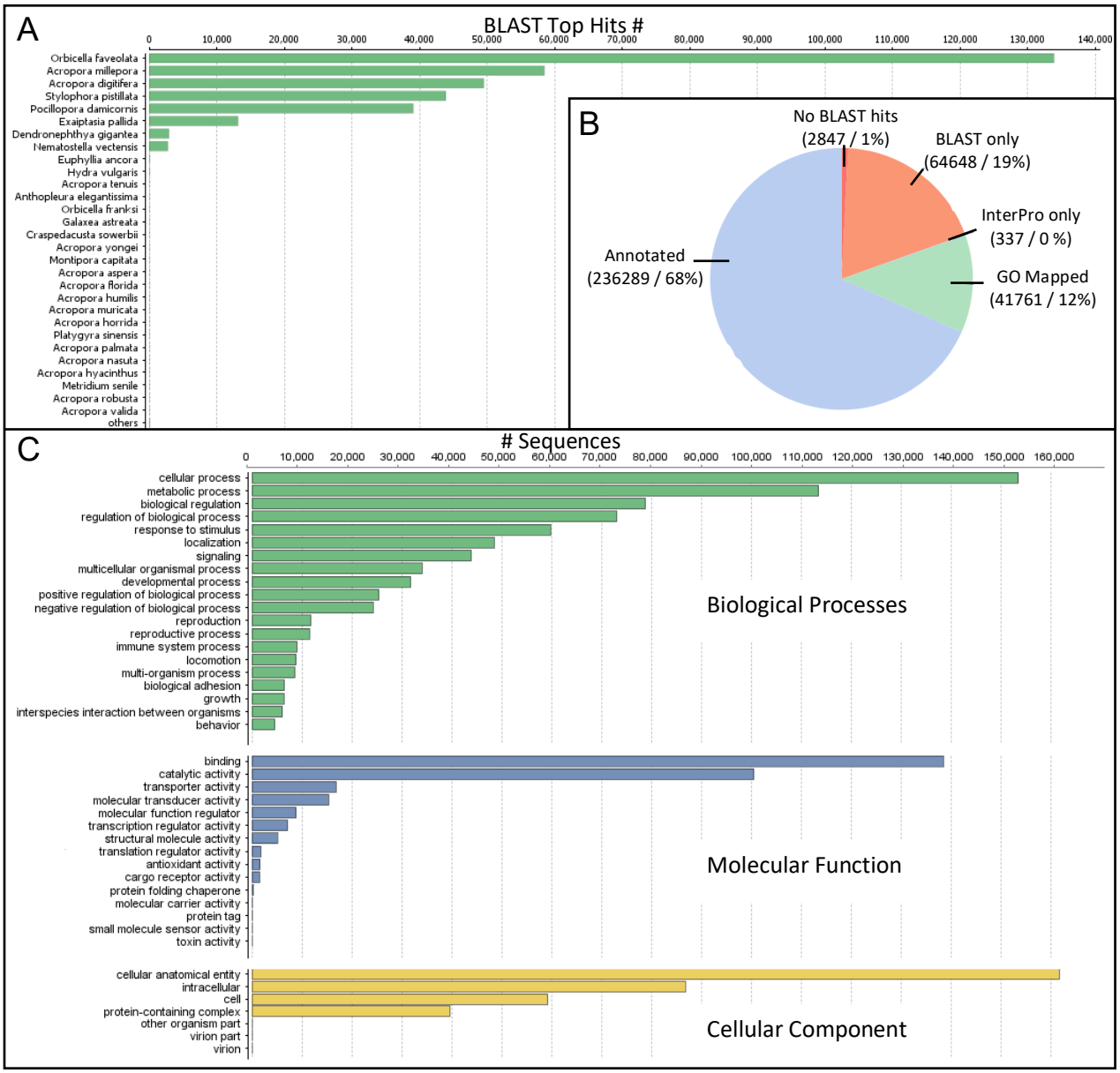

Figure 4.4 A) BLAST alignment and B) annotation statistics for the *Siderastrea siderea* transcriptome with C) level 2 GO functional classification

4.3.3 Gene expression following exposures

Samples were collected from each exposure and RNA was extracted and sequenced for gene expression analysis following each test. After filtering out poor quality RNA samples, libraries were prepared and amplified for the 73 remaining samples before being sent for sequencing, but 16 of these samples were not sequenced due to degraded libraries (Table S4.4 and S4.5). However, 57 libraries from multiple exposures were sequenced with acceptable

coverage and quality scores. For the remainder of this dissertation, the results of gene expression sample analysis will focus on *A. cervicornis* exposures, with the remainder of the sequenced libraries discussed elsewhere.

All sequenced *A. cervicornis* libraries passed fastqc analysis before and after length and adapter trimming. Sequences were aligned to their respective reference transcriptome with an average alignment rate of 47.9% (Table S4.6). Using the subset of aligned sequences from each library, count tables were generated for each sample in order to facilitate comparison of gene expression. This generated a list of 22K genes in *A. cervicornis* that were being expressed, which was reduced to 15K expressed genes after low count filtering. Pairwise comparisons of gene expression within each exposure resulted in a list of differentially expressed genes that were significantly different ($p < 0.05$) than controls (Table 4.4), measured by a $\pm\log_2$ fold change for each gene. The number of differentially expressed genes for each treatment was filtered to reduce the list to genes identified in all samples of that specific exposure. This resulted in 216 genes expressed in 1MN samples, 937 genes expressed in PHE samples, and 202 genes expressed in WAF samples, which were further reduced to only genes with fold changes ±2 in each treatment.

Table 4.4 Number of differentially expressed genes in each treatment determined by pairwise comparisons.

Test	Treatment	Number Differentially Expressed Genes	
		All	Filtered
1MN	745	1973	191
	1501	1116	197
	2775	1662	204
PHE	92	3161	838
	369	4049	899
	656	4024	891
WAF	304	1413	183
	392	3959	201
	512	2140	199
	527	2451	196

The number of genes significantly up-regulated, and the number of genes significantly down-regulated compared to controls, were both consistent across the individual exposure treatments (Table 4.5). However, the mean $\log_2$ fold changes for up- and down-regulated genes generally increased in intensity (more positive or more negative) with increasing concentration of contaminant. In order to facilitate a dose-response assessment of gene expression, the up and down regulation of the filtered genes were summarized using the DEGI. Both up- and down-regulated genes in each treatment were individually summarized by this metric, which accounts for the number and intensity of genes being regulated. Both $DEGI_{UP}$ and $DEGI_{DOWN}$ generally increased with increasing exposure concentrations, and the total DEGI was used to assess the relative influence of each contaminant on the gene expression of *A. cervicornis.*

Table 4. 5 Summary of gene regulation for all *A. cervicornis* sequenced libraries

Test	Treatment	Filtered Up-Regulated			Filtered Down-Regulated			Total
		Genes	Mean foldΔ[a]	$DEGI_{UP}$	Genes	Mean foldΔ[a]	$DEGI_{DOWN}$	DEGI
1MN	745	104	3.83	398	87	-4.28	372	771
	1501	102	3.80	388	95	-4.38	416	804
	2775	105	4.09	430	99	-4.37	433	863
PHE	92	611	3.90	2383	227	-4.21	956	3340
	369	666	4.10	2731	233	-4.35	1013	3744
	656	658	4.11	2706	233	-4.37	1018	3723
WAF	304	61	4.20	256	122	-3.92	478	734
	392	67	3.99	267	134	-4.64	622	889
	512	66	4.48	296	133	-4.36	580	875
	527	63	4.47	282	133	-4.78	635	917

[a] $\log_2$ fold change

The number and pattern of overall gene expression summarized by DEGI was similar for 1MN and WAF exposures. The number of up-regulated genes was higher for 1MN samples, while the number of down-regulated genes was higher for WAF samples. The overall DEGI was similar for these samples and was used to generate dose-response curves for both exposures (Figure 4.5). Exposure to PHE resulted in similar pattern of increasing DEGI with increasing concentration, but the number of genes involved in up- or down-regulation was much higher (Figure 4.6). The model parameters were significant ($p<0.05$), and the residual standard error was low, suggesting a good fit for all three exposures.

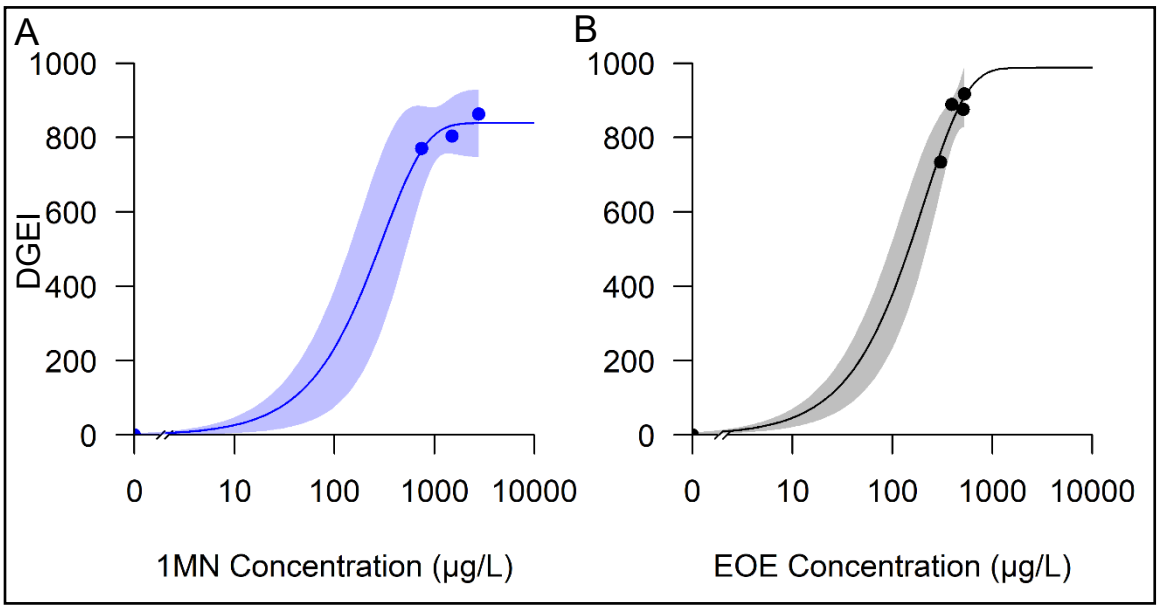

Figure 4.5 Dose-response curves for the DEGI following both 1MN and WAF exposures to *Acropora cervicornis*. Points =sample DEGI and shaded area= 95% CI.

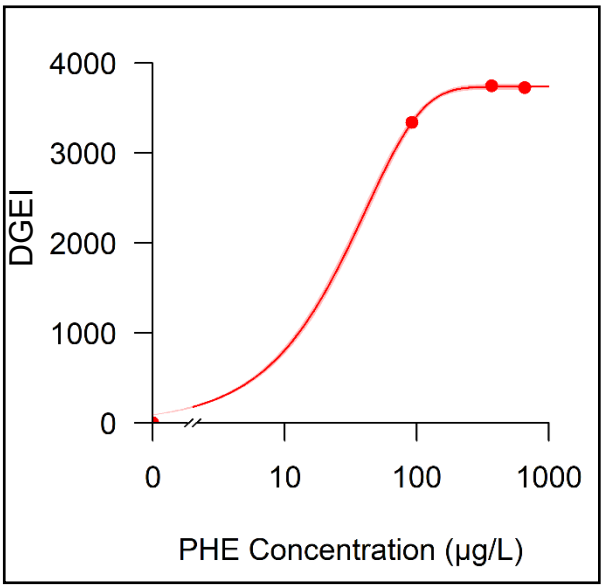

Figure 4.6 Dose-response curves for the DEGI following the PHE exposure to *Acropora cervicornis*. Points =sample DEGI and shaded area= 95% CI.

The dose-response models based on differential gene expression were used to estimate a DEC50, or the concentration that resulted in a 50% change in gene expression (of the common filtered genes), for each exposure. Exposure to 1MN resulted in an estimated DEC50 of 211 µg/L (95% CI 26-397 µg/L), PHE resulted in a DEC50 of 28 µg/L (95% CI 27-30 µg/L), and a DEC50 of 143 µg/L (95% CI 33-254 µg/L) EOE was calculated following exposure to WAF.

4.4 DISCUSSION

Impacts to organisms can be diagnosed and quantified by analyzing gene expression levels that are altered in response to environmental contaminants. Reference genomic information is required to identify the genes being expressed within each coral species during each laboratory exposures. Although recent advances have increased the availability of coral genetic information, reference transcriptomes were not readily available for these coral species. Therefore, transcriptomes of three of the coral species used in this study, and one additional species, were sequenced and annotated to provide a reference for identification of genes being expressed following each exposure.

4.4.1 Reference transcriptomes

Sequencing the transcriptome of each coral species yielded an average of 100.19 million reads per library, which were assembled into 553,000 to 1.2 billion contigs after quality and adapter filtering, depending on the species. The number of raw reads, assembled contigs, and assembly statistics of the four species described here are comparable to other previously published anthozoan transcriptomes (Shinzato et al. 2011, Traylor-Knowles et al. 2011, Moya et al. 2012, Barshis et al. 2013, Shinzato et al. 2014, Kitchen et al. 2015, Liew et al. 2016). Additionally, read number and total length were typically higher and resulted in a higher number of contigs than were previously identified in *P. astreoides* (Kenkel et al. 2013) and S. siderea (Davies et al. 2016) transcriptomes.

Contigs for all coral species were identified by BLAST homology searches, resulting in a substantial portion of each transcriptome that lacked matches in the database (46% *A. cervicornis*, 63-65% for *P. astreoides, P. divaricata,* and *S. siderea*), which is similar to four previously sequenced coral transcriptomes, including *Montastrea cavernosa* (Kitchen et al. 2015). This is potentially the result of previous biases in taxonomic composition of existing databases, and ongoing gene sequencing efforts may reduce this unidentified portion of these transcriptomes. The *A. cervicornis* transcriptome had the fewest number of contigs, but the

highest proportion identified as coral (37%) and symbiont (11.7%) in origin. The transcriptomes of the other coral species had consistent proportions of contigs identified as symbiont in origin (5%), with ≈24% coral contigs in the *Porites* sp, and 17% coral contigs in *S. sidera.* Gene ontology (GO) terms were assigned to a large proportion of the *A. cervicornis* (72%), *P. astreoides* (66%), and *S. sidera* (68%) contigs that were identified as coral during BLAST alignments, providing tentative gene identities and functional classification for a large number of sequences in each assembly.

The annotation of *A. cervicornis, P. astreoides*, and *S. siderea* transcriptomes resulted in functional identities for genes in each coral species, revealing a large number of sequences in each of the three domains. For all three species, the top five categories of each domain were identical, with similar proportions of genes in each. The level 2 GO classification provides a broad overview of the function of genes sequenced, and classifying these same genes at level 3 GO results in identification of sequences involved in many regulatory processes (Figure 4.7). The biological process domain was dominated by genes involved in processes related to organic substance, primary/cellular, and nitrogen-compound metabolism, regulation of cellular processes, and cellular response to stimulus. Dominant molecular functions include protein binding, organic/ heterocyclic compound binding, and ion binding, and cellular components were dominated by sequences with functions involved in organelle, membrane, and cytoplasm regulation.

Past research has identified genes of a "chemical defensome" in marine invertebrates, which includes an integrated network of genes and pathways that allow an organism to defend against toxic chemicals (Goldstone et al. 2006). This includes stress activated receptors and transcription factors, efflux pumps, oxidizing enzymes, reducing and conjugating enzymes, antioxidant proteins, and heat shock proteins. Genes involved in the chemical defensome have been previously identified in the *Acropora digitifera* genome (Shinzato et al. 2012), and were also identified here. Although this dissertation is not meant to provide an in-depth examination of the molecular mechanisms involved in detoxification, the following is a brief description of the 258 accession numbers linked to the chemical defensome that were identified in the coral transcriptomes described here.

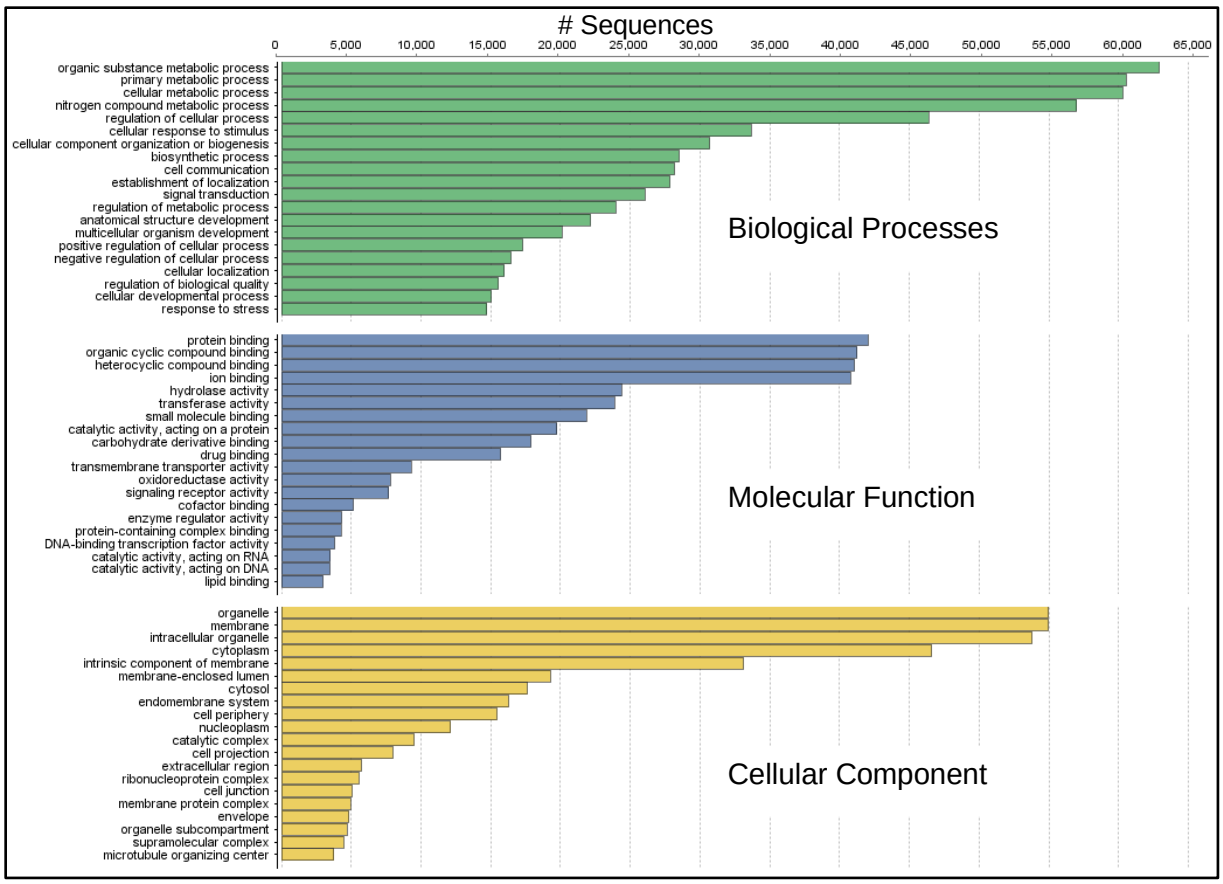

Figure 4.7 The number of sequences with Level 3 Gene Ontology classification for *A. cervicornis* coral contigs. The top 20 categories are listed for each domain

The first stage in the chemical defensome is environmental sensing by stress activated receptors, whereas the bHLH-PAS family of transcription factors responds to variety of ligands and initiates cellular response. The most studied of these is the aryl hydrocarbon receptor, which binds xenobiotic response elements in the genome and induces transcription of genes involved in detoxification (Nikinmaa and Rytkönen 2012). The contaminant may cause immediate harm depending on its toxic mode of action or if possible, efflux proteins such as the ATP binding cassette (ABC) will remove the toxicant from the cell via energy dependent processes (Venn et al. 2009). Subfamily B of the ABC protein family contains P-glycoprotein, termed the multi-xenobiotic resistance protein (MXR), and is able to transport a wide variety of substrates. Toxicant entering the cell could also induce biotransformation pathways, where cellular components inactivate and eliminate the toxicant. If the toxicant entering the cell is to be oxidized and removed, the xenobiotic and detoxification response is initiated (Downs et al. 2011, Downs et al. 2012).

The mixed-function oxidase (MFO) system is the main pathway induced during exposure to xenobiotics (Rotchell and Ostrander 2011), and has been identified in numerous cnidarian species (Ramos and Garcia 2007, Downs et al. 2012). This pathway includes cytochrome p450 monooxygenase (CYP450) and numerous other conjugating and antioxidant enzymes which have been previously correlated with increases in aromatic hydrocarbons in tissues. Polycyclic aromatic hydrocarbons (PAHs) are chemicals containing two or more benzene rings, and metabolism of PAHs may lead to reactive intermediate metabolites that interact with proteins and nucleic acids, leading to tissue damage (Ramos and Garcia 2007). The MFO is induced by PAHs in order to detoxify the compounds by oxidation (phase 1) and subsequent conjugation of functional groups (phase 2) to increase lipophilicity and render the compound more easily excretable.

The main component of oxidation in the MFO is cytochrome p450 monooxygenase (CYP450) (Downs et al. 2012), which catalyzes the monooxygenation reaction of non-polar organic compounds involving the NADPH-cytochrome reductase enzyme complex and adds oxygen to CYP450, creating an unstable free radical that acts as an oxidizing agent for substrates (Ramos and Garcia 2007). Following the oxidation by CYP450, the compound is conjugated with endogenous substrates (glutathione, sulfates, and acetate) to produce a more polar molecule to be more easily excreted (Downs et al. 2012). The conjugating enzymes (epoxide hydrolase and glutathione-S-transferase (GST)) add hydrophilic groups to phase 1 products, which are then transported by MXR out of the cell. If expression of GST is increased, the detoxification response is active, and the hydrophilic products are being managed by the cell for transport to lysosomes for metabolism, containment, or excretion.

This process also produces metabolites in the form of reactive oxygen species (ROS) (Rotchell and Ostrander 2011). ROS are responsible for lipid peroxidation, protein degradation, DNA damage, and apoptosis in vertebrates (Woo et al. 2014). In corals, there are various environmental stressors that induce the formation of ROS, including temperature fluctuations, high light levels, and bacterial infections, which affect signal transduction cascades, transcription factors, and lipids. To combat the formation of ROS, organisms rely on antioxidant defense mechanisms. Specific enzymes in the MFO system, including superoxide dismutase (SOD), catalase (CAT), and glutathione peroxidase (GPX), regulate the production of oxyradicals and are responsible for protecting the cell (Ramos and Garcia 2007, Downs et al. 2012).

Induction of the MFO system has been characterized in numerous cnidarian species, including *Acropora millepora, Hydra vulgaris, Favia fragum*, *Siderastrea siderea*, and *Orbicella annularis* (Ramos and Garcia 2007, Downs et al. 2012). In these organisms, CYP450 contents and activities of conjugating and antioxidant enzymes have been correlated with increases in PAHs in tissues, and are therefore used as biomarkers for PAH exposure (Ramos and Garcia 2007). Although these genes were identified in the reference transcriptomes, the gene expression results of *A. cervicornis* did not reveal a substantial number of these genes being significantly regulated.

4.4.2 Gene expression

Libraries prepared from *A. cervicornis* samples were sequenced, resulting in alignment rates between 40.4 and 56.5% for all samples. The gene expression sample alignment rates are similar to the proportion of contigs identified as coral (37%) and symbiont (12%) in the reference transcriptome for *A. cervicornis.* This was expected, as the reference transcriptomes only contained sequences that were previously identifiable as coral, zooxanthellae, and other organism. In any case, the list of sequences identified in all gene expression samples was used to generate count tables as a means of evaluating differential gene expression across different exposure treatments. After filtering the count tables, pairwise comparisons resulted in a list of differentially expressed genes for each exposure treatment. In order to evaluate the effects of contaminants on gene expression, the list of differentially expressed genes were further filtered to include only genes present in all samples of the exposure.

The differential expression and filtering steps resulted in up- and down-regulated genes with fold changes indicative of their deviation from control expression levels for all exposure treatments. Although this list of genes for each treatment was not filtered for the presence of the chemical defensome, it did indicate a significant change in expression with increasing contaminant concentration for roughly 200 genes in 1MN and WAF exposures, and over 900 genes in the PHE exposure before filtering for only $\log_2$ fold changes above 2/below -2. The similarity in gene expression between 1MN and WAF suggests molecular responses were similar in these two exposures. Examination of the significantly expressed genes in the biological processes domain from exposure to 1MN and WAF had the most sequences related to oxidation-reduction processes and transmembrane transport. This suggests the contaminants altered the expression of more genes that may be involved with the oxidation and reduction/conjugation of

these compounds compared to other processes. Additionally, exposure to 1MN and WAF induced changes in expression many transmembrane transport genes, which suggests an increase in the transportation of compounds in or out of the cell. The same biological processes were altered in the PHE exposure, but were less similar, and also included establishment of localization in the cell, and protein phosphorylation.

The gene expression results of *A. cervicornis* exposures resulted in significant changes in gene expression compared to controls in all exposures. The main goal of this chapter was to establish a concentration of each compound that significantly altered the gene expression of *A. cervicornis*. Initially, counts of chemical defensome genes were targeted, but low counts of these genes were filtered out, and the list of genes significantly expressed across each exposure treatment was utilized to estimate the DEC50 for each contaminant. As a means of including the number and intensity of the up- and down-regulated genes, the DEGI for each treatment was calculated and regressed against the concentration of each contaminant causing the altered expression. This resulted in estimates of DEC50 for *A. cervicornis* that were consistently lower than previous effect concentrations calculated for each compound (EC50 and IC50). The DEC50s were nearly an order of magnitude lower than the EC50 estimates previously made with observational effect data (Table 4.6) and highlight the potential to define effects of contaminants based on impacts at concentrations well below those which induce visible signs of stress.

Table 4.6 Comparison of sublethal endpoints calculated from *A. cervicornis* exposures

Exposure	IC50YIELD[a]	EC50[a]	DEC50[a]
1MN	1540	1945	211
PHE	NA	216	28
WAF	386	670[a]	143

[a] calculated endpoints (µg/L); [b] > highest concentration and estimate extrapolated

Changes to the transcriptome are very sensitive and altered regulation of genes is expected to occur at exposure levels much lower than those inducing visible damage. The lower DEC50 calculated for each exposure indicated this sensitivity, and results showed altered expression levels at low concentrations compared to controls. At these levels, impacts to coral physiology would result from partitioning of resources away from processes related to

maintaining normal homeostasis, and toward stress response. Additionally, if exposure to these compounds occurred during times of gametogenesis, energy partitioning may divert resources toward cellular defense mechanisms, which could result in decreased fecundity. Although gene regulation measured here was not based on the genes of the chemical defensome, it was the result of all genes consistently regulated across all exposure treatments.

The gene expression patterns provided the means to estimate DEC50 for *A. cervicornis*, but also resulted in a snapshot of the cellular machinery responsible for responding to these contaminants. The genes most regulated by exposures contained the highest number of sequences related to oxidation-reduction and transmembrane transport, indicating the potential to detoxify xenobiotics via MFO pathways, or to depurate compounds through membranes via mucus secretion, as discussed in Chapter 2. Exploration of these genes may identify the presence of complex molecular processes related to the depuration or detoxification of petroleum contaminants that increased the resilience of this coral species compared to other organisms. Furthermore, differences in the number of sequences involved in these functional categories between each species may shed light on the sensitivity differences previously identified through sublethal and lethal indicators of effect.

4.5 CONCLUSIONS

The coral transcriptomes sequenced here revealed numerous genes linked to the chemical defensome and other stress response pathways, and provided the reference to identify genes expressed during multiple hydrocarbon exposures. In the case of the most sensitive coral examined here, *A. cervicornis*, gene expression was significantly altered in all treatments, of all exposures. The significant transcriptomic regulation indicated cellular machinery responsible for limiting impacts in low level exposures, thus resulting in a delay in response and increased EC50s compared to organisms which lack the combined capability of depuration and detoxification. Future sequencing of coral transcriptomes in response to environmental influences and chemical contaminant exposures will aid in identifying the mechanisms for increased resilience of a somewhat sensitive organism.

CHAPTER 5- RISK ASSESSMENT AND POTENTIAL EFFECTS ON CORAL

5.1 INTRODUCTION

Oil Spill Preparedness and Response considers coral reefs, with particular focus on the impacts on the coral animal itself, one of the highest valued natural resources for protection in Net Environmental Benefit Analysis (NEBA) of response methods and environmental damage. The majority of this dissertation has focused on defining the impacts of petroleum hydrocarbon exposure to multiple species of scleractinian corals in order to generate a better understanding of the potential effects of oil spills on corals. Laboratory exposures with single petroleum hydrocarbons were used to generate the endpoint data necessary to provide inputs to a toxicological model, in an effort to generate the most useful and comparable data. Further testing with oil and chemically dispersed oil utilized toxic units to validate model predictions of aqueous concentrations and effects, and compare relative toxicity for two coral species. This research has shown corals to be comparatively more resilient to narcotic chemical exposure in a laboratory setting, when compared to other species.

5.1.1 Overcoming limitations of laboratory toxicity testing

Predicting effects of real-world exposures using laboratory test results is limited by complexity and scale, and extrapolating information from laboratory toxicity tests can be troublesome due to the variety of methodologies used to obtain results in previous tests (Bejarano et al. 2014, Redman and Parkerton 2015, National Academies of Sciences and Medicine 2019). Complexity in exposure durations and concentrations used, methods of media preparation generating a variety of compounds in the dissolved fractions, and analytical differences between chemical analyses can prevent comprehensive conclusions from being made with regard to oil toxicity to coral (Turner and Renegar 2017). The variety of results obtained from these methods are also complicated by the complexity of oil and hydrocarbons themselves. Additionally, tests using variable dilution to produce exposure media are complicated to interpret because of a lack in chemical characterization of the diluted media, which is known to be altered in response to changing microdroplet concentrations post-dilution (National Academies of Sciences and Medicine 2019). There is also a lack of data capturing environmental realism, whereas the scale of the real world is typically not represented in laboratory exposures. As an example, the rapid dilution of dispersed oil in the ocean is often overlooked in laboratory studies

(including those described in this dissertation), which are designed to be held constant to elicit a toxic response and facilitate the use of results in validating toxicological models.

Despite the problems with extrapolating results to real world spills, laboratory tests identify endpoints for mortality and other sublethal effects that can be used to generate sensitivity distributions useful for making decisions regarding oil spill response. In order to further increase the use of toxicity tests in extrapolating to real spills, the complexity and differences in methodology need to be standardized. The National Academies of Sciences and Medicine (2019) suggested a list of standardization practices that includes detailed characterization of source oil and media, description of WAF mixing energies, dispersant to oil ratios, variable loading methods, and expanded characterization of dosing media, all aimed at increasing comparability between toxicity tests. However, even with standardized practices in place, the complexity and scale of the real world cannot be replicated in toxicity testing.

To address this challenge, the focus has shifted away from reproducing field conditions in the laboratory, towards providing information to calibrate and validate toxicity models at environmentally realistic concentrations. That is, rather than simulating the stochasticity of environmental variables while maintaining exposure concentration and durations similar to field levels, laboratory tests should focus on producing data to improve toxicity model predictions of effect at environmentally realistic levels (National Academies of Sciences and Medicine 2019). The Spill Impact Model Application Package (SIMAP) originally designed by McCay (2003), used a combination of fate and biological effects models to predict the impacts of spilled oil. This integrated model has since been updated and used in many competitive risk assessments (CRA) and NEBA/SIMA activities to assess potential impacts of spilled oil in different environments and scenarios (French-McCay 2002, 2004, Bock et al. 2018, French-McCay et al. 2018). The fate of spilled oil is complex, and requires numerous submodels (see (McCay 2003) for original sources) that increase error in the overall model due to aleatory and epistemic uncertainty (Hoffman and Hammonds 1994, National Academies of Sciences and Medicine 2019). Models are only as accurate as the input data, and laboratory sensitivity studies can aid in understanding the level of uncertainty in models, thus limiting the contribution of aleatory errors by defining the variability in model inputs. For example, a small adjustment in the droplet size submodel will have profound effects on the modelled transport of the oil, thus altering the effects estimates produced.

5.1.2 Fate of oil spills

When oil is spilled into the marine environment, transport on the water surface or within the water column begins immediately. Advection from water currents, surface wind drift, and buoyancy all transport oil components throughout the water column and surface, possibly ending in shoreline stranding. Oil is mostly immiscible, but dissolution does occur for a small semi-soluble fraction as a function of the surface area of the oil-water interface. Oil on the surface or in the water column can be degraded (physically or biologically), adhere to sediments, strand on shorelines following transport, or be entrained by natural or chemical dispersion (NRC 2003, 2005). Entrainment in the water column is increased by chemical dispersants because of a decrease in oil droplet size that reduces droplet surfacing.

There are numerous processes that affect the physical fate of spilled oil, and the SIMAP model simulates the three-dimensional distribution of whole oil and oil components on the surface, in the water column, in sediments, and stranded on the shoreline (French-McCay 2004). Because of the complexity of oil and the varying composition, SIMAP groups compounds by physical-chemical properties into pseudo components to facilitate modeling fates and impacts organisms. In order to estimate impacts, the dominant fate processes simulated in the SIMAP model include transport, shoreline stranding, spreading, evaporation, emulsification, entrainment by surface waves, surf entrainment, resurfacing of entrained oil, dissolution, volatilization, adsorption to particulate matter, adherence, and degradation (biodegradation, photo-oxidation, and others).

The relative importance of these fate processes depends on the location of the spilled oil, most notably whether it is on the surface, or at depth. Buoyancy mechanisms can initially control the transportation of an oil spill that occurs below the surface, but wind and water currents are also dominating factors controlling oil fate (NRC 2003). Some processes controlling the fate of spilled oil on the surface are evaporation, natural dispersion while being transported, degradation and emulsification (McCay 2003, NRC 2003, French-McCay 2004, French-McCay et al. 2018). Oil spills resulting from a surface release, immediately interact with the air-water interface and begin to spread by gravitational or shear forces that readily increases the surface area of oil and therefore increase evaporation (McCay 2003). Few hydrocarbons are soluble, but water column concentrations will be increased in the semi-soluble fraction in the first few meters below the floating oil (Bejarano et al. 2013, National Academies of Sciences and Medicine 2019).

Unmitigated floating oil is dangerous to exposed organisms, and the immediate transport of oil by wind and surface currents increases the potential of exposure to sensitive shoreline habitats if stranding occurs (NRC 2003). Additionally, volatilization and evaporation are high, which produces a more weathered oil product that may be potentially more toxic following photodegradation while on the sea surface (Martinez et al. 2007). Oil on the surface also forms emulsions, increasing the water content of the oil and complicating response efforts.

The fate of spilled oil resulting from a subsea release is initially controlled by dissolution, entrainment, and biodegradation in the water column, but oil droplets released at depth will eventually rise to the surface due to buoyancy mechanisms, with larger droplets travelling faster (French-McCay 2004, French-McCay et al. 2018). Initially, there is no interaction with the atmosphere, so no evaporation or volatilization can occur, but instead the surface area of the oil droplet controls dissolution to the water column for soluble and semi-soluble components. Additionally, because the oil becomes entrained in the water column (3D) and not the water surface (2D), the surface area will remain higher for biodegradation, until the oil is degraded, or it eventually resurfaces.

5.1.3 Effects of oil spills

Water column toxicity of physically and chemically dispersed oil is directly related to the concentration and duration of the exposure exceeding the toxic threshold, as well as the spatial and temporal distribution and sensitivity of impacted marine life (National Academies of Sciences and Medicine 2019). The dissolution rate of compounds in oil is very sensitive to droplet size, because it involves mass transfer across surface area of droplets (French-McCay 2004). The amount of dissolved hydrocarbon is a function of the mass entrained and the droplet size distribution, which are heavily influenced by evaporation before entrainment, oil viscosity and surface tension, and energy in the system. Solubility is the main driver of toxicity to benthic organisms like corals, and most of the compounds in oil are immiscible and will float on the surface of the water. Fresh oil floating on the surface contains a high proportion of lighter-weight, volatile organic compounds (VOCs), that are acutely toxic but readily evaporate into the atmosphere without reaching appreciable concentrations in the water column. While the oil is fresh, the less volatile semi-soluble mono- and polyaromatic hydrocarbons (MAHs and PAHs), dissolve into the water column at a level dependent upon the partitioning properties of the individual compounds. In terms of exposure to coral, the sparingly soluble MAHs and PAHs

contribute the most to the toxicity of fresh oil, exhibiting narcosis as their partitioning-dependent toxic mode of action.

Weathered oil exhibits a similar mode of toxicity, except the toxicity decreases with weathering due to evaporative losses of the volatile components (VOCs, MAHs, most PAHs) that would partition into organismal lipid. As oil interacts with the environment on the sea surface, weathering processes impact the oil's composition by removing some fractions and altering others. Evaporation of the dominating toxic contributors reduces the toxicity over time as the toxic contribution becomes limited to only the compounds that are likely not soluble enough to reach exposure levels of any concern near corals. However, weathering also occurs from ultraviolet radiation, which can cause photosensitization and or photodegradation of the contaminant into a more toxic form. These degraded products could be more soluble and dissolve into the water column and exert narcotic toxicity, or perhaps may be activated to exert a more polar toxic effect.

Ultimately, the effects of any oil spill depend on the habitats and ecological resources potentially impacted by the spill and associated response options. Modelling the impacts associated with oil spills requires knowledge of environmental compartments (ECs) impacted, as well as the valued ecosystem components (VECs) that reside in each habitat (Bock et al. 2018). ECs are determined based on the behavior of spilled oil and the individual populations of organisms within each location, and are used to identify similar habitat types (shoreline, coast, shelf, etc.) that can be subdivided further (shoreline divided into rocky shore, sand beach, marsh, etc.). Spilled oil can exhibit various behaviors in different ECs, altering the fate of oil and adjusting impacts to VECs. VECs are determined based on the societal, ecological, cultural and archaeological value, or based on recovery potential or ecosystem services provided. This process accounts for sensitivity and value of each organism within the EC impacted and aids in determining the level of impact associated with different oil spill response options.

5.1.4 Spill response options

Understanding the goals and priorities of a response prior to a spill is extremely important and often requires input from many agencies and local stakeholders. This often occurs during response-planning stages because selecting the best response option to an oil spill requires understanding which options are available and feasible. After ensuring human safety, the second highest priority of oil spill response is to reduce environmental damage (National Academies of

Sciences and Medicine 2019). Response options available for most oil spills include mechanical containment and recovery, protective booming and shoreline clean-up, in situ burning, surface and subsea dispersant use, and a natural attenuation "do-nothing" approach. Each response option alters the fate and effects of the oil, resulting in accompanying benefits and trade-offs.

Mechanical containment was designed to prevent the spreading and transport of oil away from the spill site using booms and other devices. Containment is typically accompanied by recovery, which utilizes surface skimming technology to concentrate and permanently remove the oil from the water. This method of response is well-accepted and readily deployed in the immediate window of opportunity, but is typically inefficient when volumes or durations of spills are high. Mechanical containment and recovery usually recover no more than 10% of the oil spilled and requires large amounts of oily-waste storage and disposal, making it labor and equipment intensive (National Academies of Sciences and Medicine 2019). In addition, in situ burning is sometimes coupled with mechanical containment, which burns oil as a means of removing it from the water surface. Burning has a high elimination rate and no recovery of oil, but usually requires fresh oil for ignition and special approvals and permits. Additionally, burning produces a localized decrease in air quality and produces a burn residue that may sink or be difficult to recover. Protection of sensitive habitats is also accomplished with mechanical devices similar to those used in containment. Booms and other barriers are placed near sensitive resources to exclude approaching oil and divert it to a less sensitive/valuable location. Should mechanical containment fail, or oil be diverted to a more resilient location, shoreline cleanup is another available option for removing spilled oil.

Some oil spills occur in sea conditions which are not conducive to mechanical containment or recovery, and these situations may require other response options, like chemical dispersants. Dispersants can be utilized on surface or subsea spills; acting to reduce droplet size and limit the expression of surface oil by increasing the water-column concentration. Trade-offs of dispersant use may be complex and depend heavily on the environmental conditions.

5.2 POTENTIAL OIL SPILL IMPACTS TO FLORIDA CORAL REEFS

5.2.1 Surface oil spill

The likely oil spill scenario that may impact coral reefs in Broward County, FL is related to their proximity to Port Everglades, the dominant petroleum import location for the majority of the Florida population. Port Everglades regularly receives a large amount of refined petroleum

(fiscal year 2019= 125,874,000 barrels; www.porteverglades.net) in the form of gasoline, jet and diesel fuel, as well as crude oil. Ship groundings and anchor events have previously impacted the shoreline and corals in this area, as anchorages for the port lie within close proximity to many shallow water coral reefs (Figure 5.1). Dredging of the channel is currently approved and scheduled to widen and deepen the port, in order to facilitate the transport of larger, near-capacity tanker ships that can keep up with increased demand. This increases the potential for an accident related to one of the larger tanker ships like the AFRAMAX, with a capacity of 700,000 barrels of product (111 million liters) when completely full.

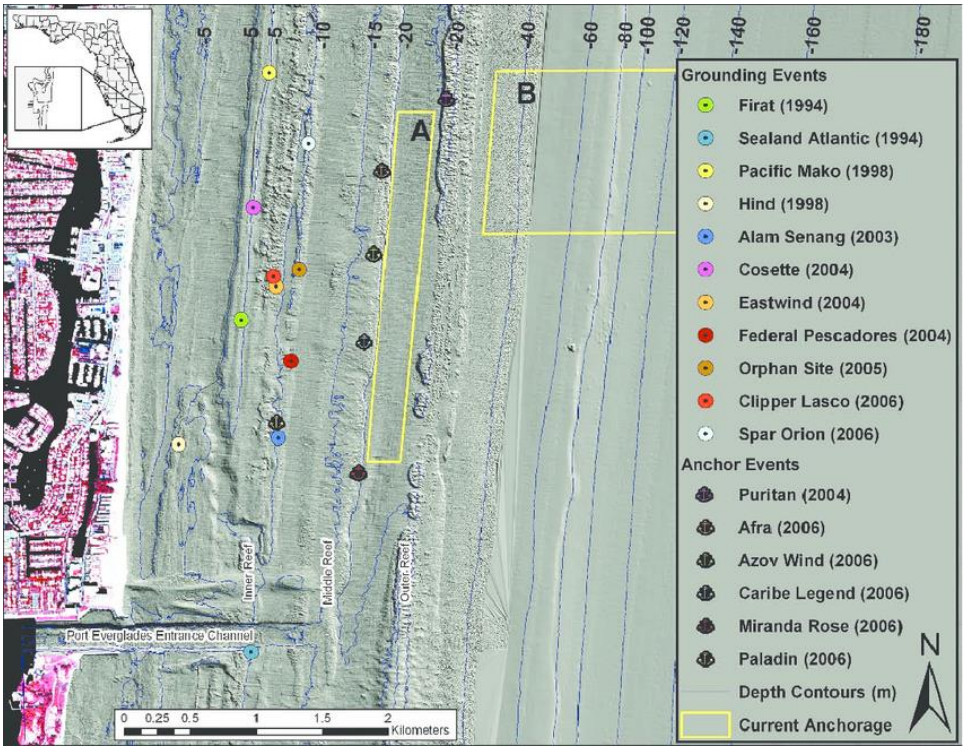

Figure 5.1 Map of Port Everglades, Florida ship groundings and anchor events reproduced from Banks et al. (2008).

If a cargo spill from an AFRAMAX tanker were to occur, it would be within close proximity to the coast, perhaps inside Port Everglades during docking or offloading product. The close proximity to shoreline would provide ample opportunity to respond to the spill quickly, and the initial response would be to contain the source of the spill with mechanical booms and as much recovery as feasible, although the physical sea state at the time of the spill must be calm enough to deploy these response options. Although this will inevitably be overwhelmed by the

amount of product spilled, some containment and collection is necessary, and will at the very least slow the spread and transport of oil toward the shoreline. Before the next set of response options are considered, it is important to assess the assumed fate of the spilled oil if a natural attenuation and monitoring approach were to be chosen. Much of the petroleum cargo entering Port Everglades is refined product enriched in VOCs, and a large volume will evaporate to the atmosphere or dissolve into the water column. Spilled oil on the surface, and more importantly in the water column, would be continuously cycled in and out of the port by semi-diurnal tides. The typical weather conditions for Port Everglades include onshore winds around 5-10 knots which would direct these volatilized compounds and all remaining surface oil toward the shoreline.

In a recent comparative risk assessment of spill response options in the area of another coral reef (Walker et al. 2018), the goal was to limit the spreading of spilled oil and extent of contamination to the surface, water column, benthos, and shoreline. In the current scenario, a combined response effort would be required to accommodate the protection of ECs, specifically the shoreline and associated sensitive habitats. After the initial mechanical recovery attempts at the source, physical protection of valued resources should be employed where possible. Winds are likely to move unmitigated surface oil toward shorelines, containment and diversion booms should be used to protect sensitive shoreline systems from stranding oil. Whether value is ecologically, societally, or economically based, sensitive nearshore habitats (corals and mangroves) and beaches would direct a majority of the response focus. Protection of every sensitive shoreline is unfeasible in many cases where the amount of time between contaminant release and shoreline stranding is limited.

A majority of the product entering Port Everglades is refined fuel that is highly volatile and light weight, and would produce a high amount of evaporation at the surface. Chemical dispersants are not generally applied to volatile, refined petroleum product, as spreading, dissolution, and evaporation will disperse the product naturally. In addition, dispersants are not pre-approved for use in US waters within 3 nm of shore in less than 10 m depth (National Academies of Sciences and Medicine 2019). However, spills within close proximity to sensitive shores and in depths of greater than 10 m may be prime candidates for use of chemical dispersants in order to remove surface oil and reduce damage to the most valued environmental component, but only when the oil is dispersible.

In this scenario, high amounts of evaporation and natural dispersion would limit the response options beyond mechanical containment and exclusion. Refined petroleum products have a higher proportion of sparingly soluble compounds compared to crude oil, and water concentrations of VOCs, MAHs, and low-ring PAHs would be increased near the source of contamination. The semi-diurnal tides in South Florida would intermittently expose water column organisms, including corals and other benthic organisms outside of the port during ebb tide. The rapid dilution of these compounds would limit effects to the coral animal, and severe damage would not be likely, as the internal defense mechanisms of these coral species have been proven capable of detoxifying or depurating these semi-soluble compounds.

5.2.2 Subsurface oil spill

Another potential risk to corals in South Florida is related to the increased oil exploration near Cuba, which entails deep-sea drilling off the northern coast near the Florida Straits. Ocean currents in this location are highly dynamic and contain many meso-scale eddies, some of which move eastward and are related to the Florida Current and the evolution of the Loop current in the Gulf of Mexico (Kourafalou et al. 2017). A major oil spill in this area resulting from loss of well control could have numerous pathways, one of which includes upwelling along the Cuban coast and entering the Florida Straits where transport would bring oil very near the Florida Keys and Miami-Dade/Broward County reefs (Paris et al. 2020).

The close proximity of Florida and the future Cuban oil exploration sites makes Florida reefs and other sensitive shorelines vulnerable targets in the event of an oil spill in these areas (Drouin et al. 2019). In a modelling exercise recently completed for a simulated deep-sea well blow-out in the northern Gulf of Mexico, the no response/natural attenuation approach resulted in the most floating oil and the highest amounts of atmospheric loss through volatilization (French-McCay et al. 2018). If an oil spill (surface or deep) of large magnitude were to occur in the northeastern drilling sites of the Cuban exploration area, a large amount of floating surface oil would likely be transported toward the US coastline. Surface oil transport was modelled in a simulated “worst-case” scenario spill in this area (Figure 5.2), and showed surface oil impacting a majority of the FL coastline within days of the spill (Drouin et al. 2019).

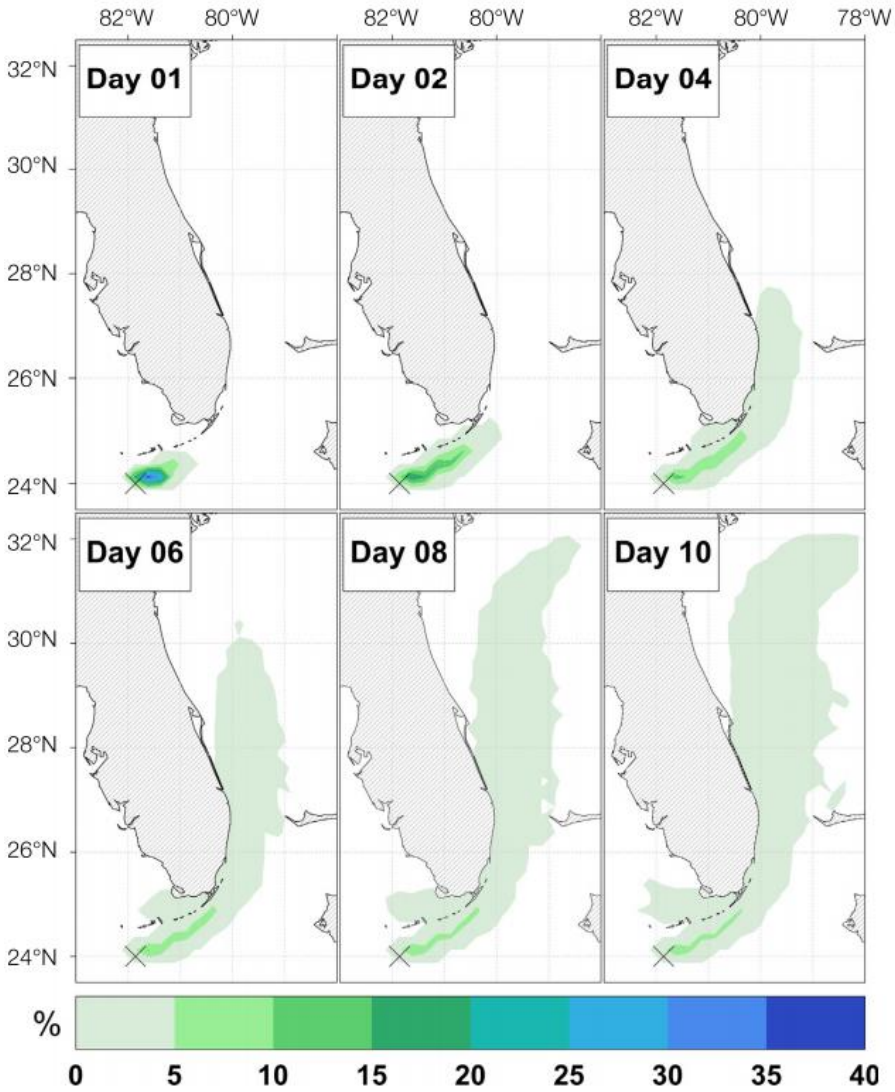

Figure 5.2 Probability distribution map of floating oil particles released in the "worst-case" scenario of an oil spill resulting from Cuban exploration. Reproduced with permission from (Drouin et al. 2019).

Surface oil spills are dangerous, but a loss of deep well control at offshore drilling platforms remains a primary risk factor for spills (Paris et al. 2020). A deep-sea blowout similar to the *Deepwater Horizon* was simulated for the Cuban West coast, and showed oil primarily constrained to the subsea below 400 m, and secondarily at the surface (0-20 m). Results of the simulation showed oil transported in all directions, including into the Florida Current toward the SE United States and Atlantic, with a large fraction remaining suspended in the water column. Interestingly, transport of the surface slicks and deep plumes were independent due to the dynamic currents and bathymetry of the location. The deep plume did not cross the Yucatan

Straits and was constrained to the coast by deep currents around a seamount and the steep coast of Cuba, while surface slicks crossed both the Yucatan and Florida Straits. Additionally, the deep plume remained the largest mass of the spill throughout the simulation, due to bathymetry and current constraints, acting as a continuous supply of weathered oil to the surrounding water.

Limiting expression of surface oil would aid in preventing impacts to the Florida coast in the event of a well blowout similar to the previous scenario. Many of the same response options deployed in a surface oil spill can also be applied to a deep-well blowout, but only once the oil reaches the surface. A combination of response options would be required to reduce surface expression of oil from a deep-well blowout in the Cuban exploration area. In another location, the use of mechanical recovery, in situ burning, and surface dispersant application were all shown to reduce the surface expression of oil following a modeled deep-well blowout (French-McCay et al. 2018). Floating oil mass, volume, and area were all significantly reduced by these response options, but inclusion of subsea dispersant injection (SSDI) further reduced surface oil, and increased biodegradation. In model runs without the use of SSDI, roughly 60% of the oil reached the surface and volatilized to the atmosphere. In fact, in any model run without SSDI, the surface and atmosphere combined to account for nearly 80% of the oil at most times, with the remaining mass divided between the water column, or collected by other surface response options.

In the event of a deep well blowout off the Cuban coast, limiting impacts to Florida coasts would require the use of SSDI to reduce the surface expression of oil, and increase transportation of the oil far downfield. Oil droplet size influences a majority of the fate processes for oil spilled at depth, and smaller droplets with a higher surface area to volume ratio have increased dissolution potential (National Academies of Sciences and Medicine 2019). The high contact rate of SSDI would produce much smaller droplet sizes that become entrained in the water column, where the high surface area to volume ratio promotes faster dissolution and biodegradation. This entrainment in the water column results in very long surfacing times, with droplets potentially carried long distances, surfacing as sheens (French-McCay et al. 2018) . The decrease in surface expression of oil from subsea dispersant therefore produces higher dissolved water column concentrations that dilutes rapidly in 3 dimensions (National Academies of Sciences and Medicine 2019). In this scenario, SSDI application would decrease the potential for

shoreline oiling, while increasing the water column concentration of oil that is transported away and diluted.

If winds are forecasted to transport surface oil onshore, and overall goals are to limit this exposure, effective application of dispersants would reduce surface oil and increase water column concentrations. The number one trade-off associated with dispersant use is an increase in water column concentrations organisms are exposed to, which is especially problematic if the water depth is shallow enough for these concentrations to increase exposure to the benthos. However, increased concentrations associated with subsea dispersant application have been shown to decline rapidly. The decision to expose one EC while preventing exposure in another is one that requires intricate knowledge of the priorities for each specific spill response.

5.3 FINAL RECOMMENDATIONS FOR CORAL

If oil were to spill in the area of a coral reef, multiple response options may be employed to limit the potential impacts. After human health is protected, the secondary focus shifts towards reducing environmental consequences of the spilled oil by employing response options with the greatest protection and fastest recovery of the resources deemed most at risk. Whether the protection is assigned due to societal, ecological, cultural and archaeological value, or based on recovery potential or ecosystem services provided, coral reefs rank among the highest valued resource for protection in an oil spill scenario. Selecting the proper response option not only requires knowledge of the fate of the oil and potentially affected resources, but also understanding what options are available and feasible, and how they align with goals of the response. Importantly, in the US, dispersant use is not pre-authorized for use in shallow water less than 10 m depth, or within 3 nautical miles from shore, where most coral reefs reside. Additionally, most US spills are too small or too close to shore for dispersants to be a viable option.

Most oil spills that affect coral reefs will likely be surface spills in the nearshore environment, in depths of less than 100 m. Corals are benthic organisms that are exposed to the dissolved fraction of oil, which limits the potential impacts from floating oil. This suggests a natural attenuation approach for spill response, however, because nearshore coral ecosystems rely heavily on adjacent mangroves and seagrasses, response options should consider all three communities. A recent NEBA exercise in Hawaii (Walker et al. 2018) outlined a multifaceted response that sought to limit oil spreading and extent of contamination on surface waters, the

water column, benthos and shoreline. The combination of response options included natural attenuation, mechanical recovery and containment, chemical dispersion, resource protection though physical barriers, and shoreline clean-up. This combination of options suggested for Hawaii would be applicable to many nearshore environments of similar depth regime (quickly increasing depth with distance from shore), but may require adjustment in different physical environments or locations with already stressed nearshore systems, like Broward County.

Overall, a response in coral reef environments should focus on protection of the entire surrounding ecosystem (seagrass, mangrove, and coral reef), as the interplay between the three compartments controls the health of the overall ecosystem. Results from the TROPICS experiment also highlight the tradeoffs associated with response options in these nearshore environments and revealed less long-lasting effects in the chemically dispersed plots compared to physically dispersed oil plots (Renegar et al. 2017a). With that said, a combination of response options similar to the Hawaii NEBA is suggested. Immediate source control and mechanical containment and recovery should always be implemented, followed by physical protection of sensitive shorelines with mechanical booms, which may have inherent effects associated with their use. If fate models suggest shoreline impacts are high even with mechanical containment and recovery, the use of chemical dispersants to reduce shoreline stranding of oil should be considered. Shorelines in proximity to coral reefs are typically lined with very sensitive habitats, and damage from chronic exposure resulting from oil trapped in the sediments is a concern.

Limiting the stranding of oil by dispersion would result in exposing the water column to higher levels of droplets/dissolved compounds in the short term. Although higher initial concentrations would be experienced, the rapid dilution should limit exposure durations to a time scale less than required to cause effects to the coral animal. The main tradeoff associated with protecting the shoreline by dispersing spilled oil is an increased water column concentration. This increased water concentration has potential to cause impacts to coral, similar to those observed here, but would presumably be controlled by the cellular and genetic machinery previously identified. Although this seems to be acceptable in terms of coral resilience, coral reefs are habitat for a very large diversity of crustaceans and small fish. As indicated by the lower critical target lipid body burdens calculated from the target lipid model (McGrath et al. 2018), some of these organisms are considerably more sensitive to hydrocarbon exposure than corals. It remains unclear whether the dispersion of oil into the water column, or shoreline

stranding producing chronic releases of oil from sediments, would cause more harm to the species more sensitive than coral. However, the life cycle of many of these more sensitive species is short, and a brief exposure that rapidly dilutes may be less harmful than the effects of floating oil reaching mangroves and seagrass communities producing acute effects and chronic exposures.

5.4 CONCLUSIONS

Coral reefs are one of the highest valued resources for protection during oil spill response activities, but have been determined here to be more resilient to exposure when compared to other organisms. Single-compound, oil, and dispersed-oil exposures were used to validate common toxicological models and compare the toxicity of oil and dispersed oil for two coral species, confirming that corals are more resilient to petroleum exposure than a majority of other organisms. This suggests effects from hydrocarbon spills would be limited in comparison to other organisms in the same environment, and response options should consider the entire ecosystem as a whole, and not just coral. Additionally, when concentrations permit (<100 mg/L oil loading), chemical dispersants could potentially reduce overall impacts to the entire ecosystem by limiting shoreline stranding of oil. The resulting increased water-column concentrations would remain below harmful levels in terms of the coral animal, and could potentially reduce the impacts of surface oil on the nearshore system.

ACKNOWLEDGMENTS

Thank you to the Gulf of Mexico Research Initiative for providing the funds for this research (Agreement #: G-231807) I would like to first thank my committee; D. Abigail Renegar, PhD; Jose Lopez, PhD; Thomas Parkerton, PhD; and Bernhard Riegl, PhD, for all of their guidance and support throughout this research project and my career at Nova Southeastern University. I would like to thank my lab members for all of their contributions; Josh Stocker, Eileen Whitemiller, Dawn Bickam, Edward Young, Kyle Pisano, and Yvain Desplat. I would also like to thank Paul Schuler for the numerous opportunities and guidance provided throughout this dissertation.

REFERENCES

FastQC: A Quality Control Tool for High Throughput Sequence Data. Andrews, S. 2010. http://www.bioinformatics.babraham.ac.uk/projects/fastqc.

Aurand, D, and G Coelho. 2005. "Cooperative Aquatic Toxicity Testing of Dispersed Oil and the Chemical Response to Oil Spills: Ecological Effects Research Forum (CROSERF)." *Ecosystem Management and Associates, Inc. Technical Report 07-03*:105 + Appendices.

Banks, Kenneth, Bernhard Riegl, Vincent Richards, Brian Walker, Kevin Helmle, Lance Jordan, Janet Phipps, Mahmood Shivji, Richard Spieler, and Richard Dodge. 2008. "The Reef Tract of Continental Southeast Florida (Miami-Dade, Broward and Palm Beach Counties, USA)." In, 175-220.

Barata, Carlos, Albert Calbet, Enric Saiz, Laura Ortiz, and Josep Maria Bayona. 2005. "Predicting single and mixture toxicity of petrogenic polycyclic aromatic hydrocarbons to the copepod Oithona davisae." *Environmental Toxicology and Chemistry* 24 (11):2992-2999. doi: 10.1897/05-189R.1.

Barshis, Daniel J., Jason T. Ladner, Thomas A. Oliver, François O. Seneca, Nikki Traylor-Knowles, and Stephen R. Palumbi. 2013. "Genomic basis for coral resilience to climate change." *Proceedings of the National Academy of Sciences* 110 (4):1387-1392. doi: 10.1073/pnas.1210224110.

Bejarano, A. C., J. R. Clark, and G. M. Coelho. 2014. "Issues and challenges with oil toxicity data and implications for their use in decision making: a quantitative review." *Environ. Toxicol. Chem.* 33 (4):732-42. doi: 10.1002/etc.2501.

Bejarano, Adriana, Edwin Levine, and Alan Mearns. 2013. "Effectiveness and potential ecological effects of offshore surface dispersant use during the Deepwater Horizon oil spill: a retrospective analysis of monitoring data." *Environmental Monitoring & Assessment* 185 (12):10281-10295.

Bera, G., T. Parkerton, A. Redman, N. R. Turner, D. A. Renegar, J. L. Sericano, and A. H. Knap. 2018. "Passive dosing yields dissolved aqueous exposures of crude oil comparable to the CROSERF (Chemical Response to Oil Spill: Ecological Effects Research Forum) water accommodated fraction method." *Environ Toxicol Chem* 37 (11):2810-2819. doi: 10.1002/etc.4263.

Bock, Michael, Hilary Robinson, Richard Wenning, Deborah French-McCay, Jill Rowe, and Ann Hayward Walker. 2018. "Comparative risk assessment of oil spill response options for a deepwater oil well blowout: Part II. Relative risk methodology." *Marine Pollution Bulletin* 133:984-1000. doi: https://doi.org/10.1016/j.marpolbul.2018.05.032.

Bolger, Anthony M., Marc Lohse, and Bjoern Usadel. 2014. "Trimmomatic: a flexible trimmer for Illumina sequence data." *Bioinformatics (Oxford, England)* 30 (15):2114-2120. doi: 10.1093/bioinformatics/btu170.

Butler, JD, TF Parkerton, DJ Letinski, GE Bragin, MA Lampi, and KR Cooper. 2013. "A novel passive dosing system for determining the toxicity of phenanthrene to early life stages of zebrafish." *Science of The Total Environment* 463:952-958.

Butler, Joshua D. 2013. "The application of a passive dosing system for determining zebrafish early life stage toxicity of hydrocarbons for use in calibrating a predictive model to acute and chronic endpoints." Doctor of Philosophy PhD Dissertation, Graduate Program of Environmental Sciences, Rutgers, The State University of New Jersey.

Capuzzo, Judith M. 1987. "Chapter 8: biological effects of petroleum hydrocarbons: Assessments from experimental results." In *Long-term Environmental Effects of Offshore Oil & Gas Development*, edited by D.F. Boesch and N.N. Rabalais, 343-410. New York: Elsevier.

Davies, Sarah W., Adrian Marchetti, Justin B. Ries, and Karl D. Castillo. 2016. "Thermal and pCO2 Stress Elicit Divergent Transcriptomic Responses in a Resilient Coral." *Frontiers in Marine Science* 3 (112). doi: 10.3389/fmars.2016.00112.

Davies, Specer P. 1989. "Short-term growth measurements of corals using an accurate buoyant weighing technique." *Marine Biology* 101 (3):389-395. doi: 10.1007/BF00428135.

Di Toro, Dominic M., and Joy A. McGrath. 2000. "Technical basis for narcotic chemicals and polycyclic aromatic hydrocarbon criteria. II. Mixtures and sediments." *Environmental Toxicology and Chemistry* 19 (8):1971-1982. doi: 10.1002/etc.5620190804.

Di Toro, Dominic M., Joy A. McGrath, and David J. Hansen. 2000. "Technical basis for narcotic chemicals and polycyclic aromatic hydrocarbon criteria. I. Water and tissue." *Environmental Toxicology and Chemistry* 19 (8):1951-1970. doi: 10.1002/etc.5620190803.

Downs, Craig A., Gary K. Ostrander, Luc Rougee, Teina Rongo, Sean Knutson, David E. Williams, Wendy Mendiola, Jackalyn Holbrook, and Robert H. Richmond. 2012. "The use of cellular diagnostics for identifying sub-lethal stress in reef corals." *Ecotoxicology* 21 (3):768-782. doi: http://dx.doi.org/10.1007/s10646-011-0837-4.

Downs, Craig A., Cheryl M. Woodley, John E. Fauth, Sean Knutson, Martina Maria Burtscher, Lisa A. May, Athena R. Avadanei, Julie L. Higgins, and Gary K. Ostrander. 2011. "A survey of environmental pollutants and cellular-stress markers of Porites astreoides at six sites in St. John, U.S. Virgin Islands." *Ecotoxicology* 20 (8):1914. doi: 10.1007/s10646-011-0729-7.

Drouin, K. L., A. J. Mariano, E. H. Ryan, and L. C. Laurindo. 2019. "Lagrangian simulation of oil trajectories in the Florida Straits." *Marine Pollution Bulletin* 140:204-218. doi: https://doi.org/10.1016/j.marpolbul.2019.01.031.

Edge, S. E., T. L. Shearer, M. B. Morgan, and T. W. Snell. 2013. "Sub-lethal coral stress: Detecting molecular responses of coral populations to environmental conditions over space and time." *Aquatic Toxicology* 128 (Supplement C):135-146. doi: https://doi.org/10.1016/j.aquatox.2012.11.014.

French-McCay, D. P. 2002. "Development and application of an oil toxicity and exposure model, OilToxEx." *Environ Toxicol Chem* 21 (10):2080-94.

French-McCay, D. P. 2004. "Oil spill impact modeling: development and validation." *Environ Toxicol Chem* 23 (10):2441-56. doi: 10.1897/03-382.

French-McCay, Deborah, Deborah Crowley, Jill J. Rowe, Michael Bock, Hilary Robinson, Richard Wenning, Ann Hayward Walker, John Joeckel, Tim J. Nedwed, and Thomas F. Parkerton. 2018. "Comparative Risk Assessment of spill response options for a deepwater oil well blowout: Part 1. Oil spill modeling." *Marine Pollution Bulletin* 133:1001-1015. doi: https://doi.org/10.1016/j.marpolbul.2018.05.042.

Geyer, H. J., I. Scheunert, R. Bruggemann, M. Matthies, C. E. Steinberg, V. Zitko, A. Kettrup, and W. Garrison. 1994. "The relevance of aquatic organisms' lipid content to the toxicity of lipophilic chemicals: toxicity of lindane to different fish species." *Ecotoxicol Environ Saf* 28 (1):53-70. doi: 10.1006/eesa.1994.1034.

Geyer, Harald J., Christian E. Steinberg, Irene Scheunert, Rainer Brüggemann, Werner Schütz, Antonius Kettrup, and Karl Rozman. 1993. "A review of the relationship between acute toxicity (LC50) of γ-hexachlorocyclohexane (γ-HCH, Lindane) and total lipid content of different fish species." *Toxicology* 83 (1):169-179. doi: https://doi.org/10.1016/0300-483X(93)90100-7.

Goldstone, J. V., A. Hamdoun, B. J. Cole, M. Howard-Ashby, D. W. Nebert, M. Scally, M. Dean, D. Epel, M. E. Hahn, and J. J. Stegeman. 2006. "The chemical defensome: Environmental sensing and response genes in the Strongylocentrotus purpuratus genome." *Developmental Biology* 300 (1):366-384. doi: https://doi.org/10.1016/j.ydbio.2006.08.066.

Haapkylae, J., F. Ramade, and B. Salvat. 2007. "Oil pollution on coral reefs: A review of the state of knowledge and management needs." *Vie et Milieu* 57 (1-2):95-111.

Hoffman, F. Owen, and Jana S. Hammonds. 1994. "Propagation of Uncertainty in Risk Assessments: The Need to Distinguish Between Uncertainty Due to Lack of Knowledge and Uncertainty Due to Variability." *Risk Analysis* 14 (5):707-712. doi: 10.1111/j.1539-6924.1994.tb00281.x.

Imbs, A. B. 2013. "Fatty acids and other lipids of corals: Composition, distribution, and biosynthesis." *Russian Journal of Marine Biology* 39 (3):153-168. doi: 10.1134/S1063074013030061.

Imbs, A. B., and I. M. Yakovleva. 2012. "Dynamics of lipid and fatty acid composition of shallow-water corals under thermal stress: an experimental approach." *Coral Reefs* 31 (1):41-53. doi: 10.1007/s00338-011-0817-4.

Karako-Lampert, Sarit, Didier Zoccola, Mali Salmon-Divon, Mark Katzenellenbogen, Sylvie Tambutté, Anthony Bertucci, Ove Hoegh-Guldberg, Emeline Deleury, Denis Allemand, and Oren Levy. 2014. "Transcriptome Analysis of the Scleractinian Coral Stylophora pistillata." *PLOS ONE* 9 (2):e88615. doi: 10.1371/journal.pone.0088615.

Kenkel, C. D., E. Meyer, and M. V. Matz. 2013. "Gene expression under chronic heat stress in populations of the mustard hill coral (Porites astreoides) from different thermal environments." *Molecular Ecology* 22 (16):4322-4334. doi: 10.1111/mec.12390.

Kipka, U., and D. M. Di Toro. 2009. "Technical basis for polar and nonpolar narcotic chemicals and polycyclic aromatic hydrocarbon criteria. III. A polyparameter model for target lipid partitioning." *Environ Toxicol Chem* 28 (7):1429-38. doi: 10.1897/08-364.1.

Kitchen, Sheila A., Camerron M. Crowder, Angela Z. Poole, Virginia M. Weis, and Eli Meyer. 2015. "De Novo Assembly and Characterization of Four Anthozoan (Phylum Cnidaria) Transcriptomes." *G3 (Bethesda, Md.)* 5 (11):2441-2452. doi: 10.1534/g3.115.020164.

Knap, AH, TD Sleeter, RE Dodge, SC Wyers, HR Frith, and SR Smith. 1983. "The effects of oil spills and dispersant use on corals: a review and multidisciplinary experimental approach." *Oil and Petrochemical Pollution* 1 (3):157-169.

Kourafalou, Vassiliki, Yannis Androulidakis, Matthieu Le Hénaff, and HeeSook Kang. 2017. "The Dynamics of Cuba Anticyclones (CubANs) and Interaction With the Loop Current/Florida Current System." *Journal of Geophysical Research: Oceans* 122 (10):7897-7923. doi: 10.1002/2017jc012928.

Landrum, Peter F., Peter M. Chapman, Jerry Neff, and David S. Page. 2012. "Evaluating the aquatic toxicity of complex organic chemical mixtures: Lessons learned from polycyclic aromatic hydrocarbon and petroleum hydrocarbon case studies." *Integrated Environmental Assessment and Management* 8 (2):217-230. doi: 10.1002/ieam.277.

Langmead, Ben, and Steven L. Salzberg. 2012. "Fast gapped-read alignment with Bowtie 2." *Nature Methods* 9 (4):357-359. doi: 10.1038/nmeth.1923.

Li, Bo, and Colin N. Dewey. 2011. "RSEM: accurate transcript quantification from RNA-Seq data with or without a reference genome." *BMC Bioinformatics* 12 (1):323. doi: 10.1186/1471-2105-12-323.

Liew, Yi Jin, Manuel Aranda, and Christian R. Voolstra. 2016. "Reefgenomics.Org - a repository for marine genomics data." *Database* 2016. doi: 10.1093/database/baw152.

Lirman, D, N Formel, S Schopmeyer, JS Ault, SG Smith, D Gilliam, and Bernhard Riegl. 2013. "Percent recent mortality (PRM) of stony corals as an ecological indicator of coral reef condition." *Ecological Indicators* 44:120-127.

Loya, Y, and B Rinkevich. 1980. "Effects of oil pollution on coral reef communities." *Marine Ecology Progress Series* 3 (16):180.

Martinez, Maria Del Carmen Guzman, Patricia Ramirez Romero, and Anastazia T. Banaszak. 2007. "Photoinduced toxicity of the polycyclic aromatic hydrocarbon, fluoranthene, on the coral, Porites divaricata." *Journal of Environmental Science and Health, Part A: Toxic/Hazardous Substances & Environmental Engineering* 42 (10):1495-1502.

McCay, Deborah French. 2003. "Development and application of damage assessment modeling: example assessment for the North Cape oil spill." *Marine Pollution Bulletin* 47 (9):341-359. doi: https://doi.org/10.1016/S0025-326X(03)00208-X.

McGrath, Joy A, and Dominic M Di Toro. 2009. "Validation of the target lipid model for toxicity assessment of residual petroleum constituents: Monocyclic and polycyclic aromatic hydrocarbons." *Environmental Toxicology and Chemistry* 28 (6):1130-1148.

McGrath, Joy A., Christopher J. Fanelli, Dominic M. Di Toro, Thomas F. Parkerton, Aaron D. Redman, Miriam Leon Paumen, Mike Comber, Charles V. Eadsforth, and Klaas den Haan. 2018. "Re-evaluation of target lipid model–derived HC5 predictions for hydrocarbons." *Environmental Toxicology and Chemistry* 37 (6):1579-1593. doi: 10.1002/etc.4100.

McGrath, Joy A., Thomas F. Parkerton, and Dominic M. Di Toro. 2004. "Application of the narcosis target lipid model to algal toxicity and deriving predicted-no-effect concentrations." *Environmental Toxicology and Chemistry* 23 (10):2503-2517. doi: 10.1897/03-538.

McGrath, Joy A., Thomas F. Parkerton, Ferdi L. Hellweger, and Dominic M. Di Toro. 2005. "Validation of the narcosis target lipid model for petroleum products: Gasoline as a case study." *Environmental Toxicology and Chemistry* 24 (9):2382-2394.

Metzker, Michael L. 2009. "Sequencing technologies — the next generation." *Nature Reviews Genetics* 11:31. doi: 10.1038/nrg2626.

Moll, Pamela, Michael Ante, Alexander Seitz, and Torsten Reda. 2014. "QuantSeq 3′ mRNA sequencing for RNA quantification." *Nature Methods* 11. doi: 10.1038/nmeth.f.376.

Morgan, M. B., D. L. Vogelien, and T. W. Snell. 2001. "Assessing coral stress responses using molecular biomarkers of gene transcription." *Environmental toxicology and chemistry* 20 (3):537-543.

Morgan, Michael B., Sara E. Edge, Alexander A. Venn, and Ross J. Jones. 2017. "Developing transcriptional profiles in Orbicella franksi exposed to copper: Characterizing responses associated with a spectrum of laboratory-controlled environmental conditions." *Aquatic Toxicology* 189 (Supplement C):60-76. doi: https://doi.org/10.1016/j.aquatox.2017.05.005.

Moya, A., l. Huisman, E. E. Ball, D. C. Hayward, l. C. Grasso, C. M. Chua, H. N. Woo, J.-p. Gattuso, S. Forêt, and D. J. Miller. 2012. "Whole Transcriptome Analysis of the Coral Acropora millepora Reveals Complex Responses to CO2-driven Acidification during the Initiation of Calcification." *Molecular Ecology* 21 (10):2440-2454. doi: 10.1111/j.1365-294X.2012.05554.x.

National Academies of Sciences, Engineering, and Medicine. 2019. *The Use of Dispersants in Marine Oil Spill Response*. Washington, DC: The National Academies Press.

Nikinmaa, Mikko, and Kalle T. Rytkönen. 2011. "Functional genomics in aquatic toxicology—Do not forget the function." *Aquatic Toxicology* 105 (3, Supplement):16-24. doi: https://doi.org/10.1016/j.aquatox.2011.05.019.

Nikinmaa, Mikko, and Kalle T. Rytkönen. 2012. "From genomes to functions in aquatic biology." *Marine Genomics* 5 (Supplement C):1-6. doi: https://doi.org/10.1016/j.margen.2011.08.004.

NRC. 2003. *Oil in the Sea III: Inputs, Fates, and Effects*. National Research Council, Washington, DC: National Academy Press. Book.

NRC. 2005. *Oil Spill Dispersants: Efficacy and Effects*. National Research Council, Washington, D.C.: National Academy Press.

OmicsBox-Bioinformatics Made Easy. BioBam Bioinformatics (Version 1.3.3). 2019. www.biobam.com/omicsbox.

Paris, Claire B., Ana C. Vaz, Igal Berenshtein, Natalie Perlin, Robin Faillettaz, Zachary M. Aman, and Steven A. Murawski. 2020. "Simulating Deep Oil Spills Beyond the Gulf of Mexico." In *Scenarios and Responses to Future Deep Oil Spills: Fighting the Next War*,

edited by Steven A. Murawski, Cameron H. Ainsworth, Sherryl Gilbert, David J. Hollander, Claire B. Paris, Michael Schlüter and Dana L. Wetzel, 315-336. Cham: Springer International Publishing.

Ramos, R., and E. Garcia. 2007. "Induction of mixed-function oxygenase system and antioxidant enzymes in the coral Montastraea faveolata on acute exposure to benzo(a)pyrene." *Comparative Biochemistry and Physiology C-Toxicology & Pharmacology* 144 (4):348-355. doi: 10.1016/j.cbpc.2006.11.006.

Redman, A. D. 2015. "Role of entrained droplet oil on the bioavailability of petroleum substances in aqueous exposures." *Marine Pollution Bulletin* 97 (1–2):342-348. doi: http://dx.doi.org/10.1016/j.marpolbul.2015.05.068.

Redman, Aaron D, Josh D Butler, Daniel J Letinski, and Thomas F Parkerton. 2017. "Investigating the role of dissolved and droplet oil in aquatic toxicity using dispersed and passive dosing systems." *Environmental toxicology and chemistry* 36 (4):1020-1028.

Redman, Aaron D, Thomas F Parkerton, Joy A McGrath, and Dominic M Di Toro. 2012a. "PETROTOX: An aquatic toxicity model for petroleum substances." *Environmental Toxicology and Chemistry* 31 (11):2498-2506.

Redman, Aaron D., Joy A. McGrath, William A. Stubblefield, Al W. Maki, and Dominic M. Di Toro. 2012b. "Quantifying the concentration of crude oil microdroplets in oil–water preparations." *Environmental Toxicology and Chemistry* 31 (8):1814-1822. doi: 10.1002/etc.1882.

Redman, Aaron D., and Thomas F. Parkerton. 2015. "Guidance for improving comparability and relevance of oil toxicity tests." *Marine Pollution Bulletin* 98 (1–2):156-170. doi: http://dx.doi.org/10.1016/j.marpolbul.2015.06.053.

Renegar, D. Abigail, Paul Schuler, Nicholas Turner, Richard Dodge, Bernhard Riegl, Anthony Knap, Gopal Bera, Ronan Jézéquel, and Bradford Benggio. 2017a. "TROPICS field study (Panama), 32-year site visit: Observations and conclusions for near shore dispersant use NEBA and tradeoffs." *International Oil Spill Conference Proceedings* 2017 (1):3030-3050. doi: 10.7901/2169-3358-2017.1.3030.

Renegar, D. Abigail, Nicholas R. Turner, Bernhard M. Riegl, Richard E. Dodge, Anthony H. Knap, and Paul A. Schuler. 2017b. "Acute and sub-acute toxicity of the polycyclic aromatic hydrocarbon 1-methylnaphthalene to the shallow-water coral Porites divaricata: Application of a novel exposure protocol." *Environmental Toxicology and Chemistry* 36 (1):212-219. doi: 10.1002/etc.3530.

Renegar, DA, Nicholas Turner, Bernhard Riegl, Richard E Dodge, Anthony H Knap, and Paul Schuler. 2015. "Quantifying Hydrocarbon Toxicity to Shallow-Water Corals: Range Finding Exposure." Gulf of Mexico Oil Spill and Ecosystem Science Conference, Houston, TX.

Ritz, Christian, Florent Baty, Jens C. Streibig, and Daniel Gerhard. 2015. "Dose-Response Analysis Using R." *PLOS ONE* 10 (12):e0146021. doi: 10.1371/journal.pone.0146021.

Rotchell, Jeanette M., and Gary K. Ostrander. 2011. "MOLECULAR TOXICOLOGY OF CORALS: A REVIEW." *Journal of Toxicology and Environmental Health-Part B-Critical Reviews* 14 (8):571-592. doi: 10.1080/10937404.2011.615112.

Ruiz-Jones, Lupita J., and Stephen R. Palumbi. 2015. "Transcriptome-wide Changes in Coral Gene Expression at Noon and Midnight Under Field Conditions." *The Biological Bulletin* 228 (3):227-241. doi: 10.1086/BBLv228n3p227.

IUPAC-NIST Solubility Data Series Version 1.1. Shaw, D.G. 1989. International Union of Pure and Applied Chemistry.

Shigenaka, Gary. 2001. Toxicity of oil to reef-building corals: A spill response perspective. Seattle, WA: NOAA Technical Memorandum NOS OR&R 8. 87 p.

Shinzato, Chuya, Mayuko Hamada, Eiichi Shoguchi, Takeshi Kawashima, and Nori Satoh. 2012. "The Repertoire of Chemical Defense Genes in the Coral Acropora digitifera Genome." *Zoological Science* 29 (8):510-517. doi: 10.2108/zsj.29.510.

Shinzato, Chuya, Mayuri Inoue, and Makoto Kusakabe. 2014. "A Snapshot of a Coral "Holobiont": A Transcriptome Assembly of the Scleractinian Coral, Porites, Captures a Wide Variety of Genes from Both the Host and Symbiotic Zooxanthellae." *PLOS ONE* 9 (1):e85182. doi: 10.1371/journal.pone.0085182.

Shinzato, Chuya, Eiichi Shoguchi, Takeshi Kawashima, Mayuko Hamada, Kanako Hisata, Makiko Tanaka, Manabu Fujie, Mayuki Fujiwara, Ryo Koyanagi, Tetsuro Ikuta, Asao Fujiyama, David J. Miller, and Nori Satoh. 2011. "Using the Acropora digitifera genome to understand coral responses to environmental change." *Nature* 476:320. doi: 10.1038/nature10249 https://www.nature.com/articles/nature10249#supplementary-information.

Singer, M. M., D. Aurand, G. E. Bragin, J. R. Clark, G. M. Coelho, M. L. Sowby, and R. S. Tjeerdema. 2000. "Standardization of the preparation and quantitation of water-accommodated fractions of petroleum for toxicity testing." *Marine Pollution Bulletin* 40 (11):1007-1016.

Smith, Kilian EC, Nathalie Dom, Ronny Blust, and Philipp Mayer. 2010. "Controlling and maintaining exposure of hydrophobic organic compounds in aquatic toxicity tests by passive dosing." *Aquatic Toxicology* 98 (1):15-24.

Tarazona, Sonia, Pedro Furió-Tarí, David Turrà, Antonio Di Pietro, María José Nueda, Alberto Ferrer, and Ana Conesa. 2015. "Data quality aware analysis of differential expression in RNA-seq with NOISeq R/Bioc package." *Nucleic Acids Research* 43 (21):e140-e140. doi: 10.1093/nar/gkv711.

Tarazona, Sonia, Fernando García-Alcalde, Joaquín Dopazo, Alberto Ferrer, and Ana Conesa. 2011. "Differential expression in RNA-seq: A matter of depth." *Genome Research* 21 (12):2213-2223. doi: 10.1101/gr.124321.111.

Towle, E. K., I. C. Enochs, and C. Langdon. 2015. "Threatened Caribbean coral is able to mitigate the adverse effects of ocean acidification on calcification by increasing feeding rate." *PLoS One* 10 (4):e0123394. doi: 10.1371/journal.pone.0123394.

Traylor-Knowles, Nikki, Brian R. Granger, Tristan J. Lubinski, Jignesh R. Parikh, Sara Garamszegi, Yu Xia, Jarrod A. Marto, Les Kaufman, and John R. Finnerty. 2011. "Production of a reference transcriptome and transcriptomic database (PocilloporaBase) for the cauliflower coral, Pocillopora damicornis." *BMC Genomics* 12 (1):585. doi: 10.1186/1471-2164-12-585.

Turner, Nicholas. 2016. "Quantifying the Toxicity of 1-Methylnaphthalene to the Shallow-Water Coral, Porites divaricata, for Use in the Target Lipid Model." Masters of Science, Department of Marine and Environmental Science, Nova Southeastern University.

Turner, Nicholas R., and D. Abigail Renegar. 2017. "Petroleum hydrocarbon toxicity to corals: A review." *Marine Pollution Bulletin* 119 (2):1-16. doi: https://doi.org/10.1016/j.marpolbul.2017.04.050.

van Wezel, A. P., and A. Opperhuizen. 1995. "Narcosis due to environmental pollutants in aquatic organisms: residue-based toxicity, mechanisms, and membrane burdens." *Crit Rev Toxicol* 25 (3):255-79. doi: 10.3109/10408449509089890.

Venn, Alexander A., Jennifer Quinn, Ross Jones, and Andrea Bodnar. 2009. "P-glycoprotein (multi-xenobiotic resistance) and heat shock protein gene expression in the reef coral Montastraea franksi in response to environmental toxicants." *Aquatic Toxicology* 93 (4):188-195. doi: https://doi.org/10.1016/j.aquatox.2009.05.003.

Wade, Terry L, Maya Morales-McDevitt, Gopal Bera, Dawai Shi, Stephen Sweet, Binbin Wang, Gerado Gold-Bouchot, Antonietta Quigg, and Anthony H Knap. 2017. "A method for the production of large volumes of WAF and CEWAF for dosing mesocosms to understand marine oil snow formation." *Heliyon* 3 (10):e00419.

Wade, Terry LTL, Stephen TST Sweet, José LJL Sericano, Norman LNL Guinasso, Arne-RA-R Diercks, Raymond CRC Highsmith, Vernon LVL Asper, Dongjoo D Joung, Alan MAM Shiller, and Steven ESE Lohrenz. 2011. "Analyses of water samples from the Deepwater Horizon oil spill: Documentation of the subsurface plume." *Monitoring and Modeling the deepwater horizon oil spill: a record-breaking enterprise*:77-82.

Walker, Ann, Debra Scholz, and Ann Hess. 2018. Hawaii Net Environmental Benefit Analysis: Consensus Evaluation of Tradeoffs Associated with Oil Spill Response Options. A Report to the Oceania Regional Response Team. SEA Consulting Group, Cape Charles, VA, 23310.

Wetterstrand, KA. 2018. "DNA Sequencing Costs: Data from the NHGRI Genome Sequencing Program (GSP)." accessed 9/3/2018. www.genome.gov/sequencingcostsdata.

Woo, Seonock, Aekyung Lee, Vianney Denis, Chaolun A. Chen, and Seungshic Yum. 2014. "Transcript response of soft coral (Scleronephthya gracillimum) on exposure to polycyclic aromatic hydrocarbons." *Environmental Science and Pollution Research International* 21 (2):901-910. doi: http://dx.doi.org/10.1007/s11356-013-1958-5.

Yamashiro, Hideyuki, Hirosuke Oku, and Kyoko Onaga. 2005. "Effect of bleaching on lipid content and composition of Okinawan corals." *Fisheries Science* 71 (2):448-453. doi: 10.1111/j.1444-2906.2005.00983.x.

Yum, Lauren K., Sebastian Baumgarten, Till Röthig, Cornelia Roder, Anna Roik, Craig Michell, and Christian R. Voolstra. 2017. "Transcriptomes and expression profiling of deep-sea corals from the Red Sea provide insight into the biology of azooxanthellate corals." *Scientific Reports* 7:6442. doi: 10.1038/s41598-017-05572-x.